Volume 35 September 2026

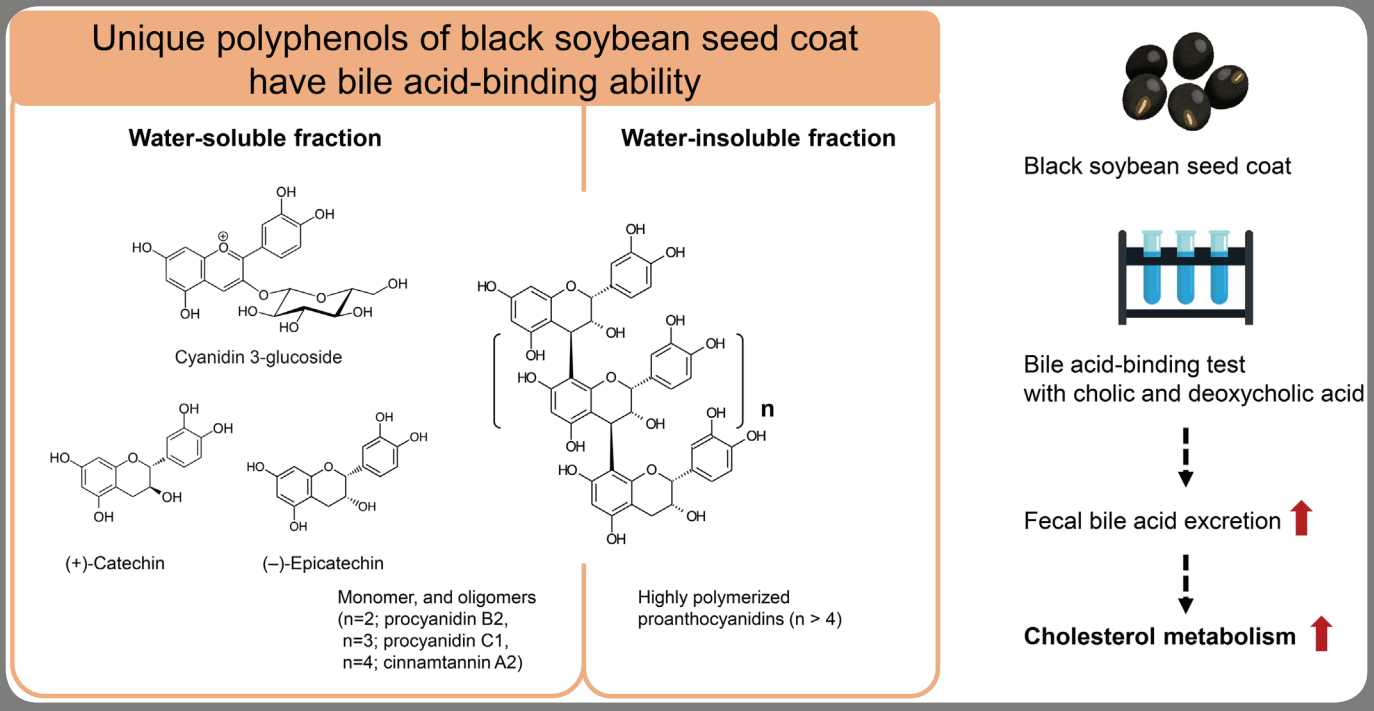
Journal of Food Bioactives

An Official Scientific Publication of the International Society for Nutraceuticals and Functional Foods (ISNFF)

An Official Journal of the International Union of Food Science and Technology (IUFoST)

Editor-in-Chief
Fereidoon Shahidi

Senior Associate Editor
Chi-Tang Ho



The International Society for Nutraceuticals and Functional Foods (ISNFF)
Publishing Services by Tsinghua University Press

Journal of Food Bioactives

Bring together the results of fundamental and applied research on food bioactives, functional food ingredients, nutraceuticals and natural health products that are known to possess or perceived to have health-promoting properties

Editorial Board

Editor-in-Chief

Fereidoon Shahidi (Canada)

Senior Associate Editor

Chi-Tang Ho

Associate Editors

Ryszard Amarowicz (Poland)
Cesarettin Alasalvar (Turkey)

Editorial Board Members

Rotimi Aluko (University of Manitoba, Canada)
Emilio Alvarez (Universidad Autónoma de Ciudad Juárez, Mexico)
Anna Arnoldi (University of Milan, Italy)
Joseph Banoub (Northwest Atlantic Fisheries Centre, St. John's, Canada)
Colin Barrow (Deakin University, Australia)
Bradley W. Bolling (University of Wisconsin, Madison, USA)
Adriano Costa de Camargo (University of Chile, Santiago, Chile)
Rong Cao (Tsao) (Guelph Research & Development Center, Agriculture and Agri-Food Canada, Ontario, Canada)
Bin Du (Heibei Normal University of Science & Technology, Qinhuangdao, China)
Richard FitzGerald (University of Limerick, Ireland)
Farah Hosseinian (Carleton University, Canada)
Charles C. Hu (Nutrilite Health Institute, Amway, USA)
Amin Ismail (University Putra Malaysia, Malaysia)
You-Jin Jeon (Jeju National University, South Korea)
Bo Jiang (Jiangnan University, China)
Hitomi Kumagai (Nihon University, Japan)
Chenyang Lu (Ningbo University, China)
Jack Losso (Louisiana State University, USA)
Kazuo Miyashita (Obihiro University of Agriculture and Veterinary Medicine, Japan)
Ganiyu Oboh (Federal University of Technology Akure, Nigeria)
Ronald B. Pegg (University of Georgia, USA)
Kenji Sato (Kyoto University, Japan)
Young-Joon Surh (Seoul National University, South Korea)
Petras R. Venskutonis (Kaunas University of Technology, Lithuania)
Chin-Kun Wang (Chung Shan Medical University, Taiwan, China)
Dao-Ying Wang Jiangsu (Academy of Agricultural Sciences, China)
Jiankang Wang (Shaanxi University of Science and Technology, China)
Yu Wang (University of Florida, USA)
Hanny C. Wijaya (Bogor Agricultural University, Indonesia)
Baojun (Bruce) Xu (Beijing Normal University-Hong Kong Baptist University United International College, China)
Wallace Yokoyama (US Department of Agriculture, Albany, USA)
Da-Yong Zhou (Dalian Polytechnic University, China)

Instructions for Authors

Journal of Food Bioactives with open access option is an official scientific publication of the International Society for Functional Foods and Nutraceuticals (ISNFF), a not-for-profit Disciplinary Interest Group of the International Union of Food Science and Technology (IUFoST) that was founded in 2007. It publishes original research articles, short communications/research notes, opinion pieces and review articles.

ISSN 2637-8752 Print
ISSN 2637-8779 Online

https://www.sciopen.com/journal/2637-8752

Journal of Food Bioactives
International Society for Nutraceuticals and Functional Foods
Review
J. Food Bioact. 2026;35:1–11

Matcha (Japanese ground green tea) and cognitive function

Klaus W. Lange[a,b,c*] and Yukiko Nakamura[a,b,c]

[a]University of Regensburg, Regensburg, Bavaria, Germany
[b]Nara Institute of Science and Technology, Ikoma, Nara, Japan
[c]Japan Society for Culture, Science and Technology, Germany
[*]**Corresponding author:** Klaus W. Lange, University of Regensburg, 93040 Regensburg, Germany. E-mail: Klaus.Lange@ur.de
DOI: 10.26599/JFB.2026.95035451
Received: June 06, 2026; **Revised received & accepted:** August 29, 2026
Citation: Lange, K.W., and Nakamura, Y. (2026). Matcha (Japanese ground green tea) and cognitive function. J. Food Bioact. 35: 1–11.

Abstract

Matcha is a finely ground powder made from shade-grown green tea leaves. It is primarily produced in Japan. Drinking matcha tea results in higher intake of green tea bioactives than drinking other types of green tea. Studies have found that matcha consumption may enhance cognitive function in situations with and without psychological stress, in the short and long term, and in different age groups. The effects of matcha on cognitive function may be due to stress reduction, improved sleep quality, an increased supply of vitamin K, altered intestinal microbiota composition, decreased oxidative stress, enhanced cholinergic brain function, and increased cortical capillary network angiogenesis. Matcha's stress-reducing efficiency appears to be influenced by differences in the quantities and ratios of its components, which may affect cognitive function. Matcha must contain high levels of theanine to have beneficial effects on stress and anxiety. Furthermore, the ratio of epigallocatechin gallate and caffeine to theanine and arginine must be low. Since not all marketed matcha products worldwide meet these conditions, quality control is important. Harnessing matcha's beneficial properties may effectively support cognitive function and prevent cognitive decline and dementia.

Keywords: Matcha; Green tea; L-theanine; Cognition; Dementia.

1. Introduction

Matcha is a finely ground powder made from shade-grown green tea leaves. According to the International Organization for Standardization (2022), matcha must be derived from the tender leaves, buds, and shoots of the *Camellia sinensis* (L.) O. Kuntze var. *sinensis*, which are grown in the shade. The leaves are steamed, dried, and ground into a fine powder without being rolled.

Powdered tea originated in China during the Tang Dynasty (618–907 CE), when tea leaves were ground into a fine powder and formed into cakes. The practice of steeping the powder in hot water is documented in "The Classic of Tea" by the Chinese tea master Lu Yu (Lu, 1995). During the Song dynasty (960–1279 CE), various tools were used to prepare a beverage called *mòchá* (powdered tea) by whisking tea powder with hot water in a bowl. Matcha was traditionally produced and consumed in Zen Buddhist monasteries (Surak, 2012). These powdered tea practices were transmitted through cultural exchanges between China and Japan around the 12th century, primarily through Zen Buddhist monks who traveled to China to obtain books and sutras from Chinese scholars and encountered *mòchá* in temples. While the practice of *mòchá* faded in China over the next few centuries, it continued in Japan and became an integral part of Japanese Zen Buddhist culture. Matcha was also highly valued by the upper classes during the Muromachi period (1336–1573 CE), when it became fashionable to drink tea from expensive Chinese ceramics. However, tea masters such as Sen no Rikyū emphasized modesty and simplicity. This gave rise to the Japanese tea ceremony, a meditative and spiritual ritual emphasizing respect, harmony, and mindfulness (*chado* or *chanoyu*).

The practice of growing tea plants in the shade by covering them with straw, reeds, or bamboo fabrics originated in Japan in the 15th century (Inoue et al., 2019). It was originally intended to protect tea sprouts from frost damage. This practice resulted in

© The author(s) 2026. Publishing Services by Tsinghua University Press
The articles published in this open access journal are distributed under the terms of the Creative Commons Attribution 4.0 International License (http://creativecommons.org/licenses/by/4.0/)

the development of the bright green Japanese matcha tea with its distinctive aroma and flavor. Shade cultivation inhibits photosynthesis in tea leaves, enhancing the synthesis and accumulation of biologically active compounds, including theanine, caffeine, chlorophyll, and various catechins, such as epigallocatechin gallate (EGCG). Consequently, the tea leaves retain a higher umami content (Ishigaki, 1981). Limiting exposure to sunlight also increases the amount of caffeine and total free amino acids (Ashihara, 2015; Horie et al., 2017) as well as the concentration of chlorophyll in the leaves. This results in a vibrant green color (Yoshida et al., 1959). Most matcha is produced in Japan, where it is an essential part of the traditional tea ceremony. It is also used to flavor and dye foods such as mochi, matcha lattes, green tea ice cream, desserts, and various confections.

Matcha tea contains 60–70% non-water-soluble ingredients, including fat-soluble vitamins (D, E, and K), dietary fiber, chlorophyll, and protein. Water-soluble ingredients include polyphenols, vitamins B1, B2, B3, and B12, fiber, amino acids (especially L-theanine), saponin, and minerals (Maeda-Yamamoto et al., 2013). Matcha tea leaves are protected from sunlight before harvesting, resulting in lower catechin content than green tea types prepared from leaves grown in sunlight (Goto et al., 1996; Ikegaya et al., 1984). However, catechin concentrations are three times higher when matcha is dissolved in water compared to loose-leaf green tea (Fujioka et al., 2016). Matcha has a higher caffeine content because the buds and young leaves of tea plants contain more caffeine than mature leaves (Ashihara and Suzuki, 2004). Matcha's high umami flavor comes from its high amino acid content, including L-theanine, glutamic acid, succinic acid, gallic acid, and theogallin (Kaneko et al., 2006; Ruan et al., 2010). Reducing light intensity through shading increases the total nitrogen, free amino acid (including theanine), and caffeine content of developing tea shoots in the early stages of the shading cycle. Meanwhile, unshaded leaves experience a decline in these quality-enhancing constituents. Sunlight breaks down theanine into glutamate and ethylamine (Anan and Nakagawa, 1974; Ashihara, 2015). Theanine levels also depend on the nitrogen absorbed by *C. sinensis* plant roots (Ruan et al., 2010). Thus, insufficient shielding from sunlight and a low nitrogen supply lead to the production of matcha that is low in theanine and high in EGCG.

Numerous research studies have examined the effects of green tea and its constituents, including catechins, L-theanine, and caffeine. Consuming green tea has been suggested to be associated with various health benefits regarding cardiovascular disease, cancer, and liver disease (Clement, 2009; Filippini et al., 2020; Lange, 2022). Additionally, research has explored the effects of green tea on mood, stress, and cognitive performance (Einöther and Martens, 2013; Lange et al., 2022a; Lange et al., 2022b; Sokary et al., 2023; Wang et al., 2022).

Consuming green tea is thought to promote clarity of mind and cognitive function. Matcha has long been consumed in Zen Buddhist monasteries due to its positive effects on the mind, consciousness, and mental well-being. The effects of green tea on cognitive performance and mood are mainly attributed to the amino acid L-theanine and the psychostimulant caffeine (Camfield et al., 2014). Caffeine can improve energy, motivation, concentration, and performance (Paulus et al., 2015). Combining caffeine and L-theanine enhances concentration, vigilance, and performance in complex cognitive tasks more than either compound alone (Einöther and Martens, 2013; Dietz and Dekker, 2017). EGCG has been found to increase calmness and reduce stress (Scholey et al., 2012).

Consuming matcha tea leads to a much higher intake of green tea phytochemicals than drinking other types of green tea (Dietz and Dekker, 2017). Although matcha and green tea are both produced from the same plant, *Camellia sinensis*, they have different compositions due to their different cultivation, processing, and preparation methods. The quantities of compounds contained in green tea and matcha differ significantly. The ingestion of EGCG after consuming matcha tea has been found to be three times higher than after consuming other high-quality green teas (Weiss and Anderton, 2003). Matcha tea infusions provide significantly more antioxidant compounds than green tea. The oxygen radical absorbance capacity per gram of matcha tea powder is about ten times higher than that of average green tea (Dietz and Dekker, 2017).

Previous studies have found that three compounds found in matcha tea—L-theanine, EGCG, and caffeine—can affect cognitive performance. In recent years, several randomized controlled studies have examined the effects of matcha tea on cognitive function.

2. Randomized controlled trials investigating the effects of matcha on human cognitive function

2.1. Study by Dietz et al. (2017)

The first human intervention study examined the impact of consuming a realistic amount of matcha tea powder (4 g), equivalent to two servings of matcha tea, on the cognitive performance of individuals who consume moderate to habitual amounts of caffeine (Dietz et al., 2017). The study employed a randomized, placebo-controlled, repeated-measures, single-blind design to administer matcha tea and a solid food product (snack bar) containing matcha. Matcha tea contains approximately twice as much caffeine as L-theanine (Aucamp et al., 2000). Unlike other intervention studies that investigated the effects of tea on cognition and administered L-theanine and caffeine at a ratio of 2:1 in favor of L-theanine, Dietz et al. (2017) used a more realistic ratio of 2:1 in favor of caffeine.

A total of 23 healthy young participants (19 females and four males, with an average age of 24.7 years and an age range of 20 to 35 years) participated in four testing sessions. During each session, the participants consumed one of the following products: matcha tea, a matcha bar (each containing 4 g of matcha powder), a placebo tea, or a placebo bar. Participants completed a set of cognitive tests assessing attention, information processing, working memory, and episodic memory at baseline and 60 minutes after consuming each product. Cognitive performance was evaluated using a computerized battery of cognitive tests based on the Cognitive Drug Research methodology. This battery's sensitivity to acute cognitive improvements after the administration of various substances has been established (Wesnes, 2002; Wesnes, 2003). The battery's cognitive tasks assessed immediate word recall, simple reaction time, digit vigilance, choice reaction time, spatial working memory, numeric working memory, delayed word recall, delayed word recognition, and delayed picture recognition (Dietz et al., 2017).

Overall, this study investigated the effects of consuming two average portions of matcha, either as a beverage or incorporated into a snack bar, on the cognitive performance of healthy young individuals. The results showed that matcha had little effect on most cognitive tasks compared to the placebo conditions. However, consuming matcha products showed statistically significant improvements in tasks primarily assessing basic attention abilities and psychomotor speed. The beverage performed better than the snack bar, particularly in tasks assessing spatial working memory speed and delayed picture recognition. Interactions with glucose or other compounds present in the bar may have negatively affected

the bioavailability of matcha. Thus, the role of the food matrix (liquid versus solid) requires further investigation. Additionally, no change in participants' mood, as assessed by the Profile of Mood States (POMS), was observed.

2.2. Study by Sakurai et al. (2020)

Another trial aimed to evaluate the effects of daily matcha tea powder supplementation on cognitive function in community-dwelling elderly individuals without a diagnosis of dementia or mild cognitive impairment (Sakurai et al., 2020). The study was a randomized, placebo-controlled, double-blind 12-week trial. Participants received 1.5 g of matcha powder or a placebo black tea-flavored powder twice daily for 12 weeks. Their cognitive function was evaluated using the Montreal Cognitive Assessment (MoCA) (Nasreddine et al., 2005) and the Mini-Mental State Examination (MMSE) (Folstein et al., 1975). Memory function was evaluated using the Wechsler Memory Scale–Delayed Recall (WMS-DR) (Wechsler, 2010). Of the participants, 54 completed all cognitive tests at the beginning and end of the trial (15 men and 39 women with a mean age of 73.6 years and an age range of 60 to 84 years; n = 28 in the active condition and n = 26 in the placebo condition).

There were no statistically significant changes in cognitive test scores (MoCA and MMSE) between the beginning of the trial and the 12-week follow-up, nor between the active and placebo groups. There was also no significant change in memory test scores between the active and placebo groups (Sakurai et al., 2020). However, a sex-specific analysis revealed a statistically significant improvement in the MoCA score in the active group of females compared to the placebo group. Further analysis of the MoCA's cognitive domains found significant improvement in the language domain for female participants in the active group compared to the placebo group. No significant changes were observed in MMSE scores or memory testing. In the male subgroup, no significant changes in the MoCA, MMSE, or memory function scores were found between the active and placebo groups (Sakurai et al., 2020).

The beneficial effects of matcha on cognition in female participants aligns with previous findings showing that healthy elderly women had improved working memory after taking a large dose of decaffeinated green tea extract (Liu et al., 2018). Additionally, the lack of positive effects of matcha on men's cognitive abilities may be due to the significantly smaller number of male participants compared to females. This study used three cognitive tests: two screening tests for dementia and a logical memory delayed recall test. Using tests that assess more complex cognitive functions may have revealed additional effects of matcha tea on cognitive functioning. In summary, the findings of this study suggest that daily matcha powder supplementation may protect against cognitive decline in community-dwelling elderly women.

2.3. Study by Baba et al. (2021c)

Psychological stress may affect cognitive function. A randomized, placebo-controlled, parallel-group, double-blind study investigated the effects of matcha intake on the attentional function of young adults after mild acute stress (Baba et al., 2021c). The study included 42 healthy men and women aged 25 to 34 years whose stress levels were assumed to be work-related. Participants were randomly assigned to the matcha or placebo group. Those in the matcha group consumed 2 g of matcha daily for two weeks. Mild psychological stress was induced using the Uchida-Kraepelin test, which involves adding single-digit numbers for 30 minutes and is thought to increase sympathetic nervous system activity (Li et al., 2004). Then, memory, attention, facial expression recognition, working memory, visual information processing, and motor function were assessed using the Cognitrax cognitive function test battery developed by CNS Vital Signs (Gualtieri and Johnson, 2006). Subjective levels of fatigue were evaluated using a visual analog scale before the Uchida-Kraepelin test and after the Cognitrax tests (Baba et al., 2021c).

Compared to baseline, the visual analog scale responses obtained after the Uchida-Kraepelin and Cognitrax tests indicated increased fatigue and decreased concentration, thinking ability, and energy levels, suggesting that taking these tests induced mild stress. Matcha intake did not affect the participants' fatigue, concentration, thinking ability, or energy levels. However, the matcha group had significantly faster reaction times on the Stroop test for attentional function than the placebo group. Additionally, the matcha group demonstrated a statistically significant increase in correct responses for positive emotions in the emotion perception test. This test evaluates social cognitive function by measuring the ability to recognize facial expressions, which deteriorates with fatigue (van der Helm et al., 2010). No significant differences between groups were observed in the other tests. Taken together, these results suggest that matcha mitigates the decline in attentional function and has a beneficial effect on social cognition after exposure to mild stress in young adults.

2.4. Study by Baba et al. (2021b)

Another study examined the effects of matcha on cognitive function in middle-aged and older adults exposed to mild, acute psychological stress. Furthermore, the role of the caffeine in matcha in improving cognitive function was investigated by comparing the effects of matcha and caffeine (Baba et al., 2021b). Since previous studies showed that the effects of catechins (Baba et al., 2020) and L-theanine (Baba et al., 2021a) on cognitive function differ depending on intake duration, the effects of single and continuous matcha administration for 12 weeks were examined. In a randomized, placebo-controlled, parallel-group, double-blind study, 51 healthy Japanese men and women aged 50 to 69 years who had self-reported a decline in cognitive function were randomly assigned to one of three groups: matcha, caffeine, or placebo. Participants ingested nine capsules daily, containing either matcha (2 g total), caffeine, or a placebo. The daily caffeine intake (66 mg) was the same in the matcha and caffeine groups. The effects of matcha, caffeine, and placebo were examined after the first capsule (single dose) and after 12 weeks of continuous intake under mild stress conditions. Mild acute stress was induced using the Uchida–Kraepelin test (UKT) (Li et al., 2004), and tests from the Cognitrax battery were used to examine cognitive function (Gualtieri and Johnson, 2006).

The main results of this study are as follows. Caffeine improved attentional function after a single dose, which may explain the reduced reaction time after consuming matcha. The effect of caffeine on accelerating reaction time and focus appears to be only acute. However, matcha was found to improve work performance more than caffeine. Additionally, continuous intake was more beneficial for the matcha group under stress than for the caffeine group (Baba et al., 2021b). In summary, ingesting matcha (which contains caffeine) improves attention and work performance under psychological stress compared to caffeine alone. Future studies should analyze the effects of different caffeine and theanine dosages, the ratio of theanine to caffeine, and the interaction between caffeine, theanine, and catechins.

2.5. Study by Uchida et al. (2024)

A cross-sectional observational study showed that the risk of cognitive decline, as indicated by a score below 26 on the Japanese version of the Mini Mental State Examination (MMSE-J), was significantly lower among individuals who consumed at least 200 milliliters of green tea daily. These results suggested a positive correlation between regular green tea consumption and maintained cognitive function (Kuriyama et al., 2006). Thus, a recent 12-month, randomized, placebo-controlled, parallel-group, double-blind clinical study examined the potential of matcha to delay cognitive decline in community-dwelling older adults aged 60 to 85 years (Uchida et al., 2024). To examine the effects of matcha consumption in the early stages of cognitive impairment, the study included individuals with mild cognitive impairment and subjective cognitive decline (Molinuevo et al., 2017). Although mild subjective cognitive decline is not classified as a disease, several studies have suggested an association between subjective cognitive decline and an increased risk of developing cognitive impairment (Mitchell et al., 2014; Pike et al., 2022). Ninety-nine participants (64 with subjective cognitive decline and 35 with mild cognitive impairment) were randomized into two groups: one receiving 2 g of matcha daily and the other receiving a placebo.

Cognitive testing and other assessments were performed at the beginning and end of the 12-month intervention period. The primary outcome measures were the Japanese version of the Montreal Cognitive Assessment (MoCA-J) and the Alzheimer's Disease Cooperative Study-Activities of Daily Living (ADCS-ADL) scores. Additional outcome measures included the Mini-Mental State Examination-Japanese version (MMSE-J), the Repeatable Battery for the Assessment of Neuropsychological Status-Japanese version (RBANS), the Alzheimer's Disease Assessment Scale-Cognitive Subscale-Japanese version (ADAS-Jcog), and the CNS Vital Signs computerized neurocognitive battery (Gualtieri and Johnson, 2006; Iverson et al., 2007). The CNS Vital Signs battery tests used to assess cognitive functioning in this study included the Stroop test, as well as tests of shift attention, continuous performance, and perception of emotion. These tests used scores of social acuity, reaction time, complex attention, cognitive flexibility, executive function, and simple attention. Additionally, sleep quality was assessed using the Japanese version of the Pittsburgh Sleep Quality Index (PSQI) (Doi et al., 2000).

Compared to the placebo group, the matcha group showed no statistically significant changes in MoCA-J and ADCS-MCI-ADL scores. However, matcha consumption led to significant improvements in certain cognitive functions, such as social acuity, as assessed by the perception of facial emotions test. Additionally, PSQI scores indicated an improvement in sleep quality from baseline to 12 months with matcha consumption (Uchida et al., 2024).

The absence of effects of matcha on the primary outcomes, the Montreal Cognitive Assessment-Japanese version (MoCA-J) and the Alzheimer's Disease Cooperative Study-Activities of Daily Living (ADCS-ADL), may be due to their insensitivity to slight changes in cognitive function. These tools are commonly used for clinical diagnoses of cognitive impairment and dementia rather than for assessing early stages of cognitive decline. Studies have shown that facial emotion recognition is affected in individuals with subjective cognitive decline and mild cognitive impairment (Pietschnig et al., 2016; Weiss et al., 2008). Furthermore, a cross-sectional analysis of over 4,000 individuals revealed impaired recognition of facial emotions in the early stages of cognitive impairment (Virtanen et al., 2017). The study by Uchida et al. (2024) suggests that matcha consumption may enhance social cognition. The decreasing trend in the PSQI score in the matcha group may be due to theanine. Theanine intake (200 mg/day) for four weeks has been shown to significantly decrease the PSQI score in healthy adults (Hidese et al., 2019).

In conclusion, this study's findings suggest that regular matcha consumption may improve emotional perception and sleep quality in elderly individuals with mild cognitive impairment, offering an effective cognitive enhancement strategy. However, this needs to be confirmed by future studies with larger sample sizes that employ more objective measures to examine sleep architecture.

Table 1 presents a summary of randomized controlled trials investigating the effects of matcha on human cognitive function.

3. Potential mechanisms involved in matcha's effects on cognitive functioning

3.1. Stress reduction

Both physical and psychological stress can affect the neuronal functioning related to cognition in the hippocampus and other brain regions (Kim and Kim, 2023). Perceived stress can have long-term physiological and psychological consequences, and it has recently been suggested to be independently associated with prevalent and incident cognitive impairment (Kulshreshtha et al., 2023). Furthermore, exposure to chronic stress appears to considerably contribute to the development of cognitive dysfunction in various mental disorders (Girotti et al., 2024).

The stress-reducing and anti-anxiolytic effects of green tea are commonly attributed to L-theanine (Wang et al., 2022). The potential of matcha to reduce stress, as well as the effects of its quantity and ratio on stress reduction, were examined in a mouse model of psychosocial stress. The outcome variable was suppression of hypertrophy of the adrenal glands, which play a critical role in stress response (Unno et al., 2018). Adrenal hypertrophy has been shown to be suppressed by antidepressant and anxiolytic medications (Unno et al., 2013).

To induce psychosocial stress, the mice were exposed to confrontational stress related to their territory for 24 hours after being reared individually for six days. Their adrenal glands became significantly enlarged, reaching peak size after 24 hours. The experimental dose of matcha was chosen based on human consumption, with 2–3 g of matcha for humans corresponding to 33–50 mg/kg for mice. The stress-reducing effects of matcha were assessed by weighing the adrenal glands. The effects of matcha and its components were examined in 15 groups of mice, for a total of 86 animals. The mice consumed a powdered diet containing matcha or its components for seven days (single rearing for six days and confrontational stress for one day). The administered matcha samples varied in their molar amounts of caffeine and EGCG (Unno et al., 2018).

Theanine and arginine are the most and second most abundant amino acids in Japanese matcha, respectively. They were confirmed to have a significant stress-reducing effect. Meanwhile, glutamate and glutamine, the third and fourth most abundant amino acids, showed no effect (Unno et al., 2016). Suppressing adrenal hypertrophy required a theanine dosage of 0.32 mg/kg or more (Unno et al., 2016). Theanine intake was found to suppress adrenal hypertrophy in a dose-dependent manner, and a similar correlation was observed for arginine. No relationship was seen between caffeine intake and adrenal hypertrophy.

The effect of theanine on adrenal gland weight was reversed when the molar concentration of caffeine was twice as high and the molar ratio of EGCG was equal. However, a 0.7 molar ratio of ar-

Table 1. Randomized controlled trials of the effects of matcha on cognitive functions in humans

Authors	Participants	Independent variables	Dependent variables	Results	Conclusions	Limitations
Dietz et al. (2017)	23 young adults (4 men, 19 women; mean age 24.7 years).	Matcha tea, matcha bar (single dose of 4 g of matcha powder), placebo tea, placebo bar.	Cognitive performance (attention, information processing, working memory, episodic memory) assessed 60 min after matcha or placebo administration.	Significant improvements in basic attention abilities and psychomotor speed after intake of matcha tea and matcha bar (better performance after matcha tea than matcha bar). Little effect on other cognitive tasks.	Improved basic attentional functions after matcha intake. Food matrix plays a role.	Small sample size. Limited generalization.
Sakurai et al. (2020)	54 elderly adults without mild cognitive impairment or dementia (15 men, 39 women; mean age 73.6 years).	Daily matcha tea powder (1.5 g) or placebo for 12 weeks.	MoCA, MMSE, Wechsler Memory Scale–Delayed Recall.	No significant changes in MoCA and MMSE after 12 weeks. No significant differences in MoCA, MMSE, and memory test scores between active and placebo groups. Significant improvement in MoCA score and MoCA language domain in females of active group versus placebo. No changes in men.	Possible protective effect of matcha powder against cognitive decline in elderly women.	Short intervention period of 12 weeks. Small number of male participants.
Baba et al. (2021b)	42 young adults (16 men, 26 women; mean age 29.8 years).	Daily matcha (2 g) or placebo for 2 weeks.	Subjective fatigue. Cognitive functions (Cognitrax battery) under mild psychological stress.	No effect of matcha on fatigue, concentration, or thinking. Significantly faster reaction times in attentional function. Significant increase in correct responses for positive emotions in emotion perception test.	Mitigating effect of matcha on decline in attentional function. Beneficial effect of matcha on social cognition.	Short intervention period of 2 weeks. Limited generalization.
Baba et al. (2021a)	51 middle-aged and elderly adults (23 men, 28 women; mean age 58 years) with self-reported decline in cognitive function.	Single dose and continuous administration for 12 weeks of matcha (2 g), caffeine (66 mg, same as in matcha), or placebo.	Cognitive functions (Cognitrax battery) under mild stress.	Only acute beneficial effect of caffeine on reaction time and focus. Better improvement of work performance by matcha than caffeine. Better effects of continuous intake of matcha under stress compared to caffeine.	Improved attention and work performance after matcha under mild psychological stress compared to caffeine alone.	Short intervention period of 12 weeks. Limited generalization.
Uchida et al. (2024)	99 older adults (64 with subjective cognitive decline, 35 with mild cognitive impairment).	Daily matcha (2 g) or placebo for 12 months.	MoCA-J, ADCS-ADL, MMSE-J, RBANS, ADAS-Jcog, Cognitrax cognitive battery, PSQI	Significantly improved perception of facial emotions after matcha intake. Improved sleep quality (PSQI) with matcha intake. No significant changes in MoCA-J and ADCS-MCI-ADL scores after matcha intake.	Improved emotional perception and sleep quality in mild cognitive impairment. Possible cognitive enhancement.	Small sample size. No objective measures of sleep quality.

ginine to theanine counteracted the antagonizing effects of caffeine and EGCG, suggesting an essential role of arginine in suppressing adrenal hypertrophy. The molar ratio of caffeine and EGCG to theanine and arginine was 1.8 in samples that effectively reduced stress and ≥3.6 in samples that were ineffective (Unno et al., 2018). These findings suggest that the molar ratios of arginine, caffeine, and EGCG influence the stress-reducing effects of theanine.

In conclusion, the dose-dependent suppression of adrenal hypertrophy in mice after consuming matcha suggests a stress-reducing effect. However, the molar ratio of arginine, caffeine, and EGCG appears to influence the stress-reducing effects of theanine. For an effective stress-reducing outcome, the molar ratio of caffeine and EGCG to theanine and arginine should be less than two.

Based on the results of the animal study, test-matcha, which was expected to have a stress-reducing effect, and placebo-matcha, which was not, were selected for a randomized, parallel-group, single-blind trial (Unno et al., 2018). Thirty-nine healthy students (23 men and 16 women with a mean age of 23 years) were randomly assigned to the test-matcha group (n = 19) or the placebo-matcha group (n = 20). The participants consumed test- or placebo-matcha tea daily for 15 days, ingesting 3 g of matcha per day. The caffeine content of the test and placebo matcha was not different. The 7-day period of routine university life and the first eight days of the students' practice program outside the university were analyzed. Salivary α-amylase activity was measured as an indicator of stress and sympathetic nervous system activation in response to physiological and psychosocial stress (van Stegeren et al., 2006). Anxiety in response to stress was assessed using the Japanese State-Trait Anxiety Inventory (STAI).

Before the practice phase outside the university, the STAI values of the participants who consumed test-matcha were significantly lower than those of the placebo-matcha group. By the eighth day of practice, however, there was no significant difference between the two groups. Although the baseline level of α-amylase activity before consuming matcha did not differ between participants in the test- and placebo-matcha groups, the level at the university was significantly lower in the test-matcha group. Throughout the practice program, α-amylase activity was lower in the test-matcha group. Subjective stress levels after practice were slightly lower in the test group than in the placebo group. In summary, matcha tea ingestion resulted in a statistically significant decrease in anxiety levels and reduction in physiological stress compared to the placebo group (Unno et al., 2018).

The stress-reducing effect of matcha was also tested in cookies containing either test-matcha (caffeine and EGCG to theanine and arginine molar ratio of 1.79) or placebo-matcha (caffeine and EGCG to theanine and arginine molar ratio of 10.64). Healthy university students consumed three pieces of cookie containing 4.5 g of matcha daily for 15 days (Unno et al., 2019). Salivary α-amylase activity decreased significantly in the test-matcha group compared to the placebo group. Thus, the caffeine and EGCG to theanine and arginine ratio appears to be an essential indicator for stress suppression. In summary, matcha in confectionery products has a stress-reducing effect. However, to have this effect, matcha must contain less caffeine and EGCG than twice the molar amount of theanine and arginine. The daily intake of matcha in confectionery products with a low caffeine and EGCG-to-theanine and arginine molar ratio may provide stress-reducing benefits to individuals who do not drink green tea.

In conclusion, healthy individuals who consumed 3 g of matcha tea daily showed significant reductions in anxiety and physiological stress. Stress reduction was also observed with cookies formulated with a specific ratio of matcha components (theanine, arginine, caffeine, and EGCG).

3.2. Sleep quality

There appears to be a close relationship between sleep quality and cognitive function (Xu et al., 2011; Sun et al., 2013; Yaffe et al., 2014). In a longitudinal study of individuals aged 50 to 80, the risk of developing mild cognitive impairment over an average observation period of 5.2 years was significantly higher for participants with a PSQI score greater than 5 (indicating poor sleep quality) than for those with a score of 5 or less (Brachem et al., 2020). These findings suggest that improving sleep quality may positively impact cognitive function. Aging is commonly associated with deteriorating sleep quality, and sleep disturbances and short sleep duration are risk factors for dementia (Sabia et al., 2021). Sleep deprivation can lead to inflammation and an increased amyloid-β burden in the brain (Shokri-Kojori et al., 2018; Irwin and Vitiello, 2019). Uchida et al. (2024) found that older adults with subjective cognitive decline or mild cognitive impairment experienced statistically significant improvements in social cognition and reduced PSQI scores after consuming 2 g of matcha daily for 12 months. Thus, matcha may benefit cognitive functioning in the elderly by improving sleep quality.

Theanine in matcha has been shown to improve sleep quality and cognitive function. However, caffeine is believed to negatively impact sleep quality. A recent randomized, placebo-controlled, parallel-group, double-blind study investigated the effects of matcha on various sleep parameters (Baba et al., 2024). Healthy men and women aged 27 to 64 consumed 2.7 grams of matcha daily for four weeks. No statistically significant differences were found between the matcha and control groups regarding sleep latency, total sleep time, wake time after sleep onset, or sleep efficiency, as assessed by electroencephalography (EEG). However, a sleep questionnaire completed immediately after waking revealed an increased satisfaction with sleep time. Additionally, EEG measures indicated a significant reduction in wake-up time following matcha consumption. Furthermore, Beck Depression Inventory-II scores tended to decrease (Baba et al., 2024). In summary, continuous matcha consumption may improve subjective sleep quality and emotional stability without significantly altering objectively measured sleep parameters. This may contribute to stress reduction and improved cognition (see section 3.1).

3.3. Vitamin K

Matcha powder contains several compounds, including EGCG, caffeine, and theanine, that have been linked to cognitive function. These compounds can significantly improve cognitive performance by modulating dopaminergic, cholinergic, and glutamatergic activities in the brain, either separately or synergistically (Dietz and Dekker, 2017). Matcha tea contains higher concentrations of fat-soluble nutrients, such as vitamins K and E, and lutein, than regular green tea. These nutrients have been reported to positively impact cognitive function (Nouchi et al., 2020; Presse et al., 2013). Low lifetime intake of vitamin K has been found to lead to mild cognitive impairment in aged rats (Carrié et al., 2011).

Several research findings suggest a relationship between vitamin K levels and cognitive functioning, indicating that vitamin K plays a role in brain function (Alisi et al., 2019). A deficiency in vitamin K may be associated with the onset of cognitive impairment (Ferland, 2012). Furthermore, vitamin K has procoagulant efficacy. Vitamin K antagonists are therefore widely used as oral anticoagulants, but they may negatively affect the volume of certain brain regions (Brangier et al., 2018) and cognitive functions,

such as verbal fluency and memory (Ferland et al., 2016).

Sakurai et al. (2020) attempted to explore the link between dietary habits and cognitive function in their study (see section 2.2). The researchers performed a multiple regression analysis to determine the relationship between daily nutrient intake (excluding the trial's test drinks), as assessed using the Brief Self-administered Diet History Questionnaire (Kobayashi et al., 2012), and the MoCA score difference for female participants. Higher vitamin K intake in the daily diet showed a statistically significant inverse correlation with increased MoCA scores after matcha administration. This suggests that matcha's positive effect on cognition may be more pronounced in individuals with lower daily vitamin K intake, as matcha consumption can supplement prevalent vitamin K deficiencies. Therefore, an adequate daily intake of vitamin K may be important for cognitive functioning, and the vitamin K in matcha tea may help maintain adequate levels and improve cognitive performance. Supplementing deficient vitamin K levels could possibly ameliorate cognitive deficits. However, further randomized trials with large samples and standardized methods for cognitive evaluation, dietary intake of vitamin K, and serum levels are needed to confirm the hypothesis that low vitamin K levels are related to cognitive decline.

3.4. Gut microbiota

The human gastrointestinal tract is home to diverse microbial species that can greatly impact brain function. Bidirectional communication along the gut–brain axis involves neural, metabolic, endocrine, and immune pathways and occurs between the intestines and the central nervous system (Bagheri et al., 2026). Research has reported a relationship between gut microbiota and cognitive function or impairment in various mental disorders (Lange, Lange, Nakamura, and Kanaya, 2020; Meyer et al., 2022). Emerging research suggests that enhancing cognition may be possible through human gut microbiota (Zhang et al., 2025). Matcha tea contains more nutrients, such as catechins and insoluble dietary fiber, than regular green tea and is believed to have positive effects on gut microbiota (Kochman et al., 2020).

A recent study examined the impact of matcha tea on gut microbiota. Young adults were randomly assigned to one of two groups: the matcha tea group (n = 16), which received 1.5 g of matcha tea, and the placebo group (n = 17). Both groups were required to drink the provided beverages for two weeks (Morishima et al., 2023). Feces were collected from the participants before and after the treatment period and analyzed using 16S rRNA metagenomic sequencing to determine the composition of the fecal microbiota. Beta diversity (or difference or dissimilarity) in microbial community composition was shown to be significantly altered two weeks after continuous matcha tea consumption, but not in the placebo group. The matcha tea group had 30 genera of bacteria that changed significantly, while the placebo group only had three. Bacterial genera whose abundance changed significantly before and after matcha tea consumption included *Fusobacterium* and *Coprococcus* (Morishima et al., 2023). Decreased abundance of *Fusobacterium* and increased abundance of *Coprococcus* in the gut microbiota of the matcha tea group are thought to confer potential health benefits to the host. A high proportion of *Fusobacterium* has been found in the gut microbiota of patients with inflammatory bowel disease and colorectal cancer (Lee et al., 2016; Repass, 2018), while a lower abundance of *Coprococcus* has been reported in people with inflammatory bowel disease (Nishino et al., 2018). EGCG appears to inhibit the growth of *Fusobacterium* (Liu et al., 2020), while insoluble dietary fiber may increase *Coprococcus* abundance in the intestinal microbiota (Chen et al., 2019).

In conclusion, consuming matcha tea for two weeks altered the fecal microbiota. Further research is needed to determine whether matcha affects bacterial genera related to cognitive functions.

3.5. Other mechanisms

Various other mechanisms have been suggested to explain the effects of matcha on cognitive functioning. Matcha's antioxidant function, conferred by EGCG, may play a role in cognitive functioning since neurons are vulnerable to oxidative stress due to their high content of unsaturated fatty acids. Therefore, matcha may prevent cognitive impairment by suppressing oxidative stress and protecting the integrity of the brain's antioxidant systems (Kim et al., 2020).

Studies have shown that matcha improves cognitive dysfunction induced by metabolic imbalance in mice fed a high-fat diet (Kim et al., 2020). This study found that matcha protects against insulin resistance and cognitive impairment caused by cerebral inflammatory responses. Matcha improved short-term and long-term memory and spatial cognitive function by regulating glucose tolerance.

Matcha can also prevent cognitive impairment by improving the function of the central cholinergic transmission system, which is closely linked to cognitive function (Kim et al., 2020). In mice, a high-fat diet was shown to increase the expression of acetylcholinesterase, which catalyzes the breakdown of the neurotransmitter acetylcholine. A high-fat diet also triggers the aggregation of amyloid-β, inducing neuronal death in the brain (Kim et al., 2020). However, matcha intake improved cholinergic function by downregulating acetylcholinesterase and reducing amyloid-β expression, while also upregulating choline acetyltransferase in the hippocampus and cerebral cortex (Kim et al., 2020).

The central nervous system requires an adequate capillary network to maintain undisturbed brain function. Due to the age-related reduction in cortical capillaries, the discovery of the angiogenic potential and protective effects of matcha and its components, vitamin K_1 and lutein, on capillary aging in the cerebral cortex of mice could have clinical significance (Iwai et al., 2021).

4. Future directions

Epidemiological studies have shown that the high consumption of certain foods in Japan may have health and longevity benefits (Lange and Nakamura, 2024, 2025a, 2025b, 2026a, 2026b). In this respect, green tea and matcha have attracted attention due to their bioactive components, which may benefit human health, including cognitive function.

4.1. Effects of matcha on cognitive decline and dementia

Aging is often associated with the deterioration of cognitive function, which appears to depend on lifestyle factors, including nutrition (Lange et al., 2026). For example, several food bioactives, including polyunsaturated fatty acids (Lange, 2020a, 2020b) and natural antioxidants (Lange, 2018; Lange and Li, 2018; Lange, Lange, Nakamura, and Li, 2020), have been suggested to reduce the risk of cognitive decline and dementia. Considering the positive impact of matcha on cholinergic function in the brain (see section 3.5), one might wonder if matcha consumption can prevent

cognitive decline and dementia. A systematic review of observational studies found that green tea consumption may reduce the risk of mild cognitive impairment, cognitive impairment, dementia, and Alzheimer's disease (Kakutani et al., 2019). Other findings also suggest a beneficial role of matcha in preventing neurodegeneration and dementing disorders.

EGCG may serve as a neuroprotective agent due to its ability to influence the inflammatory processes associated with neurodegeneration (Valverde-Salazar et al., 2023). EGCG can also inhibit the co-aggregation of amyloid proteins, such as amyloid-β and human islet amyloid polypeptide. These proteins are associated with the development of Alzheimer's disease (Li et al., 2024). EGCG and other catechins found in green tea may prevent age-related cognitive decline by increasing the expression of genes involved in synaptic plasticity in the hippocampus (Unno et al., 2020). Additionally, systemic inflammation induced by lipopolysaccharides plays a significant role in neurodegeneration. EGCG inhibits the production of reactive oxygen species induced by lipopolysaccharides, suggesting its neuroprotective efficacy in inflammation-mediated neurodegenerative diseases (Liu et al., 2016).

Caffeine may also have neuroprotective effects against dementia (Merighi et al., 2023). It may decrease the risk of cognitive decline (Ritchie et al., 2007) and slow the aging process in the brain by reversing oxidative processes and reducing neuroinflammation (Ullah et al., 2015). The beneficial effects of caffeine in preventing neurodegeneration are also related to a reduction in amyloid-β deposition (Arendash et al., 2009). In a prospective cohort study of over 130,000 people with up to 43 years of follow-up, higher consumption of caffeinated coffee was associated with more favorable cognitive outcomes and a statistically significant association with a lower risk of dementia, while intake of decaffeinated coffee was not found to be significantly associated with dementia risk (Zhang et al., 2026).

Among 8,766 community-dwelling Japanese individuals, no statistically significant correlations were observed between green tea intake and hippocampal or total brain volume (Shibata et al., 2025). However, green tea consumption was inversely correlated with cerebral white matter lesions, suggesting a potential role of matcha in preventing dementia (Shibata et al., 2025). Further research is needed to confirm and expand upon the current findings regarding the role of matcha in preventing cognitive decline and dementia.

4.2. Quality of matcha marketed in Japan and other countries

The number of people consuming green tea and matcha for health benefits is increasing worldwide. The theanine content of matcha varies depending on the quality of the green tea used to make it. Matcha is rich in theanine and low in catechin. However, not all marketed matcha products satisfy these conditions. Low-grade green teas with low amino acid content have also been reported to be sold as "matcha" (Horie et al., 2018). A recent study examined the components of matcha sold in Japan and other countries. When humans ingest 3 g of matcha daily, matcha containing levels of theanine exceeding 17 mg/g may reduce stress. Fifty out of 76 Japanese samples met this condition. However, of the 67 samples sold in other countries, only six met this criterion (Unno et al., 2018). Additionally, for matcha to have stress-reducing efficacy, the molar ratio of caffeine and EGCG to theanine and arginine must be less than two. Thirty-two of the 76 Japanese samples and one of the 67 non-Japanese samples met this condition (Unno et al., 2018). This study assessed the stress-reducing effect of matcha (at a dose of 3 g daily) sold in Japan and other countries. It was expected that about 42% of the matcha marketed in Japan would suppress stress, as opposed to only one of the matcha products sold abroad because the amounts of theanine and arginine were low while the amounts of caffeine and EGCG were high. Thus, not all marketed matcha satisfied the condition of high theanine and low catechin levels. Therefore, greater attention is needed when evaluating the cognitive and mental effects of matcha. The low amino acid content and the counteracting effect of caffeine and EGCG on theanine are rarely considered. This may lead to confusing findings. For example, a Profile of Mood States (POMS) assessment revealed no significant change in mood after consuming 4 g of matcha tea (Dietz et al., 2017). However, the molar ratio of caffeine and EGCG to theanine was greater than two. The POMS results may have differed if a matcha sample with lower caffeine and EGCG content had been used. In conclusion, quality checks are critical when using matcha samples to study cognitive function.

4.3. Side effects of matcha

Consuming matcha can have unwanted side effects since it involves ingesting relatively large amounts of oxalate due to its cultivation in the shade (Morita and Tuji, 2002). Oxalate binds to calcium ions to form calcium oxalate, which may cause kidney stones. Therefore, it may be necessary to evaluate the maximum daily intake of matcha tea for individuals who are sensitive to urinary stone formation. Additionally, oxalate can remove calcium from the body, which could lead to osteoporosis and heart disorders. Further research in this respect is required.

5. Conclusion

Because of how matcha is farmed and harvested, drinking matcha tea results in a much higher intake of green tea bioactive compounds than drinking other types of green tea. Studies in humans have shown that matcha consumption may enhance cognitive function in situations with and without psychological stress, in the short and long term, and in different age groups.

The mechanisms involved in matcha's effects on cognitive functioning may include stress reduction, improved sleep quality, an increased supply of vitamin K, altered intestinal microbiota composition, decreased oxidative stress, enhanced cholinergic brain function, and increased cortical capillary network angiogenesis.

The quantities and ratios of matcha components appear to influence the efficiency of its stress-reducing activity, which may affect cognitive function. Caffeine and EGCG counteract the stress-reducing effect of theanine, while arginine enhances it. To have beneficial effects on stress, anxiety, and mood, matcha must contain high levels of theanine and arginine while having a low ratio of EGCG and caffeine to theanine and arginine. Quality control in this respect is essential, as not all marketed matcha products worldwide meet these conditions.

In summary, harnessing matcha's stress-reducing properties and other benefits may effectively support overall daily well-being and cognitive functioning and possibly prevent cognitive decline and dementia.

References

Alisi, L., Cao, R., Angelis, C.d.e., Cafolla, A., Caramia, F., Cartocci, G., Librando, A., and Fiorelli, M. (2019). The relationships between vitamin K

and cognition: A review of current evidence. Front. Neurol. 10: 239.
Anan, T., and Nakagawa, M. (1974). Effect of light on chemical constituents in the tea leaves. Nippon Nogeikagaku Kaishi (J. Jpn. Agricult. Chem. Soc.) 48: 91–96.
Arendash, G.W., Mori, T., Cao, C., Mamcarz, M., Runfeldt, M., Dickson, A., Rezai-Zadeh, K., Tane, J., Citron, B.A., Lin, X., Echeverria, V., and Potter, H. (2009). Caffeine reverses cognitive impairment and decreases brain amyloid-beta levels in aged Alzheimer's disease mice. J. Alzheimers Dis. 17: 661–680.
Ashihara, H. (2015). Occurrence, biosynthesis and metabolism of theanine (γ-glutamyl-L-ethylamide) in plants: A comprehensive review. Nat. Prod. Commun. 10: 803–810.
Ashihara, H., and Suzuki, T. (2004). Distribution and biosynthesis of caffeine in plants. Front. Biosci. 9: 1864–1876.
Aucamp, J.P., Hara, Y., and Apostolides, Z. (2000). Simultaneous analysis of tea catechins, caffeine, gallic acid, theanine and ascorbic acid by micellar electrokinetic capillary chromatography. J. Chromatogr. A 876: 235–242.
Baba, Y., Inagaki, S., Nakagawa, S., Kaneko, T., Kobayashi, M., and Takihara, T. (2020). Effect of daily intake of green tea catechins on cognitive function in middle-aged and older subjects: A randomized, placebo-controlled study. Molecules 25: 4265.
Baba, Y., Inagaki, S., Nakagawa, S., Kaneko, T., Kobayashi, M., and Takihara, T. (2021a). Effects of l-theanine on cognitive function in middle-aged and older subjects: A randomized placebo-controlled study. J. Med. Food 24: 333–341.
Baba, Y., Inagaki, S., Nakagawa, S., Kobayashi, M., Kaneko, T., and Takihara, T. (2021b). Effects of daily matcha and caffeine intake on mild acute psychological stress-related cognitive function in middle-aged and older adults: A randomized placebo-controlled study. Nutrients 13: 1700.
Baba, Y., Kaneko, T., and Takihara, T. (2021c). Matcha consumption maintains attentional function following a mild acute psychological stress without affecting a feeling of fatigue: A randomized placebo-controlled study in young adults. Nutr. Res. 88: 44–52.
Baba, Y., Takihara, T., and Okamura, N. (2024). Matcha does not affect electroencephalography during sleep but may enhance mental well-being: A randomized placebo-controlled clinical trial. Nutrients 16: 2907.
Bagheri, S., Ryszkiel, I., and Stanek, A. (2026). Gut microbiota impact on cognitive function in humans. Nutrients 18: 369.
Brachem, C., Winkler, A., Tebrügge, S., Weimar, C., Erbel, R., Jöckel, K.-H., Stang, A., Dragano, N., Moebus, S., Kowall, B., and Jokisch, M. (2020). Associations between self-reported sleep characteristics and incident mild cognitive impairment: The Heinz Nixdorf Recall Cohort Study. Sci. Rep. 10: 6542.
Brangier, A., Celle, S., Roche, F., Beauchet, O., Ferland, G., and Annweiler, C. (2018). Use of vitamin K antagonists and brain morphological changes in older adults: An exposed/unexposed voxel-based morphometric study. Dement. Geriatr. Cogn. Disord. 45: 18–26.
Camfield, D.A., Stough, C., Farrimond, J., and Scholey, A.B. (2014). Acute effects of tea constituents L-theanine, caffeine, and epigallocatechin gallate on cognitive function and mood: A systematic review and meta-analysis. Nutr. Rev. 72: 507–522.
Carrié, I., Bélanger, E., Portoukalian, J., Rochford, J., and Ferland, G. (2011). Lifelong low-phylloquinone intake is associated with cognitive impairments in old rats. J. Nutr. 141: 1495–1501.
Chen, T., Chen, D., Tian, G., Zheng, P., Mao, X., Yu, J., He, J., Huang, Z., Luo, Y., Luo, J., and Yu, B. (2019). Soluble fiber and insoluble fiber regulate colonic microbiota and barrier function in a piglet model. Biomed. Res. Int. 2019: 7809171.
Clement, Y. (2009). Can green tea do that? A literature review of the clinical evidence. Prev. Med. 49: 83–87.
Dietz, C., and Dekker, M. (2017). Effect of green tea phytochemicals on mood and cognition. Curr. Pharm. Des. 23: 2876–2905.
Dietz, C., Dekker, M., and Piqueras-Fiszman, B. (2017). An intervention study on the effect of matcha tea, in drink and snack bar formats, on mood and cognitive performance. Food Res. Int. 99: 72–83.
Doi, Y., Minowa, M., Uchiyama, M., Okawa, M., Kim, K., Shibui, K., and Kamei, Y. (2000). Psychometric assessment of subjective sleep quality using the Japanese version of the Pittsburgh Sleep Quality Index (PSQI-J) in psychiatric disordered and control subjects. Psychiatry Res. 97: 165–172.
Einöther, S.J., and Martens, V.E. (2013). Acute effects of tea consumption on attention and mood. Am. J. Clin. Nutr. 98: 1700S–1708S.
Ferland, G. (2012). Vitamin K, an emerging nutrient in brain function. Biofactors 38: 151–157.
Ferland, G., Feart, C., Presse, N., Lorrain, S., Bazin, F., Helmer, C., Berr, C., Annweiler, C., Rouaud, O., Dartigues, J.-F., Fourrier-Reglat, A., and Barberger-Gateau, P. (2016). Vitamin K antagonists and cognitive function in older adults: The Three-City Cohort Study. J. Gerontol. A Biol. Sci. Med. Sci. 71: 1356–1362.
Filippini, T., Malavolti, M., Borrelli, F., Izzo, A.A., Fairweather-Tait, S.J., Horneber, M., and Vinceti, M. (2020). Green tea (Camellia sinensis) for the prevention of cancer. Cochrane Database Syst. Rev. 3: CD005004.
Folstein, M.F., Folstein, S.E., and McHugh, P.R. (1975). "Mini-mental state" A practical method for grading the cognitive state of patients for the clinician. J. Psychiatr. Res. 12: 189–198.
Fujioka, K., Iwamoto, T., Shima, H., Tomaru, K., Saito, H., Ohtsuka, M., Yoshidome, A., Kawamura, Y., and Manome, Y. (2016). The powdering process with a set of ceramic mills for green tea promoted catechin extraction and the ROS inhibition effect. Molecules 21: 474.
Girotti, M., Bulin, S.E., and Carreno, F.R. (2024). Effects of chronic stress on cognitive function - From neurobiology to intervention. Neurobiol. Stress 33: 100670.
Goto, T., Yoshida, Y., Kiso, M., and Nagashima, H. (1996). Simultaneous analysis of individual catechins and caffeine in green tea. J. Chromatogr. A 749: 295–299.
Gualtieri, C.T., and Johnson, L.G. (2006). Reliability and validity of a computerized neurocognitive test battery, CNS Vital Signs. Arch. Clin. Neuropsychol. 21: 623–643.
Hidese, S., Ogawa, S., Ota, M., Ishida, I., Yasukawa, Z., Ozeki, M., and Kunugi, H. (2019). Effects of L-theanine administration on stress-related symptoms and cognitive functions in healthy adults: A randomized controlled trial. Nutrients 11: 2362.
Horie, H., Ema, K., Niskikawa, H., and Nakamura, Y. (2018). Comparison of the chemical components of powdered green tea sold in the US. JARQ-Jpn. Agr. Res. Q. 52: 143–147.
Horie, H., Kaori, E., and Sumikawa, O. (2017). Chemical components of matcha and powdered green tea. J. Cookery Sci. Japan 50: 182–188.
Ikegaya, K., Takayanagi, H., and Anan, T. (1984). Chemical composition of matcha (tencha). Chagyo Kenkyu Hokoku (Tea Res. J.) 60: 79–81.
Inoue, Y., Nakao, A., Yauchi, J., Sase, T., and Konishi, S. (2019). Estimating the origin of shade-grown cultivation using soil from tea plantations in Uji City, Kyoto Prefecture (in Japanese). Jpn. J. Soil Sci. Plant Nutr. 90: 424–432.
International Organization for Standardization. (2022). Matcha tea — Definition and characteristics. Available: https://www.iso.org/obp/ui/en/#iso:std:iso:tr:21380:ed-1:v1:en. Accessed February 26, 2026.
Irwin, M.R., and Vitiello, M.V. (2019). Implications of sleep disturbance and inflammation for Alzheimer's disease dementia. Lancet Neurol. 18: 296–306.
Ishigaki, K. (1981). Chemical components, taste, and flavor of tea, and cultivation of tea plants (in Japanese). Kagaku to Seibutsu (Chemistry and Biology) 19: 278–285.
Iverson, G.L., Brooks, B.L., Weiss, M.D., Gualtieri, C.T., and Johnson, L.G. (2007). Clinical usefulness of CNS vital signs for assessing neurocognition in ADHD. Clin. Neuropsychol. 21: 686.
Iwai, R., Ishii, T., Fukushima, Y., Okamoto, T., Ichihashi, M., Sasaki, Y., and Mizuatni, K.-I. (2021). Matcha and its components control angiogenic potential. J. Nutr. Sci. Vitaminol. (Tokyo) 67: 118–125.
Kakutani, S., Watanabe, H., and Murayama, N. (2019). Green tea intake and risks for dementia, Alzheimer's disease, mild cognitive impairment, and cognitive impairment: A systematic review. Nutrients 11: 1165.
Kaneko, S., Kumazawa, K., Masuda, H., Henze, A., and Hofmann, T. (2006). Molecular and sensory studies on the umami taste of Japanese green tea. J. Agric. Food Chem. 54: 2688–2694.
Kim, E.J., and Kim, J.J. (2023). Neurocognitive effects of stress: a metaparadigm perspective. Mol. Psychiatry 28: 2750–2763.
Kim, J.M., Lee, U., Kang, J.Y., Park, S.K., Kim, J.C., and Heo, H.J. (2020).

Matcha improves metabolic imbalance-induced cognitive dysfunction. Oxid. Med. Cell Longev. 2020: 8882763.
Kobayashi, S., Honda, S., Murakami, K., Sasaki, S., Okubo, H., Hirota, N., Notsu, A., Fukui, M., and Date, C. (2012). Both comprehensive and brief self-administered diet history questionnaires satisfactorily rank nutrient intakes in Japanese adults. J. Epidemiol. 22: 151–159.
Kochman, J., Jakubczyk, K., Antoniewicz, J., Mruk, H., and Janda, K. (2020). Health benefits and chemical composition of matcha green tea: A review. Molecules 26: 85.
Kulshreshtha, A., Alonso, A., McClure, L.A., Hajjar, I., Manly, J.J., and Judd, S. (2023). Association of stress with cognitive function among older black and white US adults. JAMA Netw. Open 6: e231860.
Kuriyama, S., Hozawa, A., Ohmori, K., Shimazu, T., Matsui, T., Ebihara, S., Awata, S., Nagatomi, R., Arai, H., and Tsuji, I. (2006). Green tea consumption and cognitive function: A cross-sectional study from the Tsurugaya Project 1. Am. J. Clin. Nutr. 83: 355–361.
Lange, K.W. (2018). Red wine, resveratrol, and Alzheimer's disease. Mov. Nutr. Health Dis. 2: 31–38.
Lange, K.W. (2020a). Lipids in the treatment of neurodegenerative diseases. In: Shahidi, F. (Ed.). Bailey's industrial oil and fat products (7th ed.), Vol. 7. Wiley, pp. 370–391.
Lange, K.W. (2020b). Omega-3 fatty acids and mental health. Glob. Health J. 4: 18–30.
Lange, K.W. (2022). Tea in cardiovascular health and disease: a critical appraisal of the evidence. Food Sci. Hum. Wellness 11: 445–454.
Lange, K.W., and Li, S. (2018). Resveratrol, pterostilbene, and dementia. Biofactors 44: 83–90.
Lange, K.W., Lange, K.M., and Nakamura, Y. (2022a). Green tea, epigallocatechin gallate and the prevention of Alzheimer's disease: clinical evidence. Food Sci. Hum. Wellness 11: 765–770.
Lange, K.W., Lange, K.M., Nakamura, Y., and Kanaya, S. (2020). Is there a role of gut microbiota in mental health? J. Food Bioact. 9: 4–9.
Lange, K.W., Lange, K.M., Nakamura, Y., and Li, S. (2020). Do natural antioxidants play a role in Alzheimer's disease? J. Food Bioact. 11: 2–10.
Lange, K.W., and Nakamura, Y. (2024). Japanese food culture and human health - what we can learn from Japan. J. Dis. Prev. Health Promot. 8: 9–12.
Lange, K.W., and Nakamura, Y. (2025a). Amazake (Japanese fermented rice beverage) and its potential health benefits. Food Sci. Hum. Wellness 14: 9250076.
Lange, K.W., and Nakamura, Y. (2025b). Japanese cuisine and its health benefits: food bioactives, dietary features, and public health. J. Food Bioact. 31: 1–7.
Lange, K.W., and Nakamura, Y. (2026a). Japanese-style diet and life expectancy. J. Food Bioact. 34: 22–30.
Lange, K.W., and Nakamura, Y. (2026b). The Japanese diet of 1975 and health promotion: What can we learn from Japan? J. Dis. Prev. Health Promot. 10: 10–14.
Lange, K.W., Nakamura, Y., and Lange, K.M. (2026). Food and nutrition in the prevention of dementia-A mini-review. J. Food Bioact. 33: 10–15.
Lange, K.W., Nakamura, Y., Lange, K.M., and Zhao, H. (2022b). Tea and depression. Food Sci. Hum. Wellness 11: 476–482.
Lee, Y., Eun, C.S., Lee, A.R., Park, C.H., and Han, D.S. (2016). Fusobacterium isolates recovered from colonic biopsies of inflammatory bowel disease patients in Korea. Ann. Lab. Med. 36: 387–389.
Li, G.Y., Ueki, H., Kawashima, T., Sugataka, K., Muraoka, T., and Yamada, S. (2004). Involvement of the noradrenergic system in performance on a continuous task requiring effortful attention. Neuropsychobiology 50: 336–340.
Li, X., Zhang, Y., Yang, Z., Zhang, S., and Zhang, L. (2024). The inhibition effect of epigallocatechin-3-gallate on the co-aggregation of amyloid-β and human islet amyloid polypeptide revealed by replica exchange molecular dynamics simulations. Int. J. Mol. Sci. 25: 1636.
Liu, J.-B., Zhou, L., Wang, Y.-Z., Wang, X., Zhou, Y., Ho, W.-Z., and Li, J.-L. (2016). Neuroprotective activity of (-)-epigallocatechin gallate against lipopolysaccharide-mediated cytotoxicity. J. Immunol. Res. 2016: 4962351.
Liu, Y., Fly, A.D., Wang, Z., and Klaunig, J.E. (2018). The effects of green tea extract on working memory in healthy women. J. Nutr. Health Aging 22: 446–450.
Liu, Z., Bruijn, W.J.C.d.e., Bruins, M.E., and Vincken, J.-P. (2020). Reciprocal interactions between epigallocatechin-3-gallate (EGCG) and human gut microbiota in vitro. J. Agric. Food Chem. 68: 9804–9815.
Lu, Y. (1995). The classic of tea. Origins and rituals. Ecco Press, Hopewell, NJ.
Maeda-Yamamoto, M., Tachibana, H., Sameshima, Y., and Kuriyama, S. (2013). Green tea (cv. Benifuuki) powder and catechins availability. In: Preedy, V.R. (Ed.). Tea in Health and Disease Prevention. Elsevier, pp. 115–125.
Merighi, S., Travagli, A., Nigro, M., Pasquini, S., Cappello, M., Contri, C., Varani, K., Vincenzi, F., Borea, P.A., and Gessi, S. (2023). Caffeine for prevention of Alzheimer's disease: Is the A2A adenosine receptor its target? Biomolecules 13: 967.
Meyer, K., Lulla, A., Debroy, K., Shikany, J.M., Yaffe, K., Meirelles, O., and Launer, L.J. (2022). Association of the gut microbiota with cognitive function in midlife. JAMA Netw. Open 5: e2143941.
Mitchell, A.J., Beaumont, H., Ferguson, D., Yadegarfar, M., and Stubbs, B. (2014). Risk of dementia and mild cognitive impairment in older people with subjective memory complaints: meta-analysis. Acta Psychiatr. Scand. 130: 439–451.
Molinuevo, J.L., Rabin, L.A., Amariglio, R., Buckley, R., Dubois, B., Ellis, K.A., Ewers, M., Hampel, H., Klöppel, S., Rami, L., Reisberg, B., Saykin, A.J., Sikkes, S., Smart, C.M., Snitz, B.E., Sperling, R., van der Flier, W.M., Wagner, M., and Jessen, F. (2017). Implementation of subjective cognitive decline criteria in research studies. Alzheimers Dement. 13: 296–311.
Morishima, S., Kawada, Y., Fukushima, Y., Takagi, T., Naito, Y., and Inoue, R. (2023). A randomized, double-blinded study evaluating effect of matcha green tea on human fecal microbiota. J. Clin. Biochem. Nutr. 72: 165–170.
Morita, A., and Tuji, M. (2002). Nitrate and oxalate contents of tea plants (Camellia sinensis L.) with special reference to types of green tea and effect of shading. Soil Sci. Plant Nutr. 48: 547–553.
Nasreddine, Z.S., Phillips, N.A., Bédirian, V., Charbonneau, S., Whitehead, V., Collin, I., Cummings, J.L., and Chertkow, H. (2005). The Montreal Cognitive Assessment, MoCA: A brief screening tool for mild cognitive impairment. J. Am. Geriatr. Soc. 53: 695–699.
Nishino, K., Nishida, A., Inoue, R., Kawada, Y., Ohno, M., Sakai, S., Inatomi, O., Bamba, S., Sugimoto, M., Kawahara, M., Naito, Y., and Andoh, A. (2018). Analysis of endoscopic brush samples identified mucosa-associated dysbiosis in inflammatory bowel disease. J. Gastroenterol. 53: 95–106.
Nouchi, R., Suiko, T., Kimura, E., Takenaka, H., Murakoshi, M., Uchiyama, A., Aono, M., and Kawashima, R. (2020). Effects of lutein and astaxanthin intake on the improvement of cognitive functions among healthy adults: A systematic review of randomized controlled trials. Nutrients 12: 617.
Paulus, R., Roth, A., Titus, L., Chen, R., Bridges, M.C., and Woodyard, S. (2015). Impact of various caffeine vehicles on mood and cognitive, neurological and physiological functions over five hours. Ohio J. Sci. 115: 12–23.
Pietschnig, J., Aigner-Wöber, R., Reischenböck, N., Kryspin-Exner, I., Moser, D., Klug, S., Auff, E., Dal-Bianco, P., Pusswald, G., and Lehrner, J. (2016). Facial emotion recognition in patients with subjective cognitive decline and mild cognitive impairment. Int. Psychogeriatr. 28: 477–485.
Pike, K.E., Cavuoto, M.G., Li, L., Wright, B.J., and Kinsella, G.J. (2022). Subjective cognitive decline: Level of risk for future dementia and mild cognitive impairment, a meta-analysis of longitudinal studies. Neuropsychol Rev. 32: 703–735.
Presse, N., Belleville, S., Gaudreau, P., Greenwood, C.E., Kergoat, M.-J., Morais, J.A., Payette, H., Shatenstein, B., and Ferland, G. (2013). Vitamin K status and cognitive function in healthy older adults. Neurobiol. Aging 34: 2777–2783.
Repass, J. (2018). Replication study: Fusobacterium nucleatum infection is prevalent in human colorectal carcinoma. Elife 7: e25801.
Ritchie, K., Carrière, I., Mendonca, A.d.e., Portet, F., Dartigues, J.F., Rouaud, O., Barberger-Gateau, P., and Ancelin, M.L. (2007). The neuroprotective effects of caffeine: A prospective population study (the Three City Study). Neurology 69: 536–545.
Ruan, J., Haerdter, R., and Gerendás, J. (2010). Impact of nitrogen supply on carbon/nitrogen allocation: A case study on amino acids and cat-

echins in green tea Camellia sinensis (L.) O. Kuntze plants. Plant. Biol (Stuttg.) 12: 724–734.
Sabia, S., Fayosse, A., Dumurgier, J., van Hees, V.T., Paquet, C., Sommerlad, A., Kivimäki, M., Dugravot, A., and Singh-Manoux, A. (2021). Association of sleep duration in middle and old age with incidence of dementia. Nat. Commun. 12: 2289.
Sakurai, K., Shen, C., Ezaki, Y., Inamura, N., Fukushima, Y., Masuoka, N., and Hisatsune, T. (2020). Effects of matcha green tea powder on cognitive functions of community-dwelling elderly individuals. Nutrients 12: 3639.
Scholey, A., Downey, L.A., Ciorciari, J., Pipingas, A., Nolidin, K., Finn, M., Wines, M., Catchlove, S., Terrens, A., Barlow, E., Gordon, L., and Stough, C. (2012). Acute neurocognitive effects of epigallocatechin gallate (EGCG). Appetite 58: 767–770.
Shibata, S., Noguchi-Shinohara, M., Shima, A., Ozaki, T., Usui, Y., Taki, Y., Uchida, K., Honda, T., Hata, J., Ohara, T., Mikami, T., Maeda, T., Mimura, M., Nakashima, K., Iga, J., Takebayashi, M., Ninomiya, T., and Ono, K. (2025). Green tea consumption and cerebral white matter lesions in community-dwelling older adults without dementia. NPJ Sci. Food 9: 2.
Shokri-Kojori, E., Wang, G.-J., Wiers, C.E., Demiral, S.B., Guo, M., Kim, S.W., Lindgren, E., Ramirez, V., Zehra, A., Freeman, C., Miller, G., Manza, P., Srivastava, T., De Santi, S., Tomasi, D., Benveniste, H., and Volkow, N.D. (2018). β-Amyloid accumulation in the human brain after one night of sleep deprivation. Proc. Natl. Acad. Sci. U S A 115: 4483–4488.
Sokary, S., Al-Asmakh, M., Zakaria, Z., and Bawadi, H. (2023). The therapeutic potential of matcha tea: A critical review on human and animal studies. Curr. Res. Food Sci. 6: 100396.
Sun, J., Kang, J., Wang, P., and Zeng, H. (2013). Self-relaxation training can improve sleep quality and cognitive functions in the older: A one-year randomised controlled trial. J. Clin. Nurs. 22: 1270–1280.
Surak, K. (2012). Making tea, making Japan: Cultural nationalism in practice. Stanford University Press, Stanford, CA.
Uchida, K., Meno, K., Korenaga, T., Liu, S., Suzuki, H., Baba, Y., Tagata, C., Araki, Y., Tsunemi, S., Aso, K., Inagaki, S., Nakagawa, S., Kobayashi, M., Kakuma, T., Asada, T., Ota, M., Takihara, T., and Arai, T. (2024). Effect of matcha green tea on cognitive functions and sleep quality in older adults with cognitive decline: A randomized controlled study over 12 months. PLoS One 19: e0309287.
Ullah, F., Ali, T., Ullah, N., and Kim, M.O. (2015). Caffeine prevents d-galactose-induced cognitive deficits, oxidative stress, neuroinflammation and neurodegeneration in the adult rat brain. Neurochem. Int. 90: 114–124.
Unno, K., Furushima, D., Hamamoto, S., Iguchi, K., Yamada, H., Morita, A., Horie, H., and Nakamura, Y. (2018). Stress-reducing function of matcha green tea in animal experiments and clinical trials. Nutrients 10: 1468.
Unno, K., Furushima, D., Hamamoto, S., Iguchi, K., Yamada, H., Morita, A., Pervin, M., and Nakamura, Y. (2019). Stress-reducing effect of cookies containing matcha green tea: Essential ratio among theanine, arginine, caffeine and epigallocatechin gallate. Heliyon 5: e01653.
Unno, K., Hara, A., Nakagawa, A., Iguchi, K., Ohshio, M., Morita, A., and Nakamura, Y. (2016). Anti-stress effects of drinking green tea with lowered caffeine and enriched theanine, epigallocatechin and arginine on psychosocial stress induced adrenal hypertrophy in mice. Phytomedicine 23: 1365–1374.
Unno, K., Iguchi, K., Tanida, N., Fujitani, K., Takamori, N., Yamamoto, H., Ishii, N., Nagano, H., Nagashima, T., Hara, A., Shimoi, K., and Hoshino, M. (2013). Ingestion of theanine, an amino acid in tea, suppresses psychosocial stress in mice. Exp. Physiol. 98: 290–303.
Unno, K., Pervin, M., Taguchi, K., Konishi, T., and Nakamura, Y. (2020). Green tea catechins trigger immediate-early genes in the hippocampus and prevent cognitive decline and lifespan shortening. Molecules 25: 1484.
Valverde-Salazar, V., Ruiz-Gabarre, D., and García-Escudero, V. (2023). Alzheimer's disease and green tea: Epigallocatechin-3-gallate as a modulator of inflammation and oxidative stress. Antioxidants (Basel) 12: 1460.
van der Helm, E., Gujar, N., and Walker, M.P. (2010). Sleep deprivation impairs the accurate recognition of human emotions. Sleep 33: 335–342.
van Stegeren, A., Rohleder, N., Everaerd, W., and Wolf, O.T. (2006). Salivary alpha amylase as marker for adrenergic activity during stress: Effect of betablockade. Psychoneuroendocrinology 31: 137–141.
Virtanen, M., Singh-Manoux, A., Batty, G.D., Ebmeier, K.P., Jokela, M., Harmer, C.J., and Kivimäki, M. (2017). The level of cognitive function and recognition of emotions in older adults. PLoS One 12: e0185513.
Wang, L., Brennan, M., Li, S., Zhao, H., Lange, K.W., and Brennan, C. (2022). How does the tea L-theanine buffer stress and anxiety. Food Sci. Hum. Wellness 11: 467–475.
Wechsler, D. (2010). The Wechsler Memory Scale. 4th ed. Pearson Assessments, London, UK.
Weiss, D.J., and Anderton, C.R. (2003). Determination of catechins in matcha green tea by micellar electrokinetic chromatography. J. Chromatogr. A 1011: 173–180.
Weiss, E.M., Kohler, C.G., Vonbank, J., Stadelmann, E., Kemmler, G., Hinterhuber, H., and Marksteiner, J. (2008). Impairment in emotion recognition abilities in patients with mild cognitive impairment, early and moderate Alzheimer disease compared with healthy comparison subjects. Am. J. Geriatr. Psychiatry 16: 974–980.
Wesnes, K. (2002). Assessing cognitive function in clinical trials: latest developments and future directions. Drug Discov. Today 7: 29–35.
Wesnes, K. (2003). The Cognitive Drug Research computerised assessment system: Application to clinical trials. In: de Deyn, P.P., Thiery, E., and D'Hooge, R. (Ed.). Memory: Basic concepts, disorders and treatment. Uitgeverij Acco, pp. 453–472.
Xu, L., Jiang, C.Q., Lam, T.H., Liu, B., Jin, Y.L., Zhu, T., Zhang, W.S., Cheng, K.K., and Thomas, G.N. (2011). Short or long sleep duration is associated with memory impairment in older Chinese: The Guangzhou Biobank Cohort Study. Sleep 34: 575–580.
Yaffe, K., Falvey, C.M., and Hoang, T. (2014). Connections between sleep and cognition in older adults. Lancet Neurol. 13: 1017–1028.
Yoshida, H., Inuzuka, M., Fuchinoue, H., Shimoda, M., Nomura, S., and Watanabe, H. (1959). Fundamental studies on the production of tea leaves for kabusecha (part 1). The influences of shade on the biological conditions of tea leaves (in Japanese). Tea Ind. Res. Rep. 13: 30–38.
Zhang, R., Ding, N., Feng, X., and Liao, W. (2025). The gut microbiome, immune modulation, and cognitive decline: Insights on the gut-brain axis. Front. Immunol. 16: 1529958.
Zhang, Y., Liu, Y., Li, Y., Li, Y., Gu, X., Kang, J.H., Eliassen, A.H., Wang, M., Rimm, E.B., Willett, W.C., Hu, F.B., Stampfer, M.J., and Wang, D.D. (2026). Coffee and tea intake, dementia risk, and cognitive function. JAMA 335: 961–974.

Journal of Food Bioactives
International Society for Nutraceuticals and Functional Foods
Review
J. Food Bioact. 2026;35:12–23

Microbial biotransformation of plant-derived bioactive compounds: structural modifications, enhanced bioavailability, and functional food applications

Ying Ni[a,b,c,d], Wensheng Zhang[a,b,c,d*], Yao Sun[a,b,c,d], Zhengyong Yu[a,b,c,d] and Youhua Xu[e]

[a]Beijing Key Laboratory of Intelligent Innovation and Application for the Whole Industry Chain of TCM Nutrition and Health, Beijing Normal University, Beijing 100875, China
[b]Engineering Research Center of Natural Medicine, Ministry of Education, Beijing Normal University, Zhuhai, 519087, China
[c]Guangdong Provincial Observation and Research Station for Coupled Human and Natural Systems in Land-ocean Interaction Zone, Beijing Normal University, Zhuhai 519087, China
[d]Faculty of Arts and Sciences, Beijing Normal University, Zhuhai, 519087, China
[e]Faculty of Chinese Medicine, Macau University of Science and Technology, Macao SAR, PR China
[*]**Corresponding author:** Wensheng Zhang, Beijing Key Laboratory of Intelligent Innovation and Application for the Whole Industry Chain of TCM Nutrition and Health, Beijing Normal University, Beijing 100875, China. E-mail: zws@bnu.edu.cn
DOI: 10.26599/JFB.2026.95035452
Received: August 14, 2026; **Revised received & accepted:** September 02, 2026
Citation: Ni, Y., Zhang, W., Sun, Y., Yu, Z., and Xu, Y. (2026). Microbial biotransformation of plant-derived bioactive compounds: structural modifications, enhanced bioavailability, and functional food applications. J. Food Bioact. 35: 12–23.

Abstract

Plant-derived bioactive compounds, including polyphenols, polysaccharides, alkaloids, terpenoids/saponins, lignans and glucosinolates, are widely valued for their health-promoting potential, yet poor bioavailability and, in several cases, biological inactivity in native form limit their translation into functional food ingredients. Microbial biotransformation, carried out by naturally occurring gut microbiota, food-fermentation microorganisms and plant-associated endophytic fungi, offers a means of overcoming these limitations through mild, highly selective enzymatic modification. This review synthesizes current evidence on microbial biotransformation across five major classes of plant bioactive compounds, examining the natural microbial sources involved, the core enzymatic mechanisms, including glycosidases, esterases, oxidoreductases, decarboxylases and demethylases, responsible for these conversions, and the resulting changes in bioavailability and bioactivity for each compound class. Beyond the compound-specific discussion, we identify a smaller set of structural modifications, namely deglycosylation, molecular weight reduction, hydroxylation, demethylation, ring cleavage and decarboxylation, that recur across otherwise unrelated compound classes and account for much of the functional benefit associated with microbial processing. We discuss current applications in fermented functional foods and postbiotics, together with the principal obstacles, including strain stability, substrate specificity in complex matrices, and regulatory characterization, that constrain industrial-scale deployment, and outline multi-omics-guided and precision-fermentation strategies likely to shape future progress in this field.

Keywords: Microbial biotransformation; Gut microbiota; Plant bioactive compounds; Bioavailability; Structure-activity relationship; Functional food.

© The author(s) 2026. Publishing Services by Tsinghua University Press
The articles published in this open access journal are distributed under the terms of the Creative Commons Attribution 4.0 International License (http://creativecommons.org/licenses/by/4.0/)

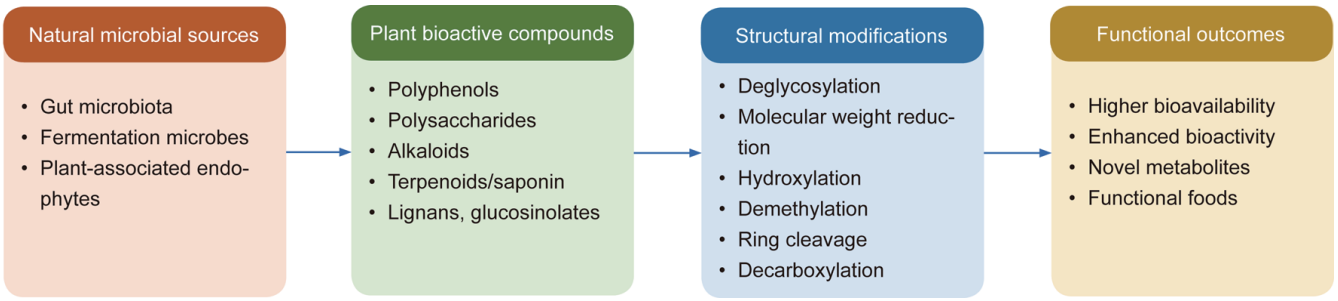


Figure 1. Conceptual framework of this review.

1.. Introduction

Plant-derived bioactive compounds have long occupied a central place in the search for functional food ingredients and nutraceuticals. More than 25,000 phytonutrients have so far been identified across fruits, vegetables and other plant-based foods, spanning polyphenols, flavonoids, isoflavones, carotenoids, phenolic acids, lignans, saponins and related classes, and a substantial body of evidence links these molecules to antioxidant, anti-inflammatory, antimicrobial and metabolic benefits(Tufail et al., 2025). Yet the translation of this chemical richness into reliable physiological effect is far from straightforward. Many bioactive food compounds are poorly absorbed: relative urinary excretion of ingested polyphenols, a compound-specific measure of overall systemic bioavailability, has been reported to range from as little as 0.3% to 43% depending on the specific polyphenol, reflecting the enormous structure-dependent variability in this class(Manach et al., 2005; Rein et al., 2013). It is this factor that has pushed researchers toward strategies capable of modifying these compounds before, or as, they reach systemic circulation.

Several approaches exist for tackling this limitation,including nanoencapsulation, chemical derivatization and physical processing, but each carries its own drawbacks. Chemical modification typically requires harsh reagents and generates by-products that complicate downstream purification for food-grade use (Giri et al., 2021); nanocarrier systems improve delivery but add cost and, in some cases, raise unresolved questions about nanoparticle safety (Tong et al., 2022; Ke et al., 2024). Because microbial biotransformation relies on the catalytic machinery already present in living cells, it tends to proceed under mild aqueous conditions, with a degree of regio- and stereoselectivity that is difficult to replicate synthetically (Qin and Dong, 2023). This enzymatic selectivity allows the generation of derivatives with specific structural features important for optimizing potency or improving metabolic stability, while microbial transformation also offers a more practical and cost-effective route than conventional chemical synthesis, since the reactions proceed under mild conditions in aqueous environments without the need for complex synthetic methodology(Qin and Dong, 2023; Rustamova et al., 2024). For an industry under pressure to deliver “clean label” ingredients, this matters as much as the chemistry itself.

The conversation around microbial biotransformation of plant compounds has, for the most part, developed along separate and rarely intersecting tracks. One body of work concerns the human gut microbiota and the metabolites it generates from dietary polyphenols and saponins as they pass through the colon (Mithul Aravind et al., 2021; Chen et al., 2022). A second, literature deals with food fermentation microbes (lactic acid bacteria, yeasts, Aspergillus and Rhizopus species) employed deliberately to modify raw plant material during processing(Cheng et al., 2025). A third, the key focus is on the plant-associated microorganisms themselves: endophytic fungi and rhizosphere bacteria that, through long co-evolution with their hosts, have acquired biotransformation capabilities of striking specificity (Orozco-Mosqueda and Santoyo, 2021). Owing to prolonged co-evolution with host plants, endophytic fungi have developed distinctive biotransformation abilities that can substantially affect the synthesis and breakdown of plant secondary metabolites, including flavonoids, polysaccharides and terpenes (Liu et al., 2021). These three groups are rarely discussed together, despite acting on overlapping pools of substrates through frequently overlapping enzymatic mechanisms.

Therefore, our review covers five major classes of plant bioactive compounds, including polysaccharides, polyphenols, alkaloids, terpenoids/saponins, and a smaller group comprising lignans, glucosinolates and other glycosides (Figure 1). A key research question is accordingly proposed: what structural changes does microbial transformation actually impose, and do these changes follow any recognizable pattern regardless of which compound class is involved?

2. Natural microbial sources and key biotransformation mechanisms

2.1. Sources of natural microorganisms

The human colon harbours a dense and metabolically versatile microbial community capable of acting on plant compounds that escape upper gastrointestinal digestion (Ruan et al., 2020). Gut microbes including Escherichia coli, Bifidobacterium, Eubacterium, Lactobacillus, Bacteroides and Streptococcus participate in the biotransformation of natural products, generating metabolites that are often more readily absorbed and pharmacologically active than their parent compounds (Zhao et al., 2022). A second distinct group consists of the organisms deliberately employed in food processing, including lactic acid bacteria represented by Lactobacillus plantarum and L. acidophilus, yeasts, and filamentous fungi including Aspergillus niger and Rhizopus species (Li et al., 2020a; Akpoghelie et al., 2025). These are not incidental passengers but selected biocatalysts, often chosen precisely for an enzymatic profile suited to a given substrate. Lactobacillus acidophilus, for instance, grows on mono- and diglucosyl dietary plant glycosides bearing small aromatic aglycones, using phosphotransferase system transporters together with phospho-β-glucosidases to take up and deglucosylate these compounds before externalizing the resulting bioactive aglycones (Theilmann et al., 2017). The distinction between this group and gut microbiota is partly artificial,

but the deliberate, controllable nature of fermentation makes it the more tractable system for food-industry application.

Endophytic fungi and rhizosphere bacteria form the third source. Having coexisted with their host plants over evolutionary time, these organisms have often evolved enzyme systems tailored to the specific phytochemicals their hosts produce (Huang and Wang, 2026). Increased understanding of the interactions between endophytic fungi and plants has led to the discovery of new chemical compounds and processes, with endophytes capable of degrading or modifying not only inorganic and organic small molecules but also a wide range of plant secondary metabolites (Aishwarya et al., 2025). One frequently cited illustration involves Fusarium sp. C39, an endophyte isolated from Dioscorea nipponica, which has been shown to biotransform the steroidal saponins of the host rhizome and increase diosgenin content through a fermentation process involving glycolytic cleavage, ring closure, dehydrogenation and carbonylation reactions (Huang et al., 2022). A 2020 analysis of patent filings identified 245 patents covering secondary-metabolite production or biotransformation applications of endophytic fungi, spanning pharmaceutical, agricultural and food uses, underscoring the scale of applied interest in this microbial source (Torres-Mendoza et al., 2020). Endophytic fungi additionally offer something the other two sources cannot easily provide: a documented capacity for genuinely novel chemistry, positioning them as promising biocatalysts for green-chemistry-oriented synthesis of new structural analogues and pharmaceutical intermediates, rather than predictable hydrolysis of existing structures (Choudhary et al., 2021).

2.2. Core enzymatic mechanisms

Despite their ecological differences, the three microbial groups described above rely on a surprisingly compact set of enzymatic tools.

Glycosidases, principally β-glucosidases and β-glucuronidases, are perhaps the most consequential of these (Stathaki et al., 2024). Most plant polyphenols, saponins and many alkaloids occur naturally as glycosides, with one or more sugar moieties attached to a lipophilic aglycone core (Bhambhani et al., 2021; El-Saadony et al., 2024; Fordos et al., 2025). The hydrolysis of these glycosidic bonds by microbial β-glucosidases and related glycosidases releases polyphenol aglycones that are more lipophilic and, in most cases, more bioactive than their glycosylated precursors, since the attached sugars otherwise hinder absorption across the gastrointestinal epithelium (Palafox-Carlos et al., 2011; Saric and Sivamani, 2016). The same logic extends well beyond polyphenols: β-glucuronidase from E. coli HGU-3 hydrolyzes baicalin to yield baicalein, while β-glucosidase produced by Eubacterium L-8 and β-glucuronidase from Streptococcus LJ-22 convert glycyrrhizin into 18β-glycyrrhetinic acid, illustrating how a single enzymatic mechanism operates across structurally unrelated compound classes (Son et al., 2021; Zhao et al., 2022; Hsu et al., 2023). Esterases and tannases perform a complementary role, releasing phenolic acids that would otherwise remain bound to cell-wall polysaccharides or esterified to other phenolics (Yang et al., 2023). Feruloyl esterases produced by Bifidobacterium animalis, Lactobacillus reuteri, L. helveticus and L. fermentum hydrolyze chlorogenic acid to liberate caffeic acid, a reaction with direct consequences for antioxidant capacity, since the freed phenolic acid is generally more reactive than its esterified form (Raimondi et al., 2015; Song and Baik, 2017; Aguirre Santos et al., 2018; Rogozinska et al., 2021; Balaj et al., 2022).

Beyond hydrolysis, oxidoreductases—including cytochrome P450 monooxygenases in fungi and various dehydrogenases in bacteria—carry out hydroxylation, dehydrogenation and ring-opening reactions that hydrolytic enzymes alone cannot achieve (Lu et al., 2019; Qin et al., 2022; Hilberath et al., 2025). For example, gradually converting the main ginsenosides into rarer forms with higher biological activity, and fungi hydroxylating the terpene skeleton at positions where it is difficult to have selective effects in chemical synthesis (Li et al., 2023a,b; Gao et al., 2024). Such microbial biotransformations, with their improved selectivity, stability and enantiomeric purity, align closely with the broader goals of green chemistry, offering an eco-friendly alternative to conventional organic synthesis for generating structurally novel molecules (Kuriata-Adamusiak et al., 2012a). In addition, a smaller but practically important set of enzymes—decarboxylases and demethylases—acts on phenolic acids and alkaloids respectively, removing carboxyl or methyl groups to alter both stability and receptor-binding behavior (Hu et al., 2020; Deng et al., 2024). Although less broadly distributed than glycosidases, these enzymes feature prominently in several of the compound-class discussions that follow, particularly where alkaloid detoxification is concerned.

3. Biotransformation of components

3.1. Biotransformation of polyphenols

In functional food research, polyphenols are among the most extensively characterized classes of plant bioactive compounds, yet their translation from cell-culture observations to reliable in vivo effects has proved stubbornly difficult (de Araújo et al., 2021). A central reason is their uneven absorption. Only around 5–10% of ingested polyphenols are absorbed intact in the proximal gastrointestinal tract as native compounds — a narrower, absorption-site-specific metric distinct from the compound-specific relative urinary excretion range (0.3–43%) noted in the Introduction, which additionally captures metabolites generated after colonic microbial processing (Manach et al., 2005; Liu et al., 2024a). The majority of ingested polyphenol mass therefore passes into the colon, where it undergoes extensive biotransformation by resident microbiota to generate secondary metabolites that often reach substantially higher plasma concentrations and display superior pharmacokinetic profiles compared with the parent compounds (Jiang et al., 2026). From this perspective, the colon microbiota is not merely a bystander in polyphenol metabolism but the primary determinant of what ultimately reaches systemic circulation.

Among the various polyphenol subclasses, free phenolic acids such as ferulic, caffeic and gallic acid illustrate the transformation logic most directly. These compounds occur abundantly in cereals, coffee and fruits, but a substantial fraction reaches the colon in esterified or matrix-bound forms rather than as free compounds (Song et al., 2020; Wu et al., 2021). Microbial esterases and feruloyl esterases cleave these bonds, releasing the free phenolic acids that can then be absorbed or further metabolized (Oliveira et al., 2019). The hydrolysis of glycosidic bonds by β-glucosidases and related glycosidases releases polyphenol aglycones that are both more lipophilic and more bioactive than their glycosylated forms, since the attached sugar moieties restrict gastrointestinal uptake (Kroon et al., 2004; Rizzo et al., 2017; Curiel et al., 2024). Fermentation driven by microbial glycosidases, esterases and decarboxylases alters polyphenol chemical structure in ways that improve solubility, stability and antioxidant activity, and the resulting metabolites support gut health partly through promotion of ben-

eficial bacteria such as Lactobacillus and Bifidobacterium while suppressing pathogenic species (Alharbi, 2026).

A parallel and equally well-documented pattern is seen among the flavonoids, where the conversion of glycosidic forms to bioactive aglycones is again the most consequential transformation (Ahn-Jarvis et al., 2017). Intestinal bacteria produce hydrolytic enzymes capable of hydrolyzing natural isoflavone glycosides, releasing unconjugated aglycones such as daidzein and genistein that are more estrogenic and more readily absorbed than their glycosylated precursors (Hur et al., 2000; Intharuksa et al., 2025); deglycosylation is thus a critical determinant of isoflavone absorption, metabolism and biological activity (Marín et al., 2015). Daidzein can be further reduced by anaerobic gut bacteria through a sequence involving dihydrodaidzein and tetrahydrodaidzein intermediates to yield equol, a metabolite with substantially higher affinity for estrogen receptors than any of the precursors (Muthyala et al., 2004; Soukup et al., 2021). Soy isoflavones, particularly daidzein, are metabolized by gut microbes into equol and related bioactive compounds, but only 20–35% of adults consuming a Western diet harbour the microbial consortia capable of producing these metabolites in vivo(Soukup et al., 2023; Zhuo et al., 2026). The individual differences in equol production indicate that the functional outcomes of polyphenol intake are partially dependent on the consumer's microbiota rather than the compounds themselves. In addition, lactic acid bacteria, including Lactobacillus plantarum, Streptococcus thermophilus and Pediococcus pentosus degrade high-molecular-weight procyanidins, breaking down dimers such as procyanidin B2 and B3 while simultaneously increasing concentrations of smaller phenolic metabolites including kaempferol derivatives (Li et al., 2013; Kim et al., 2019). And the structural simplification achieved by fermentation is associated with enhanced antioxidant and probiotic potential (Wen et al., 2023).

Ellagitannins, abundant in pomegranates, walnuts, strawberries and raspberries, are minimally absorbed intact, and their bioavailability as parent compounds is very low (Tomás-Barberán et al., 2017; Zhang et al., 2023a). Specific gut bacteria including Enterocloster bolteae and Parabacteroides gordonii biotransform ellagic acid into urolithins through a sequence of reactions comprising lactone ring cleavage, decarboxylation and progressive dehydroxylation (Leng et al., 2025). The resulting urolithins are s tructurally far simpler than their ellagitannin precursors but are the compounds actually detected in plasma, establishing them as the likely effectors of the health effects attributed to ellagitannin-rich diets (García-Villalba et al., 2022). Antioxidant activity among urolithin derivatives correlates with the number of hydroxyl groups as well as molecular lipophilicity (Li et al., 2024); the most potent antioxidants are urolithins C and D, which outperform the parent ellagic acid and punicalagins in cell-based assays (Bialonska et al., 2009). The progressive dehydroxylation that occurs along the conversion pathway thus represents a structure–activity trade-off: later-stage metabolites such as urolithin A are more readily absorbed but less antioxidant than earlier intermediates, while highly hydroxylated forms are potent but remain poorly bioavailable.

3.2. Biotransformation of polysaccharides

Unlike polyphenols, plant polysaccharides are not typically thought of as compounds that need to be "activated" by microbial transformation. Their bioactivities, including immunomodulation, antioxidant properties and prebiotic effects, are generally attributed to their intact high-molecular-weight structures (Salehi and Rashidinejad, 2025; Cao et al., 2026). Yet there is growing evidence that the structural changes imposed by microbial and enzymatic processing, far from destroying these activities, can selectively amplify them, particularly in the context of gut health (Wang et al., 2019; Cao et al., 2022; Rong et al., 2026).

Microbial enzymes, including cellulases, pectinases, xylanases and amylases produced by gut bacteria and filamentous fungi, depolymerize polysaccharide chains to lower-molecular-weight fractions, with measurable consequences for bioactivity (Rowland et al., 2018; Pant et al., 2022). Enzymatic degradation of Lilium polysaccharide significantly reduced molecular weight through enzymolysis, leading to increased exposure of internal functional groups and altered monosaccharide composition; antioxidant capacity was enhanced by hydrolysis, and the degraded fractions showed distinct prebiotic profiles relative to the parent polysaccharide, tending to promote beneficial bacteria such as Megamonas, Bacteroides and Parabacteroides while the intact polymer inhibited harmful Fusobacterium (Peng et al., 2025). This molecular weight dependence on bioactivity is not uniform, however, and depends on the specific polysaccharide backbone and the assay in question. Fractionation of apple pectin-derived oligosaccharides by molecular weight revealed that the highest-molecular-weight fractions (30–100 kDa) showed superior prebiotic effects on lactobacilli, while intermediate fractions (3–10 kDa and 10–30 kDa) exerted stronger bifidogenic effects and better inhibition of pathogenic bacteria including Escherichia coli and Salmonella enteric (Wilkowska et al., 2025). Therefore, microbial depolymerization is not just about breaking down polysaccharides into smaller and more uniformly active fragments. Instead, it produces a series of products, and the individual biological activities of these products depend on their size, composition, and branching. In addition, microbial biotransformation does not affect polysaccharide molecular weight alone. It can also alter the types and proportions of constituent monosaccharides and the degree of chain branching. Fermentation by lactic acid bacteria and fungi tends to selectively cleave more accessible linkages while leaving resistant branched regions intact, producing modified structures with altered charge density, water-binding capacity and receptor interaction profiles (Wang et al., 2023a; Zhao et al., 2025). Comparison of litchi polysaccharide fractions differing in molecular weight showed that the lower-molecular-weight fraction contained relatively more neutral sugar, arabinose, galactose and rhamnose but less uronic acid; this lower-molecular-weight fraction showed higher solubility, lower viscosity, stronger stimulation of macrophage secretion of pro-inflammatory cytokines and better promotion of beneficial lactobacilli and bifidobacteria (Zou et al., 2023). Whether such structural shifts are universally associated with enhanced activity or simply reflect the liberation of previously inaccessible monosaccharide sequences remains an open question.

At the far end of microbial depolymerization, polysaccharides are broken down into oligosaccharides that selectively feed beneficial gut bacteria and into short-chain fatty acids (SCFAs) such as acetate, propionate and butyrate (Frolova et al., 2022; Wang et al., 2023b). These downstream products are responsible for some of the most documented gut health effects of dietary fiber, yet these SCFA-generating and prebiotic effects are frequently the product of microbial structural modification rather than an intrinsic property of the unmodified plant polysaccharide, since native forms often show comparatively low bioactivity prior to fermentation (Kasubuchi et al., 2015; Wang et al., 2024). The demand for natural value-added products derived from microbial biotransformation is rapidly increasing in both the food and pharmaceutical sectors, with growing scientific focus on microbial bioconversions that produce cost-effective, selective and functionally enriched compounds from natural substrates (Khosroshahi et al., 2025). The conversion of plant polysaccharides to SCFA-generating sub-

strates by microbial fermentation thus represents one of the more direct connections between the topic of this review and functional food outcomes.

3.3. Biotransformation of alkaloids

Whereas the main problem with polyphenols is one of bioavailability, and with polysaccharides one of solubility, alkaloids are often intrinsically bioavailable but present in forms whose pharmacological profiles are shaped in unpredictable ways by first-pass intestinal metabolism (Wang et al., 2017a; Tian et al., 2018). Microbial biotransformation thus plays a dual role here: in some cases improving the efficiency and selectivity of absorption, in others detoxifying compounds whose native structures are associated with cytotoxic or adverse effects.

Among plant alkaloids, berberine has become the paradigmatic example of how gut microbiota can reshape alkaloid pharmacology. Berberine is an isoquinoline alkaloid found in several plants across genera including Berberis and Coptis, and it has documented activity against metabolic syndrome, dyslipidaemia and glucose dysregulation (Li et al., 2020b). Its oral bioavailability in native form, however, is poor (Cui et al., 2024). Higher levels of nitroreductase activity in gut microbiota increase intestinal concentrations of dihydroberberine, a reduced metabolite that is more efficiently absorbed than berberine itself (Feng et al., 2015); this microbial conversion has been associated with improved lipid metabolism outcomes in both rats and humans (Wang et al., 2017b). In addition, berberine also modulates gut microbiota composition, and the metabolic outcomes of berberine supplementation appear to depend substantially on the microbial ecosystem into which it is introduced. Key gut bacteria including Blautia species are involved in the demethylation of berberine to berberrubine and thalifendine, metabolites that may contribute to berberine's effects on gut health alongside SCFA production (Dehau et al., 2023). Therefore, individuals whose gut microbiota are well-equipped to reduce and demethylate berberine may obtain substantially different outcomes from supplementation than those lacking these microbial capabilities.

A structurally distinct but mechanistically separate case involves caffeine and other methylxanthines, among the most widely consumed alkaloids globally (Barone and Roberts, 1996; Gramza-Michałowska et al., 2021). Systemic clearance of caffeine in humans is dominated by hepatic metabolism, with only about 0.5–3.0% of an ingested dose excreted unchanged by the kidneys; hepatic cytochrome P450 1A2 (CYP1A2) accounts for over 90% of the initial N-demethylation steps that convert caffeine to paraxanthine, theobromine and theophylline (Liu and Xu, 2026). Microbial N-demethylation of caffeine and related methylxanthines has, by contrast, been characterized primarily in environmental and food-associated microorganisms rather than in the resident human gut microbiota: soil-derived bacteria such as *Pseudomonas putida* CBB5 sequentially N-demethylate caffeine and theophylline via distinct but convergent pathways terminating in xanthine (Yu et al., 2009), while fungal strains isolated from fermenting Pu-erh tea, including *Aspergillus sydowii*, carry out analogous N-demethylation of theobromine during tea processing (Zhou et al., 2020). Whether the human gut microbiota performs a quantitatively meaningful equivalent of this reaction in vivo remains an open question.

Beyond improving the bioavailability of beneficial alkaloids, microbial biotransformation can also render toxic or irritant alkaloids safer for consumption, a function that is easy to overlook but arguably just as important from a food-safety standpoint. The steroidal glycoalkaloids α-solanine and α-chaconine, which together account for the great majority of glycoalkaloid content in potato tubers (Liu et al., 2024b). Microbial deglycosylation proceeds through sequential removal of the trisaccharide side chain, generating β- and γ-glycoalkaloid intermediates before yielding the aglycone solanidine; this stepwise loss of sugar residues alters the compounds' interaction with cell membranes and correspondingly reduces their cytotoxicity (Wei et al., 2025). The enzymatic basis of this pathway has been resolved in some detail: bacterial isolates such as *Arthrobacter* sp. S41 harbour a dedicated gene cluster encoding the deglycosylating enzymes responsible for complete degradation of both compounds (Hennessy et al., n.d.), while a related enzyme portfolio comprising α-rhamnosidase (RhaA), β-glucosidase (GluA) and β-galactosidase (GalA), drawn from the GH78, GH3 and GH2 glycoside hydrolase families respectively, has been characterized in a gut-associated bacterium of the potato tuber moth and shown to carry out the same stepwise deglycosylation (Wang et al., 2022). Therefore, structural modifications do not all consistently proceed in the direction of enhancing bioactivity. In the case of steroidal glycoalkaloids, the same deglycosylation chemistry that elsewhere increases potency instead serves a protective, detoxifying function.

3.4. Biotransformation of terpenoids and saponins

Terpenoids and saponins represent one of the largest and most structurally diverse groups of plant secondary metabolites, encompassing monoterpenes, sesquiterpenes, diterpenes, triterpenes and steroidal saponins (Câmara et al., 2024). Their biotransformation by natural microorganisms has attracted considerable research interest, partly because the products of microbial transformation are often more potent or more bioavailable than the parent compounds, and partly because bacteria and fungi are capable of chemo-, regio- and stereospecific hydroxylations of complex substrates that are extremely difficult to achieve through conventional chemical synthesis (Cano-Flores et al., 2020). Cytochrome P450 monooxygenase systems in particular confer high catalytic specificity toward the hydroxylation, demethylation and deglycosylation of complex ring structures characteristic of terpenoids and steroidal alkaloids, reactions for which chemical routes generally lack comparable selectivity (Xu et al., 2026).

The ginsenosides of *Panax ginseng* and *P. notoginseng* provide the most extensively studied example of terpenoid biotransformation by food-grade microorganisms. Most ginsenosides are poorly absorbed across the human gastrointestinal tract in their native form, owing to poor intestinal permeability associated with their extensive glycosylation (Dong and Huang, 2025). Protopanaxadiol-type ginsenosides bearing multiple sugar chains, such as Rb1 and Rb2, require deglycosylation by gut or food-fermentation microbiota to generate more absorbable metabolites (Mohanan et al., 2018a; Liu et al., 2026). Microbial β-glucosidases and related hydrolases progressively remove these sugar chains to yield rare ginsenosides, including compound K, Rg3 and Rh2, whose reduced glycosylation confers greater lipophilicity, stronger membrane affinity and substantially enhanced bioactivity relative to their glycosylated precursors (Kim et al., 2022; Liu et al., 2026). Compound K was itself first characterized as a hydrolysate of ginsenosides Rb1, Rb2 and Rc generated by soil bacterial hydrolysis, and was subsequently re-identified as a product of enteric bacterial metabolism of Rb1 and Rb2 in the intestine, a discovery that established the gut microbiota as a physiologically relevant site of ginsenoside transformation (Yang et al., 2015). The directionality of conversion is determined by microbial β-glucosidase specificity: different organisms cleave sugars at distinct positions and in different sequences, meaning that the product spectrum is partly

microbial-species-dependent, and that the metabolic capacity to generate compound K from Rb1 varies considerably between individuals according to their gut microbiota composition (Kim et al., 2013). Fermentation of ginseng with *Aspergillus cristatus* JH-5, a food-safe fungal strain with documented use in tea processing, and resulted in the de novo accumulation of rare ginsenosides Rg3(S) and Rg3(R) to a total content of 0.23% dry weight, compounds entirely undetectable in unfermented ginseng (Su et al., 2026). Rg3 and compound K carry documented antitumour, anti-inflammatory and immunomodulatory properties not shared by the major ginsenosides from which they derive, acting through pathways including PI3K/Akt signalling, caspase-mediated apoptosis and NF-κB inhibition (Yang et al., 2015; Mohanan et al., 2018b; Tang et al., 2021; Zhang et al., 2022; Lee et al., 2025b; Cui et al., 2026). And the key structural difference, reduced glycosylation of the protopanaxadiol or protopanaxatriol skeleton, is precisely the change that microbial β-glucosidases impose (Tran et al., 2023). Laboratory conversion rates reaching 98.19% for Rg3 and 95.89% for Rh2 have been reported, though improving conversion efficiency and reducing production costs remain the primary bottlenecks for industrial-scale manufacture (Xu et al., 2023).

A structurally related but botanically distinct example is found in the steroidal saponins of *Dioscorea* species, principally dioscin, which serve as precursors for the semi-synthesis of diosgenin, a steroidal aglycone that underpins the industrial manufacture of oral contraceptives, corticosteroids and other pharmaceutically important steroid hormones (Mandal et al., 2025; Li et al., 2026). Diosgenin is conventionally liberated from dioscin by concentrated acid hydrolysis, a process that generates substantial acidic effluent and offers only moderate yields; this has driven sustained interest in microbial and enzymatic alternatives capable of cleaving the relevant glycosidic bonds under milder, more selective conditions (Zhang et al., 2023b). Deglycosylation proceeds through sequential removal of the terminal rhamnosyl and glucosyl residues attached to the diosgenin core, a two-step mechanism resolved in molecular detail in the endophytic fungus *Talaromyces stollii* CLY-6, whose genome encodes a dedicated α-L-rhamnosidase that hydrolyzes the terminal rhamnoside followed by a β-D-glucosidase that releases the residual glucose units (Cheng et al., 2021). Endophytic and related fungi isolated from *Dioscorea* tissue have proved particularly effective biocatalysts for this transformation: *Penicillium dioscin* achieves diosgenin yields exceeding 90% through direct solid-state biotransformation of *Dioscorea zingiberensis* rhizome (Dong et al., 2015), while *Fusarium* sp. C39, an endophyte isolated specifically from *Dioscorea nipponica*, has been shown to substantially increase diosgenin content through fermentation of the host rhizome (Huang et al., 2022).

Moving from triterpenoid and steroidal saponins to the volatile terpene classes, fungal and bacterial biotransformation of monoterpene and sesquiterpene skeletons represent a category of reaction with the regio- and stereoselectivity achievable by microbial oxidoreductase systems. Stereoselective hydroxylation, epoxidation, Baeyer–Villiger oxidation, and stereo- and enantioselective reduction of ketones to secondary alcohols have been documented as a standard toolkit of green chemistry for the synthesis of chiral terpenoid derivatives not readily accessible through conventional organic synthesis (Kuriata-Adamusiak et al., 2012a). Pinene, an inexpensive and abundant monoterpene substrate, illustrates the practical scope of this approach: fungal, yeast and bacterial isolates from citrus residues have been used to convert α-pinene into verbenol, while plant cell cultures of *Rauvolfia sellowii* achieve enantiomerically enriched verbenone from both (–)- and (+)-α-pinene enantiomers with moderate yields (Neves et al., 2026). Within the p-menthane monoterpene series, the regio- and enantioselectivity of microbial Baeyer–Villiger oxidation has been attributed to the specific orientation of the substrate's isopropyl group within the enzyme active site, while yeast strains such as *Hormonema* sp. are capable of stereoselective reduction of the carbonyl group in menthone, illustrating the fine stereochemical control achievable by whole-cell biocatalysts that has no straightforward synthetic parallel (Grabarczyk et al., 2020).

3.5. Other plant components: lignans, glucosinolates and glycosides

Plant lignans occur predominantly as glycosidic conjugates in seeds, whole grains and some vegetables, with flaxseed representing the richest single dietary source, containing lignan precursor levels 75- to 800-fold higher than any other plant food (Mareai, 2011). Their conversion to bioactive mammalian lignans requires the concerted, sequential action of several distinct gut bacterial species, each responsible for a discrete step in the pathway. After ingestion, secoisolariciresinol diglucoside (SDG) is first deglycosylated to its aglycone, secoisolariciresinol (SECO); this initial step has been attributed to strains of *Bacteroides distasonis*, *B. fragilis*, *B. ovatus* and *Clostridium cocleatum* (Clavel et al., 2006). SECO is then demethylated, a reaction catalysed by strains including *Peptostreptococcus productus*, *Eubacterium callanderi* and *Eubacterium limosum* (Clavel et al., 2006). Before undergoing dehydroxylation by *Clostridium scindens* and *Eggerthella lenta* to yield enterodiol, which is subsequently oxidized to enterolactone (Wang et al., 2000). Both enterodiol and enterolactone can undergo further phase I and phase II biotransformation, with extensive formation of glucuronide and sulfate conjugates prior to systemic circulation (Patel et al., 2012). The health significance of this multi-step pathway rests on the fact that it is enterolactone and enterodiol, not the parent SDG, that reach the bloodstream and exert the antioxidative, antitumour and estrogenic or anti-estrogenic activities associated with flaxseed consumption (Bowers et al., 2019). The microbial metabolic pathway from SDG through enterodiol to enterolactone is thus the route by which the health benefits of flaxseed lignan intake are actually delivered to the host (Zhu et al., 2024). The capacity to complete this multi-step conversion efficiently varies substantially between individuals according to gut microbiota composition, since the pathway depends on the co-occurrence of functionally distinct bacterial guilds rather than on any single organism.

Glucosinolates, which are present in cruciferous vegetables, mainly exist in the form of biologically inert precursors until they are hydrolyzed (Nguyen et al., 2020). Plant myrosinase ordinarily performs this hydrolysis upon cell disruption (Lv et al., 2022). However, cooking inactivates the plant enzyme, and because mammals themselves lack any endogenous myrosinase-like activity, glucosinolates that survive food processing transit to the large intestine largely intact, where their fate depends entirely on resident microbial enzymes (Marshall et al., 2023). Gut bacteria possessing myrosinase-like activity, demonstrated experimentally using germ-free and gnotobiotic animal models as well as characterized pure cultures including *Lactobacillus* strain LEM220, hydrolyze these intact glucosinolates to release isothiocyanates that are then absorbed across the intestinal epithelium (Narbad and Rossiter, 2018). The bioactive isothiocyanates generated through this pathway, principally sulforaphane, act through the Keap1–Nrf2 signalling axis alongside PI3K/AKT/mTOR and NF-κB pathways to activate phase II detoxification enzymes, and have documented chemopreventive properties across multiple cancer cell models (Polozsányi et al., 2024).

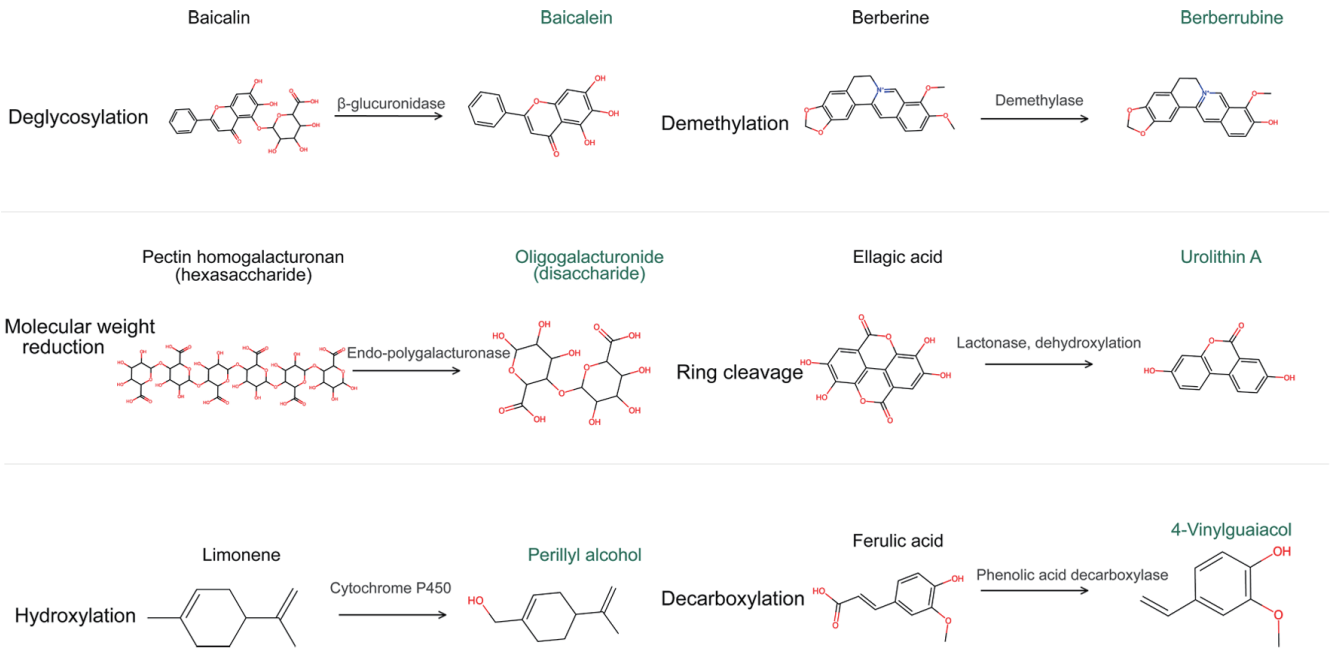


Figure 2. Representative examples of the major structural-modification archetypes described in this review.

3.6. Cross-cutting structural patterns and their functional consequences

The compound classes reviewed above—polyphenols, polysaccharides, alkaloids, terpenoids and saponins, lignans and glucosinolates—undergo transformations that appear specific to each substrate: ring opening in flavonoids, depolymerization in polysaccharides, N-demethylation in alkaloids, sequential deglycosylation in saponins and lignans (Figure 2). Existing treatments of microbial biotransformation typically address these classes separately, either as dedicated reviews of a single compound category or as multi-class surveys organized class by class without a unifying structural framework (Mutafova et al., 2016). This section instead identifies the smaller set of structural operations that recur across classes and summarizes their functional consequences in a single comparative table (Table 1).

Removal of sugar moieties by β-glucosidases, β-glucuronidases and related glycoside hydrolases is the most broadly distributed of these operations, occurring in polyphenol glycosides, isoflavone glucosides, ginsenosides, plant lignans, glucosinolates and steroidal saponins. The resulting aglycone is consistently more lipophilic and more readily transported across intestinal epithelial membranes than its glycosylated precursor, which accounts for the frequent association between deglycosylation and improved bioavailability; the enzymes and positional specificity involved differ by substrate, and this determines whether a product simply becomes easier to absorb or acquires additional, qualitatively different activity. Molecular weight reduction plays an analogous role for polysaccharides and for condensed polyphenols such as procyanidins and tannins, where depolymerization to intermediate oligomeric fractions tends to produce material with more favorable biological properties than either the intact polymer or fully hydrolyzed monomers. Chain length therefore functions as a structural

Table 1. Recurring structural modifications and their functional consequences across compound classes

Structural modification	Compound classes	Representative enzymes	Functional consequence
Deglycosylation	Polyphenols, saponins, alkaloids, lignans, glucosinolates	β-glucosidase, β-glucuronidase, glycoside hydrolase	Increased bioavailability and lipophilicity; altered bioactivity
Molecular weight reduction	Polysaccharides, condensed tannins, procyanidins	Cellulase, pectinase, xylanase, tannase	Increased solubility; altered prebiotic and immunomodulatory activity
Hydroxylation	Terpenoids, phenolic acids	Cytochrome P450, hydroxylase	Increased antioxidant capacity and receptor specificity
Demethylation	Alkaloids, lignans	Demethylase, reductase	Altered bioactivity, estrogenic or metabolic profile
Ring cleavage/fission	Flavonoids, tannins, lignans	Reductase, lyase, decarboxylase	Novel metabolite scaffolds (urolithins, enterolactone, equol)
Decarboxylation	Phenolic acids	Phenolic acid decarboxylase	Altered antioxidant stability, volatility and flavour

variable in its own right, separate from monomer composition. A further category involves modification of the carbon skeleton itself. Cytochrome P450-mediated hydroxylation, documented in terpenoid and phenolic acid biotransformation, alters receptor-binding geometry and metabolic stability. Bacterial demethylation, observed in alkaloids such as berberine and in lignan intermediates en route to enterolactone, removes methyl groups that would otherwise hinder receptor engagement. Ring fission, illustrated by the conversion of ellagitannins to urolithins, generates metabolites structurally unrelated to the parent compound.

A separate observation concerns the dependence of these transformations on microbiota composition rather than on the compound alone. Equol production from daidzein is limited to individuals whose gut microbiota include the requisite bacterial consortium, reported at 20–35% of adults on a Western diet (Zhuo et al., 2026). Urolithin metabotypes classify individuals by which urolithin species their microbiota generate from the same ellagitannin intake, with a subset producing none (García-Villalba et al., 2022). For example, enterolactone yield from SDG shows comparable dependence on specific bacterial taxa at each pathway step.

4. Applications and limitations

Fermentation of plant material with defined starter cultures, rather than reliance on gut microbial action after ingestion, allows the bioactive metabolites described in this review to be generated during processing, reducing dependence on the consumer's own microbiota. Fermentation pathways differ by microbial platform: lactic acid bacteria are the most commonly applied organisms owing to their established safety record and enzymatic capacity, while yeasts and filamentous fungi are used where more extensive restructuring of the plant matrix is required (Travičić et al., 2026). The resulting preparations, characterized as postbiotics when their activity does not depend on live cell viability, are more readily standardized and evaluated for regulatory approval than products relying on live cultures. A related strategy pairs substrate selection with the deliberate choice of microbial strain to target a specific transformation product, as in the use of *Aspergillus cristatus* for rare ginsenoside production or specific bacterial isolates for lignan conversion in fermented flaxseed (Zhu et al., 2024; Su et al., 2026). Demand for such targeted bioconversion products is increasing in both the food and pharmaceutical sectors (Khosroshahi et al., 2025).

Several recent examples illustrate the transition from laboratory-scale biotransformation to industrially relevant production. For rare ginsenoside compound K, an engineered *Pichia pastoris* strain displaying a surface-anchored *Sulfolobus solfataricus* β-glucosidase achieved a 93.8% bioconversion rate and a titer of 6.42 mg/mL following fermentation optimization that increased enzyme activity by 58.9% over the parent strain (Luo et al., 2026). A complementary process combining *Aspergillus tubingensis* fermentation with commercial cellulase reached 8.06 g/L (13.0 mM) compound K after 168 h at a productivity of 48 mg/L/h — a 2.0-fold increase in titer and 1.7-fold increase in productivity over conventional fermentation alone (Lee et al., 2025a). For ginsenosides Rh2 and Rg3, a metabolically engineered *Saccharomyces cerevisiae* strain carrying the full biosynthetic pathway achieved approximately 300 mg/L Rh2 in a 5-L fed-batch bioreactor (Wang et al., 2015), while a related engineered yeast platform reached 3.4 g/L of a glycosylated ginsenoside analogue in a 3-L bioreactor, though product adhesion to the bioreactor wall was identified as a specific engineering obstacle requiring further process optimization (Sun et al., 2026). For urolithin A, industrial translation has progressed furthest among the compounds discussed in this review. Amazentis's branded ingredient Mitopure™ has been evaluated in a randomized, double-blind, placebo-controlled trial (ATLAS) in healthy, overweight, middle-aged adults, in which oral urolithin A at 500 mg or 1,000 mg daily for four months improved muscle strength, exercise performance, and biomarkers of mitochondrial health relative to placebo, providing one of the more direct examples of a microbially-derived plant metabolite advanced through controlled clinical evaluation into a defined commercial ingredient (Singh et al., 2022). In parallel, microbial fermentation routes are under active development: the strain *Enterococcus faecium* FUA027, isolated from human faecal samples and characterized by whole-genome sequencing, converts ellagic acid to urolithin A and has been proposed as a candidate production strain, with genomic screening confirming the absence of transmissible antibiotic-resistance genes relevant to food-safety approval (Xia et al., 2023). Ingredient suppliers including Daicel Corporation now additionally offer fermentation-derived urolithin A, indicating that chemical synthesis, engineered microbial fermentation, and screened natural isolates are being pursued commercially in parallel for the same target molecule (Sun et al., 2025).

These cases illustrate considerations that separate laboratory-scale biotransformation from industrial deployment. Engineered strains must be optimized for enzyme stability and expression level, not conversion efficiency alone. Bioreactor-scale processes must address compound-specific physical challenges such as product adhesion to reactor surfaces. Commercial translation can proceed along more than one route for the same target molecule, from clinically validated branded ingredients to fermentation-derived alternatives offered by ingredient suppliers and candidate production strains still under laboratory characterization. A full techno-economic comparison across chemical synthesis, engineered fermentation, and screened wild-type strains has not yet been published for most compounds discussed in this review and remains an important direction for future work connecting biotransformation research to food-industry application.

Several obstacles limit the scale at which these methods can be deployed. Strain stability across repeated fermentation cycles is not assured, particularly for endophytic fungi whose activity may depend on host-plant signals absent from industrial fermentation conditions. The same enzymatic selectivity that is advantageous for a purified substrate becomes a liability when applied to crude plant extracts containing multiple compound classes, since the enzyme may act on unintended substrates present in the mixture. Regulatory approval of novel fermented ingredients requires characterization of the complete product spectrum and safety evaluation of each transformation product individually, a requirement that adds cost and time to development. Finally, the interindividual variability documented throughout this review means that even a well-characterized fermented ingredient may not produce uniform effects across all consumers, since residual reliance on the consumer's own gut microbiota is rarely eliminated entirely.

Funding

This work was supported by the Guangdong-Macao Science and Technology Innovation Joint Research Special Fund (2023A0505020013, 2025A0505010005); Macau Science and Technology Development Fund (0104/2024/AGJ);Guangdong Provincial Observation and Research Station for Coupled Human and Natural Systems in Land-ocean Interaction Zone (2024B1212040003).

References

Aguirre Santos, E.A., Schieber, A., and Weber, F. (2018). Site-specific hydrolysis of chlorogenic acids by selected Lactobacillus species. Food Res. Int. 109: 426–432.

Ahn-Jarvis, J.H., Teegarden, M.D., Schwartz, S.J., Lee, K., and Vodovotz, Y. (2017). Modulating conversion of isoflavone glycosides to aglycones using crude beta-glycosidase extracts from almonds and processed soy. Food Chem. 237: 685–692.

Aishwarya, P., Sabarinathan, K.G., Gomathy, M., Meenakshisundaram, P., Manonmani, K., and Kar, A.A. (2025). Endophytes as bioenhancers of plant growth: An overview. Fitoterapia 181: 106355.

Akpoghelie, P.O., Edo, G.I., Ali, A.B.M., Yousif, E., Zainulabdeen, K., Owheruo, J.O., Isoje, E.F., Igbuku, U.A., Essaghah, A.E.A., Makia, R.S., Ahmed, D.S., Umar, H., and Alamiery, A.A. (2025). Lactic acid bacteria: Nature, characterization, mode of action, products and applications. Process Biochem. 152: 1–28.

Alharbi, N.A.A. (2026). Polyphenol metabolites in fermented foods: biotransformation, bioavailability, and functional roles. Front. Nutr. 13: 1767453.

Balaj, G., Tamanai-Shacoori, Z., Olivier-Jimenez, D., Sauvager, A., Faustin, M., Bousarghin, L., David-Le Gall, S., Guyot, S., Nebija, D., Tomasi, S., and Abasq, M.L. (2022). An insight into an intriguing oxidative biotransformation pathway of 5-O-caffeoylquinic acid by a gut bacterium. Food Funct. 13: 6195–6204.

Barone, J.J., and Roberts, H.R. (1996). Caffeine consumption. Food Chem. Toxicol. 34: 119–129.

Bhambhani, S., Kondhare, K.R., and Giri, A.P. (2021). Diversity in Chemical Structures and Biological Properties of Plant Alkaloids. Molecules 26: 3374.

Bialonska, D., Kasimsetty, S.G., Khan, S.I., and Ferreira, D. (2009). Urolithins, Intestinal Microbial Metabolites of Pomegranate Ellagitannins, Exhibit Potent Antioxidant Activity in a Cell-Based Assay. J. Agric. Food Chem. 57: 10181–10186.

Bowers, L.W., Lineberger, C.G., Ford, N.A., Rossi, E.L., Punjala, A., Camp, K.K., Kimler, B.K., Fabian, C.J., and Hursting, S.D. (2019). The flaxseed lignan secoisolariciresinol diglucoside decreases local inflammation, suppresses NFκB signaling, and inhibits mammary tumor growth. Breast Cancer Res. Treat. 173: 545–557.

Câmara, J.S., Perestrelo, R., Ferreira, R., Berenguer, C.V., Pereira, J.A.M., and Castilho, P.C. (2024). Plant-Derived Terpenoids: A Plethora of Bioactive Compounds with Several Health Functions and Industrial Applications—A Comprehensive Overview. Molecules 29: 3861.

Cano-Flores, A., Gómez, J., Escalona-Torres, I.S., and Velasco-Bejarano, B. (2020). Microorganisms as Biocatalysts and Enzyme Sources. In: Blumenberg, M., Shaaban, M., and Elgaml, A. (Ed.). Microorganisms. IntechOpen, London.

Cao, L., Du, C., Zhai, X., Li, J., Meng, J., Shao, Y., and Gao, J. (2022). Codonopsis pilosula Polysaccharide Improved Spleen Deficiency in Mice by Modulating Gut Microbiota and Energy Related Metabolisms. Front. Pharmacol. 13: 862763.

Cao, S.-X., Li, L.-Y., Ding, Y.-Y., Luo, X., Huang, F., Sun, Y., So, K.-F., Tan, H.-L., and He, R.-R. (2026). Advances in bioactive polysaccharides: Structural characterization, signaling mechanisms, and therapeutic applications. Cell Invest. 2: 100063.

Chen, Z., Zhang, Z., Liu, J., Qi, H., Li, J., Chen, J., Huang, Q., Liu, Q., Mi, J., and Li, X. (2022). Gut Microbiota: Therapeutic Targets of Ginseng Against Multiple Disorders and Ginsenoside Transformation. Front. Cell. Infect. Microbiol. 12: 853981.

Cheng, L., Zhang, H., Cui, H., Davari, M.D., Wei, B., Wang, W., and Yuan, Q. (2021). Efficient enzyme-catalyzed production of diosgenin: inspired by the biotransformation mechanisms of steroid saponins in Talaromyces stollii CLY-6. Green Chem. 23: 5896–5910.

Cheng, Z., Yang, J., Yan, R., Wang, B., Bai, Y., Miao, Z., Sun, J., Li, H., Wang, X., and Sun, B. (2025). Interactive mechanism-guided microbial interaction dynamics in food fermentations: Lactic acid bacteria and yeasts as a case example. Food Biosci. 68: 106453.

Choudhary, M., Gupta, S., Dhar, M.K., and Kaul, S. (2021). Endophytic Fungi-Mediated Biocatalysis and Biotransformations Paving the Way Toward Green Chemistry. Front. Bioeng. Biotechnol. 9: 664705.

Clavel, T., Henderson, G., Engst, W., Doré, J., and Blaut, M. (2006). Phylogeny of human intestinal bacteria that activate the dietary lignan secoisolariciresinol diglucoside. FEMS Microbiol. Ecol. 55: 471–478.

Cui, Y., Li, J., Liu, C., Yu, G., Shi, J., Li, X., Qi, J., Guo, R., Fan, H., Zhang, S., Wang, C., Chen, K., and Luo, Z. (2026). Ginsenoside Rg3 in Cancer Therapy: Pharmacokinetics, Molecular Mechanisms, and Synergistic Combinations. Am. J. Chin. Med. 54: 1499–1530.

Cui, Y., Zhou, Q., Jin, M., Jiang, S., Shang, P., Dong, X., and Li, L. (2024). Research progress on pharmacological effects and bioavailability of berberine. Naunyn-Schmiedeberg's Arch. Pharmacol. 397: 8485–8514.

Curiel, J.A., de la Bastida, A.R., Langa, S., Peirotén, Á., and Landete, J.M. (2024). Characterization and stabilization of GluLm and its application to deglycosylate dietary flavonoids and lignans. Appl. Microbiol. Biotechnol. 108: 80.

de Araújo, F.F., de Paulo Farias, D., Neri-Numa, I.A., and Pastore, G.M. (2021). Polyphenols and their applications: An approach in food chemistry and innovation potential. Food Chem. 338: 127535.

Dehau, T., Cherlet, M., Croubels, S., Van De Vliet, M., Goossens, E., and Van Immerseel, F. (2023). Berberine-microbiota interplay: orchestrating gut health through modulation of the gut microbiota and metabolic transformation into bioactive metabolites. Front. Pharmacol. 14: 1281090.

Deng, H., Gu, Q., Yu, X., Zhou, J., and Liu, X. (2024). Surface-displayed phenolic acid decarboxylase for increased vinylphenolic pyranoanthocyanins in blueberry wine. Curr. Res. Food Sci. 8: 100730.

Dong, J., Lei, C., Lu, D., and Wang, Y. (2015). Direct Biotransformation of Dioscin into Diosgenin in Rhizome of Dioscorea zingiberensis by Penicillium dioscin. Indian J. Microbiol. 55: 200–206.

Dong, Z., and Huang, B. (2025). The Role of Gut Microbiota in Modulating Ginseng Pharmacokinetics and Pharmacodynamics. Med. Plant Res. 15(4): 169–177.

El-Saadony, M.T., Yang, T., Saad, A.M., Alkafaas, S.S., Elkafas, S.S., Eldeeb, G.S., Mohammed, D.M., Salem, H.M., Korma, S.A., Loutfy, S.A., Alshahran, M.Y., Ahmed, A.E., Mosa, W.F.A., Abd El-Mageed, T.A., Ahmed, A.F., Fahmy, M.A., El-Tarabily, M.K., Mahmoud, R.M., Abu-Qamar, S.F., El-Tarabily, K.A., and Lorenzo, J.M. (2024). Polyphenols: Chemistry, bioavailability, bioactivity, nutritional aspects and human health benefits: A review. Int. J. Biol. Macromol. 277: 134223.

Feng, R., Shou, J.-W., Zhao, Z.-X., He, C.-Y., Ma, C., Huang, M., Fu, J., Tan, X.-S., Li, X.-Y., Wen, B.-Y., Chen, X., Yang, X.-Y., Ren, G., Lin, Y., Chen, Y., You, X.-F., Wang, Y., and Jiang, J.-D. (2015). Transforming berberine into its intestine-absorbable form by the gut microbiota. Sci. Rep. 5: 12155.

Fordos, S., Amin, S., Abid, N., Pasha, I., Khan, M.K.I., Amin, A., Gulzar, M., Subtain, M., and Abdi, G. (2025). Saponins: Advances in extraction techniques, functional properties, and industrial applications. Appl. Food Res. 5: 101146.

Frolova, M.S., Suvorova, I.A., Iablokov, S.N., Petrov, S.N., and Rodionov, D.A. (2022). Genomic reconstruction of short-chain fatty acid production by the human gut microbiota. Front. Mol. Biosci. 9: 949563.

Gao, Y., Feng, Y., Chang, Y., Zhu, Z., Zhao, H., Xu, W., Zhao, M., Xiao, Y., Tian, L., and Xiu, Y. (2024). Biotransformation of Ginsenoside Rb1 to Ginsenoside Rd and 7 Rare Ginsenosides Using Irpex lacteus with HPLC-HRMS/MS Identification. ACS Omega 9: 22744–22753.

García-Villalba, R., Giménez-Bastida, J.A., Cortés-Martín, A., Ávila-Gálvez, M.Á., Tomás-Barberán, F.A., Selma, M.V., Espín, J.C., and González-Sarrías, A. (2022). Urolithins: a Comprehensive Update on their Metabolism, Bioactivity, and Associated Gut Microbiota. Mol. Nutr. Food Res. 66: 2101019.

Giri, P., Pagar, A.D., Patil, M.D., and Yun, H. (2021). Chemical modification of enzymes to improve biocatalytic performance. Biotechnol. Adv. 53: 107868.

Grabarczyk, M., Mączka, W., Żołnierczyk, A.K., and Wińska, K. (2020). Transformations of Monoterpenes with the p-Menthane Skeleton in the Enzymatic System of Bacteria, Fungi and Insects. Molecules 25: 4840.

Gramza-Michałowska, A., Sidor, A., and Kulczyński, B. (2021). Methylxanthines in Food Products. In: Jeszka-Skowron, M., Zgoła-Grześkowiak, A., Grześkowiak, T., and Ramakrishna, A. (Ed.). Analytical Methods in the Determination of Bioactive Compounds and Elements in Food.

Springer International Publishing, Cham, pp. 83–100.
Hennessy, R.C., Nielsen, S.D., Greve-Poulsen, M., Larsen, L.B., Sørensen, O.B., and Stougaard, P. (2020). Discovery of a Bacterial Gene Cluster for Deglycosylation of Toxic Potato Steroidal Glycoalkaloids α-Chaconine and α-Solanine. J. Agric. Food Chem. 65(5): 1390–1396.
Hilberath, T., Hollmann, F., Tieves, F., and Zhang, W. (2025). Peroxygenase-catalysed oxyfunctionalisation reactions. Methods Enzymol. 714: 425–443.
Hsu, Y.-C., Hsieh, W.-C., Chen, S.-H., Li, Y.-Z., Liao, H.-F., Lin, M.-Y., and Sheu, S.-M. (2023). 18β-glycyrrhetinic Acid Modulated Autophagy is Cytotoxic to Breast Cancer Cells. Int. J. Med. Sci. 20: 444–454.
Hu, D., Gao, Y.-H., Yao, X.-S., and Gao, H. (2020). Recent advances in dissecting the demethylation reactions in natural product biosynthesis. Curr. Opin. Chem. Biol. 59: 47–53.
Huang, J., and Wang, Q. (2026). Land plant evolution: from microbial interaction to horizontal gene transfer. Trends Plant Sci. 31: 327–336.
Huang, N., Yu, D., Huo, J., Wu, J., Chen, Y., Du, X., and Wang, X. (2022). Study of Saponin Components after Biotransformation of Dioscorea nipponica by Endophytic Fungi C39. J. Anal. Methods Chem. 2022: 2943177.
Hur, H.-G., Lay, J.O. Jr, Beger, R.D., Freeman, J.P., and Rafii, F. (2000). Isolation of human intestinal bacteria metabolizing the natural isoflavone glycosides daidzin and genistin. Arch. Microbiol. 174: 422–428.
Intharuksa, A., Arunotayanun, W., Na Takuathung, M., Chaichit, S., Prasansuklab, A., Chaikhong, K., Sirichanchuen, B., Chupradit, S., and Koonrungsesomboon, N. (2025). Daidzein and Genistein: Natural Phytoestrogens with Potential Applications in Hormone Replacement Therapy. Int. J. Mol. Sci. 26: 6973.
Jiang, T.A., Prioult, G., and Quann, E. (2026). Microbial Biotransformation of Polyphenols and Bioactive Substrates: Implications for Metabolite-Guided Synbiotics. J. Nutr. 156: 101621.
Kasubuchi, M., Hasegawa, S., Hiramatsu, T., Ichimura, A., and Kimura, I. (2015). Dietary Gut Microbial Metabolites, Short-chain Fatty Acids, and Host Metabolic Regulation. Nutrients 7: 2839–2849.
Ke, C., Zhang, S., Yang, X., and Li, L. (2024). Comparative study of Maillard reaction and blending between soybean protein isolate and soluble soybean polysaccharide: Physicochemical, structure and functional properties. Int. J. Biol. Macromol. 282: 137101.
Khosroshahi, E.D., Razavi, S.H., Salami, M., and Ubeyitogullari, A. (2025). Recent advances in bioprocessing of medicinal plants through fermentation: A promising approach to maximize nutritional/functional value, bioactive potential, and health benefits. Food Biosci. 70: 107045.
Kim, H.J., Oh, T.K., Kim, Y.H., Lee, J., Moon, J.M., Park, Y.S., and Sung, C.M. (2022). Pharmacokinetics of Ginsenoside Rb1, Rg3, Rk1, Rg5, F2, and Compound K from Red Ginseng Extract in Healthy Korean Volunteers. Evidence-Based Complementary Altern. Med. 2022: 1–10.
Kim, J.S., Kim, J.H., Palaniyandi, S.A., Lee, C.C., You, J.W., Yang, H., Yoon Park, J.H., Yang, S.H., and Lee, K.W. (2019). Yak-Kong Soybean (Glycine max) Fermented by a Novel Pediococcus pentosaceus Inhibits the Oxidative Stress-Induced Monocyte-Endothelial Cell Adhesion. Nutrients 11: 1380.
Kim, K.-A., Jung, I.-H., Park, S.-H., Ahn, Y.-T., Huh, C.-S., and Kim, D.-H. (2013). Comparative Analysis of the Gut Microbiota in People with Different Levels of Ginsenoside Rb1 Degradation to Compound K. PLOS ONE 8: e62409.
Kroon, P.A., Clifford, M.N., Crozier, A., Day, A.J., Donovan, J.L., Manach, C., and Williamson, G. (2004). How should we assess the effects of exposure to dietary polyphenols in vitro? Am. J. Clin. Nutr. 80: 15–21.
Kuriata-Adamusiak, R., Strub, D., and Lochyński, S. (2012a). Application of microorganisms towards synthesis of chiral terpenoid derivatives. Appl. Microbiol. Biotechnol. 95: 1427–1436.
Lee, Y.-I., Song, W.-S., and Oh, D.-K. (2025a). Enhanced production of ginsenoside compound K by synergistic conversion of fermentation with *Aspergillus tubingensis* and commercial cellulase. Front. Bioeng. Biotechnol. 12: 1538031.
Lee, Y.-P., Chan, H.-T., Li, T.-H., Chu, L.J., Lee, S.-L., Chang, Y.-Q., and Wang, R.Y. (2025b). Anticancer Mechanisms of Ginsenoside Compound K: A Review. Diseases 13: 143.
Leng, P., Wang, Y., and Xie, M. (2025). Ellagic Acid and Gut Microbiota: Interactions, and Implications for Health. Food Sci. Nutr. 13: e70133.
Li, C., Sun, J., Han, J., Lin, Y., Fan, R., Yang, J., Feng, Y., Xu, W., Li, H., and Xu, S. (2026). Synthesis and neuroprotective activity evaluation of diosgenin derivatives based on a biocatalytic-chemosynthetic combinatorial strategy. Eur. J. Med. Chem. 311: 118825.
Li, C., Zhou, J., Du, G., Chen, J., Takahashi, S., and Liu, S. (2020a). Developing Aspergillus niger as a cell factory for food enzyme production. Biotechnol. Adv. 44: 107630.
Li, D.-D., Yu, P., Xiao, W., Wang, Z.-Z., and Zhao, L.-G. (2020b). Berberine: A Promising Natural Isoquinoline Alkaloid for the Development of Hypolipidemic Drugs. Curr. Top. Med. Chem. 20: 2634–2647.
Li, M., Ma, M., Wu, Z., Liang, X., Zheng, Q., Li, D., An, T., and Wang, G. (2023a). Advances in the biosynthesis and metabolic engineering of rare ginsenosides. Appl. Microbiol. Biotechnol. 107: 3391–3404.
Li, S., Chen, L., Yang, T., Wu, Q., Lv, Z., Xie, B., and Sun, Z. (2013). Increasing antioxidant activity of procyanidin extracts from the pericarp of Litchi chinensis processing waste by two probiotic bacteria bioconversions. J. Agric. Food Chem. 61: 2506–2512.
Li, X., Chou, M.-Y., Bonito, G.M., and Last, R.L. (2023b). Anti-fungal bioactive terpenoids in the bioenergy crop switchgrass (Panicum virgatum) may contribute to ecotype-specific microbiome composition. Commun. Biol. 6: 917.
Li, Z.-R., Jia, R.-B., Mo, Y., Wang, H., Luo, D., Zhou, C., and Zhao, M. (2024). Comparative Study on the Antioxidative Effects and α-Glucosidase Inhibitory Potential In Vitro among Ellagic Acid and Its Metabolites Urolithins. J. Agric. Food Chem. 72: 26711–26721.
Liu, T., Li, W., Liu, D., and Xue, B. (2026). Research Progress on Anticancer Mechanism of Ginsenoside Regulating Tumor Microenvironment. Curr. Issues Mol. Biol. 48: 329.
Liu, X., and Xu, S. (2026). Unraveling the complexities of caffeine: metabolism, genetics, evolution, and health. Hereditas 163: 36.
Liu, X., Zhou, Z.-Y., Cui, J.-L., Wang, M.-L., and Wang, J.-H. (2021). Biotransformation ability of endophytic fungi: from species evolution to industrial applications. Appl. Microbiol. Biotechnol. 105: 7095–7113.
Liu, Y., Deng, J., Zhao, T., Yang, X., Zhang, J., and Yang, H. (2024a). Bioavailability and mechanisms of dietary polyphenols affected by non-thermal processing technology in fruits and vegetables. Curr. Res. Food Sci. 8: 100715.
Liu, Y., Liu, X., Li, Y., Pei, Y., Jaleel, A., and Ren, M. (2024b). Potato steroidal glycoalkaloids: properties, biosynthesis, regulation and genetic manipulation. Mol. Hortic. 4: 43.
Lu, W., Feng, J., Chen, X., Bao, Y.-J., Wang, Y., Wu, Q., Ma, Y., and Zhu, D. (2019). Distinct Regioselectivity of Fungal P450 Enzymes for Steroidal Hydroxylation. Appl. Environ. Microbiol. 85: e01182–19.
Luo, Y., Wang, P., Wang, R., Hui, J., Zhu, C., Fu, R., and Fan, D. (2026). Efficient Biosynthesis of Rare Ginsenoside Compound K Using Engineered *Pichia pastoris* with Surface-Anchored *Sulfolobus solfataricus* β-Glucosidase. J. Agric. Food Chem. 74: 1154–1166.
Lv, Q., Li, X., Fan, B., Zhu, C., and Chen, Z. (2022). The Cellular and Subcellular Organization of the Glucosinolate-Myrosinase System against Herbivores and Pathogens. Int. J. Mol. Sci. 23: 1577.
Manach, C., Williamson, G., Morand, C., Scalbert, A., and Rémésy, C. (2005). Bioavailability and bioefficacy of polyphenols in humans. I. Review of 97 bioavailability studies. Am. J. Clin. Nutr. 81: 230S–242S.
Mandal, N., Pathak, A., Gauliya, K., Manjhi, M.K., Gupta, A., Upadhyay, D.C., Khan, M.L., Koiri, R.K., Saad, T., and Upadhyay, C.P. (2025). Reprogramming of Diosgenin-Specialized Metabolism in Plants and Its Medicinal Applications. Physiol. Plant. 177: e70621.
Mareai, S. (2011). Secoisolariciresinol Diglucoside: A potent multifarious bioactive phytoestrogen of flaxseed. Res. Rev. Biomed. Biotechnol. 2: 1–24.
Marín, L., Miguélez, E.M., Villar, C.J., and Lombó, F. (2015). Bioavailability of Dietary Polyphenols and Gut Microbiota Metabolism: Antimicrobial Properties. BioMed Res. Int. 2015: 905215.
Marshall, S.A., Young, R.B., Lewis, J.M., Rutten, E.L., Gould, J., Barlow, C.K., Giogha, C., Marcelino, V.R., Fields, N., Schittenhelm, R.B., Hartland, E.L., Scott, N.E., Forster, S.C., and Gulliver, E.L. (2023). The broccoli-derived antioxidant sulforaphane changes the growth of gastrointestinal microbiota, allowing for the production of anti-inflammatory metabolites. J. Funct. Foods 107: 105645.

Mithul Aravind, S., Wichienchot, S., Tsao, R., Ramakrishnan, S., and Chakkaravarthi, S. (2021). Role of dietary polyphenols on gut microbiota, their metabolites and health benefits. Food Res. Int. 142: 110189.

Mohanan, P., Subramaniyam, S., Mathiyalagan, R., and Yang, D.-C. (2018a). Molecular signaling of ginsenosides Rb1, Rg1, and Rg3 and their mode of actions. J. Ginseng Res. 42: 123–132.

Mutafova, B., Fernandes, P., Mutafov, S., Berkov, S., and Pavlov, A. (2016). Microbial Transformations of Plant Secondary Metabolites. In: Pavlov, A., and Bley, T. (Ed.). Bioprocessing of Plant In Vitro Systems. Springer, Cham, pp. 1–41.

Muthyala, R.S., Ju, Y.H., Sheng, S., Williams, L.D., Doerge, D.R., Katzenellenbogen, B.S., Helferich, W.G., and Katzenellenbogen, J.A. (2004). Equol, a natural estrogenic metabolite from soy isoflavones: convenient preparation and resolution of R- and S-equols and their differing binding and biological activity through estrogen receptors alpha and beta. Bioorg. Med. Chem. 12: 1559–1567.

Narbad, A., and Rossiter, J.T. (2018). Gut Glucosinolate Metabolism and Isothiocyanate Production. Mol. Nutr. Food Res. 62: 1700991.

Neves, C.M.B., Wessel, D.F., Neves, M. da G.P.M.S., and Simões, M.M.Q. (2026). Sustainable Approaches toward Valuable Chemicals by Transformation and Biotransformation of Monoterpenes and Monoterpenoids. ACS Sustainable Resour. Manage. 3: 1276–1300.

Nguyen, V.P.T., Stewart, J., Lopez, M., Ioannou, I., and Allais, F. (2020). Glucosinolates: Natural Occurrence, Biosynthesis, Accessibility, Isolation, Structures, and Biological Activities. Molecules 25: 4537.

Oliveira, D.M., Mota, T.R., Oliva, B., Segato, F., Marchiosi, R., Ferrarese-Filho, O., Faulds, C.B., and Santos, W.D. dos (2019). Feruloyl esterases: Biocatalysts to overcome biomass recalcitrance and for the production of bioactive compounds. Bioresour. Technol. 278: 408–423.

Orozco-Mosqueda, M. del C., and Santoyo, G. (2021). Plant-microbial endophytes interactions: Scrutinizing their beneficial mechanisms from genomic explorations. Curr. Plant Biol. 25: 100189.

Palafox-Carlos, H., Ayala-Zavala, J.F., and González-Aguilar, G.A. (2011). The Role of Dietary Fiber in the Bioaccessibility and Bioavailability of Fruit and Vegetable Antioxidants. J. Food Sci. 76: R6–R15.

Pant, A., Maiti, T.K., Mahajan, D., and Das, B. (2023). Human Gut Microbiota and Drug Metabolism. Microb. Ecol. 86: 97–111.

Patel, D., Vaghasiya, J., Pancholi, S.S., and Paul, A. (2012). Therapeutic Potential of Secoisolariciresinol Diglucoside: A Plant Lignan. Int. J. Pharm. Sci. Drug Res. 4(1): 15–18.

Peng, K., Zhang, Y., Zhang, Q., Wang, Y., Liu, Y., and Cui, X. (2025). Impact of Enzymatic Degradation Treatment on Physicochemical Properties, Antioxidant Capacity, and Prebiotic Activity of Lilium Polysaccharides. Foods 14: 246.

Polozsányi, Z., Galádová, H., Kaliňák, M., Jopčík, M., Kaliňáková, B., Breier, A., and Šimkovič, M. (2024). The Antimicrobial Effects of Myrosinase Hydrolysis Products Derived from Glucosinolates Isolated from Lepidium draba. Plants 13: 995.

Qin, D., and Dong, J. (2023). Multi-Level Optimization and Strategies in Microbial Biotransformation of Nature Products. Molecules 28: 2619.

Qin, Z., Yu, S., Chen, J., and Zhou, J. (2022). Dehydrogenases of acetic acid bacteria. Biotechnol. Adv. 54: 107863.

Raimondi, S., Anighoro, A., Quartieri, A., Amaretti, A., Tomás-Barberán, F.A., Rastelli, G., and Rossi, M. (2015). Role of bifidobacteria in the hydrolysis of chlorogenic acid. MicrobiologyOpen 4: 41–52.

Rein, M.J., Renouf, M., Cruz-Hernandez, C., Actis-Goretta, L., Thakkar, S.K., and Silva Pinto, M. da (2013). Bioavailability of bioactive food compounds: a challenging journey to bioefficacy. Br. J. Clin. Pharmacol. 75: 588–602.

Rizzo, M., Ventrice, D., Giannetto, F., Cirinnà, S., Santagati, N.A., Procopio, A., Mollace, V., and Muscoli, C. (2017). Antioxidant activity of oleuropein and semisynthetic acetyl-derivatives determined by measuring malondialdehyde in rat brain. J. Pharm. Pharmacol. 69: 1502–1512.

Rogozinska, M., Korsak, D., Mroczek, J., and Biesaga, M. (2021). Catabolism of hydroxycinnamic acids in contact with probiotic Lactobacillus. J. Appl. Microbiol. 131: 1464–1473.

Rong, X.-Q., Zhang, X.-M., Yan, L., Tan, Y., and Lu, C. (2026). The Structure-Decoding-Conversion-Effect Paradigm of Natural Polysaccharides for Gut Microbiota Remodeling in Ulcerative Colitis. Nutrients 18: 1297.

Rowland, I., Gibson, G., Heinken, A., Scott, K., Swann, J., Thiele, I., and Tuohy, K. (2018). Gut microbiota functions: metabolism of nutrients and other food components. Eur. J. Nutr. 57: 1–24.

Ruan, W., Engevik, M.A., Spinler, J.K., and Versalovic, J. (2020). Healthy Human Gastrointestinal Microbiome: Composition and Function After a Decade of Exploration. Dig. Dis. Sci. 65: 695–705.

Rustamova, N., Huang, G., Isokov, M., Movlanov, J., Farid, R., Buston, I., Xiang, H., Davranov, K., and Yili, A. (2024). Modification of natural compounds through biotransformation process by microorganisms and their pharmacological properties. Fitoterapia 179: 106227.

Salehi, M., and Rashidinejad, A. (2025). Multifaceted roles of plant-derived bioactive polysaccharides: A review of their biological functions, delivery, bioavailability, and applications within the food and pharmaceutical sectors. Int. J. Biol. Macromol. 290: 138855.

Saric, S., and Sivamani, R.K. (2016). Polyphenols and Sunburn. Int. J. Mol. Sci. 17: 1521.

Singh, A., D'Amico, D., Andreux, P.A., Fouassier, A.M., Blanco-Bose, W., Evans, M., Aebischer, P., Auwerx, J., and Rinsch, C. (2022). Urolithin A improves muscle strength, exercise performance, and biomarkers of mitochondrial health in a randomized trial in middle-aged adults. Cell Rep. Med. 3: 100633.

Son, S.-H., Kang, J., Ahn, M., Nam, S., Jung, Y.W., Lee, K.Y., Jeon, Y.H., Byun, Y., and Lee, K. (2021). Synthesis and Biochemical Evaluation of Baicalein Prodrugs. Pharmaceutics 13: 1516.

Song, H., Zhang, L., Wu, L., Huang, W., Wang, M., Zhang, L., Shao, Y., Wang, M., Zhang, F., Zhao, Z., Mei, X., Li, T., Wang, D., Liang, Y., Li, J., Xu, T., Zhao, Y., Zhong, Y., Chen, Q., and Lu, B. (2020). Phenolic acid profiles of common food and estimated natural intake with different structures and forms in five regions of China. Food Chem. 321: 126675.

Song, Y.-R., and Baik, S.-H. (2017). Molecular cloning, purification, and characterization of a novel thermostable cinnamoyl esterase from Lactobacillus helveticus KCCM 11223. Prep. Biochem. Biotechnol. 47: 496–504.

Soukup, S.T., Engelbert, A.K., Watzl, B., Bub, A., and Kulling, S.E. (2023). Microbial Metabolism of the Soy Isoflavones Daidzein and Genistein in Postmenopausal Women: Human Intervention Study Reveals New Metabotypes. Nutrients 15: 2352.

Soukup, S.T., Stoll, D.A., Danylec, N., Schoepf, A., Kulling, S.E., and Huch, M. (2021). Metabolism of Daidzein and Genistein by Gut Bacteria of the Class Coriobacteriia. Foods 10: 2741.

Stathaki, A., Pantidi, G., Thomopoulou, M., and Koudounas, K. (2024). β-Glucosidases in specialized metabolism: Towards a new understanding of the gatekeepers of plant chemical arsenal. Curr. Opin. Plant Biol. 82: 102638.

Su, F., Duan, T., Liu, R., Ding, X., Mao, S., Zhang, Y., Li, J., Wu, Q., and Zhang, C. (2026). Genomic and metabolomic insights into the enhancement of rare ginsenosides in *Panax ginseng* through solid-state fermentation by *Aspergillus cristatus* JH-5. Front. Microbiol. 17: 1785529.

Sun, X.-Y., Peng, Y., Gong, T., Chen, J.-J., Chen, T.-J., Yang, J.-L., and Zhu, P. (2026). Engineering a yeast cell factory for high-level production of unnatural ginsenoside 3β-O-Glc-DM. Microb. Cell Fact. 25: 83.

Sun, Z., Gao, L., Ju, Z., and Zhang, L. (2025). Multi-Dimensional Analysis of Key Points in the Biological Activity, Chemical Synthesis and Biotransformation of Urolithin A. Fermentation 11: 603.

Tang, M., Xie, X., Yang, Y., and Li, F. (2021). Ginsenoside compound K- a potential drug for rheumatoid arthritis. Pharmacol. Res. 166: 105498.

Theilmann, M.C., Goh, Y.J., Nielsen, K.F., Klaenhammer, T.R., Barrangou, R., and Abou Hachem, M. (2017). Lactobacillus acidophilus Metabolizes Dietary Plant Glucosides and Externalizes Their Bioactive Phytochemicals. mBio 8: e01421–17.

Tian, X., Xu, Z., Chen, M., Hu, P., Liu, F., Sun, Z., Liu, H., Guo, X., Li, Z., and Huang, C. (2018). Simultaneous determination of eight bioactive compounds by LC-MS/MS and its application to the pharmacokinetics, liver first-pass effect, liver and brain distribution of orally administrated Gouteng-Baitouweng (GB) in rats. J. Chromatogr. B: Anal. Technol. Biomed. Life Sci. 1084: 122–131.

Tomás-Barberán, F.A., González-Sarrías, A., García-Villalba, R., Núñez-Sánchez, M.A., Selma, M.V., García-Conesa, M.T., and Espín, J.C. (2017). Urolithins, the rescue of "old" metabolites to understand a "new" concept: Metabotypes as a nexus among phenolic metabolism, microbiota dysbiosis, and host health status. Mol. Nutr. Food

Res. 61: 1500901.
Tong, Q., Li, T., Jiang, L., Wang, Z., and Qian, Y. (2022). Nanoparticle, a promising therapeutic strategy for the treatment of infective endocarditis. Anatolian J. Cardiol. 26: 90–99.
Torres-Mendoza, D., Ortega, H.E., and Cubilla-Rios, L. (2020). Patents on Endophytic Fungi Related to Secondary Metabolites and Biotransformation Applications. J. Fungi 6: 58.
Tran, T.N.A., Son, J.-S., Awais, M., Ko, J.-H., Yang, D.C., and Jung, S.-K. (2023). β-Glucosidase and Its Application in Bioconversion of Ginsenosides in Panax ginseng. Bioengineering 10: 484.
Travičić, V., Pezo, L., Sulejmanović, M., Tenji, D., Perović, M., Ćetković, G., and Ćetković, N. (2026). State-of-the-Art Perspectives on Postbiotic-Oriented Systems Derived from Fermented Medicinal Plant Extracts. Foods 15: 864.
Tufail, T., Fatima, S., Bader Ul Ain, H., Ikram, A., Noreen, S., Rebezov, M., AL-Farga, A., Saleh, R., and Shariati, M.A. (2025). Role of Phytonutrients in the Prevention and Treatment of Chronic Diseases: A Concrete Review. ACS Omega 10: 12724–12755.
Wang, G., Xie, L., Huang, Z., and Xie, J.-H. (2023a). Recent advances in polysaccharide biomodification by microbial fermentation: production, properties, bioactivities, and mechanisms. Crit. Rev. Food Sci. Nutr. 64: 1–25.
Wang, H.-Y., Wang, C., Guo, S.-C., Chen, Z.-C., Peng, Z.-T., Duan, R., Dong, T.T.X., and Tsim, K.W.K. (2019). Polysaccharide deriving from Ophiopogonis Radix promotes metabolism of ginsenosides in the present of human gut microbiota based on UPLC-MS/MS assay. J. Pharm. Biomed. Anal. 175: 112779.
Wang, L.-Q., Meselhy, M.R., Li, Y., Qin, G.-W., and Hattori, M. (2000). Human Intestinal Bacteria Capable of Transforming Secoisolariciresinol Diglucoside to Mammalian Lignans, Enterodiol and Enterolactone. Chem. Pharm. Bull. 48: 1606–1610.
Wang, P., Wei, Y., Fan, Y., Liu, Q., Wei, W., Yang, C., Zhang, L., Zhao, G., Yue, J., Yan, X., and Zhou, Z. (2015). Production of bioactive ginsenosides Rh2 and Rg3 by metabolically engineered yeasts. Metab. Eng. 29: 97–105.
Wang, Q., Chen, H., Yin, M., Cheng, X., Xia, H., Hu, H., Zheng, J., Zhang, Z., and Liu, H. (2023b). *In vitro* digestion and human gut microbiota fermentation of Bletilla striata polysaccharides and oligosaccharides. Front. Cell. Infect. Microbiol. 13: 1105335.
Wang, W., Du, G., Yang, G., Zhang, K., Chen, B., and Xiao, G. (2022). A multifunctional enzyme portfolio for α-chaconine and α-solanine degradation in the Phthorimaea operculella gut bacterium Glutamicibacter halophytocola S2 encoded in a trisaccharide utilization locus. Front. Microbiol. 13: 1023698.
Wang, X., Zheng, M., Liu, J., Huang, Z., Bai, Y., Ren, Z., Wang, Z., Tian, Y., Qiao, Z., Liu, W., and Feng, F. (2017a). Differences of first-pass effect in the liver and intestine contribute to the stereoselective pharmacokinetics of rhynchophylline and isorhynchophylline epimers in rats. J. Ethnopharmacol. 209: 175–183.
Wang, Y., Tong, Q., Shou, J.-W., Zhao, Z.-X., Li, X.-Y., Zhang, X.-F., Ma, S.-R., He, C.-Y., Lin, Y., Wen, B.-Y., Guo, F., Fu, J., and Jiang, J.-D. (2017b). Gut Microbiota-Mediated Personalized Treatment of Hyperlipidemia Using Berberine. Theranostics 7: 2443–2451.
Wang, Z., Zheng, Y., Dai, Y., Yang, R., Zhao, R., Sun, G., Zhou, W.-W., Feng, S., Feng, Y., Li, N., Yang, J., Zhang, H., and An, L. (2024). Effect of probiotic fermentation on the extraction rate and bioactivity of plant-based polysaccharides: A review. Innovative Food Sci. Emerging Technol. 98: 103863.
Wei, Z., Wang, H., Zhong, R., Chen, L., Vigors, S., and Zhang, H. (2025). Biodegradation of α-solanine and α-chaconine: Insights into microbial detoxification and enzymatic deglycosylation pathways. Food Chem.: X 31: 102968.
Wen, J., Sui, Y., Li, S., Shi, J., Cai, S., Xiong, T., Cai, F., Zhou, L., Zhao, S., and Mei, X. (2023). Phenolic Profile and Bioactivity Changes of Lotus Seedpod and Litchi Pericarp Procyanidins: Effect of Probiotic Bacteria Biotransformation. Antioxidants 12: 1974.
Wilkowska, A., Nowak, A., Motyl, I., and Oracz, J. (2025). The Molecular Weight of Enzymatically Modified Pectic Oligosaccharides from Apple Pomace as a Determinant for Biological and Prebiotic Activity. Molecules 30: 46.
Wu, S., Shen, D., Wang, R., Li, Q., Mo, R., Zheng, Y., Zhou, Y., and Liu, Y. (2021). Phenolic profiles and antioxidant activities of free, esterified and bound phenolic compounds in walnut kernel. Food Chem. 350: 129217.
Xia, M., Mu, S., Fang, Y., Zhang, X., Yang, G., Hou, X., He, F., Zhao, Y., Huang, Y., Zhang, W., Shen, J., and Liu, S. (2023). Genetic and Probiotic Characteristics of Urolithin A Producing Enterococcus faecium FUA027. Foods 12: 1021.
Xu, K., Sheng, Y., Deng, Y., Han, H., and Zeng, B. (2026). Research Progress in Biotransformation of Plant and Phytochemicals by Aspergillus: Active Metabolites and Industrial Applications. Fermentation 12: 282.
Xu, W., Lyu, W., Duan, C., Ma, F., Li, X., and Li, D. (2023). Preparation and bioactivity of the rare ginsenosides Rg3 and Rh2: An updated review. Fitoterapia 167: 105514.
Yang, F., Chen, C., Ni, D., Yang, Y., Tian, J., Li, Y., Chen, S., Ye, X., and Wang, L. (2023). Effects of Fermentation on Bioactivity and the Composition of Polyphenols Contained in Polyphenol-Rich Foods: A Review. Foods 12: 3315.
Yang, X.-D., Yang, Y.-Y., Ouyang, D.-S., and Yang, G.-P. (2015). A review of biotransformation and pharmacology of ginsenoside compound K. Fitoterapia 100: 208–220.
Yu, C.L., Louie, T.M., Summers, R., Kale, Y., Gopishetty, S., and Subramanian, M. (2009). Two Distinct Pathways for Metabolism of Theophylline and Caffeine Are Coexpressed in *Pseudomonas putida* CBB5. J. Bacteriol. 191: 4624–4632.
Zhang, J., Tong, Y., Lu, X., Dong, F., Ma, X., Yin, S., He, Y., Liu, Y., Liu, Q., and Fan, D. (2022). A derivant of ginsenoside CK and its inhibitory effect on hepatocellular carcinoma. Life Sci. 304: 120698.
Zhang, M., Cui, S., Mao, B., Zhang, Q., Zhao, J., Zhang, H., Tang, X., and Chen, W. (2023a). Ellagic acid and intestinal microflora metabolite urolithin A: A review on its sources, metabolic distribution, health benefits, and biotransformation. Crit. Rev. Food Sci. Nutr. 63: 6900–6922.
Zhang, X., Zhang, Y., Guo, Y., Xue, P., Xue, Z., Zhang, Y., Zhang, H., Ito, Y., Dou, J., and Guo, Z. (2023b). Research progress of diosgenin extraction from *Dioscorea zingiberensis* C. H. Wright: Inspiration of novel method with environmental protection and efficient characteristics. Steroids 192: 109181.
Zhao, Y., Wang, M., Li, H., Zhang, Z., and Li, H. (2025). Advances in Modification Strategies of Polysaccharides and Their Applications. J. Food Sci. 91: e70779.
Zhao, Y., Zhong, X., Yan, J., Sun, C., Zhao, X., and Wang, X. (2022). Potential roles of gut microbes in biotransformation of natural products: An overview. Front. Microbiol. 13: 956378.
Zhou, B., Ma, C., Zheng, C., Xia, T., Ma, B., and Liu, X. (2020). 3-Methylxanthine production through biodegradation of theobromine by Aspergillus sydowii PT-2. BMC Microbiol. 20: 269.
Zhu, J., Cai, Z., Song, Z., Li, Y., Shim, Y.Y., Reaney, M.J.T., Lee, Y.Y., Wang, Y., and Zhang, N. (2024). Bioconversion of lignans in flaxseed cake by fermented tofu microbiota and isolation of *Enterococcus faecium* strain ZB26 responsible for converting secoisolariciresinol diglucoside to enterodiol. Food Chem. 457: 140077.
Zhuo, J., Li, B., and Tian, M. (2026). Biological Activities, Health Benefits and Synthesis of Equol and Its Derivatives: A Comprehensive Review. Food Sci. Nutr. 14: e71443.
Zou, X., Cai, J., Xiao, J., Zhang, M., Jia, X., Dong, L., Hu, K., Yi, Y., Zhang, R., and Huang, F. (2023). Purification, Characterization and Bioactivity of Different Molecular-Weight Fractions of Polysaccharide Extracted from Litchi Pulp. Foods 12: 194.

Journal of Food Bioactives
International Society for Nutraceuticals and Functional Foods
Review
J. Food Bioact. 2026;35:24–37

Coreopsis tinctoria and its bioactives in the prevention and management of diabetes and diabetic complications

Wenyu Zhang[a], Yixing Zhu[a], Junfeng Shen[a*] and Alexander Gosslau[b,c*]

[a]College of Biology and Agricultural Resources and Hubei Key Laboratory for EFGIR, Huanggang Normal University, Huanggang, 438000, China
[b]Department of Science, City University of New York, BMCC, 199 Chambers Street, New York, NY 10007, USA
[c]Department of Chemistry and Chemical Biology, Rutgers University, 123 Bevier Road, Piscataway, New Jersey 08854, USA
[*]**Corresponding author:** Junfeng Shen, College of Biology and Agricultural Resources and Hubei Key Laboratory for EFGIR, Huanggang Normal University, Huanggang, 438000, China; Alexander Gosslau, Department of Science, City University of New York, BMCC, 199 Chambers Street, New York, NY 10007, USA. E-mail: jfshen@hgnu.edu.cn (JS) and agosslau@bmcc.cuny.edu (AG)
DOI: 10.26599/JFB.2026.95035453
Received: April 25, 2026; **Revised received & accepted:** July 29, 2026
Citation: Zhang, W., Zhu, Y., Shen, J., and Gosslau, A. (2026). *Coreopsis tinctoria* and its bioactives in the prevention and management of diabetes and diabetic complications. J. Food Bioact. 35: 24–37.

Abstract

Diabetes, one of the major metabolic diseases, has become a major public health concern worldwide leading to chronic lesions in various organs such as kidney and cardiovascular disease, severely impacting quality of life and life expectancy. Current drug treatments for diabetes have varying degrees of side effects. Therefore, finding natural, safe, and effective functional foods to prevent and control diabetes and its complications has become a research hotspot. *Coreopsis tinctoria* Nutt. (*C. tinctoria*) is rich in polyphenols (e.g. flavonoids), polysaccharides, and other bioactive components, possessing various health benefits. Studies have shown that *C. tinctoria* flavonoids lower blood sugar levels through multiple pathways, including suppressing oxidative stress, decreasing the inflammatory cascade, regulating glucose and lipid metabolism, increasing insulin sensitivity and improving insulin resistance. This review briefly summarizes the research progress on diabetes and its complications, and details the mechanisms of action of *C. tinctoria* bioactives in prevention and treatment of diabetes and its complications. The aim is to provide the molecular mechanisms of *C. tinctoria* and its bioactives for a potential application of *C. tinctoria* in controlling diabetes and its complications.

Keywords: *Coreopsis tinctoria* Nutt.; Diabetes mellitus; Diabetic complications; Oxidative stress; Inflammation.

1. Introduction

Diabetes mellitus (DM) is a complex metabolic disorder characterized by chronic hyperglycemia. Its pathogenesis involves defects in insulin secretion, insulin resistance (IR), abnormal hepatic glucose output, impaired glucose uptake in muscle and adipose tissue, and the interaction of genetic and environmental factors (Chaudhury et al., 2017; Lu et al., 2024; Zhao et al., 2026). According to data from the International Diabetes Federation (IDF) in 2025, the number of adults aged between 20–79 years living with diabetes and its pathological conditions has reached approximately 589 million worldwide and is projected to increase substantially over the coming decades. It is estimated that by 2050, the number of people with diabetes worldwide will reach 853 million (IDF diabetes atlas, 2025). Persistent hyperglycemia contributes to progressive structural and functional damage in multiple organs and tissues, including eyes, kidneys, cardiovascular system, peripheral nerves, and blood vessels among others, seriously affecting their quality of life and life expectancy (Galicia-Garcia et al., 2020; Vlassara and Uribarri, 2017; Zhao et al., 2026). At present, the main treatment for diabetes is insulin injection (for type I and advanced diabetes patients) or oral hypoglycemic drugs for type II, but these treatments are accompanied by varying degrees of side

© The author(s) 2026. Publishing Services by Tsinghua University Press
The articles published in this open access journal are distributed under the terms of the Creative Commons Attribution 4.0 International License (http://creativecommons.org/licenses/by/4.0/)

effects (Chaudhury et al., 2017; Romero et al., 2017; Lu et al., 2024). Therefore, the search for natural, safe and effective drugs for prevention and treatment of diabetes has become a hot topic in the fields of food science and natural product research. (Donath, 2014; Nanda et al., 2023)

Coreopsis tinctoria Nutt., abbreviated as *C. tinctoria*, is a plant of the Asteraceae family that originated in the United States and Africa, and is now widely cultivated around the world. Currently in China, *C. tinctoria* is mainly distributed in the area of Kunlun Mountains at an altitude of about 3,000 meters. It is one of the distinctive alpine wild plants to the Xinjiang Uyghur Autonomous region, China , and is recognized for its unique properties (Guo et al., 2023, 2025). *C. tinctoria* is rich in flavonoids, polysaccharides, volatile oils, amino acids and other bioactive components. The main functional components of *C. tinctoria* include essential oils, polyphenols, polysaccharides, amino acids, saponins, and phenylpropanoids among others (Begmatov et al., 2020; Shen et al., 2021; Xu et al., 2021). Polyphenols comprise an important class of bioactives in *C. tinctoria*, with a total polyphenol content of more than 20% in dry weight (Hayat et al., 2020). Its flavonoids are a major part of polyphenols, mainly including flavones, chalcones, flavonols, dihydroflavones, and isoflavones among others (Guo et al., 2015, 2025; Shen et al., 2021). Among them, the chalcone marein and dihydroflavonoid flavanomarein are the main flavonoid components in *C. tinctoria*, accounting for more than 50% of the total flavonoid content (Guo et al., 2023; Lam et al., 2016).

Traditionally, *C. tinctoria* has been used to hypertension, prevent diabetes and other metabolic diseases. Modern pharmacological studies have demonstrated a variety of bioactive activities such as antioxidant, anti-inflammatory, hypoglycemic, lipid-lowering, anti-fibrotic, anti-cancer, anti-ageing, and anti atherosclerosis effects (Du et al., 2026; Guo et al., 2025; Zhu et al., 2026a; Li, et al., 2024; Shen et al., 2021; Sun et al., 2027; Zhang et al., 2023; Zhao et al., 2025b). Accumulating evidence indicates that *C. tinctoria* may exert beneficial effects against diabetes and its associated complications. (Abdurehman et al., 2026; Ma et al., 2023; Yang et al., 2025; Zhu et al., 2026a, 2026b). It helps maintain glycemic homeostasis and modulate biomarkers related to diabetic complications, potentially through coordinated actions on multiple key target organs and tissues, including the liver, kidneys, pancreatic islets, and vascular endothelium among others (Guo et al., 2022; Liu et al., 2022; Zhang et al., 2022; Yu et al., 2019). Herein, we review the recent studies on the efficacy and mechanism of *C. tinctoria* in managing diabetes and its complications

2. Antidiabetic mechanisms of *C. tinctoria* and its bioactives

2.1. Antioxidant and anti-inflammatory effects

2.1.1. *C. tinctoria*

Oxidative stress is one of the important pathogenic mechanisms of diabetes. When the antioxidant defense mechanism is insufficient, the clearance of reactive oxygen species (ROS) decreases, leading to excessive accumulation of ROS in the body, which in turn stimulates the release of inflammatory cytokines, forming a vicious cycle and exacerbating the pathological process of diabetes (Mehndiratta et al., 2024; Yao et al., 2020; Zamanian et al., 2024; Zhao et al., 2025a). *C. tinctoria* has exhibited antioxidant activity and can effectively clear excessive reactive oxygen species (ROS) in the body. The DPPH free radical scavenging EC_{50} capacity of the aqueous extract of *C. tinctoria* was demonstrated to be 21 μg/mL (Dias et al., 2010). The IC_{50} values of the DPPH free radical scavenging activity of the alcoholic extract (EEC) and aqueous extract (WEC) of *C. tinctoria* were 0.298 ± 0.051 and 0.759 ± 0.067 mg/mL, respectively. The ABTS assay, measuring the total antioxidant activity of EEC and WEC was equivalent to 0.268 ± 0.003 and 0.383 ± 0.046 mg/mL of Trolox (Cai et al., 2016). In evaluating the inhibition of lipid peroxidation through the determination of the anti-lipid peroxidation capacity of the linoleic acid system, both n-butanol extract and ethyl acetate extract of *C. tinctoria* were more effective than ascorbic (Zhang et al., 2019). Marein, flavanomarein, and *C. tinctoria* extract reduced the levels of malondialdehyde (MDA) and ROS while increasing SOD and GSH-Px activities in the cell supernatant.(Guo et al., 2022; Zhao et al., 2025a). Among them, marein, flavanomarein, *C. tinctoria* polysaccharides and extracts were most effective to protect against the high glucose-induced damage of HUVEC cells by reducing the expression of VEGF ICAM-1 and MCP-1, and inhibiting the proliferation and migration of vascular endothelial cells (Shen et al., 2021; Zhu et al., 2026a). Gavage administration of 100–400 μg/kg/d *C. tinctoria* extract to streptozotocin (STZ)-induced diabetic rats was demonstrated to enhance the activity of SOD and Glutathione Peroxidase (GPO) in rat serum leading to a reduction of the content of MDA (Shu et al., 2017a). In another study, a dose of 0.2 g/kg/d, *C. tinctoria* extracted in water, methanol or ethanol increased GSH and SOD activity and reduced MDA levels. (Zhang et al., 2017).

In a high glucose-induced HUVEC model, a *C. tinctoria* fraction containing marein, flavanomarein, isochlorogenic acid A, dicaffeoylquinic acids, coreopsin, flavanocorepsin, luteolin-7-*O*-glucoside, 5, 7, 3′,5′,-tetrahydroxyflavanone-*O*-hexoside, and other polyphenolic compounds, upregulated IRS-1, Akt, and eNOS expression and increased the levels of p-IRS-1^{Ser307}, p-Akt ^{Ser473}, and p-$eNOS^{Ser1177}$, while reducing NOX4, TNF-α, IL-6, sVCAM, sICAM, and NF-κB expression ($P < 0.01$) (Li et al., 2020). At dosages of 200–600 mg/kg/d, a n-butanol extract of *C. tinctoria* restored the expression levels of CAT, GSH, GSH-PX, and SOD in STZ-induced hyperglycemic and hyperlipidemic mice (Zhang et al., 2019). In summary, *C. tinctoria* extract and its monomeric compounds can inhibit excessive ROS accumulation in the body thus playing a role in the prevention and treatment of diabetes and its complications by alleviating oxidative stress (Figure 1).

C. tinctoria extracts and marein have demonstrated anti-inflammatory effects in diabetes-associated renal complications, particularly diabetic nephropathy (Yao et al., 2019; Yu et al., 2019). In diabetic rats, *C. tinctoria* extract attenuated renal inflammation, as evidenced by reduced expression of the inflammatory mediators MCP-1 and ICAM-1, together with suppression of renal injury and fibrosis (Yu et al., 2019). Both *C. tinctoria* ethyl acetate extract and marein markedly suppressed high-glucose-induced inflammatory responses. Specifically, they reduced NF-κB and NF-κB p65 activation and MCP-1 expression, indicating that inhibition of the NF-κB/MCP-1 axis is an important anti-inflammatory mechanism (Yao et al., 2019).

2.1.2. Marein-mediated antioxidant and anti-inflammatory effects

Marein, a major bioactive flavonoid of *Coreopsis tinctoria* Nutt., has shown notable anti-inflammatory activity in several experimental models, particularly under hyperglycemic and diabetes-associated pathological conditions. In high-glucose-stimulated rat mesangial HBZY-1 cells, marein attenuated the inflammatory

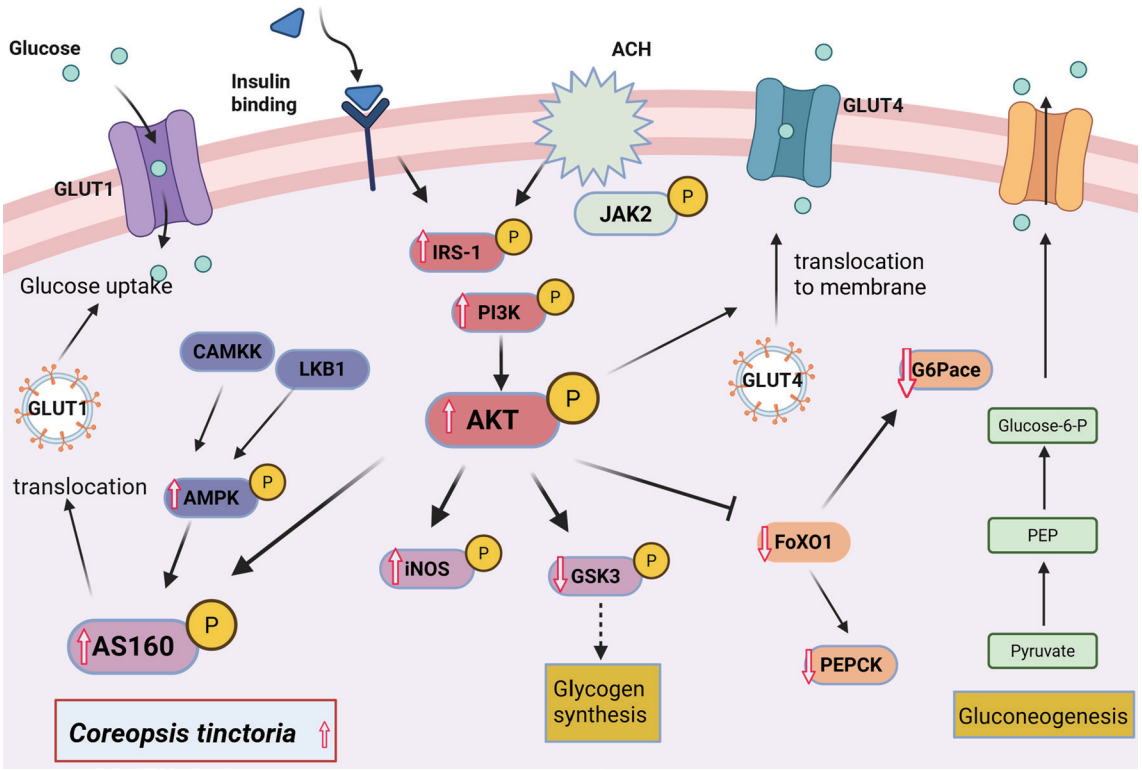


Figure 1. The possible molecular mechanisms of *Coreopsis tinctoria* leading to an improved diabetic insulin resistance.

response by suppressing NF-κB signaling and monocyte chemoattractant protein-1 (MCP-1) expression, while simultaneously activating AMPK and inhibiting TGF-β1/Smad signaling (Yao et al., 2019). Pharmacological modulation of NF-κB further supported this mechanism, as marein enhanced the suppression of NF-κB p65 and MCP-1 produced by an NF-κB inhibitor, suggesting that the NF-κB/MCP-1 axis represents an important target underlying its anti-inflammatory action. Because MCP-1 promotes monocyte/macrophage recruitment and activation in diabetic kidneys, its inhibition may contribute to the attenuation of chronic renal inflammation and subsequent fibrotic remodeling. Marein also decreased fibronectin and collagen IV in this model, indicating a close interaction between its anti-inflammatory and antifibrotic activities during diabetic nephropathy (Yao et al., 2019). These cellular findings are supported by *in vivo* evidence in db/db mice, in which long-term administration of marein ameliorated renal dysfunction, glomerulosclerosis, and ectopic lipid accumulation and, importantly, reduced renal expression of the pro-inflammatory mediators IL-6 and MCP-1 (Guo et al., 2020). Mechanistically, marein directly inhibited renal sodium-glucose cotransporter 2 (SGLT2) and enhanced activation of the AMPK/ACC/PGC-1α pathway, thereby improving glucose/lipid metabolic disturbances in the diabetic kidney. Concomitant decreases in IL-6 and MCP-1, together with reduced fibronectin and collagen I, suggest that the metabolic, anti-inflammatory, and antifibrotic effects of marein are closely interconnected. These findings are particularly relevant because they extend the anti-inflammatory activity of marein from HG-stimulated cell systems to an established animal model of type 2 diabetes and diabetic nephropathy (Guo et al., 2020).

In a high glucose-induced inflammatory injury model, marein inhibited excessive ROS generation and NF-κB activation, along with reduced apoptosis and extracellular matrix degradation in human nucleus pulposus cells exposed to high glucose (Yao et al., 2020). High glucose increased MMP-3 and MMP-13 and decreased collagen II and aggrecan, whereas marein ameliorated these alterations. These observations suggest that suppression of the ROS/NF-κB axis may represent a more general mechanism through which marein protects tissues from chronic hyperglycemia-associated cellular injury (Yao et al., 2020). Additional evidence for a direct anti-inflammatory action of marein comes from the study by Li et al. (2022), in which this investigation employed an LPS-induced inflammatory model. In RAW264.7 macrophage/osteoclast precursor cells, marein dose-dependently suppressed LPS-induced production of TNF-α, IL-1β, PGE2, and COX-2, while reducing RANK, TRAF6, MMP-9, cathepsin K, and carbonic anhydrase II expression. Marein also inhibited phosphorylation of IκBα and activation of NF-κB. More specifically, marein decreased the p-IκBα/IκBα ratio and reduced TNF-α, IL-1β, PGE2, and COX-2, supporting inhibition of IκBα phosphorylation/NF-κB signaling as a key molecular basis for its anti-inflammatory activity. This model has demonstrated the independent mechanistic evidence that marein can directly interfere with NF-κB-mediated inflammatory signaling (Li et al., 2022).

Taken together, existing evidence indicates that NF-κB is one of the most consistently implicated inflammatory signaling pathways targeted by marein, resulting in reduced expression of chemokines, cytokines, and inflammatory enzymes, including MCP-1, IL-6, TNF-α, IL-1β, COX-2, and PGE2. The effects of marein on AMPK activation and ROS suppression may further contribute to the modulation of NF-κB signaling, thereby linking improvements in cellular energy metabolism and oxidative stress with the attenuation of inflammatory responses. In diabetic complications such as nephropathy, this anti-inflammatory activity is closely associated with the inhibition of TGF-β/Smad signaling

and extracellular matrix accumulation, which may help attenuate the progression from chronic metabolic stress and inflammation to renal fibrosis. Overall, the available evidence supports marein as an important anti-inflammatory constituent of *C. tinctoria*, particularly in hyperglycemia-associated renal injury. However, most of the mechanistic evidence remains preclinical, and further studies are needed to clarify its molecular targets, establish pharmacologically relevant exposure levels, and determine its anti-inflammatory efficacy in humans.

2.2. Effects of C. tinctoria and marein on glucose and lipid metabolism

Glucose metabolism disorders are characterized by functional abnormalities in hormonal or enzymatic regulation and pathological changes in tissues and organs involved in glucose, fructose, and other carbohydrate metabolism. (Fadaka et al., 2017). Lipid metabolism disorder refers to the abnormal levels of lipids and their metabolites in the blood and tissues of the body (Galicia-Garcia et al., 2020; Lu et al., 2024). Glucose and lipid metabolism disorder can damage human organs. Therefore, correcting glucose and lipid metabolism disorder is one of the important means of treating diabetes. In recent years, it had been have found that marein increases glucose uptake in high glucose-induced HepG2 cells, and improves hexokinase activity and glycogen synthesis (Jiang et al., 2018). At a dose of 50–100 μmol/L, kaempferol significantly improved glucose consumption impairment caused by palmitic acid treatment in L02 cells leading to normal growth of L02 cells (Huangfu et al., 2024). In rat or mouse models, it has been demonstrated that aqueous and ethyl acetate extracts of *C. tinctoria* can improve STZ-induced glucose intolerance in rats (Dias et al., 2010; Dias et al., 2010a). In another study, *C. tinctoria* and Kaempferol significantly decreased body weight and the levels of fasting blood glucose in DIO mice. They also improved glucose tolerance and significantly reduced HbA1c levels, restored gut microbiota balance and significantly increased the abundance of *Desulfovibrio* and *Butyricimonas*, which have been associated with improved glucose metabolism and intestinal health. (Zhang et al., 2022). In alloxan-induced diabetic mice, *C. tinctoria* extract at 0.75–3 g/kg/d reduced blood glucose and glycated serum protein (GSP) levels in a dose-dependent manner, improved glucose tolerance, and reduced the area under the glucose tolerance curve (Fan et al., 2013). Both ethanol extract (0.4–1.6 g/kg/d) and water extract (0.3–1.2 g/kg/d) of *C. tinctoria* reduced glycated hemoglobin (HbA1c), levels of total cholesterol (TC), triglycerides (TG), and low-density lipoprotein cholesterol (LDL-C) and increased high-density lipoprotein cholesterol (HDL-C) levels in SD rats (Lan et al., 2014). Also an ethyl acetate extract of *C. tinctoria* (0.15 g/kg/d) effectively reduced random blood glucose and serum TG and LDL levels in diabetic rats (Zhang et al., 2015). Also, the positive effects of ethyl acetate extract of *C. tinctoria* on lipid metabolism were demonstrated by reduced lipid accumulation in hepatocytes and decreased formation of fat vacuoles in liver slices. (Jiang et al., 2018). Another study showed that the aqueous extract of *C. tinctoria* (0.1 g/kg/d) significantly increased adiponectin and HDL-C levels in KKAy type 2 diabetic mice (Wu et al., 2017).

Marein improved high glucose-induced insulin resistance in HepG2 cells by promoting glucose uptake through the CaMKK/AMPK/GLUT1 pathway, enhancing glycogen synthesis via the IRS/Akt/GSK-3β pathway, and suppressing gluconeogenesis through the Akt/FoxO1 pathway. Notably, marein significantly increased the phosphorylation of AMP-activated protein kinase (AMPK) and the 160-kDa Akt substrate (AS160), thereby enhancing GLUT1 translocation to the plasma membrane (Jiang et al, 2016a). In H_2O_2-induced oxidative stress in HepG2 cells, marein alleviated oxidative damage and lipid accumulation by reducing ROS, MDA, TC, TG, and LDL-C levels while increasing cell viability, SOD, GSH-Px, and HDL-C levels. These effects were potentially mediated by activation of the SIRT1/Nrf2 signaling pathway (Zhao et al., 2025a).

In summary, marein and different extracts of *C. tinctoria* were able to improve glucose and lipid metabolism disorders and thus play a regulatory role in diabetes-related indicators.

2.3. Effects on insulin sensitivity and reduce insulin resistance

Insulin resistance (IR) refers to the decreased efficiency of insulin in promoting glucose uptake and utilization due to decreased sensitivity of target organs and their receptors to insulin. In the IR state, the body compensates by secreting excessive insulin to produce hyperinsulinemia in order to maintain blood glucose homeostasis (Reaven, 2005). Therefore, improving IR has become an important strategy for controlling and reducing the incidence of diabetes. Pancreatic β cells regulate blood glucose by secreting insulin. When the function of pancreatic β cells is impaired or number of cells decreases, it leads to abnormal insulin secretion, thereby causing hyperglycemia symptoms. In animal models, alcoholic and aqueous extracts of *C. tinctoria* reduced fasting blood glucose and serum insulin levels, increased insulin sensitivity, and alleviated insulin resistance (Lan et al., 2014; Zhang et al., 2016). Water extract of *C. tinctoria* (0.2 g/kg/d) reduced fasting blood glucose and serum insulin in KKAy type 2 diabetic mice and increased insulin sensitivity index (Zhang et al., 2016). At 100–400 μg/(g/d), *C. tinctoria* extract reduced fasting blood glucose and 2 h postprandial blood glucose in diabetic rats, and significantly promoted insulin secretion, leading to improved pancreatic tissue morphology thus protecting pancreatic β cells (Shu et al., 2017a). The extraction of *C. tinctoria* in ethyl acetate (300–600 mg/kg) increased the insulin sensitivity index and improved insulin tolerance (Jiang et al., 2018). In a high fat diet-induced obese C57BL/6J mouse model, it has been demonstrated that water extract of *C. tinctoria* improved energy metabolism and alleviated obesity-induced hyperglycemia at dosages of 4 and 10 g/kg/d, exhibiting the best recovery effect of insulin sensitivity at 4 g/kg/d (Huangfu et al., 2024). The dosage in this study is very high for human consumption, but the concentrations of bioactive components in *C. tinctoria* were not listed and served as preliminary evaluation needed to find an optimal lower dose (Huangfu et al., 2024). These studies showed that extracts or components of *C. tinctoria* can regulate blood glucose and insulin-related indicators by modulating pancreatic β-cell function and improving insulin resistance.

A number of studies have revealed that marein has improved insulin sensitivity and reduced insulin resistance (Li et al., 2021; Zhang et al., 2022, 2024). In an 8-week study using db/db mice, marein administration significantly reduced fasting blood glucose and blood lipid levels by improving insulin resistance, increasing serum adiponectin levels, and alleviating glucose and lipid metabolism disorders (Li et al., 2021). Marein also ameliorated glomerular and tubular basement membrane thickening, glomerulosclerosis, and tubular fibrosis, thereby improving renal insufficiency, protecting kidney function, and delaying pathological progression. Furthermore, marein increased PI3K expression and Akt phosphorylation at Ser473, as well as the LC3-II/LC3-I ratio and the expression of Beclin1 and ATG5. It also increased FGFR1 expression in the kidneys and serum levels of FGF21 and FGF. These findings suggest that marein protects renal function

in diabetic mice and may alleviate diabetic nephropathy by improving insulin resistance through the IRS1/PI3K/Akt signaling pathway (Li et al., 2021). In an *in vitro* study, Marein improved high glucose-induced insulin resistance in HepG2 cells by promoting glucose uptake through the CaMKK/AMPK/GLUT1 pathway, enhancing glycogen synthesis via the IRS/Akt/GSK-3β pathway, and suppressing gluconeogenesis through the Akt/FoxO1 pathway (Jiang et al., 2016).

2.4. Regulation of related enzyme activity and gene/protein expression

Glucose transporters are encoded by the *SLC2* (Solute carrier family 2) gene family and belong to the major facilitator superfamily of membrane transport proteins. They are key regulators of glucose flux and contribute to tissue-specific glucose uptake and metabolism in the liver, skeletal muscle and adipose tissue, thereby maintaining blood glucose homeostasis. To date, 14 types of glucose transporter isoforms have been identified, among which glucose transporter 4 (GLUT4) is the most important glucose transporter in adipocytes and myocytes. Therefore, insulin-regulated GLUT4 membrane transport is crucial for maintaining blood glucose homeostasis (Cueto-Ureña et al., 2026; Wang et al., 2025).

The fractionation of *C. tinctoria* by Li et al. (2020) yielded fraction A-2-2 mainly containing coreopside, marein, luteolin-7-*O*-glucoside and 3′,5,5′,7-tetrahydroxyflavanone-*O*-hexoside,,and fraction A-2-3, mainly containing zephyranin-7-*O*-β-D-glucopyranoside, polyphenols, flavonoid, isochlorogenic acid A, dicaffeoquinic acid and coreopside. Both fractions upregulated the expression of IRS-1, Akt and iNOS in the high glucose-induced HUVEC model, and increased the levels of p-IRS-1, Ser307, p-Akt-Ser473 and p-iNOS, Ser1177, thereby playing a protective role against endothelial dysfunction (Li et al., 2020). In another study, *C. tinctoria* extract at 100–400 mg/kg/d promoted the expression of regulatory factors insulin receptor substrate 1 (IRS-1), phosphatidylinositide 3-kinase (P13K), and GLUT4 protein, and improved insulin resistance in diabetic rats through the IRS-1/P13K/GLUT4 signaling pathway (Shu et al., 2017b). The ethanol extract of *C. tinctoria* had been demonstrated to regulate the protein and gene expression of Toll-like receptor 4 (TLR4), NF-κB, MAPK and cyclooxygenase 2 (COX-2) in the liver tissue of mice fed a high-fat diet, leading to reduced liver inflammation and oxidative stress (Abdurehman et al., 2023). In db/db mice, *C. tinctoria* ethanol extract reduced 24-h urinary albumin excretion alleviated pathological fibrotic kidney damage, and reduced the expression of miR-192 and miR-200b in mouse kidneys, thereby further regulating the expression of downstream proteins PI3K p85α, P-AKT, P-smad3 and COL4α1 to protect the kidneys of diabetic mice (Yu et al., 2019). In db/db mice, 15 weeks of treatment with the flavonoid-rich fraction of *C. tinctoria* (CTF) markedly improved glucose and lipid metabolism, as reflected by normalized glucose, insulin, glucagon, and HbA1c levels and improved profiles of total cholesterol, triglycerides, LDL, and nonesterified fatty acids. CTF also improved hepatic function, as indicated by changes in ALT and AST levels. Integrated transcriptomic and network pharmacology analyses revealed that CTF regulated 48.2% of the 6,357 genes dysregulated in db/db mice, with mitochondrial electron transport and the tricarboxylic acid (TCA) cycle identified as major affected pathways. Collectively, these findings suggest that CTF exerts antidiabetic effects partly by restoring hepatic mitochondrial metabolism and correcting mitochondrial dysfunction-associated metabolic disturbances (Ma et al., 2023).

Marein is a main bioactive component of *C. tinctoria*, or dominant in many species of *C. tinctoria* species (Zhou et al., 2026; Zhu et al., 2026b). It had been demonstrated that marein activated the phosphorylation of AMP-activated protein kinase (AMPK) and Akt substrate 160 kDa (AS160) in HepG2 liver cancer cells, causing an enhanced translocation of glucose transporter 1 (GLUT1) to the cell membrane, thus improving glucose uptake. Also, the phosphorylation of insulin receptor substrate (IRS-1) and GSK-3β was inhibited which led to an increase of glycogen synthesis via reduced expression levels of FoxO1, G6Pase and PEPCK, thereby inhibiting gluconeogenesis (Jiang et al., 2016a).

Thus, *C. tinctoria* extract and its components such as marein can play an anti-diabetic role by improving insulin resistance and inhibiting inflammation via regulation of protein expression and multiple signaling pathways.

2.5. Other mechanisms of action

The ethanol and water extracts of *C. tinctoria* inhibited α-glucosidase activity, with IC_{50} concentrations of 0.067 ± 0.004 and 0.125 ± 0.005 mg/mL, respectively, which were slightly higher than the IC_{50} of acarbose (0.038 ± 0.003 mg/mL) (Cai et al., 2016). *In vivo* studies have found that the extract of *C. tinctoria* can regulate 48.2% of 6357 disordered genes in the mitochondrial electron transport chain and tricarboxylic acid cycle of db/db mice. After dietary intervention with *C. tinctoria* extract, 11 genes in mitochondrial metabolism (*Slc2a2, Ogt, Cd36, Cd36, Cd36, Cd36, Cd36, Cd36, Slc27a4, Slc27a4, Slc27a4*) were improved to varying degrees (Ma et al., 2023). Marein (50 mg/kg/d) alleviated and corrected liver and pancreatic tissue morphology and damage in db/db mice, reduced the expression of liver autophagy-related protein P62, and increased the expression levels of LC3II/I, Beclin1 and ATG5, thus alleviating diabetic conditions (Zhang et al., 2024; Li, Tao, Mao, 2021; Li et al., 2021). *C. tinctoria* extract and its monomeric compounds also inhibited α-glucosidase, regulating cell autophagy, improving mitochondrial dysfunction and tissue morphology. The biological activity of *C. tinctoria* and its components in different cell and animal models are summarized in Table 1.

3. The mechanism of *C. tinctoria* in combating diabetic complications

Diabetes is a metabolic disorder primarily characterized by persistently elevated blood glucose levels. Its etiology is complex, involving a combination of genetic factors, environmental factors, and lifestyle choices. If diabetes is poorly controlled, it can lead to a wide range of complications. These complications are broadly categorized into two main groups: microvascular complications and macrovascular complications. Common microvascular complications include diabetic nephropathy, diabetic retinopathy, and diabetic neuropathy. Macrovascular complications encompass cardiovascular diseases—such as coronary heart disease and stroke—as well as peripheral vascular diseases, including lower-extremity arteriosclerosis, vascular stenosis, or vascular occlusion (Galicia-Garcia et al., 2020; Zhao et al., 2026). The biological activity of *C. tinctoria* and its components against conditions of diabetic nephropathy, cardiomyopathy, retinopathy, and encephalopathy in different cell and animal models are summarized in Table 2.

3.1. Diabetic nephropathy

Diabetic nephropathy is one of the microvascular complications

Table 1. Mechanism of anti-diabetic action of *C. tinctoria*

Biological activity	*C. tinctoria* and its components	Dosage	Cell/Animal model	Dosing method/ Timing	Mechanism of action
Antioxidant and anti-inflammatory	Marein	5 μmol/L	H_2O_2-treated HepG2 cells	Incubation with compounds for 24 h	Reduced levels of MDA, ROS, and LDH; increased SOD and GSH-Px activities; restored SIRT1 and Nrf2 levels decreased expression of inflammatory factors VEGF, ICAM-1, and MCP-1 (Zhao et al., 2025a)
	Marein	10, 25, 50 μmol/L	Chondrocytes	Incubation with compounds for 24 h	Enhanced Nrf2 phosphorylation, induced HO-1 and NQO1 expression, inhibited NO synthesis, suppressed activation of NF-κB pathway (Yin et al., 2025)
	C. tinctoria extract	100, 200, 400 μg/g	Wistar rats	Gavage for 4 weeks	Reduced blood glucose and MDA levels; increased SOD and GSH-Px activities in diabetic rats (Shu et al., 2017)
	Water, methanol, and ethanol extracts of *C. tinctoria*	0.2 g/kg	Wistar rats	Gavage for 4 weeks	Increased serum GS, SOD, IND, and CP levels; reduced MDA levels (Zhang et al., 2017)
	C. tinctoria extract	1, 2, 4 g/kg	Kunming mice	Gavage for 14 d	Increased SOD activity; decreased MDA levels (Huangfu et al., 2024)
	n-Butanol extract of *C. tinctoria*	200, 400, 600 mg/kg bw	T2DM mice	Gavage for 28 d	Increased CAT, GSH, GSH-Px, and SOD activities (Zhang et al., 2019)
Improvement of glucose and lipid metabolism disorders	Marein	5, 10, 20, 40 μmol/L	HepG2 cells	Incubation for 24 h	Promoted glucose uptake; increased hexokinase activity and glycogen synthesis; reduced PEPCK and G6Pase expression; regulated glucose metabolism pathways (Jiang et al., 2018)
	Kaempferol	1.5625, 3.125, 6.25, 12.5, 25, 50, 100 μmol/L	L02 cells	Incubation for 24 h	Improved impaired glucose consumption (Huangfu et al., 2024)
	C. tinctoria extract	0.75, 1.5, 3 g/kg	ICR mice	Gavage for 30 d	Reduced fasting blood glucose and glycated serum protein; decreased serum TC and TG levels (Fan et al., 2013)
	C. tinctoria extracts	Ethanol extracts: 0.4, 0.8, 1.6 g/kg; water extracts: 0.3, 0.6, 1.2 g/kg	SD rats	Gavage for 4 weeks	Reduced levels of HbA1c, TG, TC, and LDL-C; increased HDL-C levels (Lan et al., 2014)
	Ethyl acetate extract of *C. tinctoria*	0.15, 0.3, 0.6 g/kg	SD rats	Gavage for 4 weeks	Reduced levels of blood glucose, HbA1c, TG, and LDL (Zhang et al., 2015)
	Water extract of *C. tinctoria*	4 g/kg	DIO mice	Gavage for 8 weeks	Improved glucose tolerance and metabolism, reduced HbA1c levels, restored gut microbiota balance (Zhang et al, 2022)
	Kunlun snow chrysanthemum water extract	0.1, 0.2, 0.4 g/kg	KKAy mice	Gavage for 35 d	Increased adiponectin, resistin, and HDL-C levels; decreased TC, TG, and LDL-C levels (Wu et al., 2017)

(continued)

Table 1. *(continued)*

Biological activity	*C. tinctoria* and its components	Dosage	Cell/Animal model	Dosing method/ Timing	Mechanism of action
Improvement of insulin resistance	Marein and *C. tinctoria* polysaccharides	Marein: 100, 200, 400 μmol/L; polysaccharides: 25, 50, 100, 200 μg/mL	MIN6 cells	Incubation for 24 h	Increased cell proliferation and insulin secretion; decreased Bax expression; increased Bcl-2 expression (Liu et al., 2017)
	Ethanol and water extracts of *C. tinctoria*	Ethanol extract: 0.4, 0.8, 1.6 g/kg; water extract: 0.3, 0.6, 1.2 g/kg	SD rats	Gavage for 4 weeks	Reduced levels of fasting blood glucose and serum insulin; increased insulin sensitivity index (Lan et al., 2014)
	Water extract of *C. tinctoria*	0.1, 0.2, 0.4 g/kg	KKAy mice	Gavage for 5 weeks	Reduced fasting blood glucose and serum insulin levels; improved insulin sensitivity (Zhang et al., 2016)
	Kunlun snow chrysanthemum extract	100, 200, 400 μg/g	Wistar rats	Gavage for 4 weeks	Reduced fasting and 2-h postprandial blood glucose; promoted insulin secretion; protected pancreatic β-cells (Shu et al., 2017a)
	Ethyl acetate extract of *C. tinctoria*	150, 300, 600 mg/kg	SD rats	Gavage for 8 weeks	Reduced blood glucose and insulin levels; increased insulin sensitivity index; improved insulin tolerance (Jiang et al., 2018)
	Water and ethanol extracts of *C. tinctoria*	4, 10 g/kg bw	C57BL/6J mice	Gavage for 8 weeks	Increased serum insulin levels; improved glucose tolerance and insulin tolerance (Huangfu et al., 2024)
Regulation of enzymes and gene/protein expression	Marein	5, 10 μmol/L	HepG2 cells	Incubation for 24 h	Promoted glucose uptake via CaMKK/AMPK/GLUT1; increased glycogen synthesis via IRS/Akt/GSK-3β; reduced gluconeogenesis via Akt/FoxO1, improved insulin resistence in HepG2 cells induced by high glucose (Jiang et al, 2016a)
	Active fractions of *C. tinctoria*	6.25, 12.5, 25, 50 μg/mL	HUVEC cells	Incubation for 24 h	Upregulated IRS-1, Akt, and eNOS expression; increased phosphorylation levels; improved endothelial function via JAK2/IRS-1/PI3K/Akt/eNOS pathway (Li et al., 2020)
	Kunlun snow chrysanthemum extract	100, 200, 400 mg/kg	Wistar rats	Gavage for 4 weeks	Improved insulin resistance through IRS-1/PI3K/ GLUT4 signaling pathway (Shu et al., 2017b)
	C. tinctoria extract	150, 300 mg/kg/d	C57BL/6J mice	Gavage for 8 weeks	Suppressed hepatic inflammation via NF-κB/iNOS/ COX-2/NLRP3/MAPK; improved oxidative stress via Nrf2/HO-1 pathway (Abdurehman et al., 2023)
Improvement of mitochondrial dysfunction	*C. tinctoria* extract	200, 400 mg/kg bw	db/db mice	Gavage for 15 weeks	Regulated mitochondrial electron transport chain and TCA cycle; affected 48.2% of dysregulated genes in db/db mice (Ma et al., 2023)
Autophagy regulation	Marein	50 mg/kg	db/db mice	Gavage for 8 weeks	Improved liver and pancreas morphology; decreased P62 expression; increased LC3II/I, Beclin1, and ATG5 expression (Zhang et al., 2024)
Autophagy regulation	Marein	50 mg/kg	db/db mice	Gavage for 8 weeks	Upregulated PI3K/Akt phosphorylation, LC3-II/I, Beclin1, ATG5, and renal FGFR1 expression; increased serum FGF21 and FGF23 levels (Li et al., 2021)

Table 2. Mechanism of anti-diabetic complication of *C. tinctoria*

Biological activity	*C. tinctoria* and its components	Dosage	Cell/animal model	Dosing method/Timing	Mechanism of action
Diabetic nephropathy	Ethyl acetate extract of *C. tinctoria*	25, 50, 100, 150 mg/L	HBZY-1 cells	Incubation for 24 h	Inhibited proliferation of rat glomerular mesangial cells induced by high glucose and reduced mRNA and protein expression of TGF-β1 and collagen IV (Yao et al., 2017)
	C. tinctoria flavonoids	25, 50, 100 μg/mL	HBZY-1 cells	Incubation for 24 h	Suppressed mesangial fibrosis by regulating the TGF-β1/Smads/Nox4 signaling pathway and reduced fibronectin and α-SMA expression (Zhang et al., 2018)
	Flavanomarein	1, 10, 20, 40, 60, 80 μmol/L	HK-2 cells	Culture for 24 h	Inhibited epithelial–mesenchymal transition (EMT) by decreasing α-SMA, fibronectin, and vimentin expression through inhibition of the Syk/TGF-β1/Smad pathway (Zhang et al., 2020)
	Marein	66 μmol/L	HK-2 cells	Culture for 6 h	Inhibitd SGLT2 expression and reduced glucose analogue uptake; increased p-AMPK/pACC to ameliorate high-glucose-induced cellular dysfunction (Guo et al., 2020)
	Marein	3, 10 μmol/L	HRGEC cells	Culture for 24 h	Increased PI3K and p-AKT (Ser473)/AKT and LC3 protein levels while decreasing p62 expression (Li et al., 2022)
	Ethyl acetate extract of *C. tinctoria*	150, 300, 600 mg/kg	SD rats	Gavage for 4 weeks	Reduced expression of pro-inflammatory cytokines MCP-1 and ICAM-1; decreased fibronectin and collagen IV and inhibitd the TGF-β1/Smad pathway to alleviate renal hypertrophy and fibrosis (Yao et al., 2015)
	Ethyl acetate extract	300 mg/kg	SD rats	Gavage for 4 weeks	Alleviated renal tubular dilation, glomerular shrinkage, inflammatory cell infiltration, and basement membrane thickening; decreased renal Vimentin, α-SMA, TGF-β1, and p-Smad2 expression (Jiang et al., 2019)
	Ethanol extract	300 mg/kg	db/db mice	Gavage for 10 weeks	Reduced 24-h urinary albumin excretion and renal injury; down-regulated miR-192 and miR-200b while increased ZEB2 expression, thereby modulating the PTEN/PI3K/AKT pathway to attenuate renal fibrosis (Yu et al., 2019)
	Ethyl acetate extract	150, 300, 600 mg/kg	SD rats	Gavage for 4 weeks	Suppressed α-SMA expression and renal fibrotic deposition via the RhoA/ROCK/Nox4 signaling pathway, thereby attenuating early renal injury (Yao et al., 2019)
	Marein	50 mg/kg/day	db/db mice	Gavage for 12 weeks	Inhibitd SGLT2 expression, activated AMPK/ACC/PGC-1α signaling, and suppressed IL-6, MCP-1, FN, and COL1 expression (Guo et al., 2020)
	Marein	50 mg/kg	db/db mice	Gavage for 12 weeks	Improved glomerular and tubular basement membrane thickening, glomerulosclerosis, and tubular fibrosis by regulating the PI3K/Akt signaling pathway and improved insulin resistance (Song et al., 2023)

(continued)

Table 1. *(continued)*

Biological activity	*C. tinctoria* and its components	Dosage	Cell/animal model	Dosing method/Timing	Mechanism of action
	Marein	50 mg/kg	db/db mice	Gavage for 8 weeks	Reduced fibronectin, vimentin, TGF-β, and FGFR1 expression while increasing CD31 expression (Zhang et al., 2023)
Diabetic cardiomyopathy	Marein	25, 50, 100 mg/kg	isoproterenol-stimulated mice	Gavage for 8 weeks	Reduced the protein expression levels of α-smooth muscle actin, collagen type I, and collagen type III; decreased the protein levels of TGF-β1, HIF-1α, p-Smad2/3, and total Smad2/3. (Niu et al., 2024)
	Marein	50 mg/kg	db/db mice	Gavage for 8 weeks	Improved myocardial hypertrophy, reduced collagen fiber deposition, and decreased expression of FN1, vimentin, and TGF-β1 in myocardial tissue (Tian et al., 2024)
Diabetic retinopathy	Active fraction of *C. tinctoria*	150, 300 mg/kg	db/db	Gavage for 10 weeks	Attenuates oxidative stress, down-regulates VEGF and ICAM-1, and increased Bcl-2 expression, and up-regulates LC3 and Bcl-2 in high-glucose-treated HUVEC cells (Li et al., 2021)
	Marein	50, 100, 200 μmol/L	HRMEC cells (CP-H130)	Incubation	Reduced apoptosis, Bax and LDH levels, and MDA content, increased Bcl-2 levels, and SOD activity (Jin et al., 2023)
	Marein	50 mg/kg	db/db mice	Gavage for 12 weeks	Lowerd blood glucose, TG, TC, and LDL levels; alleviated pathological retinal changes (retinal edema, cell shrinkage, abnormal nuclear morphology); suppressed expression of VEGF, PI3K, fibrin and spleen tyrosine kinase; increased the of epithelial marker E-cadherin expression (Song et al., 2023)
Diabetic encephalopathy	Marein	1.25, 2.5, 5, 10, 20, 40 μmol/L	PC12 cells	Drug-containing culture for 24 h	Attenuated MG-induced mitochondrial dysfunction, increased GlO1 activity, p-AMPKα (Thr172), and Bcl-2 expression, and reduced Bax, caspase-3, and ICAD activity (Jiang et al., 2016)
	Water extract	500, 2,000 mg/kg	Kunming mice	Gavage for 6 weeks	Reduced oxidative stress, regulated acetylcholine (ACh) levels and acetylcholinesterase (AChE) activity, and improved cholinergic system function (He et al., 2020)
	C. tinctoria flavonoids	50, 100, 200 mg/kg	SHR rats (SPF)	Gavage for 11 weeks	Lowered blood pressure, increased SOD, GSH, CAT, reduced ROS accumulation, suppressed TNF-α, IL-1β, IL-6 and Ang-II, alleviated cognitive impairment and histopathological alterations (Wu et al., 2026)

of diabetes. It is a secondary kidney disease characterized by glomerular sclerosis and is also the main cause of end-stage renal failure (Jha et al., 2024). Diabetic nephropathy has a high impact on irreversible kidney damage, which is an important cause of death in patients with type I and type II diabetes. Studies have shown that the ethyl acetate extract and flavonoid extract of *Coreopsis lanceolata* can exert a protective effect on diabetic nephropathy by inhibiting fibrosis of the glomerular mesangium induced by high glucose and high lipid in rats (Yao et al., 2017; Zhang et al., 2018).

In db/db mice with diabetic nephropathy, *C. tinctoria* alcohol extract improved metabolic abnormalities and renal injury, as evidenced by reductions in body weight, fasting blood glucose, HbA1c, and 24-h urinary albumin excretion, together with attenuation of renal pathological fibrosis. Mechanistically, diabetic nephropathy was associated with increased renal miR-192 and miR-200b expression and reduced expression of their target proteins ZEB2 and PTEN, accompanied by activation of the PI3K/AKT and Smad3 pathways and increased COL4α1 expression. The treatment with *C. tinctoria* alcohol extract reversed these molecular alterations, increasing PTEN while reducing PI3K p85α, p-AKT (Ser473), p-Smad3 (Ser425), and COL4α1 expression. Collectively, these findings suggest that *C. tinctoria* extract protects against diabetic nephropathy by alleviating collagen accumulation and renal fibrosis, potentially through modulation of the miR-192/ZEB2/PTEN/PI3K/AKT signaling axis (Yu et al., 2019). Ethyl acetate extracts of *C. tinctoria* at doses of 150 – 600 mg/kg ameliorated the deposition of fibrotic substances in the kidneys of diabetic rats and suppressed the urinary levels of α1-microglobulin (α1-MG), and β2-microglobulin (β2-MG). Furthermore, by modulating the RhoA/Rho-associated kinase (ROCK)/Nox4 signaling pathway, these extracts inhibited the expression of α-SMA in renal tissue and reduced renal fibrotic deposition in diabetic rats, thereby attenuating early-stage renal injury in the animal model (Yao et al., 2019). Similar studies have demonstrated that marein significantly ameliorated the thickening of glomerular and tubular basement membrane, as well as glomerular sclerosis and tubulointerstitial fibrosis in db/db mice (Li, 2020). I*n vitro* experiments have shown that an ethyl acetate extract of *C. tinctoria* at 150–600 mg/kg decreased the expression levels of β2-MG and α1-MG in urine, inhibited the inflammatory and fibrotic process, downregulated the TGF-β1/Smad signaling pathway, and activated renal AMPKα phosphorylation to improve renal hypertrophy and fibrosis (Yao et al., 2015). Electroacupuncture combined with *C. tinctoria* extract induced an alleviation of renal tubular dilation, reduced glomerular shrinkage, improved inflammatory cell infiltration, and reduced the expression of renal fibrosis protein in diabetic rats (Jiang et al., 2019).

Marein improved high glucose-induced cell dysfunction via a suppression of over-expression of SGLT2 and increasing phosphorylation (p)-AMPK/pACC in high glucose-induced HK-2 cells. It exerted its nephroprotective effects by directly inhibiting the expression of SGLT2 in renal tubules and activating the AMP-activated protein kinase (AMPK)/acetyl-CoA carboxylase (ACC)/peroxisome proliferator-activated receptor-γ coactivator-1α (PGC-1α) pathway in db/db mice (Guo et al., 2020). On the other hand, marein increased the expression of p-AKT/AKT in human glomerular vascular endothelial cells (HRGEC) and levels of microtubule-associated protein LC3, thus playing an anti-diabetic nephropathy role (Li et al., 2022).

3.2. Diabetic retinopathy

Diabetic retinopathy is a major and severe microvascular complication of diabetes and is strongly associated with the duration of chronic hyperglycemia. Its progression involves multiple interconnected pathological processes, including metabolic dysregulation, oxidative stress, inflammation, and dysfunction of the retinal neurovascular unit, collectively leading to impaired retinal neurovascular function. Clinically, diabetic retinopathy progresses from early microaneurysms to retinal hemorrhage and ischemia, with ischemia potentially triggering pathological neovascularization and the development of proliferative diabetic retinopathy. Vascular leakage can occur throughout the disease spectrum, leading to diabetic macular edema, while advanced complications include vitreous hemorrhage and tractional retinal detachment. Diabetic retinopathy is also a major cause of new-onset blindness in adults, and diabetes increases the risk of earlier and more frequent glaucoma and cataracts (ADA, 2026; Sood et al., 2023; Lee et al., 2025; Peng et al., 2025).

C. tinctoria extract improved glucose metabolism and attenuated diabetic retinopathy in a db/db diabetic mice study (Li, Tao, Mao, 2021). *C. tinctoria* extract reduced blood glucose and glycosylated hemoglobin levels and alleviated systemic oxidative stress. Histological examination showed that *C. tinctoria* partially preserved retinal architecture and reduced pathological changes, including disorganization of the ganglion cell layer, vacuolar degeneration, and retinal capillary dilation and congestion. At the molecular level, *C. tinctoria* reduced retinal expression of VEGF and ICAM1. It also increased Bcl-2 expression, particularly at the high dose (300 mg/kg), indicating a potential reduction in retinal cell apoptosis. In addition, *C. tinctoria* restored retinal PEDF expression, supporting its potential anti-inflammatory, antioxidant, and retinal-protective effects. Therefore, the findings suggest that *C. tinctoria* protects against diabetic retinopathy through multiple complementary mechanisms, including improvement of hyperglycemia, attenuation of oxidative stress, suppression of VEGF/ICAM1-associated retinal vascular injury, inhibition of apoptosis through Bcl-2, and restoration of the protective factor PEDF (Li et al., 2021). Recently, in a streptozotocin-induced diabetic retinopathy rat model, Zhang et al. (2026) investigated the protective mechanism of *C. tinctoria* from the perspective of the gut–eye axis. Using gut microbiota sequencing, fecal metabolomics, and lipidomics, the study demonstrated that *C. tinctoria* intervention altered the composition and abundance of gut microbiota and improved lipid metabolism. Differential fecal metabolites were predominantly lipids, with *C. tinctoria* particularly alleviating metabolic disturbances in glycerophospholipids and sphingolipids. These findings suggest that *C. tinctoria* may ameliorate diabetic retinopathy by modulating the gut microbiota–lipid metabolism axis and thereby influencing inflammation-related pathways (Zhang et al., 2026).

Marein exhibited a protective effect against high-glucose (HG)-induced injury in human retinal microvascular endothelial cells (HRMECs), suggesting potential therapeutic relevance to diabetic retinopathy. Treatment with marein at low, medium, and high concentrations reduced apoptosis, Bax and LDH levels, and MDA content, while increasing Bcl-2 levels, SOD activity, and SNHG7 expression in a concentration-dependent manner. Mechanistically, SNHG7 overexpression reproduced the protective effects of marein, whereas SNHG7 knockdown attenuated these effects. Collectively, these findings suggest that marein alleviates HG-induced HRMEC injury, at least partly, by upregulating SNHG7 and thereby reducing apoptosis and oxidative stress (Jin et al., 2023). In another study using db/db mice, 12 weeks of marein treatment improved glucose and lipid metabolism, significantly reducing blood glucose, TG, TC, and LDL levels. More importantly, marein alleviated pathological retinal changes associated with diabetic retinopathy, including retinal edema, cell shrinkage, and abnormal nuclear morphology, thereby improving retinal function. Both *in*

vivo and *in vitro* experiments resulted in that marein exerted retinal protective effects by suppressing the expression of VEGF, PI3K, fibrin, and spleen tyrosine kinase, while increasing the expression of the epithelial marker E-cadherin. These findings suggest that marein may ameliorate diabetic retinopathy through both systemic improvement of glucose and lipid metabolism and direct modulation of retinal pathological signaling, particularly VEGF-, PI3K-, and spleen tyrosine kinase-related pathways (Song et al., 2023).

3.3. Diabetic cardiomyopathy

Diabetic cardiomyopathy refers to a myocardial disease in diabetic patients without coronary artery disease, hypertension, valvular heart disease, or congenital heart disease, characterized by abnormal myocardial structure and function (Jia et al., 2018; Li et al., 2024; Quaiyoom and Kumar, 2024). Cardiac cells rely heavily on autophagy to effectively clear abnormal and damaged proteins and organelle functions in order to maintain normal cardiac function (Kobayashi and Liang, 2015).

One of the major key bioactives of *C. tinctoria*, marein alleviated myocardial fibrosis in isoproterenol-stimulated mice. Oral administration of marein at 25–100 mg/kg to the mice resulted in a significant reduction in the protein expression levels of α-smooth muscle actin, collagen type I, and collagen type III. Mechanistically, marein also decreased the protein expression levels of TGF-β1, hypoxia-inducible factor-1α (HIF-1α), p-Smad2/3, and Smad2/3 (Niu et al., 2024). Another study has found that marein reduced the expression of FN1, vimentin, and TGF-β1 in the myocardial tissue of db/db mice, improved myocardial structural damage, and reduced collagen fiber deposition in myocardial tissue (Tian et al., 2024). These findings suggest that marein protects against myocardial fibrosis in diabetic cardiomyopathy, thereby exerting a cardioprotective effect.

3.4. Diabetic encephalopathy

Diabetic encephalopathy (DE) is a central nervous system complication caused by diabetes, characterized by neuroinflammation and abnormal synapsis in the hippocampus, leading to cognitive impairment, decision-making difficulties, and mood disorders (Liu et al., 2018; Xu et al., 2024).

In D-galactose-induced aging mice, *C. tinctoria* bud extract significantly alleviated age-related cognitive impairment and brain aging. The extract restored body weight and brain index, improved general behavioral performance and mobility, and reduced oxidative stress by enhancing GSH-Px, SOD, and total antioxidant capacity while decreasing MDA levels. It also improved learning and memory performance, as demonstrated by reduced escape latency and increased target-quadrant crossing in the Morris water maze. Mechanistically, *C. tinctoria* bud extract partially restored acetylcholine levels and reduced AChE activity. Histological analysis further showed that the extract attenuated hippocampal neuronal loss and karyopycnosis. Therefore, *C. tinctoria* bud extract may protect against brain aging and cognitive impairment through attenuation of oxidative damage, enhancement of antioxidant defenses, restoration of cholinergic function, and preservation of hippocampal integrity (He et al., 2020). Also in a D-galactose-induced aging mice modle, the ethyl acetate extract of *C. tinctoria* improved learning and memory impairment. The protective effects were associated with modulation of oxidative stress, including changes in serum SOD and GSH-Px activities and MDA levels, together with alterations in brain neurotransmitters, particularly glutamate (Glu) and γ-aminobutyric acid (GABA), indicating that *C. tinctoria* extract may alleviate age-related cognitive dysfunction through regulation of systemic oxidative stress and brain neurotransmitter homeostasis (Li et al., 2021a). In high-fat/high-fructose diet-fed mice, *C. tinctoria* flower (CTF) administration improved glycolipid metabolism; alleviated cognitive impairment, particularly spatial and working memory deficits; improved insulin sensitivity; reduced HOMA-IR and excessive weight gain; and also enhanced hippocampal synaptic plasticity and neurotrophic responses. Mechanistically, CTF remodeled the disrupted gut microbiota, reversing the increase in Firmicutes and decrease in Bacteroidetes and increasing potentially beneficial genera such as *Roseburia*, *Akkermansia*, *Bacteroides*, and *Clostridium*, while reducing *Faecalibaculum*. These microbiota changes were accompanied by restoration of tryptophan metabolism and increased microbiota-derived indole metabolites, particularly indole-3-lactic acid (ILA) and indole-3-carboxylic acid (ICA). CTF increased hippocampal tryptophan, ICA, and ILA levels and enhanced aryl hydrocarbon receptor expression. Importantly, depletion of gut microbiota with antibiotics markedly weakened CTF-mediated improvements in cognitive performance, hippocampal postsynaptic density, and ILA/ICA levels, demonstrating that the gut microbiota is critical to the neuroprotective effect (Sun et al., 2027). In spontaneously hypertensive rats with chronic cerebral hypoperfusion, a model of hypertensive vascular dementia, 11-week administration of *C. tinctoria* flavonoids reduced systolic blood pressure, improved cerebral blood flow, alleviated both spatial and non-spatial learning and memory deficits, and also attenuated histopathological damage in memory-related brain regions, including the hippocampal dentate gyrus and corpus callosum. *C. tinctoria* flavonoids enhanced antioxidant defenses by increasing SOD, CAT, and GSH levels and reducing ROS, while suppressing neuroinflammation through inhibiting TNF-α, IL-1β, IL-6, and angiotensin II. Hippocampal transcriptomic analysis further identified multiple regulated pathways, with PI3K–Akt and MAPK signaling among the enriched pathways (Wu et al., 2026).

Methylglyoxal (MG), an endogenous toxic metabolite implicated in diabetic complications, can induce neuronal apoptosis and contribute to diabetic cognitive dysfunction. In MG-treated PC12 cells, marein markedly attenuated neuronal injury by preserving mitochondrial membrane potential and mitochondrial permeability transition pore function, reducing intracellular Ca^{2+} and ROS accumulation, restoring the GSH/GSSG ratio and ATP levels, and decreasing apoptosis. Marein increased glyoxalase I activity and phosphorylation of AMPKα (Thr172). It also increased the anti-apoptotic protein Bcl-2 while suppressing Bax, caspase-3, and ICAD activation. Overall, marein protects neurons against MG-induced damage primarily by preserving mitochondrial function and activating AMPK signaling, thereby reducing oxidative stress and mitochondrial dysfunction and ultimately suppressing neuronal apoptosis (Jiang et al., 2016). In an oxygen–glucose deprivation/reperfusion (OGD/R) model using HT22 neuronal cells, marein exhibited concentration-dependent neuroprotective effects against cerebral ischemia–reperfusion injury. Marein at 10–40 μM significantly improved OGD/R-induced loss of cell viability, restoring cell survival from approximately 40% to 80–90%, while markedly reducing intracellular ROS accumulation. Mechanistically, OGD/R markedly increased PTGS2 expression and Src phosphorylation, whereas marein treatment (20 μM) reduced PTGS2 expression by approximately 35% and the p-Src/Src ratio by approximately 30%. These findings suggest that marein may alleviate CIRI by suppressing PTGS2/SRC-associated inflammatory signaling and oxidative stress (Luo et al., 2025).

4. Concluding remarks

Diabetes has become a prevalent chronic metabolic disease worldwide. Researchers both domestically and internationally are urgently seeking effective drugs for treating diabetes through various channels. Our brief review summarizes recent data of *C. tinctoria* in its role in preventing diabetes which involves eliminating ROS free radicals, regulating glucose and lipid metabolism, increasing insulin sensitivity, inhibiting α-glucosidase, and regulating the expression of related genes and proteins. These effects resulted in lowering blood sugar levels and reduced diabetic pathologies thus suggesting a role in preventing and potentially treating diabetes and its complications. The main bioactive components of *C. tinctoria* were currently identified as flavonoid polyphenols, including marein and other flavonoid glycosides, which are crucial for the prevention and treatment of diabetes and its onset. However, due to the diverse targets of flavonoids and the complexity of their mechanisms of action, these aspects still remain unclear. Current research on *C. tinctoria* is limited to cell and animal experiments, with relatively few clinical studies and insufficient exploration of its molecular mechanisms. Furthermore, the large-scale isolation and research of monomeric compounds in *C. tinctoria* is still incomplete, resulting in a lack of systematic research on the activity and mechanisms of these monomeric compounds. Therefore, exploring its specific composition using modern technology, isolating its monomeric components, and improving the preparation process of these components can provide a foundation for research on the pharmacodynamic material basis, mechanism of action, and structure-activity relationship of *C. tinctoria* in preventing and treating diabetes and its complications. It also provides ideas and references for clinical drug development. However, how to elucidate the mechanisms of action of *C. tinctoria* in preventing and treating diabetes and its complications in cells, more animal, and even clinical settings, under the guidance of modern pharmacological theory, through multiple pathways and levels, is a key issue that urgently needs to be addressed in the development of *C. tinctoria* as natural extract used for prevention or even treatment against diabetes.

Acknowledgments

Authors wish to thank Professor Hui Zhao and Miss Yuxin Wang from Tianjin University of Commerce, Tianjin, China, for their assistance in drawing Figure 1 using BioRender software (www.biorender.com).

References

Abdurehman, D., Guoruoluo, Y., Lu, X., Li, J., Abudulla, R., Liu, G., Xin, X., and Aisa, H.A. (2023). Optimization of preparation method of hepatoprotective active components from *Coreopsis tinctoria* Nutt. and its action mechanism *in vivo*. Biomed. Pharmacother. 167: 115590–115602.

Abdurehman, D., Lu, X., Guoruoluo, Y., Liu, G., Li, J., Wu, T., Xin, X., and Aisa, A. (2026). AI-integrated multi-target validation of *Coreopsis tinctoria* polyphenols as a functional food ingredient against diabetic nephropathy. Foods 15: 2257.

ADA, American Diabetes Association Professional Practice Committee for Diabetes. (2026). 12. Retinopathy, neuropathy, and foot care: Standards of Care in Diabetes—2026. Diabetes Care (Suppl. 1): S261–S276.

Begmatov, N., Li, L., Bobakulov, K., Numonov, S., and Aisa, H.A. (2020). The chemical components of *Coreopsis tinctoria* Nutt. and their antioxidant, antidiabetic and antibacterial activities. Nat. Prod. Res. 12: 1772–1776.

Cai, W., Yu, L.J., Zhang, Y., Feng, L., Kong, S., Tan, H., Xu, H., and Huang, C. (2016). Extracts of *Coreopsis tinctoria* Nutt. flower exhibit antidiabetic effects via the inhibition of α-glucosidase activity. J. Diabetes Res. 2016: 2340276.

Chaudhury, A., Duvoor, C., Reddy Dendi, V.S., Kraleti, S., Chada, A., Ravilla, R., Marco, A., Shekhawat, N.S., Montales, M.T., Kuriakose, K., Sasapu, A., Beebe, A., Patil, N., Musham, C.K., Lohani, G.P., and Mirza, W. (2017). Clinical Review of Antidiabetic Drugs: Implications for Type 2 Diabetes Mellitus Management. Front. Endocrinol. 8: 1–12.

Cueto-Ureña, C., Martínez-Martos, J.M., and Ramírez-Expósito, M.J. (2026). Glucose Transporters: Structure, Trafficking, Physiology, and Disease Relevance. Curr. Issues Mol. Biol. 48(9): 861.

Dias, T., Mota-Filipe, H., Liu, B., Jones, P., Houghton, P.J., and Paulo, A. (2010). Recovery of oral glucose tolerance by Wistar rats after treatment with *Coreopsis tinctoria* infusion. Phytother Res. 24(5): 699–705.

Dias, T., Bronze, M.R., Houghton, P.J., Mota-Filipe, H., and Paulo, A. (2010a). The flavonoid-rich fraction of *Coreopsis tinctoria* promotes glucose tolerance regain through pancreatic function recovery in streptozotocin-induced glucose-intolerant rats. J. Ethnopharmacol. 132(2): 483–490.

Donath, M.Y. (2014). Targeting inflammation in the treatment of type 2 diabetes: time to start. Nat. Rev. Drug Discov. 13: 465–476.

Du, J., Tao, K., and Chen, X. (2026). *Coreopsis tinctoria*-loaded gels for dermal delivery: development, optimization, retention capacity, and skin photoaging repair. Pharm. Develop. Technol. 31(5): 729–743.

Fadaka, A., Ajiboye, B., Ojo, O., Adewale, O., Olayide, I., and Emuowhochere, R. (2017). Biology of glucose metabolization in cancer cells. J. Oncol. Sci. 3(2): 45–51.

Fan, L., Zhang, X., Nan, X., Li, J., Zhou, X., and Gu, J. (2013). Effects of *Kunlun Snow Chrysanthemum* on glucose and lipid metabolism in alloxan-induced diabetic mice. J. Chin. Med. Mater. 36(12): 2011–2013. doi: 10.13863/j.issn1001-4454.2013.12.043.

Galicia-Garcia, U., Benito-Vicente, A., Jebari, S., Larrea-Sebal, A., Siddiqi, H., Uribe, K.B., Ostolaza, H., and Martín, C. (2020). Pathophysiology of type 2 diabetes mellitus. Int. J. Mol. Sci. 21(17): 6275.

GBD 2021 Diabetes Collaborators. (2021). Global, regional, and national burden of diabetes from 1990 to 2021, with projections of prevalence to 2050: a systematic analysis for the Global Burden of Disease Study 2021. Lancet 402(10397): 203–234.

Guo, F., Abulati, A., Wang, J.-W., Jiang, J., Zhang, W.-X., Chen, P.-D., Yao, L., and Mao, X.-M. (2022). Flavonoids of *Coreopsis tinctoria* Nutt alleviate the oxidative stress and inflammation of glomerular mesangial cells in diabetic nephropathy via RhoA/ROCK signaling. J. Funct. Foods. 89: 104955.

Guo, L., Zhang, W., and Li, S. (2023). Research progress on separation and characterization of bioflavonoids from *Coreopsis tinctoria* Nutt. J. Food Bioact. 24: 40–45.

Guo, L., Zhang, W., Ho, C-T., and Li, S. (2015). Chemistry and nutraceutical property of Chrysanthemum (*Coreopsis tinctoria*). J. Funct. Foods. 13: 11–20.

Guo, L., Zhang, W., Wang, L., Shen, J., Ho, C-T., and Li, S. (2025). Anti-fibrotic effects of marein-enriched *Coreopsis tinctoria* flavonoids on CCl_4-induced hepatic fibrosis in rats *via* blocking the TGF-β1/Smad signaling pathway. Food Sci. Human. Wellness 14(9): 9250499.

Guo, Y., Ran, Z., Zhang, Y., Song, Z., Wang, L., Yao, L., Zhang, M., Xin, J., and Mao, X. (2020). Marein ameliorates diabetic nephropathy by inhibiting renal sodium glucose transporter 2 and activating the AMPK signaling pathway in db/db mice and high glucose–treated HK-2 cells. Biomed. Pharmacother. 131: 110684–110698.

Hayat, J., Akodad, M., Moumen, A., Baghour, B., Skalli, A., Ezrari, S., and Belmalha, S. (2020). Phytochemical screening, polyphenols, flavonoids and tannin content, antioxidant activities and FTIR characterization of Marrubium vulgare L. from 2 different localities of Northeast of Morocco. Heliyon 6(11): e05609.

He, X., Tian, Y., Lei, L., Zhi, Q., Zhao, J., and Ming, J. (2020). Protective effects of *Coreopsis tinctoria* buds extract against cognitive impairment and brain aging induced by D-galactose. J. Funct. Foods. 73: 104089–104096.

Huangfu, B., Yang, M., Xu, J., Gao, R., Hu, Y., Zhao, Y., Huang, K., and He,

X. (2024). *Coreopsis tinctoria* improves energy metabolism in obese hyperglycemic mice. Heliyon 10(6): e27449.
IDF diabetes atlas. Brussels: International Diabetes Federation. (2025). https://diabetesatlas.org. Accessed July 3, 2026.
Jha, R., Lopez-Trevino, S., Kankanamalage, H.R., and Jha, J.C. (2024). Diabetes and renal complications: an overview on pathophysiology, biomarkers and therapeutic interventions. Biomedicines 12: 1098.
Jia, G., Hill, M.A., and Sowers, J.R. (2018). Diabetic cardiomyopathy: an update of mechanisms contributing to this clinical entity. Circ. Res. 122(4): 624–638.
Jiang, B., Le, L., Liu, H., Xu, L., He, C., Hu, K., Peng, Y., and Xiao, P. (2016). Marein protects against methylglyoxal-induced apoptosis by activating the AMPK pathway in PC12 cells. Free Rad. Res. 50(11): 1173–1187.
Jiang, B., Le, L., Zhai, W., Wan, W., Hu, K., Yong, P., He, C., Xu, L., and Xiao, P. (2016a). Protective effects of marein on high glucose-induced glucose metabolic disorder in HepG2 cells. Phytomedicine 23(9): 891–900.
Jiang, J., Ablat, A., and Yao, L. (2019). Effects of electroacupuncture combined with *Coreopsis tinctoria* extract on renal expression of vimentin, α-SMA, TGF-β1, and p-Smad2 in rats with diabetic nephropathy. Chin. J. Inf. Tradit. Chin. Med. 26(6): 55–58. doi: 10.3969/j.issn.1005-5304.2019.06.012.
Jiang, B., Lv, Q., Xiang, J., Le, L., Hu, K., Xu, L., and Xiao, P. (2018). Inhibition of metabolic disorders *in vivo* and *in vitro* by main constituent of *Coreopsis tinctoria*. Chin. Herb. Med. 10(02): 157–168. doi: 10.1016/j.chmed.2018.03.004.
Jin, S., Feng, Y., Xie, J., Deng, R., Li, G., and Cui, M. (2023). Marein Alleviates High Glucose-Induced Human Retinal Microvascular Endothelial Cell Injury by Up-Regulating *SNHG7* Expression. Discov. Med. 35(178): 861–867.
Kobayashi, S., and Liang, Q.R. (2015). Autophagy and mitophagy in diabetic cardiomyopathy. BBA-Mol. Basis Dis. 1852(2): 252–61.
Lam, S.-C., Liu, X., Chen, X.-Q., Hu, D.-J., Zhao, J., Long, Z.-R., Fan, B., and Li, S.-P. (2016). Chemical characteristics of different parts of Coreopsis tinctoria in China using microwave assisted extraction and high-performance liquid chromatography followed by chemometric analysis. J. Sep. Sci. 39(15): 2919–2927.
Lan, Y., Lu, W., Li, L., Yang, Y., Long, M., and Mao, X. (2014). Effects of the ethanol extract of *Coreopsis tinctoria* on blood glucose and blood lipid levels in experimental diabetic rats. Chin. J. Drug Appl. Monit. 11(5): 272–275. CNKI:SUN:YWYY.0.2014-05-005.
Lee, D., Kim, S.J., and Lee, J. (2025). Novel therapeutic approaches for treatment of diabetic retinopathy and age-related macular degeneration. Vision 9(2): 35.
Li, H., Tao, Y., and Mao, X. (2021). Protective effect of effective components of *Coreopsis tinctoria* Nutt on retinopathy of db/db diabetic mice. Evid Based Complement Alt. Med. 2021: 9948609.
Li, H., Xu, G., Wu, D., Li, J., Cui, J., and Liu, J. (2021a). Effects of ethyl acetate extract from *Coreopsis tinctoria* on learning and memory impairment in D-galactose-induced aging mice and the underlying molecular mechanism. Food Funct. 12(6): 2531–2542.
Li, J., Xie, Y., Zheng, S., He, H., Wang, Z., Li, X., Jiao, S., Liu, D., Yang, F., Zhao, H., Li, P., and Sun, Y. (2024). Targeting autophagy in diabetic cardiomyopathy: From molecular mechanisms to pharmacotherapy. Biomed. Pharmacother. 175: 116790.
Li, T., Abulat, Z., Kadier, K., Guo, Y., Wang, L., Zhang, Y., Ran, Z., Song, Z., Zhang, F., and Mao, X. (2021). Marein regulates insulin resistance in diabetic nephropathy mice by inducing autophagy. Int. J. Morphol. 39(6): 1635–1645.
Li, Y., Guo, F., Wang, W., Lv, F., Zhang, L., Zhu, M., Yang, S., Dong, S., Zhou, M., Li, Z., Zhu, Z., Yang, Y.-M., and Zhang, Y. (2024a). Marein, a novel natural product for restoring chemo-sensitivity to cancer cells through competitive inhibition of ABCG2 function. Biochem. Pharmacol. 228: 116219.
Li, Y., Huang, C., Fu, W., Zhang, H., Lao, Y., Zhou, H., Tan, H., and Xu, H. (2020). Screening of the active fractions from the *Coreopsis tinctoria* Nutt. flower on diabetic endothelial protection and determination of the underlying mechanism. J. Ethnopharmacol. 253: 112645–112655.
Li, Y., Zhang, J., Yan, C., Chen, Q., Xiang, C., Zhang, Q., Wang, X., and Jiang, K. (2022). Marein prevented LPS-induced osteoclastogenesis by regulating the NF-κB pathway in vitro. J. Microbiol. Biotechnol. 32(2): 141–148.
Liu, J., Yao, L., Bi, X., Li, L., Li, L-L., Wang, Y., Lan, Y., and Mao, Z. (2017). Protective effects of marein, a flavonoid component from *Coreopsis tinctoria*, on pancreatic β-cells. J. Xinjiang Med. Univ. 40(4): 428–432. doi: 10.3969/j.issn.1009-5551.2017.04.005.
Liu, Y., Li, M., Zhang, Z., Ye, Y., and Zhou, J. (2018). Role of microglia-neuron interactions in diabetic encephalopathy. Ageing Res. Rev. 42: 28–39.
Liu, Y., Xiong, B., Qiu, X., Hao, H., and Sha, A. (2022). Study on the antithrombotic effect and physiological mechanism of okanin. Biomed. Pharmacol. 153: 113358.
Lu, X., Xie, Q., Pan, X., Zhang, R., Zhang, X., Peng, G., Zhang, Y., Shen, S., and Tong, N. (2024). Type 2 diabetes mellitus in adults: pathogenesis, prevention and therapy. Sig. Transduct. Target Ther. 9: 262.
Luo, W., Wang, J., Fan, Y., Yuan, M., Xie, W., Su, Y., Wang, X., Zhong, Y., Zhang, Y., Zhan, J., Mao, X., Huang, X., Long, J., Wang, X., Tang, T., and Wang, X. (2025). Elucidating multifaceted targets of marein in cerebral ischemia-reperfusion injury. Front. Chem. 13: 1651873.
Ma, P., Yu, F., Zhong, Y., Xu, L., and Xiao, P. (2023). Protective effects of flavonoids in *Coreopsis tinctoria* Nutt. in a mouse model of type 2 diabetes. J. Ethnopharmacol. 307: 116214.
Mehndiratta, M., Almeida, E.A., Chawl, D., Madhu, S.V., Garg, S., and Kar, R. (2024). Higher oxidative stress and inflammation in obese compared to lean patients with type 2 diabetes mellitus. Aspects Mol. Med. 3: e100042.
Nanda, J., Verma, N., and Mani, M. (2023). A Mechanistic Review on Phytomedicine and Natural Products in the Treatment of Diabetes. Curr. Diabetes Rev. 19(7): e221222212125.
Niu, G., Zhao, Y., Song, H., Song, Q., Yin, X., Zhu, Z., and Xu, J. (2024). Marein ameliorates myocardial fibrosis by inhibiting HIF-1α and TGF-β1/Smad2/3 Signaling pathway in isoproterenol-stimulated mice and TGF-β1-stimulated cardiac fibroblasts. Curr. Pharm. Des. 30(1): 71–80.
Peng, X., Peng, Y., Li, L., Liu, L., Zhou, G., and Cai, Y. (2025). Breakthroughs in diabetic retinopathy diagnosis and treatment using preclinical research models: current progress and future directions. Ann. Med. 57(1): 2531251.
Quaiyoom, A., and Kumar, R. (2024). An overview of diabetic cardiomyopathy. Curr. Diabetes Rev. 20(5): e121023222139.
Reaven, G.M. (2005). Insulin resistance, the insulin resistance syndrome, and cardiovascular disease. Panminerva Med. 47(4): 201–10.
Romero, R., Erez, O., Huttemann, M., Maymon, E., Panaitescu, B., Conde-Agudelo, A., Pacora, P., Yoon, B.H., and Grossman, L.I. (2017). Metformin, the aspirin of the 21st century: its role in gestational diabetes mellitus, prevention of preeclampsia and cancer, and the promotion of longevity. Am. J. Obstet. Gynecol. 217(3): 282–302.
Shen, J., Hu, M., Tan, W., Ding, J., Jiang, B., Xu, L., Hamulati, H., He, C., Sun, Y., and Xiao, P. (2021). Traditional uses, phytochemistry, pharmacology, and toxicology of *Coreopsis tinctoria* Nutt.: A review. J. Ethnopharmacol. 269: 113690.
Shu, C., Fan, Q., Yang, L., Jiang, L., Zhang, B., Kang, W., Zhang, Y., and Wan, S. (2017). Effects of Kunlun snow chrysanthemum extract on serum SOD, MDA, and GSH-PX in STZ-induced diabetic rats. Tradit. Chin. Med. Res. 30(4): 70–72. doi: 10.3969/j.issn.1001-6910.2017.04.30.
Shu, C., Fan, Q., Yang, L., Jiang, L., Zhang, B., Kang, W., Zhang, Y., and Wan, S. (2017a). Effects of *Kunlun snow chrysanthemum* extract on insulin resistance in streptozotocin (STZ)-induced diabetic rats. Tradit. Chin. Med. Res. 30(3): 66–70. doi: 10.3969/j.issn.1001-6910.2017.03.31.
Shu, C., Fan, Q., Yang, L., Jiang, L., and Zhang, B. (2017b). Effects of Kunlun snow chrysanthemum extract on insulin resistance in diabetic rats via the IRS-1/PI3K/GLUT4 signaling pathway. Chin. J. Exp. Tradit. Med. Formulae. 23(11): 122–127. doi: 10.13422/j.cnki.syfjx.2017110122.
Song, Z., Xin, J., Wei, X., Zulipiya, A., Kedireya, K., and Mao, X. (2023). Effect and Mechanism of Marein on Diabetic Retinopathy. Pakistan J. Zool. 55(6): 2785–2796.
Sood, A., Baishnab, S., Gautam, I., Choudhary, P., Lang, D.K., Jaura, R.S., and Singh, T.G. (2023). Exploring various novel diagnostic and therapeutic approaches in treating diabetic retinopathy. Inflammopharmacology 31(2): 773–786.
Sun, L., Huang, J., Wang, W., Chao, M., Chen, Y., Ma, P., Xu, L., and Xiao,

P. (2027). Protective effects of Coreopsis tinctoria flower extract on high-fat and high-fructose diet-induced cognitive deficit: Insight into gut microbiota-derived tryptophan metabolism. Food Sci. Human. Wellness 16. doi: 10.26599/FSHW.2026.9251066.

Tian, Y., Zhang, F., Zhang, B., and Li, T. (2024). Marein alleviates myocardial fibrosis in diabetic mice. Basic Clin. Med. 44(1): 51–56. doi: 10.16352/j.issn.1001-6325.2024.01.0051.

Vlassara, H., and Uribarri, J. (2014). Advanced glycation end products (AGE) and diabetes: cause, effect, or both? Curr. Diabetes Rev. 14: 1–10.

Wang, Y., Sun, Z., Zhao, Z., Pang, J., and Chen, J. (2025). Recent progress in the development of glucose transporter (GLUT) inhibitors. J. Med. Chem. 68(2): 1033–1050.

Wu, S., Li, X., and Zhang, B. (2017). Effects of the aqueous extract of *Kunlun Snow Chrysanthemum* on serum adiponectin, resistin, and blood lipid levels in KKAy mice. West. J. Tradit. Chin. Med. 30(10): 12–15. CNKI:SUN:GSZY.0.2017-10-006.

Wu, X., Sun, K., Wang, X., Hu, M., Sun, X., Jiang, B., Sun, Y., and He, C. (2026). Total Flavonoids from Snow Chrysanthemum Exert Synergistic Vascular and Neuroprotective Effects in Hypertensive Vascular Dementia Rats. Pharmaceuticals 19(5): 700.

Xu, L., Hamulati, H., He, C., Sun, Y., and Xiao, P. (2021). Traditional uses, phytochemistry, pharmacology, and toxicology of *Coreopsis tinctoria* Nutt.: A review. J. Ethnopharmacol. 269: 113690.

Xu, W., Wang, X., Hou, X., Yang, Y., Ma, R., Lv, R., and Yin, Q. (2024). The role of microglia in the pathogenesis of diabetic-associated cognitive dysfunction. Front. Endocrinol. 14: 1246979.

Yang, H., Zhang, Y., Hou, S., Liu, J., Shi, Y., and Chen, X. (2025). Mechanism study of *Coreopsis tinctoria* Nutt. on diabetes retinopathy based on liver-eye axis by UHPLC-MS. Sep. Sci. Plus. 8: E70012.

Yao, L., Jiang, J., Wang, J., and Mao, X. (2019). Effects of *Coreopsis tinctoria* on the RhoA/ROCK/Nox4 signaling pathway in renal fibrosis of diabetic rats. Chin. J. Inf. Tradit. Chin. Med. 26(1): 57–62. doi: 10.3969/j.issn.1005.5304.2019.01.014.

Yao, L., Li, J., Li, L., Li, X., Zhang, R., Zhang, Y., and Mao, X. (2019). *Coreopsis tinctoria* Nutt ameliorates high glucose-induced renal fibrosis and inflammation via the TGF-β1/SMADS/AMPK/NF-κB pathways. BMC Complementary Altern. Med. 19: 14.

Yao, L., Li, L., Li, X., Li, H., Zhang, Y., Zhang, R., Wang, J., and Mao, X. (2015). The anti-inflammatory and antifibrotic effects of *Coreopsis tinctoria* Nutt on high-glucose-fat diet and streptozotocin-induced diabetic renal damage in rats. BMC Complementary Altern. Med. 15: 314.

Yao, L., Zhang, Y., Liu, J., Li, L., Wang, Y., Lan, Y., and Mao, X. (2017). Effects of *Coreopsis tinctoria* extract on proliferation and fibrosis-related factor expression in rat glomerular mesangial cells. Chin. J. Exp. Tradit. Med. Formulae 23(19): 134–139. doi: 10.13422/j.cnki.syfjx.2017190134.

Yao, M., Zhang, J., Li, Z., Guo, S., Zhou, X., and Zhang, W. (2020). Marein protects human nucleus pulposus cells against high glucose-induced injury and extracellular matrix degradation at least partly by inhibition of ROS/NF-κB pathway, Intern. Int. Immunopharmacol. 80: 106126.

Yin, L., He, Z., Fan, Y., Niu, Z., Yao, L., Ding, S., Chen, J., Zhang, Q., Tong, Y., Bi, Q., and Cao, L. (2025). Marein ameliorates the progression of osteoarthritis: An *in vitro* and *in vivo* studies. Int. Immunopharmacol. 144: 113695.

Yu, S., Zhao, H., Yang, W., Amat, R., Peng, J., Li, Y., Deng, K., Mao, X., and Jiao, Y. (2019). The alcohol extract of *Coreopsis tinctoria* Nutt ameliorates diabetes and diabetic nephropathy in db/db mice through miR-192/miR-200b and PTEN/AKT and ZEB2/ECM pathways. Biomed. Res. Int. 2019: 5280514.

Zamanian, M.Y., Alsaab, H.O., Golmohammadi, M., Yumashev, A., Jabba, A.M., Abid, M.K., Joshi, A., Alawadi, A.H., Jafer, N.S., Kianifar, F., and Obakiro, S.B. (2024). NF-κB pathway as a molecular target for curcumin in diabetes mellitus treatment: Focusing on oxidative stress and inflammation. Cell Biochem. Funct. 42(4): e403.

Zhang, B., Shu, C., Du, M., Liu, X., Yang, L., and Li, X. (2016). Impact of aqueous extract from Kunlun snow chrysanthemum on the levels of blood glucose and insulin of the mice with type two diabetes mellitus. West. J. Tradit. Chin. Med. 29(1): 26–29. doi: 10.3969/j.issn.1004-6852.2016.01.009.

Zhang, F., Abula, Z., Kadeer, K., Song, Z., Zhang, B., Zhang, Y., Peng, X., and Li, T. (2024). Effects of marein on liver and pancreatic histomorphology and autophagy in diabetic mice. West. J. Tradit. Chin. Med. 37(2): 4–8. doi: 10.12174/j.issn.2096-9600.2024.02.02.

Zhang, F., Yang, M., Xu, J., Hu, Y., Gao, R., Huang, K., and He, X. (2022). *Coreopsis tinctoria* and its flavonoids ameliorate hyperglycemia in obese mice induced by high-fat diet. Nutrients 14(6): 1160–1170.

Zhang, N., Ma, Y., Deng, K., Mao, X., and Yao, L. (2018). Effects of flavonoid extracts from *Coreopsis tinctoria* on fibrosis of rat glomerular mesangial cells induced by high glucose and high lipid conditions and the related mechanisms. J. Chin. Med. Mater. 41(4): 949–954. doi: 10.13863/j.issn1001-4454.2018.04.038.

Zhang, N.-N., Kang, J.-S., Liu, S.-S., Gu, S.-M., Song, Z.-P., Li, F.-X., Wang, L.-F., Yao, L., Li, T., Li, L.-L., Wang, Y., Li, X.-J., and Mao, X.-M. (2020). Flavanomarein inhibits high glucose-stimulated epithelial-mesenchymal transition in HK-2 cells via targeting spleen tyrosine kinase. Sci. Rep. 10(1): 439.

Zhang, P.-P., Zhuo, B.-Y., Duan, Z.-W., Li, X., Huang, S.-L., Cao, Q., Zhao, T., Wei, S.-L., Hu, X., and Zhang, Y. (2023). Marein reduces lipid levels via modulating the PI3K/AKT/mTOR pathway to induce lipophagy. J. Ethnopharmacol. 312: 116523.

Zhang, Y., Lan, Y., Li, H., Yao, L., Li, L., Wang, J., and Mao, X. (2015). Effect of ethyl acetate extract from *Coreopsis tinctoria* on diabetic SD rats induced by STZ. Chin. Pharmacological Bull. 31(10): 1439–1442.

Zhang, Y., Hou, S., Li, N., Liu, J., Ding, Y., Liu, E., Lan, W., and Chen, X. (2026). Study on the mechanism of *Coreopsis tinctoria* Nutt. in the treatment of diabetic retinopathy based on gut microbiota. Comb. Chem. High Throughput Screening. doi: 10.2174/0113862073438400251208203012.

Zhang, Y., Luo, L., Li, Z., Li, H., Yao, X., and Luo, R. (2019). Anti-lipid peroxidation, α-glucosidase and α-amylase inhibitory effects of the extract of capitula of *Coreopsis tinctoria* Nutt. and protection effects on high-fat/high-sugar and streptozotocin-induced type 2 diabetes in mice. Chem. Biodivers. 16(12): e1900514.

Zhang, Z., Chen, X., Wang, H., and Zhang, P. (2017). Effects of *Coreopsis tinctoria* (Kunlun snow chrysanthemum) from Qinghai on blood glucose levels in diabetic rats and its possible mechanisms. Chin. J. Gerontol. 37(23): 5782–5784. doi: 10.3969/j.issn.1005-9202.2017.23.014.

Zhao, L., Liu, R., Kang, Y., Chen, Y., Xiao, Y., Cheng, X., and Zhang, L. (2025a). Marein from Coreopsis tinctoria Nutt. alleviates oxidative stress and lipid accumulation via SIRT1/Nrf2 signaling. Sci. Rep. 15(1): 18761.

Zhao, L., Xing, J., Wang, Y., Xin, L., Cheng, X., Chen, Y., Wang, P., Zhang, L., and Zhao, W. (2025b). Marein alleviates the development of atherosclerosis through targeting miR-126/lipoprotein-associated phospholipase A_2 axis. FASEB J. 39: e70360.

Zhao, L., Yuan, J., Yang, Q., Ma, J., Yang, F., Zou, Y., Liu, K., and Liu, F. (2026). Diabetes and its complications: molecular mechanisms, prevention and treatment. Signal Transduction Targeted Ther. 11(1): 22.

Zhou, X., Xu, A., and Chen, X. (2026). Extraction, pharmacological prediction and experimental verification of *Coreopsis tinctoria* flowers. Nat. Prod. Res. 40(5): 1369–1374.

Zhu, D., Li, R., Sun, Y., Li, Y., Ruan, J., and Wang, J. (2026a). *Coreopsis tinctoria* buds polysaccharides boost metformin's antihyperglycemic effect in diabetic mice via gut microbiota and metabolism modulation. Ind. Crops Prod. 240: 122574.

Zhu, Y., Guo, L., Zhu, J., Zhu, H., Liu, C., and Shen, J. (2026b). Biotransformation of *Coreopsis tinctoria* major flavonoids marein and flavanomarein. J. Food Bioact. 33: 85–93.

Journal of Food Bioactives
International Society for Nutraceuticals and Functional Foods
Original Research
J. Food Bioact. 2026;35:38–45

In vitro bile acid-binding ability of black soybean seed coat

Naho Mizuno-Nagata[a*], Hitoshi Ashida[a] and Toshiya Toda[b†]

[a]Department of Food Sciences and Nutrition, School of Food Sciences and Nutrition, Mukogawa Women's University, 6-46 Ikebiraki-cho, Nishinomiya, Hyogo 663-8558, Japan
[b]Department of Innovative Food Sciences, School of Food Sciences and Nutrition, Mukogawa Women's University, 6-46 Ikebiraki-cho, Nishinomiya, Hyogo 663-8558, Japan
[†]T.T. deceased on April 3, 2026.
[*]**Corresponding author:** Naho Mizuno-Nagata, Department of Food Sciences and Nutrition, School of Food Sciences and Nutrition, Mukogawa Women's University, 6-46 Ikebiraki-cho, Nishinomiya, Hyogo 663-8558, Japan. E-mail: mw499460@mukogawa-u.ac.jp
DOI: 10.26599/JFB.2026.95035454
Received: May 11, 2026; **Revised received & accepted:** May 31, 2026
Citation: Mizuno-Nagata, N., Ashida, H., and Toda, T. (2026). *In vitro* bile acid-binding ability of black soybean seed coat. J. Food Bioact. 35: 38–45.

Abstract

Bile acid-binding ability with dietary components is known to modulate cholesterol metabolism. However, the bile acid-binding potential of polyphenols in black soybean (*Glycine max* L.) seed coat has not yet been fully elucidated. In this study, we quantified the bile acid-binding ability of both black and yellow soybean seed coats and their polyphenols. Suspended seed coat revealed the ability to bind cholic and deoxycholic acids: the binding ability of black soybean seed coat significantly exceeded that of yellow one. This ability was observed in both water-soluble and water-insoluble fractions from black soybean seed coat. The ability of the water-soluble fraction is attributed to anthocyanins and low-molecular-weight proanthocyanidins, whereas that of the water-insoluble fraction is mainly due to highly polymerized proanthocyanidins. These findings suggest that the intake of black soybean seed coat may maintain healthy cholesterol homeostasis through the excretion of bile acids.

Keywords: Black soybeans; Bile acid-binding ability; Polyphenols; Anthocyanins; Proanthocyanidins.

1. Introduction

Bile acids are synthesized from cholesterol in the liver, secreted into the duodenum, and subsequently reabsorbed via the intestinal tract to enter enterohepatic circulation. To maintain homeostasis, the liver synthesizes nascent bile acids to replace the fraction excreted in feces. Due to their potent strong surfactant properties, bile acids are essential regulators of lipid digestion, absorption, and cholesterol metabolism (Konishi and Nabetani, 2013; Uchida, 2009). Furthermore, they exert selective pressure on the intestinal microbiota through significant antibacterial activity (Yokota et al., 2012). Consequently, fluctuations in bile acid composition and pool size can profoundly alter the gut environment. Recently there has been growing research focus on bile acid-mediated metabolic signaling and the bidirectional interactions between the bile acid and gut commensal bacteria (Therdtatha et al., 2022).

Bile acid sequestrants, such as anion-exchange resins cholestyramine and colesevelam, are established treatments for hypercholesterolemia due to their capacity to enhance fecal bile acid excretion (Scaldaferri et al., 2013). Similarly, numerous dietary components particularly fiber-rich grains and fruits have demonstrated significant bile acid-binding potential (Dongowski, 2007; Hamauzu and Mizuno, 2011; Kahlon and Chow, 2000; Kahlon and Shao, 2004; Kahlon and Smith, 2007). Furthermore, polyphenols, specifically those characterized by highly polymerized proanthocyanidin structures, exhibit strong bile acid-binding ability. Matsumoto et al. (2010) and Hamauzu and Ikeda (2022) showed not only that proanthocyanidins derived from immature persimmon fruits effectively bind bile acids *in vitro*, but also that by the *in vivo* animal models, where the administration of these compounds significantly enhanced fecal bile acid excretion, concurrently reducing hepatic lipid accumulation and plasma cholesterol concentrations in mice.

The food culture of soybean [*Glycine max* (L.) Merr.] is unique

© The author(s) 2026. Publishing Services by Tsinghua University Press
The articles published in this open access journal are distributed under the terms of the Creative Commons Attribution 4.0 International License (http://creativecommons.org/licenses/by/4.0/)

to East Asia, where a wide variety of soybeans are consumed. The seed coat of black soybeans is also rich in polyphenols, including anthocyanins and proanthocyanidins, compared to other soybeans, i.e. red-brown, green and yellow, and has been reported to have positive antioxidant and lipid metabolism effects (Furuta et al., 2003; Ganesan and Xu, 2017; Malenčić et al., 2012; Nishijima et al., 2024; Yamashita et al., 2020). However, there are no detailed studies on the bile acid-binding ability of polyphenols in black soybeans. Therefore, in this study, we measured the bile acid-binding ability of both black and yellow soybean seed coats and investigated the relationship between the polyphenols present in the seed coat.

2. Materials and methods

2.1. Preparation and extraction of soybean seed coat

Black soybean (*Glycine max* (L.) Merr. 'Iwaikuro', harvested in 2024; Hokkaido, Japan) and yellow soybean (*Glycine max* (L.) Merr. 'Yuzuru', harvested in 2024; Hokkaido, Japan) seeds were purchased from Japan Clasia Food Supply (Okayama, Japan). After lyophilization, the seed coat was separated and crushed to less than 500 µm. Aliquot of the crushed seed coat (0.5 g) was extracted with 40 mL of water at 90°C for 30 min. After centrifugation (10,900 ×*g*, 15 min), the residue was washed twice with 30 mL of water. The resulting supernatant and residue were lyophilized into powders and referred to as a water-soluble fraction and water-insoluble fraction, respectively.

2.2. Bile acid-binding ability

Bile acid-binding tests *in vitro* were performed according to the method described by Matsumoto et al. (2011). Briefly, soybean seed coat powder was suspended at 4% (w/v) in PBS solution (pH 7.4) containing bile acid and shaken at 37 °C for 10 min. The experimental bile acid concentrations were modeled after physiological levels in the human intestine (2–10 mM: Northfield and McColl, 1973): i.e., sodium cholate monohydrate (CA; Sigma-Aldrich, St. Louis, MO, USA) and sodium deoxycholate monohydrate (DCA; Nacalai Tesque, Kyoto, Japan) were used at final concentrations of 4 mM and 2 mM, respectively. These concentrations are the maximum concentrations achievable without inducing viscosity related experimental interference. The additive amount of seed coat was set to 4% (w/v), the maximum within the range where addition dependence was confirmed, after measuring the bile acid-binding rate of 1–5% black soybean seed coat beforehand. After incubation, supernatant was collected by a centrifugation (13,800 ×*g*, 5 min), and the bile acid concentration was measured using a commercially available enzyme colorimetric kit [Total bile acid-test Wako; Fujifilm Wako Pure Chemical (Fujifilm Wako), Osaka, Japan]. This assay kit uses 3α-hydroxysteroid dehydrogenase and diaphorase as enzymes; theoretically, errors caused by component-specific colors or nonspecific reactions can be offset by including a sample blank measurement. Then, the bile acid-binding rate was calculated as the rate of precipitation, obtained by subtracting the concentration of free bile acid from that of added bile acid. To ensure assay validity, cholestyramine (Sigma-Aldrich) and cellulose (Fujifilm Wako) were employed as the positive and negative controls, respectively.

First, differences of the bile acid-binding ability of the seed coat and its water-insoluble fraction from black and yellow soybeans were compared. Then, the seed coat, its insoluble and soluble fractions from black soybeans were tested. Finally, in order to clarify the bile acid-binding ability of the low-molecular polyphenols contained in black soybean seed coat, 0.033% (w/v) of (+)-catechins (Sigma-Aldrich), (–)-epicatechin (Fujifilm Wako), procyanidin B2 (Fujifilm Wako), procyanidin C1 (Cayman Chemical, Ann Arbor, MI, USA), cinnamtannin A2 (Phytolab, Vestenbergsgreuth, Germany), and cyanidin 3-glucoside [C3G; Tokiwa Phytochemical (Tokiwa), Chiba, Japan] were subjected to the bile acid-binding tests. They were analyzed in triplicate.

2.3. Component analysis

Methanol/water/trifluoroacetic acid (40:60:0.5, v/v/v; 20 mL) was added to 0.3 g of the seed coat and its water-insoluble fraction from black and yellow soybeans, and after repeated cycles of stirring and sonicating (15 min) and resting (5 min), centrifugation (4,800 ×*g*, 15 min) was performed. The same extraction was repeated twice, and then the supernatant was filled up to 100 mL (Oki et al., 2011). In addition, 20 mL of acetone/water/acetic acid (70:29.5:0.5, v/v/v) was added to the extraction residue above, and the same extraction procedure was repeated thrice. Acetone was removed by a vacuum concentration and filled up to 50 mL with 50% (v/v) methanol (Sawai et al. 2012).

Anthocyanins were analyzed using the HPLC L-7000 system equipped with Cadenza CD-C18 column (250 × 4.6 mm inner diameter (i.d.), 3 µm; Imtakt, Kyoto, Japan). The HPLC conditions were as follows: column temperature, 40°C; injection volume, 10 µL; flow rate, 0.6 mL/min; and measurement wavelength, 520 nm. Mobile phase A consisted of 0.6% (v/v) formic acid and mobile phase B consisted of 50% acetonitrile:0.6% formic acid (v/v). The gradients for mobile phase B were 15–50% (0–40 min), 50% (40–45 min), and 15% (46–60 min). C3G, delphinidin 3-glucoside (D3G; Tokiwa), and petunidin 3-glucoside (Pt3G; Tokiwa) were used as standards. Flavan-3-ol monomers and oligomers were analyzed using the HPLC 8020 system (Tosoh, Tokyo, Japan) equipped with the fluorescence detector (Nanospace 3213 SI-2; Shiseido, Tokyo, Japan), and Cadenza CL-C18 column (250 × 4.6 mm, i.d., 3 µm; Imtakt). The HPLC conditions were the same as above, except the flow rate (0.7 mL/min) and detector. The fluorescence was measured by excitation at 276 nm and detection at 316 nm (Wang et al., 2017). Mobile phase A was 0.1% (v/v) formic acid. Mobile phase B was acetonitrile, and the gradient was 5–15% (0–45 min), 15–80% (45–50 min), 80% (50–53 min), and 5% (53–70 min). The standards used were (+)-catechin, (–)-epicatechin, procyanidin B2, procyanidin C1, and cinnamtannin A2. The content of anthocyanins and flavan-3-ols in the methanol/water/trifluoroacetic acid and acetone/water/acetic acid extracts were measured respectively, and the results are expressed as combined values as the latter contained only trace amounts of them.

The insoluble fraction (5 g) from black and yellow soybean seed coat was added to 100 mL of acidified methanol (70% methanol:1% concentrated HCl, v/v) and extracted twice at 80°C for 30 min (Matsumoto et al. 2010; Takekawa and Matsumoto, 2012). The acidified methanol solution was filled up to 250 mL, and the optical absorption spectrum (190–700 nm, UV-1280; Shimadzu, Kyoto, Japan) was scanned to check the existence of anthocyanins. The absorbance (555 nm, UVmini-1240; Shimadzu) was separately measured and the total cyanidin content was calculated using cyanidin chloride (Fujifilm Wako) as a standard. Total proanthocyanidin content was determined as the (+)-catechin equivalent by measuring the absorbance (500 nm, UVmini-1240) according to the vanillin sulfate method (Sun et al., 1998).

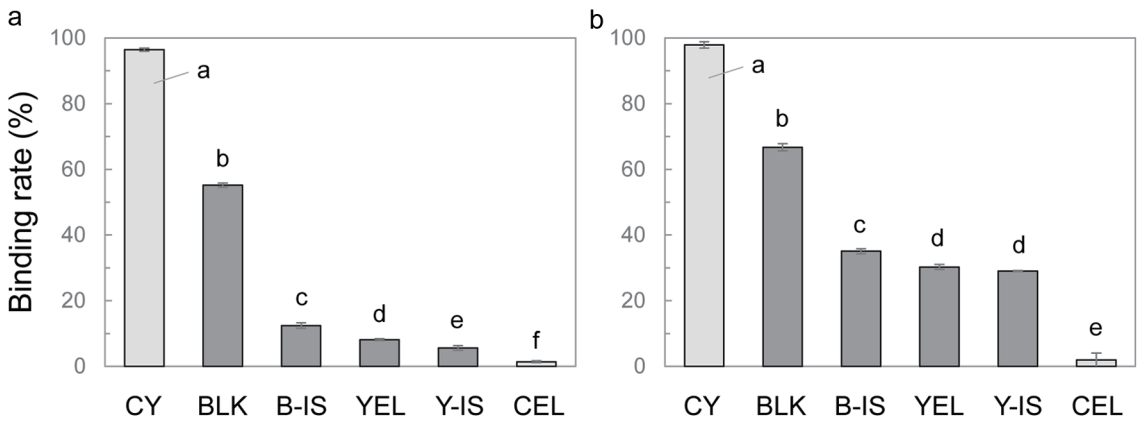


Figure 1. Bile acid-binding rate of the seed coat and its water-insoluble fraction of black and yellow soybeans (4%) with 4 mM CA (a), and 2 mM DCA (b). The binding rate of the water-insoluble fraction was adjusted based on the recovery yield relative to the seed coat. Error bars indicate the standard deviation of three measurements, and different letters indicate a statistically significant difference based on a one-way ANOVA with Tukey's post-hoc test ($p < 0.05$). CA, sodium cholate; DCA, sodium deoxycholate; CY, cholestyramine; BLK, black soybean seed coat; B-IS, black soybean water-insoluble fraction; YEL, yellow soybean seed coat; Y-IS, yellow soybean water-insoluble fraction; CEL, cellulose.

2.4. Statistical analysis

IBM SPSS Statistics v29.0.2.0 (IBM, Armonk, NY, USA) was used to perform a one-way analysis of variance (ANOVA) with Tukey's post-hoc test. Statistical significance was set at $p < 0.05$.

3. Results and discussion

3.1. Comparison of bile acid-binding ability of black and yellow soybean seed coat

The yields of the water-insoluble fraction obtained from the seed coat were 76 ± 5% and 88 ± 5% (w/w) for black and yellow soybeans, respectively. Figure 1 shows the results of bile acid-binding test conducted at a concentration of 4% of these fractions. The binding rate of the insoluble fraction was adjusted based on the recovery yield relative to the seed coat. Black and yellow soybean seed coats are bound CA and DCA. The binding rates of black soybean seed coat were 55.2% and 66.7% for CA and DCA, respectively, showing values 6.8 times and 2.2 times higher than that of yellow one. Compared to the insoluble fraction of black soybeans, the seed coat showed 4.4 times and 1.9 times higher binding rates for CA and DCA, respectively. Therefore, in black soybeans, the difference in binding rates between the seed coat and its insoluble fraction might be due to the water-soluble substances. However, the difference in binding rates between the seed coat and its insoluble fraction of yellow ones was negligible, only a few percent, for the two bile acids; thus, the water-soluble substances of yellow soybean seed coat hardly contribute to binding ability. The binding rate of the insoluble fraction of black soybeans showed significantly greater than that of yellow ones. This suggests that the substances unique to black soybean seed coat are involved in the high binding ability of the insoluble fraction.

3.2. Comparison of the seed coat, its water-insoluble and water-soluble fractions of black soybean seed coat

Black soybean seed coat has a higher binding ability than yellow one, and both the water-insoluble and water-soluble substances contained in black soybean seed coat exhibit activity (Figure 1). To investigate the differences in binding ability between water-insoluble and water-soluble fractions of black soybeans in detail, the binding rates of the seed coat, its insoluble, and soluble fractions were determined (Figure 2). They were tested at a concentration of 4%, and the absolute value of binding ability was calculated. In addition, adjusted binding rates of the insoluble and soluble fractions were also calculated based on their recovery yields relative to the seed coat (76 ± 5% and 18 ± 1% w/w, respectively), to account for their relative activity within the seed coat. The seed coat and two fractions demonstrated significant bile acid-binding activity. The absolute binding rates of the soluble fraction were 85.9% and 77.8%, significantly higher than those of the insoluble one at 20.6% and 46.4% for CA and DCA, respectively. However, the sum of the adjusted binding rates of the insoluble and soluble ones were roughly consistent with the binding rates of the seed coat. This suggests that the insoluble fraction accounted for over half of the total binding ability of black soybean seed coat. Since water-soluble fraction from yellow soybean seed coat exhibited negligible binding ability (data from Figure. 1), it is suggesting that the soluble fraction of black soybean contains bioactive compounds for the binding ability unique to the black soybean variety.

Low-molecular-weight polyphenols including anthocyanins and proanthocyanidins are characteristic of black soybean seed coat and largely absent in yellow variety (Todd and Vodkin, 1993; Takahata et al., 2001). We compared the extractable polyphenol content of the seed coat and its insoluble fraction for both varieties; anthocyanin levels are summarized in Table 1, while flavan-3-ol monomers and oligomers are detailed in Table 2. Black soybean seed coat contained a full profile of these polyphenols; among the anthocyanins, C3G composed the majority, and (–)-epicatechin and procyanidin B2 were the main flavan-3-ols. Only trace amounts of polyphenols were detected in the water-insoluble fraction, indicating that the majority of polyphenols were partitioned into the water-soluble fraction during extraction. Consequently, the amount of the component in the soluble fraction of black soybeans subjected to the bile acid-binding test was approximately 3.7-fold higher anthocyanin levels and 3.5-fold higher flavan-3-ol levels compared to the seed coat. In contrast, yellow soybean seed coat yielded no detectable anthocyanins and only negligible quan-

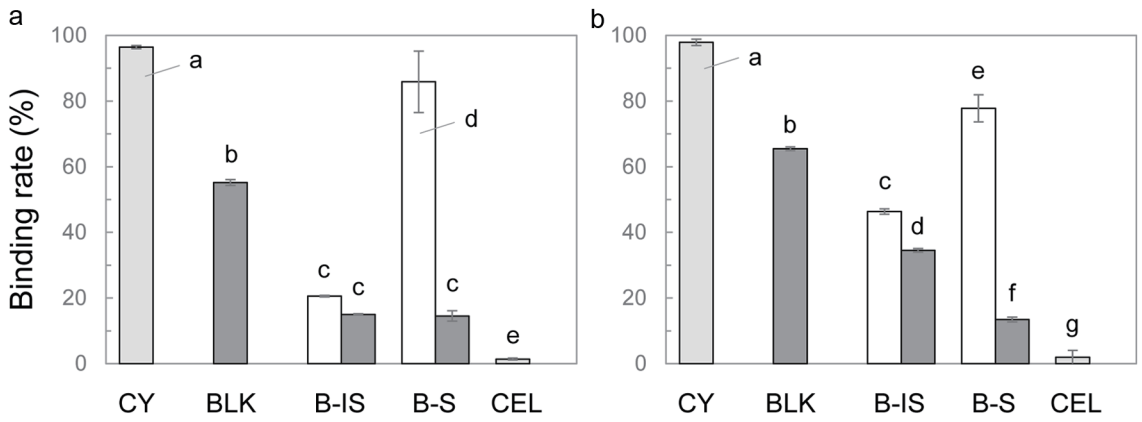


Figure 2. Bile acid-binding rate of the seed coat and its water-insoluble and water-soluble fractions of black soybean (4%) with 4 mM CA (a), and 2 mM DCA (b). The absolute binding rate of each fraction at 4 %(□) and the adjusted rate based on the recovery yield relative to the seed coat (■) are shown. Error bars indicate the standard deviation of three measurements, and different letters indicate a statistically significant difference based on a one-way ANOVA with Tukey's post-hoc test ($p < 0.05$). CA, sodium cholate; DCA, sodium deoxycholate; CY, cholestyramine; BLK, black soybean seed coat; B-IS, black soybean water-insoluble fraction; B-S, black soybean water-soluble fraction; CEL, cellulose.

tities of flavan-3-ols, further confirming the distinctness of the black soybean seed coat.

3.3. Bile acid-binding ability of polyphenols

Since black soybean seed coat and its water-soluble fraction contained high levels of anthocyanins and proanthocyanidins, particularly C3G, D3G, (–)-epicatechin, and procyanidin B2 (Tables 1 and 2), the bile acid-binding test using pure polyphenols was performed. The results are shown in Figure 3. As the pure polyphenols showed bile acid-binding ability even at low concentrations, the concentration was set to 0.033%. Bile acid-binding ability was also observed for all the polyphenol products tested with CA and DCA. Procyanidin C1 and cinnamtannin A2, the trimer and tetramer of (–)-epicatechin, respectively, exhibited higher binding ability than other polyphenols with both bile acids and than cholestyramine, the positive control, with CA. The binding rate of cholestyramine with CA was lower than that with DCA, possibly indicating that the binding ability with CA had already saturated at the concentration used in this experiment.

Regarding the interaction between proanthocyanidins and bile acids, banana-derived proanthocyanidins, which primarily trimers of (–)-epicatechin and epigallocatechin, have been reported to

Table 1. Anthocyanin contents in the untreated and water-insoluble fractions of black and yellow soybean seed coats

	Anthocyanins (mg/g)†			
	C3G	D3G	Pt3G	Total††
BLK	32.11 ± 1.54	3.24 ± 0.28	1.36 ± 0.10	36.70 ± 1.88
B-IS	0.26 ± 0.01	0.04 ± 0.01	0.01 ± 0.00	0.31 ± 0.01
YEL	n.d.	n.d.	n.d.	n.d.
Y-IS	n.d.	n.d.	n.d.	n.d.

†Mean and standard deviation of three measurements are shown based on the weight of the seed coat. ††Total of C3G, D3G, and Pt3G. C3G, cyanidin 3-glucoside; D3G, delphinidin 3-glucoside; P3G, petunidin 3-glucoside; BLK, black soybean seed coat; B-IS, black soybean water-insoluble fraction; YEL, yellow soybean seed coat; Y-IS, yellow soybean water-insoluble fraction; n.d., not detected.

Table 2. Monomer and oligomer contents of flavan-3-ol in the untreated and water-insoluble fractions of black and yellow soybean seed coats

	Flavan-3-ol monomers, oligomers (mg/g)†					
	CAT	EC	B2	C1	A2	Total††
BLK	0.20 ± 0.02	2.34 ± 0.30	2.72 ± 0.59	0.79 ± 0.17	0.37 ± 0.11	6.42 ± 1.15
B-IS	0.04 ± 0.00	0.20 ± 0.00	0.14 ± 0.03	0.04 ± 0.01	0.04 ± 0.02	0.45 ± 0.02
YEL	n.d.	Trace	Trace	n.d.	n.d.	Trace
Y-IS	n.d.	n.d.	n.d.	n.d.	n.d.	n.d.

†Mean and standard deviation of three measurements are shown based on the weight of the seed coat. ††Total of CAT, EC, B2, C1, and A2. CAT, (+)-catechin; EC, (–)-epicatechin; B2, procyanidin B2; C1, procyanidin C1; A2, cinnamtanninA2; BLK, black soybean seed coat; B-IS, black soybean water-insoluble fraction; YEL, yellow soybean seed coat; Y-IS, yellow soybean water-insoluble fraction; n.d., not detected; Trace, below the limit of quantification.

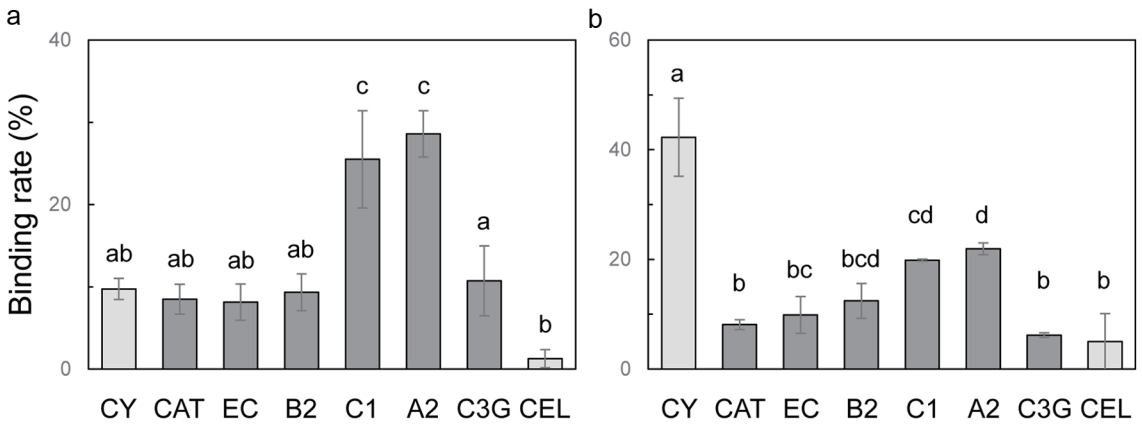


Figure 3. Bile acid-binding rate of polyphenols (0.033%) with 4 mM CA (a), and 2 mM DCA (b). Error bars indicate the standard deviation of three measurements, and different letters indicate a statistically significant difference based on a one-way ANOVA with Tukey's post-hoc test ($p < 0.05$). CA, sodium cholate; DCA, sodium deoxycholate; CY, cholestyramine; CAT, (+)-catechin; EC, (–)-epicatechin; B2, procyanidin B2; C1, procyanidin C1; A2, cinnamtannin A2; C3G, cyanidin 3-glucoside; CEL, cellulose.

adsorb to bile acids and form complexes via hydrogen bonding and hydrophobic interactions resulting from their amphilic structure (Li et al., 2019). On the other hand, although anthocyanins are highly water-soluble, they form hydrophobic platforms through self-association in the binding of pectin and anthocyanins (Liu et al., 2024). Based on the above, proanthocyanidins and anthocyanins contained in black soybeans were also thought to have formed insoluble complexes and precipitated in this experiment by binding to bile acids through hydrophobic interactions. Therefore, the large amounts of low-molecular-weight polyphenols in the soluble fraction might result in the high binding rate of the water-soluble fraction of black soybeans (Figure 2). Though the C3G content was high, procyanidin C1 and cinnamtannin A2, which showed high binding rate in pure products, may have influenced the binding ability of black soybean seed coat even in small amounts. Regarding the *in vivo* pharmacokinetics of proanthocyanidins in humans, the trimer and tetramer of (–)-epicatechin may exhibit bile acid-binding abilities in the digestive tract, since the monomers and dimers have been reported to be absorbed into the bloodstream, whereas trimers and tetramers are hardly absorbed (Zhang et al., 2016). Therefore, trimers and tetramers of proanthocyanidins that remain in the gastrointestinal tract without being absorbed are likely to effectively adsorb bile acids in the human tract as well.

3.4. Determination of bile acid-binding substances of black soybean water-insoluble fraction

The bile acid-binding ability of black soybean insoluble fraction significantly exceeded that of yellow one, suggesting that high binding affinity is mediated by bioactive substances unique to black soybean seed coat (Figure 1). To characterize these constituents, we analyzed the optical absorption spectra of the acidified methanol solution of the insoluble fractions, alongside total cyanidin and proanthocyanidin content (Table 3). Upon acid hydrolysis, the insoluble solution of black soybeans exhibited a distinct red chromophore with a maximum absorption peak (λ_{max}) at approximately 550 nm, consistent with the spectral profile of cyanidin (Figure 4). This chromogenic reaction is attributed to the acid-catalyzed hydrolysis of proanthocyanidins or anthocyanins into their respective anthocyanidin subunits. These data, coupled with the vanillin-sulfate assay results, indicate that the insoluble fraction of black soybeans contains significant quantities of high-molecular-weight proanthocyanidins. In contrast, the acidified insoluble solution of yellow soybeans showed no color change or detectable anthocyanidin and proanthocyanidin presence, confirming the absence of these polymerized structures in the yellow variety.

Polyphenols in plants are conventionally extracted using organic solvents, though hydrolyzable polyphenols, which are low-molecular-weight phenolic compounds strongly bound to polysaccharides or proteins, and non-extractable proanthocyanidins, which are high-molecular-weight structures, remain in the residue (Pérez-Jiménez and Saura-Calixto, 2015). Mizuno et al. (2024) and Peng et al. (2017) reported that non-extractable proanthocyanidins contained in the black soybean seed coat after acid hydrolysis treatment of the residue obtained by removing extractable polyphenols with aqueous–organic solvents, such as methanol and acetone. In this study, although almost no anthocyanins or monomers and oligomers of flavan-3-ol were detected in black soybean water-insoluble fraction (Tables 1 & 2), the presence of proanthocyanidins was suggested in the acidified insoluble solution (Figure 4, Table 3); therefore, it is reasonable to assume that highly polymerized proanthocyanidins were present in black soybean insoluble fraction.

Because of the high binding abilities of procyanidin C1 and

Table 3. Polyphenol contents of the acidified methanol solution of the water-insoluble fraction of black and yellow soybean seed coats

	Total cyanidins (mg/g, cyanidin equivalent)	Total proanthocyanidins (mg/g, CAT equivalent)
B-IS	66.8	1.3
Y-IS	Trace	Trace

The means of two measurements are shown based on the weight of the seed coat. The total cyanidins were calculated by the absorbance (555 nm), and the total proanthocyanidins were determined using the vanillin sulfate method. CAT, (+)-catechin; B-IS, black soybean water-insoluble fraction; Y-IS, yellow soybean water-insoluble fraction; Trace, below the limit of quantification.

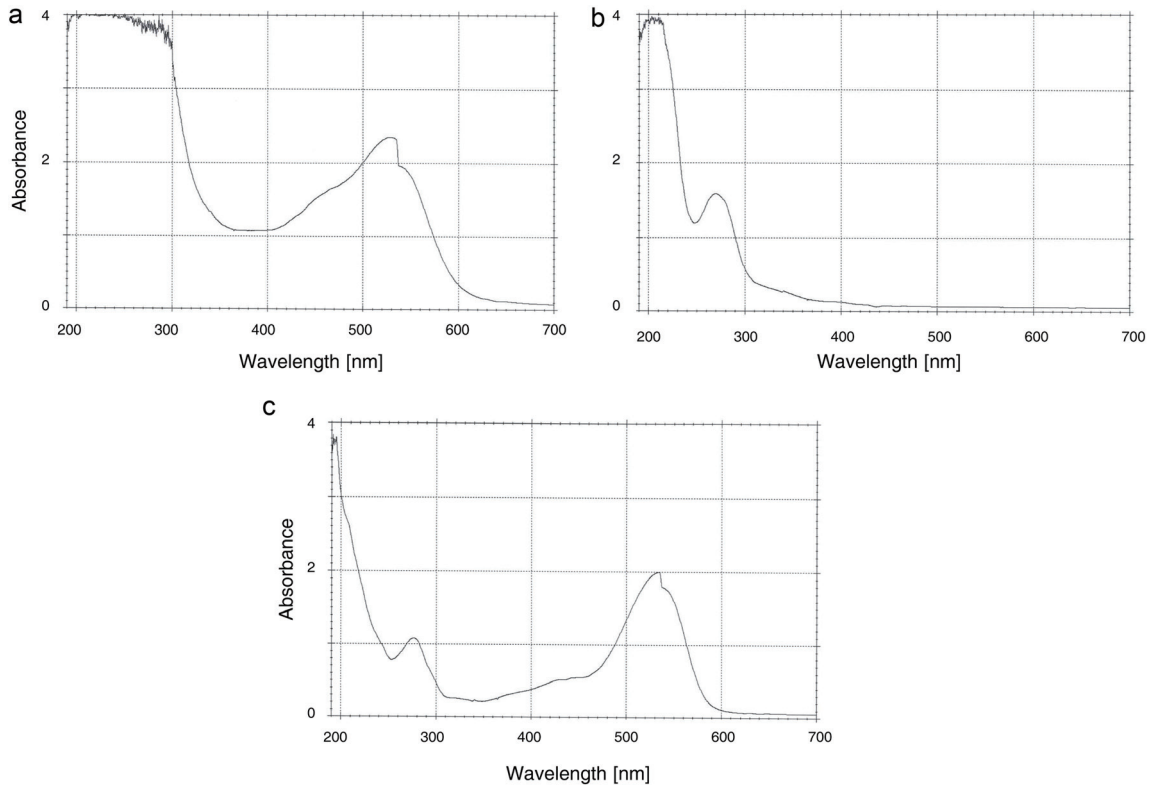


Figure 4. Optical absorption spectrum of the acidified methanol solution of the water-insoluble fraction of black soybean seed coat (a), that of yellow soybean seed coat (b), and cyanidin as a control (c).

cinnamtannin A2, the trimer and tetramer of (–)-epicatechin, respectively (Figure 3), proanthocyanidins with higher polymerization degree were presumed to also exhibit bile acid-binding ability. Takekawa and Matsumoto (2012) reported that the water-insoluble proanthocyanidin contents, measured using the vanillin hydrochloride method, correlated with CA-binding rates in extracts of 10 types of immature persimmon fruits, pears, and peaches. Hamauzu and Mizuno (2011) and Hamauzu and Suwannachot (2019) suggested that the high content of non-extractable polyphenols in dried persimmons and quinces may contribute to their strong bile acid-binding abilities. As mentioned above, Li et al. (2019) reported that, in bananas, complexes are formed by the adsorption of proanthocyanidins and bile acids, through hydrogen bonds and hydrophobic interactions. Although the proanthocyanidins of black soybeans, immature persimmon fruits, and bananas may have different structures, non-extractable proanthocyanidins of black soybeans may form similar complexes with bile acids through hydrogen bonding and hydrophobic interactions, resulting in a high bile acid-binding ability.

Bile acid sequestrants and food substances with similar properties primarily exert their effects in the small intestine, specifically from the lower jejunum to the ileum at a pH of around 7.5–8.0. A slight discrepancy existed between the pH of PBS used in this experimental system (7.4) and that of the small intestine. When the pH rises to 7.5 or higher, deprotonation of polyphenols proceeds, causing electrostatic repulsion with negatively charged bile acids, which may weaken their interactions. In contrast, in the large intestine, the pH drops again (to around 5.5–7.0) due to fermentation by intestinal bacteria. Regarding the pharmacokinetics of proanthocyanidins in humans, proanthocyanidins with a high degree of polymerization (DP>3) are rarely absorbed from the intestinal tract (Zhang et al., 2016). Therefore, regarding the interaction between polyphenols that flow into the large intestine without being reabsorbed in the ileum and bile acids, electrostatic repulsion is eliminated as the pH in the large intestine decreases; thus, the conditions of this experiment are considered to have high physiological validity. Consequently, the intake of black soybeans may contribute to improved cholesterol metabolism by allowing highly polymerized proanthocyanidins to adsorb bile acids in the intestine without digestion or absorption, thereby promoting the excretion of bile acids in feces.

Although the yellow soybean seed coat contained almost no polyphenols (Tables 1–3), the insoluble fraction showed some degree of bile acid-binding ability (Figure 1). While not examined in this study, bile-acid binding by insoluble dietary fiber of black soybeans has been reported (Lei et al., 2025). As the dietary fiber content in black and yellow soybeans is almost the same (Kan et al., 2018), insoluble dietary fiber is considered to commonly affect the bile acid-binding ability of the insoluble fractions of both black and yellow soybeans.

This study provides the first evidence of the potent bile acid-binding ability of polyphenols concentrated in black soybean seed coat. Although soybean dietary fiber also exhibits bile acid-binding ability, further comparative analyses involving diverse soybean phenotypes such as brown and alternative black varieties are required to delineate the relative functional contributions of fiber versus polyphenolic fractions. In addition, although highly polymerized proanthocyanidins exhibit strong bile acid-binding ability, their limited bioavailability suggests that they induce the liver to synthesize new bile acids from cholesterol by firmly binding to

and excreting bile acids in the lower gastrointestinal tract, thereby is thought to stimulate a systemic shift in lipid metabolism. Thus, dynamic biological reactions—such as the cascading metabolic shifts triggered by the disruption of the enterohepatic circulation and signal regulation mediated by the gut microbiota—cannot be evaluated using a single *in vitro* model. Therefore, *in vivo* evaluations in animals and humans are essential to accurately assess the unique bioavailability of black soybean seed coats and to verify their substantive effects on improving lipid metabolism.

4. Conclusion

In this study, the bile acid-binding abilities of black and yellow soybean seed coats were measured, and the relationships between the polyphenols contained in the seed coat were investigated. The results showed that the seed coats of black and yellow soybeans had bile acid-binding abilities for cholic and deoxycholic acids. The bile acid-binding rate of black soybean seed coat was significantly higher than that of yellow soybeans, and both water-soluble and water-insoluble fractions showed bile acid-binding ability. The binding ability of the water-soluble fraction was attributed to the abundance of C3G and the high binding rate observed for the pure products of flavan-3-ol monomers and oligomers. In contrast, the bile acid-binding ability of the water-insoluble fraction was influenced by highly polymerized proanthocyanidins. The results of this study reveal the high bile acid-binding ability of polyphenols contained in black soybean seed coat and suggest that ingestion of black soybean seed coat may support healthy cholesterol metabolism.

Conflict of interest

All contributing authors declare no conflicts of interest.

References

Dongowski, G. (2007). Interactions between dietary fibre-rich preparations and glycoconjugated bile acids *in vitro*. Food Chem. 104: 390–397.

Furuta, S., Takahashi, M., Takahata, Y., Nishiba, Y., Oki, T., Masuda, M., Kobayashi, M., and Suda, I. (2003). Radical-scavenging activities of soybean cultivars with black seed coats. Food Sci. Technol.Res. 9: 73–75.

Ganesan, K., and Xu, B. (2017). A critical review on polyphenols and health benefits of black soybeans. Nutrients 9: 455.

Hamauzu, Y., and Ikeda, E. (2022). *In vitro* and *in vivo* evaluation of the bile acid-binding properties of dried persimmon and its non-extractable proanthocyanidin fraction. Food Chem. 373: 131617.

Hamauzu, Y., and Mizuno, Y. (2011). Non-extractable procyanidins and lignin are important factors in the bile acid binding and radical scavenging properties of cell wall material in some fruits. Plant Foods Hum. Nutr. 66: 70–77.

Hamauzu, Y., and Suwannachot, J. (2019). Non-extractable polyphenols and *in vitro* bile acid-binding capacity of dried persimmon (Diospyros kaki) fruit. Food Chem. 293: 127–133.

Kahlon, T., and Chow, F. (2000). *In vitro* binding of bile acids by rice bran, oat bran, wheat bran, and corn bran. Cereal Chem. 77: 518–521.

Kahlon, T., and Shao, Q. (2004). *In vitro* binding of bile acids by soy bean (Glycine max), black eye bean (Vigna unguiculata), garbanzo (Cicer arietinum) and lima bean (Phaseolus lunatus). Food Chem. 86: 435–440.

Kahlon, T., and Smith, G. (2007). *In vitro* binding of bile acids by blueberries (Vaccinium spp.), plums (Prunus spp.), prunes (Prunus spp.), strawberries (Fragaria X ananassa), cherries (Malpighia punicifolia), cranberries (Vaccinium macrocarpon) and apples (Malus sylvestris). Food Chem. 100: 1182–1187.

Kan, L., Nie, S., Hu, J., Wang, S., Bai, Z., Wang, J., Zhou, Y., Jiang, J., Zeng, Q., and Song, K. (2018). Comparative study on the chemical composition, anthocyanins, tocopherols and carotenoids of selected legumes. Food Chem. 260: 317–326.

Konishi, T., and Nabetani, K. (2013). Enterohepatic circulation: Focus on the bile acid cycle. Jpn. J. Surg. Metab. Nutr. (Geka to Taisha Eiyou) 47: 41–43(in Japanese).

Lei, H., Zhang, Y., Guan, T., Liu, M., Li, Z., Liu, J., Zhao, J., and Liu, T. (2025). Modification of black soybean (Glycine max (L.) merr.) residue insoluble dietary fiber with ultrasonic, microwave, high temperature and high-pressure, and extrusion. Food Chem. 473: 143020.

Li, X., Jiao, W., Zhang, W., Xu, Y., Cao, J., and Jiang, W. (2019). Characterizing the interactions of dietary condensed tannins with bile salts. J. Agric. Food Chem. 67: 9543–9550.

Liu, Y., Tong, Y., Tong, Q., Xu, W., and Wang, Z. (2024). Effect of ultrasonic modification on the binding ability of pectin to anthocyanin. J. Sci. Food Agric. 104: 3614–3623.

Malenčić, D., Cvejić, J., and Miladinović, J. (2012). Polyphenol content and antioxidant properties of colored soybean seeds from central Europe. J. Med. Food 15: 89–95.

Matsumoto, K., Kadowaki, A., Ozaki, N., Takenaka, M., Ono, H., Yokoyama, S., and Gato, N. (2011). Bile acid-binding ability of kaki-tannin from young fruits of persimmon (Diospyros kaki) *in vitro* and *in vivo*. Phytother. Res. 25: 624–628.

Matsumoto, K., Yokoyama, S., and Gato, N. (2010). Bile acid-binding activity of young persimmon (Diospyros kaki) fruit and its hypolipidemic effect in mice. Phytother. Res. 24: 205–210.

Mizuno, N., Noshima, Y., and Toda, T. (2024). Relationship between black soybean polyphenols and seed coat color during boiling process. Food Sci. Technol. Res. 30: 591–598.

Nishijima, T., Yamashita, Y., and Ashida, H. (2024). Black soybean seed coat polyphenols have different effects on glucose and lipid metabolism in growing and young adult mice. Food Funct. 15: 1004–1020.

Northfield, T., and McColl, I. (1973). Postprandial concentrations of free and conjugated bile acids down the length of the normal human small intestine. Gut 14: 513–518.

Oki, T., Sawai, Y., Sato-Furukawa, M., and Suda, I. (2011). Validation of pH differential method for the determination of total anthocyanin content in black rice and black soybean with interlaboratory comparison. Bunseki Kagaku 60: 819–824(in Japanese).

Peng, H., Li, W., Li, H., Deng, Z., and Zhang, B. (2017). Extractable and non-extractable bound phenolic compositions and their antioxidant properties in seed coat and cotyledon of black soybean (Glycinemax (L.) merr). J. Funct. Foods 32: 296–312.

Pérez-Jiménez, J., and Saura-Calixto, F. (2015). Macromolecular antioxidants or non-extractable polyphenols in fruit and vegetables: Intake in four European countries. Food Res. Int. 74: 315–323.

Sawai, Y., Sugawara, T., Oki, T., Nishiba, Y., Ujihara, K., and Suda, I. (2012). Comparison of high-performance liquid chromatography and pH differential method: correlations for quantitation of anthocyanins in black pearl rice and soybean. J. Jpn. Soc. Food Sci. Technol. (Nippon Shokuhin Kagaku Kogaku Kaishi) 59: 104–108(in Japanese).

Scaldaferri, F., Pizzoferrato, M., Ponziani, F.R., Gasbarrini, G., and Gasbarrini, A. (2013). Use and indications of cholestyramine and bile acid sequestrants. Intern. Emerg. Med. 8: 205–210.

Sun, B., Leandro, C., Ricardo da Silva, J.M., and Spranger, I. (1998). Separation of grape and wine proanthocyanidins according to their degree of polymerization. J. Agric. Food Chem. 46: 1390–1396.

Takahata, Y., Ohnishi-Kameyama, M., Furuta, S., Takahashi, M., and Suda, I. (2001). Highly polymerized procyanidins in brown soybean seed coat with a high radical-scavenging activity. J. Agric. Food Chem. 49: 5843–5847.

Takekawa, K., and Matsumoto, K. (2012). Water-insoluble condensed tannins content of young persimmon fruits-derived crude fibre relates to its bile acid-binding ability. Nat. Prod. Res. 26: 2255–2258.

Therdtatha, P., Shinoda, A., and Nakayama, J. (2022). Crisis of the Asian gut: associations among diet, microbiota, and metabolic diseases. Biosci. Microbiota Food Heal. 41: 83–93.

Todd, J.J., and Vodkin, L.O. (1993). Pigmented soybean (Glycine max) seed

coats accumulate proanthocyanidins during development. Plant physiol. 102: 663–670.
Uchida, K. (2009). "Bile acids and bile" Sanseido. Tokyo.
Wang, L., Yamashita, Y., Saito, A., and Ashida, H. (2017). An analysis method for flavan-3-ols using high performance liquid chromatography coupled with a fluorescence detector. J. Food Drug Anal. 25: 478–487.
Yamashita, Y., Sakakibara, H., Toda, T., and Ashida, H. (2020). Insights into the potential benefits of black soybean (Glycine max L.) polyphenols in lifestyle diseases. Food Funct. 11: 7321–7339.
Yokota, A., Fukiya, S., Islam, K.S., Ooka, T., Ogura, Y., Hayashi, T., Hagio, M., and Ishizuka, S. (2012). Is bile acid a determinant of the gut microbiota on a high-fat diet? Gut microbes 3: 455–459.
Zhang, L., Wang, Y., Li, D., Ho, C.-T., Li, J., and Wan, X. (2016). The absorption, distribution, metabolism and excretion of procyanidins. Food Funct. 7: 1273–1281.

Journal of Food Bioactives
International Society for Nutraceuticals and Functional Foods
Original Research
J. Food Bioact. 2026;35:46–56

Pyroglutamyl peptide–rich rice protein hydrolysate restores cecal *N*-acetyl amino acids in high-fat-diet–fed rats, outperforming short-chain fatty acids as early microbial markers

Satoshi Miyauchi[a,b], Shiro Kajiwara[c], Tomoko Asai[a], Yasutaka Shigemura[b] and Kenji Sato[a*]

[a]Division of Applied Biosciences, Graduate School of Agriculture, Kyoto University, Kitashirakawa Oiwake-cho, Sakyo-ku, Kyoto 606 8502, Japan
[b]Department of Food and Nutrition, Tokyo Kasei University, 1-18-1 Kaga, Itabashi-ku, Tokyo 173 8602, Japan
[c]Bansyu chomiryo Co., Ltd., 948, Nozato, Himeji, Hyogo 670 0811, Japan
[*]**Corresponding author:** Kenji Sato, Division of Applied Biosciences, Graduate School of Agriculture, Kyoto University, Kitashirakawa Oiwake-cho, Sakyo-ku, Kyoto 606 8502, Japan. E-mail: kenjisato6213@gmail.com
DOI: 10.26599/JFB.2026.95035455
Received: June 12, 2026; **Revised received & accepted:** July 28, 2026
Citation: Miyauchi, S., Kajiwara, S., Asai, T., Shigemura, Y., and Sato, K. (2026). Pyroglutamyl peptide–rich rice protein hydrolysate restores cecal *N*-acetyl amino acids in high-fat-diet–fed rats, outperforming short-chain fatty acids as early microbial markers. J. Food Bioact. 35: 46–56.

Abstract

Pyroglutamyl-leucine (pyroGlu-Leu) is a food-derived modified peptide known to modulate the gut microbiota. This study examined the effects of orally administered rice protein hydrolysate (RPH) containing pyroGlu-Leu in rats fed a 45% high-fat diet that induced mild dysbiosis without obesity or severe liver dysfunction. In addition to short-chain fatty acids (SCFAs), several *N*-acetyl amino acids (NAAAs) were detected in cecal contents. The high-fat diet significantly decreased both SCFAs and NAAAs, whereas administration of RPH or synthetic pyroGlu-Leu restored the levels of NAAAs despite not recovering those of SCFAs. RPH did not alter the overall gut microbial composition but modified specific bacterial taxa that correlated with NAAA levels. These results suggest that NAAAs are gut microbiota-derived metabolites that respond more sensitively to food-derived modulation of the gut microbiota than SCFAs, and may serve as early indicators of microbiota–host metabolic interactions.

Keywords: Peptide; Pyroglutamyl peptide; Microbiota; Short-chain fatty acid; *N*-Acetyl amino acid.

1. Introduction

Pyroglutamyl peptides, which are non-enzymatically generated from peptides containing *N*-terminal glutaminyl residue, are widely present in food protein hydrolysates and fermented foods (Ejima et al., 2018; Gazme et al., 2019; Kiyono et al., 2013; Nagao et al., 2024; Rahmadian et al., 2025; Sato et al., 1998, 2013; Shirako et al., 2020). Several pyroglutamyl di- and tri-peptides have been reported to resist in vitro digestion by endoproteinases and exopeptidases (Chen et al., 2019; Ejima et al., 2018; Miyauchi et al., 2022; Sato et al., 1998). In addition, levels of certain food-derived pyroglutamyl peptide increase in the bloodstream after oral administration of food protein hydrolysates and fermented foods, such as soybean paste (miso) and fish sauce (Ejima et al., 2018; Higaki-Sato et al., 2006; Miyauchi et al., 2022; Nagao et al., 2024; Rahmadian et al., 2025; Sato et al., 2013).

Several pyroglutamyl peptides exhibit biological activities in vivo and in vitro. Among them, pyroGlu-Leu, first identified as a hepatoprotective peptide from wheat gluten hydrolysate (Sato et al., 2013)—has been reported to attenuate dextran sulfate sodium (DSS)-induced colitis and to improve gut microbial imbalance in the ratio of Firmicutes to Bacteroidetes at doses as low as 0.1 mg/kg/body weight (Wada et al., 2013). More recently, Shirako et al. (2019) demonstrated that pyroGlu-Leu enhances the secretion of host antimicrobial peptides from Paneth cells to lumen of ileum, thereby ameliorating high-fat-diet-induced gut microbial dysbio-

© The author(s) 2026. Publishing Services by Tsinghua University Press
The articles published in this open access journal are distributed under the terms of the Creative Commons Attribution 4.0 International License (http://creativecommons.org/licenses/by/4.0/)

sis. These findings suggest that pyroGlu-Leu may attenuate DSS-induced colitis by modulating gut microbiota through the stimulation of host antimicrobial peptide secretion. However, the downstream microbial metabolites involved in this process remain unclear. Short-chain fatty acids (SCFAs), major gut microbial metabolites, are known to maintain intestinal homeostasis by strengthening the intestinal barrier and modulating immune and inflammatory responses (Fusco et al., 2023; Kim et al., 2013; Parada Venegas et al., 2019). Thus, the anti-colitis effect of pyroGlu-Leu may be linked to SCFAs production through microbiota modulation.

Our previous study revealed that a rice protein hydrolysate (RPH) contains pyroglutamyl peptides, including pyroGlu-Leu at a concentration of approximately 5 μmol/g, and that oral administration of RPH increases pyroglutamyl peptide levels in the ileum (Miyauchi et al., 2022). The objective of the present study was to investigate the effects of the RPH containing pyroglutamyl peptides, including pyroGlu-Leu, on gut microbiota and SCFAs in a high-fat-diet-induced dysbiosis model.

2. Materials and methods

2.1. Rice protein hydrolysate

A rice protein hydrolysate (RPH) was prepared by Bansyu Chomiryo (Hyogo, Japan) and was identical to that used in a previous study (Miyauchi et al., 2022). Briefly, rice protein, a byproduct of rice starch production, suspended in water and enzymatically hydrolyzed using food-grade plant- and microorganism-derived proteases. The enzymatic reaction was terminated by heating, after which the hydrolysate was separated into liquid and solid fractions by filtration. The liquid fraction was collected and spray-dried. According to information from the manufacturer, the protein concentrations of the rice protein substrate and its hydrolysate (RPH), determined by the Kjeldahl method, were 83% and 86%, respectively. The RPH used in this study is a prototype intended for industrial application, and the specific enzymes and reaction conditions employed have not been disclosed. However, the composition and content of the pyroglutamyl peptides within it are described in detail in previous reports (Miyauchi et al., 2022).

2.2. Reagents

Acetonitrile (HPLC grade), and phosphate-buffered saline (pH 7.4, 10× PBS) were purchased from Nacalai Tesque (Kyoto, Japan). Triethylamine (TEA), propionic acid, and butyric acid were purchased from Fujifilm Wako Pure Chemical (Osaka, Japan). *N*-Acetyl-glycine, *N*-acetyl-L-isoleucine, *N*-acetyl-L-leucine, and *N*-acetyl-L-phenylalanine were purchased from Tokyo Chemical Industry (Tokyo, Japan), and *N*-acetyl-L-alanine was purchased from Merck (Darmstadt, Germany). *N*-(*tert*-Butoxycarbonyl)-L-pyroglutamic acid (Boc-Pyr-OH), L-leucine *tert*-butyl ester hydrochloride (H-Leu-OtBu·HCl), 1-hydroxybenzotriazole (Hobt), and 1-(3-dimethylaminopropyl)-3-ethylcarbodiimide hydrochloride (WSCI·HCl) were purchased from Watanabe Chemical Industries (Hiroshima, Japan).

2.3. Peptide synthesis

PyroGlu-Leu were synthesized by a liquid-phase method using TEA, Boc-Pyr-OH, H-Leu-OtBu·HCl, Hobt, and WSCI·HCl, as described previously (Sato et al., 2013). The synthesized pyroGlu-Leu was purified by reversed-phase high-performance liquid chromatography (RP-HPLC) using a Cosmosil 5C18MS-II column (10 mm i.d. × 250 mm, Nacalai Tesque). A binary linear gradient was applied using 0.1% formic acid (solvent A) and 0.1% formic acid in 80% acetonitrile (solvent B) at a flow rate of 2 mL/min. The gradient program was as follows: 0–20 min, 0–50% B; 20–30 min, 50–100% B; 30–35 min, 100% B; 35–35.1 min, 100–0% B; 35.1–45 min, 0% B. The column temperature was maintained at 40 °C. Peptide elution was monitored at 214 and 254 nm. The purified pyroGlu-Leu was lyophilized and used in an animal experiment.

2.4. Animal experiment

All animal procedures were conducted in accordance with the National Institutes of Health guidelines for the care and use of laboratory animals and were approved by the Animal Care Committee of the Louis Pasteur Center for Medical Research (Kyoto, Japan, approval number 202102). Five-week-old male Wistar/ST rats (130–150 g body weight) were purchased from Japan SLC (Shizuoka, Japan). During a 1-week acclimatization period, rats were housed individually under controlled temperature (24–26 °C), humidity, (40–60%) and a 12 h light–dark cycle, with free access to standard chow (MF diet, Oriental Yeast, Tokyo, Japan) and water.

After 1-week acclimatization, rats were randomly assigned to five groups (n = 4, per group): normal diet + vehicle (C), high-fat diet + vehicle (HF), high-fat diet + RPH at 20 mg/kg body weight/day (LRP), high-fat diet + RPH at 100 mg/kg body weight/day (HRP), high-fat diet + pyroGlu-Leu at 1 mg/kg body weight/day (PEL). Rats in the HF, LRP, HRP, and PEL groups were fed high-fat diet (45% kcal fat/total kcal; solid type of D12451, Research Diets, New Brunswick, NJ, USA) for 5 weeks, whereas the C group continued the standard chow. Body weight was recorded weekly.

RPH and pyroGlu-Leu were orally administered via drinking water, with concentrations adjusted daily based on the body weight and previous day's water intake. To accurately measure the daily water intake, the rats were housed individually in cages. Individual water intake was recorded daily on weekdays. For each three-day weekend period, cumulative water consumption was recorded and divided by three to estimate the average daily intake (Table S1). Actual daily doses were calculated from the treatment concentration, measured water intake, and body weight (Table S2). Food intake was monitored throughout the experiment, and total calorie intake was calculated. All rats had ad libitum access diet and drinking water throughout the experiment. At the end of 5-week feeding period, fecal samples were collected, immediately frozen at −80 °C, and stored at −80 °C until microbiota analysis. Rats were euthanized under isoflurane anesthesia, and blood was collected from the inferior vena cava. Plasma was prepared by centrifugation at 800 × *g* for 10 min in the presence of heparin. The cecum and its inner content were collected and stored at −80 °C. Plasma biochemical parameters (albumin; ALB, creatinine; CRE, aspartate aminotransferase; AST, alanine aminotransferase; ALT, alkaline phosphatase; ALP, total cholesterol; TCHO, triglyceride; TG, glucose; GLC) were measured by Oriental Yeast Co., Ltd. (Tokyo, Japan).

2.5. Identification and quantification of microbial metabolites in cecal contents

Cecal contents (50 mg) were mixed with nine volumes of ultrapure water (450 μL) and centrifuged at 13,000 × *g* for 10 min at 4 °C. The supernatant was collected as the aqueous extract. Carboxy

groups in the extract were derivatized with 2-nitrophenylhydrazine (2-NPH) using a fatty acids label kit (YMC, Kyoto, Japan) with slight modifications. Briefly, 20 µL of extract was mixed with 40 µL ultrapure water, 40 µL of 0.02 M 2-NPH hydrochloride (reagent A), and 40 µL of 0.25 M 1-(3-dimethylaminopropyl)-3-ethylcarbodiimide hydrochloride (reagent B) followed by incubation at 60 °C for 20 min. The reaction mixture was then combined with 40 µL of 1 M KOH and incubated at 60 °C for an additional 15 min. After cooling to room temperature, 20 µL of 10% formic acid was added, and the mixture was filtered through a Cosmonice filter (4 mm i.d., 0.45 µm, Nacalai Tesque).

An aliquot (10 µL) of the filtrate was analyzed by liquid chromatography–electrospray ionization tandem mass spectrometer (LC–MS/MS, LCMS 8040, Shimadzu, Kyoto, Japan). The derivatized compounds were resolved by RP-HPLC using an Inertsil ODS-3 column (2.1 mm i.d. × 250 mm, GL Sciences, Tokyo, Japan). A binary linear gradient was performed using same solvents as mentioned before at a flow rate of 0.2 mL/min. The gradient program was as follows: 0–20 min, 0–40% B; 20–35 min, 40–100% B; 35–45 min, 100% B; 45–45.1 min, 100–0% B; 45.1–55 min, 0% B. The column was maintained at 40 °C.

2-NPH derivatives were specifically detected in neutral loss mode, scanning for precursor ions undergoing a neutral loss of mass-to-charge ratio (*m/z*) 153 (the 2 NPH moiety) under collision induced dissociation at −15 eV. Product ion scans at −15 eV and −35 eV were used to estimate structures.

Quantification of acetic acid, propionic acid, butyric acid, *N*-acetyl-Gly, and *N*-acetyl-Ala were determined using LC-MS/MS in multiple reaction monitoring (MRM) mode. *N*-Acetyl-Ile, *N*-acetyl-Leu, and *N*-acetyl-Phe were quantified without the derivatization by direct LC-MS/MS injection. MRM conditions were optimized using the LabSolutions LCMS Ver. 5.5 (Shimadzu).

2.6. Microbiota analysis

Fecal samples collected at the end of the experiment were analyzed for gut microbiota composition based on 16S ribosomal RNA gene sequences (Kim et al., 2013). Analyses were outsourced to Sheep-Medical (Tokyo, Japan). Samples were suspended in 4 M guanidino thiocyanate and homogenized using zirconia beads. After centrifugation, bacterial DNA was extracted from the supernatant using a Maxwell RSC automated system (Promega Corporation, Madison, WI, USA).

The V1–V2 region of the 16S rRNA gene was amplified by polymerase chain reaction (PCR, 98 °C for 30 s:20 cycles of 98 °C for 10 s, 55 °C for 10 s, and 72 °C for 5 s). Template preparation was performed using an Ion Chef system (Thermo Fisher Scientific, Waltham, MA, USA) and sequencing was performed on an Ion S5 instrument (Thermo Fisher Scientific). Taxonomic assignment and relative abundance calculations were performed using Ion Reporter software (Thermo Fisher Scientific). Sequences were analyzed as operational taxonomic units (OTUs) using a QIIME-based workflow implemented in Ion Reporter with the default settings, and taxonomic assignment was performed using the MicroSEQ ID and Greengenes 13_5 reference databases. DNA-extraction blanks and no-template PCR negative controls were included in each analytical run; however, a defined positive-control mock community was not included.

Taxon-specific read counts were divided by the total number of classified reads in each sample and expressed as relative abundances. Thus, total-sum scaling was used to normalize the taxonomic profiles across samples, and rarefaction was not performed. Beta diversity was assessed using Bray–Curtis distances calculated from the relative-abundance data, and differences in microbial community composition were visualized by non-metric multidimensional scaling (NMDS).

2.7. Statistical analysis

Each individual rat was considered an independent experimental unit for all statistical analyses. Differences in bacterial phyla and species relative abundances as well as cecal metabolite concentrations between the HF group and the other groups were evaluated using the Steel test. To account for the simultaneous analysis of 130 bacterial taxa, the Steel-adjusted *p*-values were further adjusted separately for each group comparison using the Benjamini–Hochberg procedure. An FDR-adjusted q-value of less than 0.05 was considered statistically significant. Taxa with a Steel-adjusted *p*-value of less than 0.05 but an FDR-adjusted q-value of 0.05 or greater were regarded as exploratory findings. Differences in initial and final body weights, total food intake, and plasma biochemical parameters between the HF group and other groups were evaluated by Dunnett's test. Similarities in fecal microbiota composition were evaluated by pairwise permutational multivariate analysis of variance (PERMANOVA; Adonis) based on Bray-Curtis distances. A *p*-value of less than 0.05 was considered statistically significant.

3. Results

3.1. Identification of carboxylic compounds in rat cecal contents

Representative mass chromatograms obtained in neutral-loss scan mode for 2-NPH derivatives of carboxyl compounds in rat cecal contents are shown in Figure 1 (upper panel). The peaks marked with a–j were assigned to the 2-NPH derivatives of acetic acid (a), propionic acid (b), isobutyric acid (c) butyric acid (d), isovaleric acid (e), valeric acid (f), pyroglutamic acid (g), succinic acid (h), caproic acid, and pyruvic acid (i), respectively, based on retention time (Inoue et al., 2019) and precursor ion *m/z* values (Table 1). Pyruvic acid was detected as a derivative containing two 2-NPH units. Among these compounds, acetic, propionic, and butyric acids were the major metabolites present in cecal contents. Additional peaks marked with 1–7 were also detected in neutral-loss scan mode. The calculated molecular weights of these carboxylic compounds in these peaks did not match those of SCFAs or common organic acids from glycolysis or Krebs cycle. To evaluate their structures, product-ion scans were carried out in positive mode. Figure 1 (lower panel) shows product-ion spectrum of the precursor ion at *m/z* 253 (peak 1), which exhibited product ion (b1) derived from *N*-acetyl group (*m/z* 43) and immonium ion of glycine (*m/z* 30). In addition, b2 ion resulting from loss of the 2-NPH moiety (*m/z* 100) was also detected. These data identified peak 1 as the 2-nitrophenylhydrazide derivative of *N*-acetyl-Gly.

The precursor and product ions and the estimated structures of compounds in peaks 1–7 are summarized in Table 2. Subsequent MRM analysis using standards confirmed the presence of *N*-acetyl amino acids (NAAAs) listed in Table 2 in cecal contents. *N*-Propionyl-Ile/Leu, *N*-propionyl-Gly, and *N*-propionyl-Ala could not be validated due to unavailability of commercial standards. Peaks marked with asterisk (*) (Figure 1 upper panel) could not be assigned to known SCFAs, organic acids, or modified amino acids based on their MS/MS spectra. Peaks marked with # were derived from the derivatization reagents, as they were also detected in control injection of ultra-pure water processed with 2-NPH (data not shown).

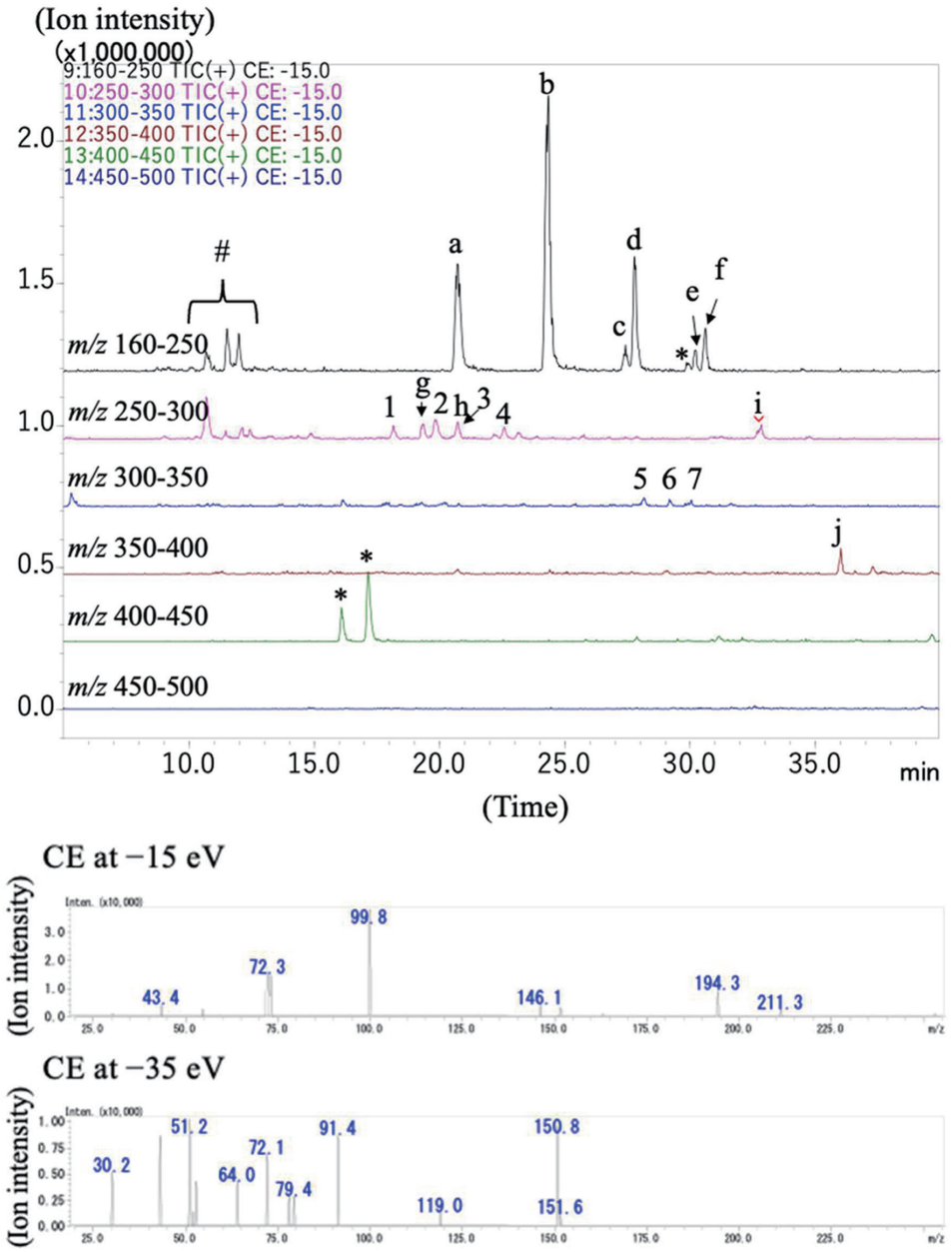


Figure 1. Mass chromatograms of 2-nitrophenylhydrazides of a cecal content of the rat in the HRP group in neutral loss scan mode (upper panel) and spectra of the product ions from precursor ions in peak 1 (lower panel). The peaks marked with lowercase in the chromatograms were estimated to be SCFAs and organic acids based on their retention time and *m/z*. The peaks marked with number were estimated to be modified amino acids consisting of SCFAs and amino acids on the basis of their *m/z* and mass spectra of product ion scanning. The peaks marked with sharp (#) were derived from the reagents and the peaks with asterisks could not be assigned to be any organic acids and modified amino acids. The product ion scan was carried out using collision energies at −35 and −15 eV.

3.2. Effects of RPH and pyroGlu-Leu on body weight gain and blood biochemical parameters

High-fat diet feeding did not significantly affect final body weight or total calorie intake (Table 3), indicating that the present 45% high-fat diet did not induce obesity. Plasma biochemical parameters, including AST, ALT, and creatinine, were not significantly altered by the high-fat diet, except for a significant increase in ALP, suggesting the absence of severe hepatic or renal dysfunction. In the PEL group, plasma TG levels were significantly higher than in the HF group; however, no other biochemical parameters differed significantly between RPH or PEL group and the HF group (Table 4).

3.3. Effects of RPH and pyroGlu-Leu on SCFAs in cecal content

Cecal SCFAs concentrations were quantified by LC-MS/MS in

Table 1. Summary of estimated SCFAs and organic acids in the rat cecal contents

Peak	Estimated compound	Precursor ion (*m/z*)
a	Acetic acid	196
b	Propionic acid	210
c	Isobutyric acid	224
d	Butyric acid	224
e	Isovaleric acid	238
f	Valeric acid	238
g	Pyroglutamic acid	265
h	Succinic acid	254
i	Capronic acid	252
j	Pyruvic anid (with two 2-NPH)	359

MRM mode. High-fat diet feeding significantly reduced the levels of acetic, propionic, and butyric acids (Figure 2a–c). Administration of RPH and pyroGlu-Leu did not significantly restore propionic or butyric acid levels compared to the HF group. Acetic acid levels were slightly but significantly increased in the HRP group (100 mg/kg body weight/day) compared to the HF group. No significant differences were observed among groups for other organic acids, including lactic, pyruvic, succinic, and malic acids (data not shown).

3.4. Effects of RPH and pyroGlu-Leu on N-acetyl amino acids (NAAAs) in cecal contents

N-acetyl-Gly and *N*-acetyl-Ala were quantified by following derivatization with 2-NPH followed by LC-MS/MS analysis under the same chromatographic conditions used for their identification. Other NAAAs (*N*-acetyl-Ile, *N*-acetyl-Leu, and *N*-acetyl-Phe) were quantified without derivatization, as they were sufficiently retained under the present LC condition.

High-fat diet feeding significantly reduced the levels of all NAAA compared to C group (Figure 3). In contrast, administration of RPH at both doses and pyroGlu-Leu significantly restored the levels of *N*-acetyl-Gly, *N*-acetyl-Ala, and *N*-acetyl Ile (Figure 3a–c). *N*-Acetyl-Leu and *N*-Acetyl-Phe showed similar trends, although significant restoration was observed only in the low-dose RPH group (20 mg/kg/day) (Figure 3d, e).

3.5. Effect of RPH and pyroGlu-Leu on fecal microbiota

Some fecal bacterial taxa could not be identified to species levels and are presented at family level. NMDS based on Bray-Curtis distances revealed no significant differences in overall microbiota composition among the HF, LRP, HRP, and PEL groups, as determined by pairwise Adonis test (Figure 4a).

At the phylum level, the HF group exhibited a significantly lower relative abundance of Bacteroidetes and significantly higher

Table 2. Summary of estimated modified amino acids in the rat cecal contents

Peak number	Estimated compound	Precursor ion (*m/z*)	Product ions (*m/z*)
1	*N*-acetyl-glycine	253	30 (Gly*), 43, 72, 100, 194, 211
2	*N*-acetyl-alanine	267	44 (Ala*), 86, 114, 208
3	*N*-propionyl-glycine	267	30 (Gly*), 57, 73, 86, 114, 194, 211
4	*N*-propionyl-alanine	281	44 (Ala*), 57, 100, 128
5	*N*-acetyl-isoleucine/leucine	309	86 (Ile/Leu*), 128, 156
6	*N*-acetyl-phenylalanine	343	120 (Phe*), 162, 190
7	*N*-propionyl-isoleucine/leucine	323	57, 86 (Ile/Leu*), 142, 170

Asterisks (*) indicate immonium ions of amino acids.

Table 3. Initial and final body weight and total food intake in rats

	C	HF	LRP	HRP	PEL
Initial body weight (g)	176.93 ± 11.68	177.75 ± 7.15	177.33 ± 6.36	177.55 ± 5.77	178.10 ± 6.30
Final body weight (g)	380.08 ± 34.36	386.95 ± 1.49	377.65 ± 18.18	385.53 ± 5.74	400.03 ± 15.41
Total food intake (kcal)	2,383.49 ± 259.79	2,440.92 ± 52.39	2,336.15 ± 162.91	2,405.56 ± 69.64	2,565.55 ± 85.26

Data are shown as mean ± standard deviation (n = 4).

Table 4. Summary of blood biochemical values in rats

	C	HF	LRP	HRP	PEL
Albumin (g/dL)	3.67 ± 0.11	3.98 ± 0.07	3.83 ± 0.05	3.88 ± 0.10	3.73 ± 0.06
Creatinine (mg/dL)	0.28 ± 0.01	0.31 ± 0.01	0.33 ± 0.02	0.32 ± 0.01	0.30 ± 0.00
AST (IU/L)	58.75 ± 2.13	63.25 ± 1.14	72.75 ± 3.66	67.00 ± 1.84	64.25 ± 2.48
ALT (IU/L)	43.25 ± 3.49	47.25 ± 2.33	53.50 ± 1.30	47.25 ± 3.96	46.50 ± 2.25
Alkaline phosphatase (IU/L)	960.00 ± 36.78**	1,323.25 ± 110.57	1,255.00 ± 42.11	1,205.50 ± 55.37	1,108.75 ± 12.46
Total cholesterol (mg/dL)	69.00 ± 3.79	79.75 ± 0.74	79.75 ± 2.97	82.25 ± 1.78	81.25 ± 4.08
Triglyceride (mg/dL)	105.50 ± 11.29	137.50 ± 9.25	163.25 ± 24.67	182.50 ± 17.90	241.00 ± 18.39**
Glucose (mg/dL)	147.75 ± 4.90	152.25 ± 1.88	147.75 ± 8.63	162.00 ± 10.68	154.25 ± 3.25

Data are shown as mean ± standard deviation (n = 4). Asterisks indicate significant difference compared to the HF group by Dunnett's test (** p < 0.01).

levels of Proteobacteria compared with C group (Figure 4c and e). Administration of RPH at 100 mg/kg/day (the HRP group) significantly attenuated the high-fat-diet-induced increase in Proteobacteria (Figure 4e) with similar trends observed in the LRP and PEL groups. No significant differences were observed among groups in relative abundances of Actinobacteria and Firmicutes, nor in the Firmicutes/Bacteroidetes ratio (Figure 4b, d, and f).

At the taxon level, several differences in relative abundance were observed based on the Steel test. The HF group showed significantly lower abundances of Porphyromonadaceae (family level ID only) and significantly higher abundances of *[Eubacterium] dolichum, Phascolarctobacterium faeccium, Enterococcus gallinarum*compared, and *Clostridium symbiosum* compared with C group (Figure 5b, g, k, l, and n). Administrations of RPH altered several taxa relative to the HF group. Low-dose RPH significantly increased Clostridiaceae (slash calls), *[Eubacterium] dolichum*, and Victivallaceae (family level ID only) (Figure 5a, b, and c), and decreased *Arthrobacter creatinoliticus* (Figure 5d). High-dose RPH significantly increased *Bacteroides* sp., *Bacteroides thetaiotaomicron*, Porphyromonadaceae (family level ID only), Eubacteriaceae (family level ID only), *Blautia producta*, *Ruminococcus flavefaciens*, and *Phascolarctobacterium faecium* (Figure 5e–k), while significantly decreasing *Arthrobacter creatinoliticus, Enterococcus gallinarum*, *Lactobacillus animalis*, and *Clostridium symbiosum*, (Figure 5d, l–n). However, none of these taxon-level differences remained statistically significant after Benjamini–

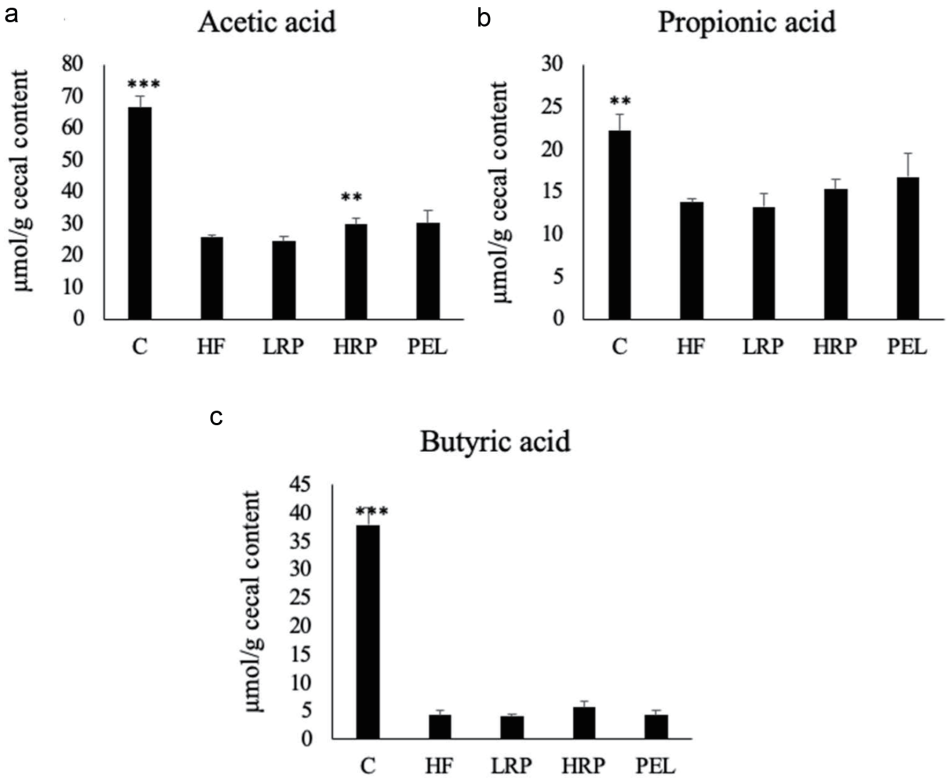


Figure 2. Concentrations of (a) acetic acid, (b) propionic acid, and (c) butyric acid in the cecal contents of rats. Data are shown as mean ± standard error (a–e, n = 4). Asterisks indicate significant differences compared to the HF group evaluated by Steel's test (** p < 0.01, *** p < 0.001).

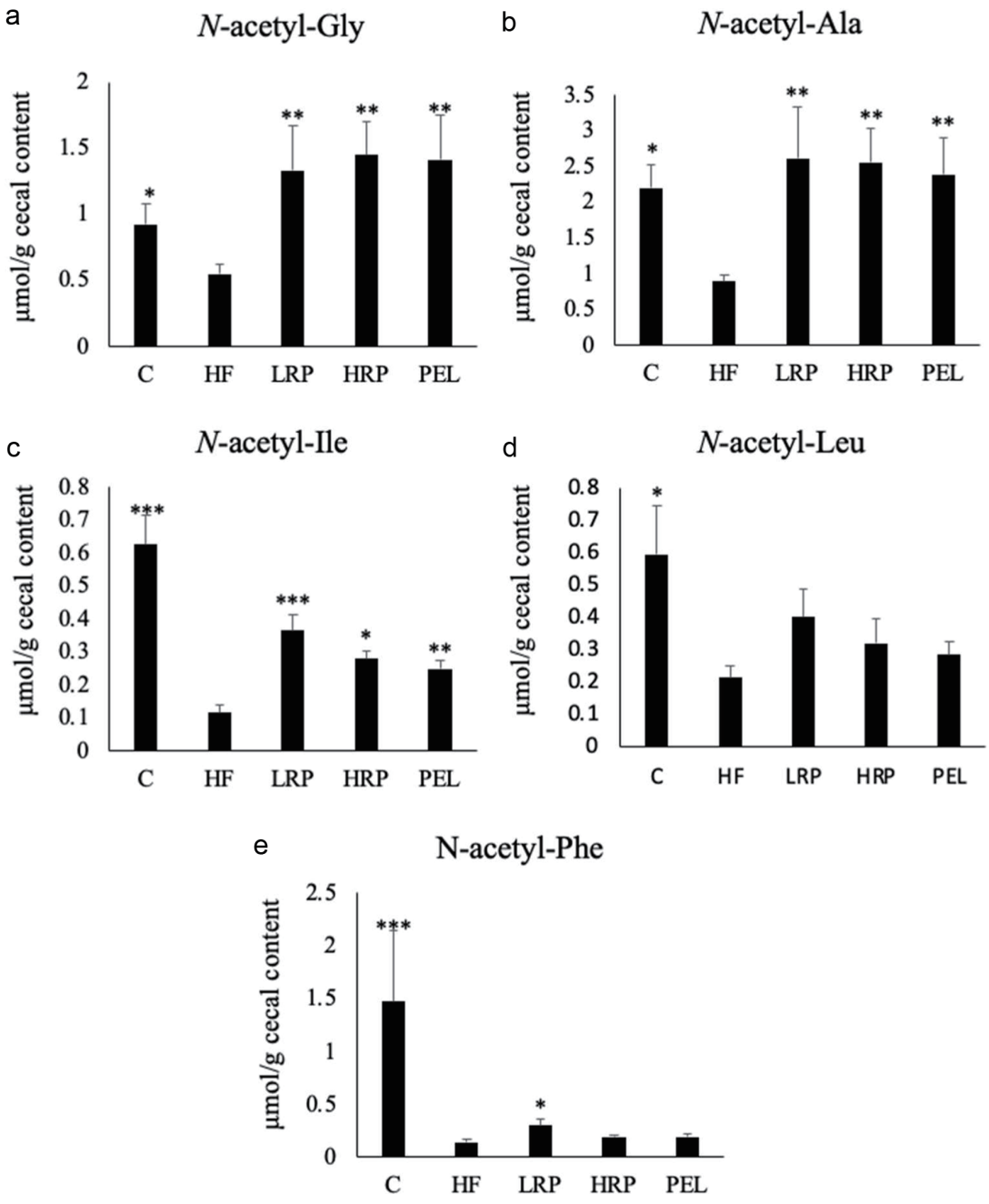


Figure 3. Concentrations of (a) *N*-acetyl-Gly, (b) *N*-acetyl-Ala, (c) *N*-acetyl-Ile, (d) *N*-acetyl-Leu, and (e) *N*-acetyl-Phe in the cecal content of rats. Data are shown as mean ± standard error (a–e, n = 4). Asterisks indicate significant differences compared to the HF group evaluated by Steel's test (* $p < 0.05$, ** $p < 0.01$, *** $p < 0.001$).

Hochberg correction across the 130 taxa examined in each group comparison. Therefore, these findings were should be regarded as exploratory.

3.6. Correlation between fecal bacterial abundances and SCFAs and NAAAs

Spearman's rank correlation coefficients between fecal bacterial species that differed significantly among groups and the levels of SCFAs and NAAAs are presented as a heat map (Figure 6). SCFAs and NAAAs exhibited similar directions of correlation (positive or negative) with the bacterial abundances; however, the strengths of these correlations differed. SCFAs showed strong positive correlations with *Bacteroides thetaiotaomicron*, Porphyromonadaceae (family level ID only), *Ruminococcus flavefaciens*, and *Phascolarctobacterium faecium*. NAAAs also correlated positively with these taxa but with weaker correlation strengths. The exact Spear-

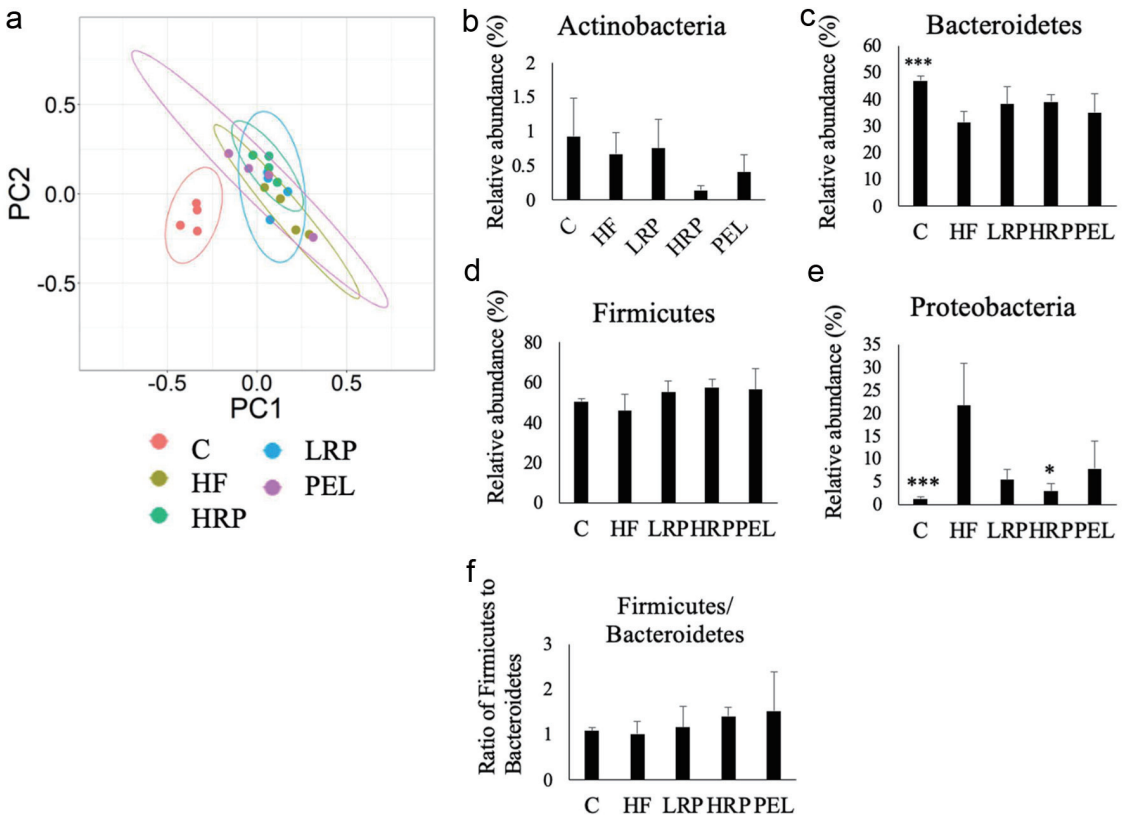


Figure 4. Non-metric multidimensional scaling (NMDS) plot of rat fecal microbiota based on Bray-Curtis distance (a) and the relative abundance of Actinobacteria (b), Bacteroidetes (c), Firmicutes (d), and Proteobacteria (e) and the ratio of Firmicutes to Bacteroidetes (f) in the rat fecal microbiota. Data are shown as mean ± standard error (b–f, n = 4). Asterisks indicate significant differences compared to the HF group by Steel test (* $p < 0.05$, *** $p < 0.001$).

man's rank correlation coefficients (ρ) and their associated p-values underlying the heat map are provided in Table S3.

In contrast, NAAAs exhibited stronger positive correlations than SCFAs with Clostridiaceae (slash calls), Eubacteriaceae (family level ID only), and Victivallaceae (family level ID only). SCFAs showed stronger negative correlations with *Enterococcus gallinarum* and *Lactobacillus animalis* than did NAAAs. Additionally, acetic acid showed a particularly strong negative correlation with *[Eubacterium] dolichum*. *Arthrobacter creatinolyticus* exhibited negative correlations with several SCFAs and NAAAs.

4. Discussion

Several studies have reported that short-chain pyroglutamyl peptides, such as pyroGlu-Leu and pyroGlu-Asn-Ile, exert beneficial effects on intestinal health, including amelioration of colitis in mouse models at low doses (0.1–1.0 mg/kg body weight) (Kiyono et al., 2016; Wada et al., 2013). These peptides have also been shown to modulate gut microbiota composition (Kiyono et al., 2016; Shirako et al., 2019; Wada et al., 2013). Shirako et al. (2019) demonstrated that pyroGlu-Leu improves high-fat-diet-induced dysbiosis by enhancing the secretion of rattusin, a host antimicrobial peptide produced in the small intestine. These studies used single synthetic pyroglutamyl peptides; however, pyroglutamyl peptides also naturally occur in fermented foods such as Japanese rice wine and miso, as well as in enzymatic hydrolysates of food proteins including wheat gluten and rice protein. Unlike fermented foods, enzymatic hydrolysates do not contain high levels of salt or alcohol, making them promising sources of pyroglutamyl peptides for use as functional food ingredients. The RPH used in the present study contained approximately 1.2 mg/g of pyroGlu-Leu and released an additional 1.2 mg/g after exopeptidase digestion (Miyauchi et al., 2022). Therefore, we compared the effects of RPH with those of synthetic pyroGlu-Leu on fecal microbiota and cecal metabolites in rats fed a high-fat diet. The doses of RPH used in this study (20 and 100 mg/kg body weight) corresponded to approximately 0.05 and 0.24 mg/kg body weight of pyroGlu-Leu, respectively, taking into account exopeptidase-mediated release.

High-fat-diet feeding is known to alter the gut microbiota, typically decreasing Bacteroidetes and increasing Firmicutes and Proteobacteria (Malesza et al., 2021; Murphy et al., 2015; Shirako et al., 2019) as well as reducing fecal SCFA concentrations (Brinkworth et al., 2009). SCFAs regulate inflammatory and immune responses in colonocytes and innate immune cells by acting as ligands of G-protein coupled receptors such as GPR41, GPR43, and GPR109A and by inhibiting histone deacetylases (Parada Venegas et al., 2019). These findings suggest that reductions in SCFAs due to high-fat diet-induced dysbiosis contribute to the onset and progression of diseases such as inflammatory bowel disease (IBD) and colorectal cancer. Indeed, high-fat-diet feeding accelerates the development of these diseases in animal models (Gruber et al., 2013; Lee et al., 2015; Shao et al., 2023). In addition to SCFAs, the present study identified *N*-acetyl amino acids (NAAAs) in cecal contents. Although several metabolomic studies have reported the presence of NAAAs in feces (Tian et al., 2024; Zierer et al., 2018), these compounds have not

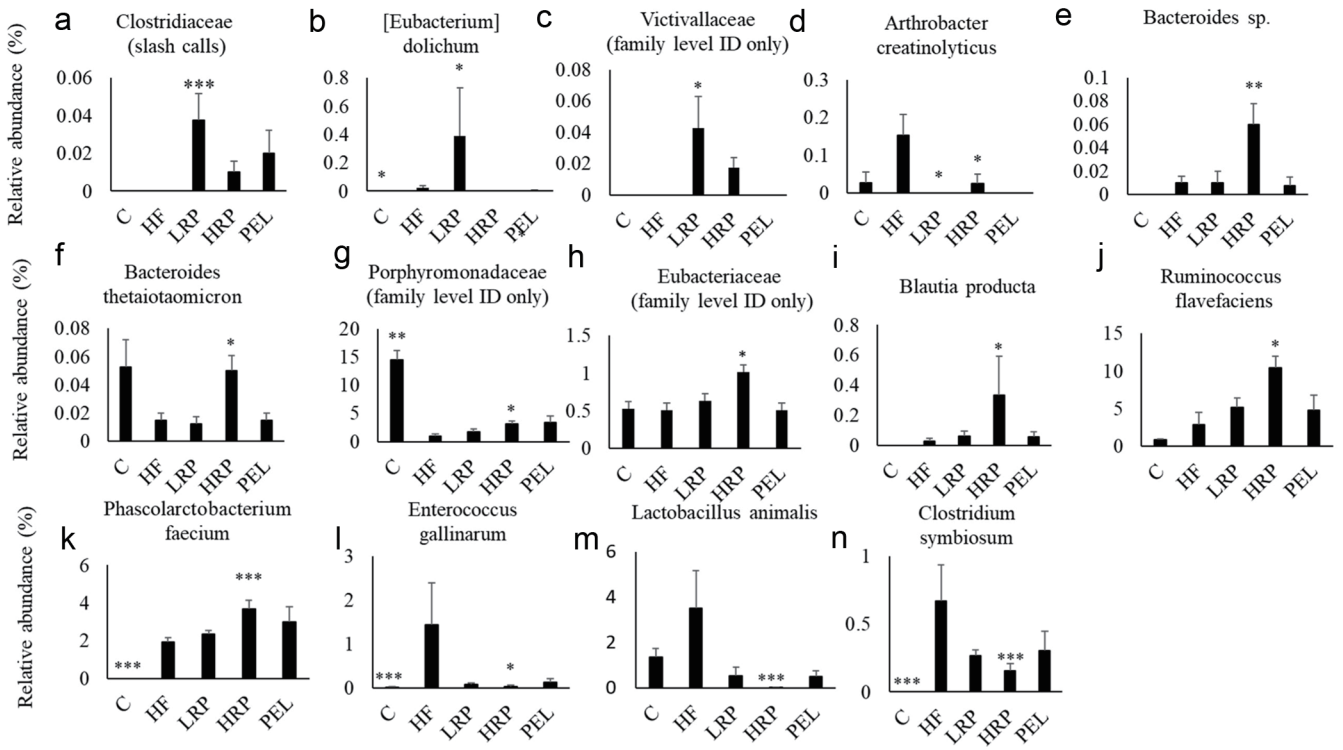


Figure 5. Relative abundance of Clostridiaceae (slash calls) (a), *[Eubacterium] dolichum* **(b), Victivallaceae (family level ID only) (c),** *Arthrobacter creatinolyticus* **(d),** *Bacteroides sp.* **(e),** *Bacteroides thetaiotaomicron* **(f), Porphyromonadaceae (family level ID only) (g), Eubacteriaceae (family level ID only) (h),** *Blautia producta* **(i),** *Ruminococcus flavefaciens* **(j),** *Phascolarctobacterium faecium* **(k),** *Enterococcus gallinarum* **(l),** *Lactobacillus animalis* **(m), and** *Clostridium symbiosum* **(n) in the rat fecal microbiota.** "Slash calls" indicate ambiguous assignments where sequences matched multiple taxa with similar confidence and could not be uniquely assigned to a single genus. Square brackets in *[Eubacterium] dolichum* denote a taxon that is currently considered misclassified in that genus and awaits formal taxonomic revision. "Family level ID only" indicates sequences that could be classified with sufficient confidence only to the family rank based on the 16S rRNA gene. Data are shown as mean ± standard error (A–N, n = 4). Asterisks indicate significant differences compared to the HF group by Steel's test (* $p < 0.05$, *** $p < 0.001$).

been quantified. Their producers and biosynthetic pathways remain unclear; however, their presence in fermented foods such as miso, soy sauce, and fish sauce (Nagao et al., 2024; Rahmadian et al., 2025) suggests that they are likely generated by microorganisms.

In the present study, feeding a 45% high-fat diet significantly altered the overall composition of the fecal microbiota (Figure 4a). However, unlike in our previous study using a 60% high-fat diet (Shirako et al., 2019), the Firmicutes/Bacteroidetes ratio was not

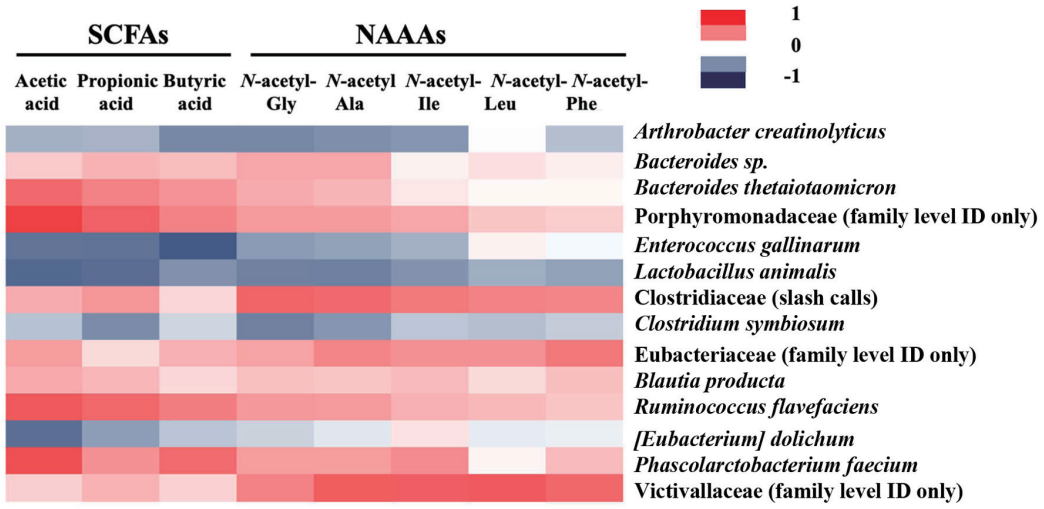


Figure 6. A heat map of Spearman's rank correlation coefficients between fecal microbial species and SCFAs and NAAAs.

significantly affected (Figure 4f). Furthermore, the present 5-week high-fat diet feeding did not increase body weight, in contrast to our previous study using the same animal strain and diet (Shirako et al., 2020). One plausible explanation for this difference is variation in the initial composition of the small-intestinal microbiota among the animals. Because metabolites produced by the small-intestinal microbiota contribute to high-fat-diet-induced obesity (Martinez-Guryn et al., 2018), the high-fat diet used in the present study may have induced only modest dysbiosis, possibly due to differences in the initial small-intestinal microbiota of the rats.

Despite the absence of obesity or liver damage, the high-fat diet significantly decreased cecal SCFA levels (Figure 2). Administration of RPH or pyroGlu-Leu did not restore SCFA levels or reverse the overall microbiota composition altered by the high-fat diet. However, both doses of RPH and pyroGlu-Leu significantly restored the levels of *N*-acetyl-Gly, *N*-acetyl-Ala, and *N*-acetyl-Ile (Figure 3), and altered the relative abundances of several bacterial taxa at the phylum and species levels (Figures 4 and 5). Recently, Kvitne et al. (2025) reported that children with very early-onset IBD exhibit lower abundances of SCFA-producing bacteria and reduced fecal levels of NAAAs such as *N*-acetyl-Met and *N*-acetyl-Ile/Leu, with positive correlations between these bacteria and NAAAs. These findings suggest that NAAAs may be synthesized by SCFA-producing bacteria and may serve as biomarkers reflecting their abundance or metabolic activity. Consistent with this, the present study showed that SCFAs and NAAAs correlated in the same direction with several bacterial species; however, the strengths of these correlations differed (Figure 6). Notably, the abundances of Clostridiaceae, Eubacteriaceae, and Victivallaceae showed stronger positive correlations with NAAAs than with SCFAs. These families include known SCFA-producing bacteria (Esquivel-Elizondo et al., 2017; Mukherjee et al., 2020; Zoetendal et al., 2003). These results suggest that oral administration of RPH and pyroGlu-Leu may enhance the growth or metabolic activity of SCFA-producing bacteria in a manner that increases NAAA production without necessarily increasing SCFA levels.

The mechanisms underlying these observations remain unclear. One possibility is that NAAAs respond more rapidly or sensitively to changes in SCFA-producing bacteria than SCFAs, which often require larger shifts in microbial fermentation to change measurably. Alternatively, RPH and pyroGlu-Leu may preferentially promote bacteria capable of producing *N*-acetyl amino acids or modulate metabolic pathways within SCFA-producing bacteria, leading to increased NAAA synthesis. Further studies are needed to clarify these mechanisms, but the present findings indicate that NAAAs may serve as early and sensitive indicators of microbiota-host co-metabolism.

The biological roles of NAAAs in the host remain largely unknown. In this study, administration of RPH and pyroGlu-Leu restored NAAA levels before the onset of adverse effects typically associated with high-fat diet feeding. Thus, the recovery of NAAAs may contribute to the beneficial effects of pyroglutamyl peptides on intestinal health reported previously (Kiyono et al., 2016; Wada et al., 2013). Takakuwa et al. (2019) reported that SCFAs and amino acids such as butyrate and leucine stimulate α-defensin secretion from mouse Paneth cells. Therefore, NAAAs restored by RPH and pyroGlu-Leu administration may modulate innate immunity in the intestine, similarly to pyroGlu-Leu, amino acids, and SCFAs. Further studies on the biological activities of *N*-acetyl amino acids are currently underway.

This study has several limitations. First, the sequencing analysis was outsourced, and detailed quality-control metrics—including sequencing depth, read-quality summaries, filtering criteria, chimera removal, and taxonomic-assignment thresholds—together with the raw sequence files were part of the contract laboratory's internal workflow and could not be retrieved retrospectively. Absolute bacterial quantification and compositional differential-abundance analysis were also not performed; therefore, the microbial data were analyzed only as relative abundances, and the taxon-level findings should be regarded as exploratory. Second, the baseline composition of the gut microbiota was not assessed, so comparability among groups before the intervention could not be directly confirmed, and the proposed contribution of the initial small-intestinal microbiota to the absence of body-weight gain remains speculative. Third, only endpoint microbiota profiles were examined, and the relatively small sample size (n = 4 per group) may limit the statistical power to detect subtle differences. These limitations should be addressed in future studies incorporating baseline and longitudinal microbiota profiling, absolute quantification, and larger group sizes.

Furthermore, modulation of the gut microbiota and its metabolites by RPH or pyroGlu-Leu may have the potential to support human health by contributing to the maintenance of a favorable intestinal environment. Based on body-surface-area scaling, the RPH doses used in this study correspond to estimated human-equivalent intakes of approximately 0.19–0.97 g/day for a 60-kg adult, whereas the pure pyroGlu-Leu dose corresponds to approximately 9.7 mg/day. The estimated RPH intakes would provide or potentially release approximately 0.47–2.34 mg of pyroGlu-Leu per day. Although pyroglutamyl peptides are absorbed by small-intestinal tissue, our previous study (Miyauchi et al., 2022) showed that they only small parts of them enter the bloodstream. Therefore, body-surface-area scaling may not fully reflect their physiological behavior. Nevertheless, even when considering intake per body weight, the estimated human-equivalent doses of RPH and pyroGlu-Leu remain realistic. Human intervention studies are required to determine whether comparable effects occur in humans and to establish effective intake levels.

5. Conclusion

The present study demonstrated the presence of NAAAs in the rat cecal contents by neutral loss scanning using LC-MS/MS following 2-NPH derivatization. Interestingly, the high-fat diet used in the present study significantly decreased cecal concentrations of NAAAs and SCFAs in rats through changes in fecal microbiota. However, administration of RPH and pyroGlu-Leu restored the levels of NAAA but not those of SCFA. Cecal concentrations of NAAA and SCFA showed similar positive correlations with the abundances of several SCFA-producing bacteria; however, the strength of these correlations differed between SCFAs and NAAAs. Collectively, these findings raise the possibility that NAAA represent an early metabolic signature of beneficial adaptations in SCFA-producing bacteria induced by pyroglutamyl peptides.

Acknowledgments

We would like to thank to the Kyoto Louis Pasteur Center for Medical Research for allowing us to perform animal experiments in their facility.

Supplementary material

Table S1. Daily water intake (mL) of rats during the 5-week experimental period.

Table S2. Actual daily doses (mg/kg body weight/day) of RPH and pyroGlu-Leu administered to rats during the 5-week experimental period.

Table S3. Spearman's rank correlations between cecal metabolite levels and fecal bacterial relative abundances.

References

Brinkworth, G.D., Noakes, M., Clifton, P.M., and Bird, A.R. (2009). Comparative effects of very low-carbohydrate, high-fat and high-carbohydrate, low-fat weight-loss diets on bowel habit and faecal short-chain fatty acids and bacterial populations. Br. J. Nutr. 101(10): 1493–1502.

Chen, L., Ejima, A., Gu, R., Lu, J., Cai, M., and Sato, K. (2019). Presence of exopeptidase-resistant and susceptible peptides in a bacterial protease digest of corn gluten. J. Agric. Food Chem. 67: 11948–11954.

Ejima, A., Nakamura, M., Suzuki, Y.A., and Sato, K. (2018). Identification of food-derived peptides in human blood after ingestion of corn and wheat gluten hydrolysates. J. Food Bioact. 2: 104–111.

Esquivel-Elizondo, S., Ilhan, Z.E., Garcia-Peña, E.I., and Krajmalnik-Brown, R. (2017). Insights into butyrate production in a controlled fermentation system via gene predictions. mSystems 2(4): e00051–17.

Fusco, W., Lorenzo, M.B., Cintoni, M., Porcari, S., Rinninella, E., Kaitsas, F., Lener, E., Mele, M.C., Gasbarrini, A., Collado, M.C., Cammarota, G., and Ianiro, G. (2023). Short-chain fatty-acid-producing bacteria: Key components of the human gut microbiota. Nutrients 15(9): 2211.

Gazme, B., Boachie, R.T., Tsopmo, A., and Udenigwe, C.C. (2019). Occurrence, properties and biological significance of pyroglutamyl peptides derived from different food sources. Food Sci. Hum. Wellness. 8: 268–274.

Gruber, L., Kisling, S., Lichti, P., Martin, F.-P., May, S., Klingenspor, M., Lichtenegger, M., Rychlik, M., and Haller, D. (2013). High fat diet accelerates pathogenesis of murine Crohn's disease-like ileitis independently of obesity. PLoS One 8(8): e71661.

Higaki-Sato, N., Sato, K., Inoue, N., Nawa, Y., Kido, Y., Nakabou, Y., Hashimoto, K., Nakamura, Y., and Ohtsuki, K. (2006). Occurrence of the free and peptide forms of pyroglutamic acid in plasma from the portal blood of rats that had ingested a wheat gluten hydrolysate containing pyroglutamyl peptides. J. Agric. Food Chem. 54: 6984–6988.

Inoue, H., Takayama, K., Takahara, C., Tabuchi, N., Okamura, N., Narahara, N., Kojima, E., Date, Y., and Tsuruta, Y. (2019). Determination of short-chain fatty acids in mouse feces by high-performance liquid chromatography using 2-nitrophenylhydrazine as a labeling reagent. Biol. Pharm. Bull. 42: 845–849.

Kim, S.-W., Suda, W., Kim, S., Oshima, K., Fukuda, S., Ohno, H., Morita, H., and Hattori, M. (2013). Robustness of gut microbiota of healthy adults in response to probiotic intervention revealed by high-throughput pyrosequencing. DNA Res. 20: 241–253.

Kiyono, T., Hirooka, K., Yamamoto, Y., Kuniishi, S., Ohtsuka, M., Kimura, S., Park, E.Y., Nakamura, Y., and Sato, K. (2013). Identification of pyroglutamyl peptides in Japanese rice wine (sake): Presence of hepatoprotective pyroGlu-Leu. J. Agric. Food Chem. 61: 11660–11667.

Kiyono, T., Wada, S., Ohta, R., Wada, E., Takagi, T., Naito, Y., Yoshikawa, T., and Sato, K. (2016). Identification of pyroglutamyl peptides with anticolitic activity in Japanese rice wine, *sake*, by oral administration in a mouse model. J. Funct. Foods. 27: 612–621.

Kvitne, K.E., Zuffa, S., Charron-Lamoureux, V., Mohanty, I., Patan, A., Mannochio-Russo, H., Zemlin, J., Burnett, L.A., Zhang, L.S., Cecala, M.C., Ersoz, C., Connelly, J.A., Halasa, N., Nicholson, M., Dorrestein, P.C., Tsunoda, S.M., and Markle, J. (2025). Fecal microbial and metabolic signatures in children with very early onset inflammatory bowel disease. NPJ Biofilms Microbiomes 12: 33.

Lee, D., Albenberg, L., Compher, C., Baldassano, R., Piccoli, D., Lewis, J.D., and Wu, G.D. (2015). Diet in the pathogenesis and treatment of inflammatory bowel diseases. Gastroenterology 148: 1087–1106.

Malesza, I.J., Malesza, M., Walkowiak, J., Mussin, N., Walkowiak, D., Aringazina, R., Bartkowiak-Wieczorek, J., and Mądry, E. (2021). High-fat, Western-style diet, systemic inflammation, and gut microbiota: A narrative review. Cells 10(11): 3164.

Martinez-Guryn, K., Hubert, N., Frazier, K., Urlass, S., Musch, M.W., Ojeda, P., Pierre, J.F., Miyoshi, J., Sontag, T.J., Cham, C.M., Reardon, C.A., Leone, V., and Chang, E.B. (2018). Small intestine microbiota regulate host digestive and absorptive adaptive responses to dietary lipids. Cell Host & Microbe. 23: 458–469.

Miyauchi, S., Kajiwara, S., and Sato, K. (2022). Metabolic fate of peptides in a rice protein hydrolysate in rat intestine and blood after oral administration. J. Food Bioact. 20: 40–55.

Mukherjee, A., Lordan, C., Ross, R.P., and Cotter, P.D. (2020). Gut microbes from the phylogenetically diverse genus Eubacterium and their various contributions to gut health. Gut Microbes. 12(1): e1802866.

Murphy, E.A., Velazquez, K.T., and Herbert, K.M. (2015). Influence of high-fat-diet on gut microbiota: A driving force or chronic disease risk. Curr. Opin. Clin. Nutr. Metab. Care 18(5): 515–520.

Nagao, A., Nakamoto, Y., Miyauchi, S., and Sato, K. (2024). Presence of modified peptides with high bioavailability and angiotensin-converting enzyme inhibitory activity in Japanese fermented soybean paste (miso). J. Agric. Food Chem. 72: 18942–18956.

Parada Venegas, D., De la Fuente, M.K., Landskron, G., González, M.J., Quera, R., Dijkstra, G., Harmsen, H.J.M., Faber, K.N., and Hermoso, M.A. (2019). Short chain fatty acids (SCFAs)-mediated gut epithelial and immune regulation and its relevance for inflammatory bowel diseases. Front. Immunol. 10: 277.

Rahmadian, Y., Miyauchi, S., Wijanarti, S., Asai, T., and Sato, K. (2025). Presence of γ-glutamyl and β-aspartyl isopeptides, diketopiperazines, pyroglutamyl peptides, in addition to normal peptides in fish and soy sauces: Structures, contents and their bioavailability. J. Food Bioact. 29: 60–76.

Sato, K., Egashira, Y., Ono, S., Mochizuki, S., Shimmura, Y., Suzuki, Y., Nagata, M., Hashimoto, K., Kiyono, T., Park, E.Y., Nakamura, Y., Itabashi, M., Sakata, Y., Furuta, S., and Sanada, H. (2013). Identification of a hepatoprotective peptide in wheat gluten hydrolysate against d-galactosamine-induced acute hepatitis in rats. J. Agric. Food Chem. 61: 6304–6310.

Sato, K., Nisimura, R., Suzuki, Y., Motoi, H., Nakamura, Y., Ohtsuki, K., and Kawabata, M. (1998). Occurrence of indigestible pyroglutamyl peptides in an enzymatic hydrolysate of wheat gluten prepared on an industrial scale. J. Agric. Food Chem. 46(9): 3403–3405.

Shao, X., Liu, L., Zhou, Y., Zhong, K., Gu, J., Hu, T., Yao, Y., Zhou, C., and Chen, W. (2023). High-fat diet promotes colitis-associated tumorigenesis by altering gut microbial butyrate metabolism. Int. J. Biol. Sci. 19(15): 5004–5019.

Shirako, S., Kojima, Y., Hasegawa, T., Yoshikawa, T., Matsumura, Y., Ikeda, K., Inagaki, N., and Sato, K. (2020). Identification of short-chain pyroglutamyl peptides in Japanese salted fermented soy paste (miso) and their anti-obesity effect. J. Food Bioact. 12: 129–139.

Shirako, S., Kojima, Y., Tomari, N., Nakamura, Y., Matsumura, Y., Ikeda, K., Inagaki, N., and Sato, K. (2019). Pyroglutamyl leucine, a peptide in fermented foods, attenuates dysbiosis by increasing host antimicrobial peptide. NPJ Sci. Food. 3: 18.

Takakuwa, A., Nakamura, K., Kikuchi, M., Sugimoto, R., Ohira, S., Yokoi, Y., Ayabe, T. (2019). Butyric acid and leucine induce α-defensin secretion from small intestinal Paneth cells. Nutrients 11: 2817.

Tian, X., Xie, Y., Yu, L., Yao, P., Dong, M., Jin, C., and Wu, N. (2024). Analysis of the gut microbiota and fecal metabolites in people living with HIV. Microbiol. Spectr. 12(11): e00238–24.

Wada, S., Sato, K., Ohta, R., Wada, E., Bou, Y., Fujiwara, M., Kiyono, T., Park, E.Y., Aoi, W., Takagi, T., Naito, Y., and Yoshikawa, T. (2013). Ingestion of low dose pyroglutamyl leucine improves dextran sulfate sodium-induced colitis and intestinal microbiota in mice. J. Agric. Food Chem. 61: 8807–8813.

Zierer, J., Jackson, M.A., Kastenmüller, G., Mangino, M., Long, T., Telenti, A., Mohney, R.P., Small, K.S., Bell, J.T., Steves, C.J., Valdes, A.M., Spector, T.D., and Menni, C. (2018). The fecal metabolome as a functional readout of the gut microbiome. Nat. Genet. 50(6): 790–795.

Zoetendal, E.G., Plugge, C.M., Akkermans, A.D.L., and de Vos, W.M. (2003). *Victivallis* vadensis gen. Nov., sp. Nov., a sugar-fermenting anaerobe from human faeces. Int. J. Syst. Evol. Microbiol. 53: 211–215.

Journal of Food Bioactives
International Society for Nutraceuticals and Functional Foods
Original Research
J. Food Bioact. 2026;35:57–68

Probiotics characterization of fermented tiger nut-millet-blended beverage

Olawale Peter Odeleye[a], Blessing Mosopeoluwa Gabriel-Ogunniyi[a,b], Grace Mosunmola Adegbola[a,c], Ruth Adefolakemi O. Gabriel-Ajobiewe[a*] and Bartholomew Saanu Adeleke[d*]

[a]Food and Applied Microbiology Unit, Department of Microbiology, Faculty of Life Sciences, Federal University, Oye-Ekiti, Nigeria
[b]Department of Microbiology and Public Health, Federal University of Agriculture, Abeokuta, Nigeria
[c]Food Microbiology Unit, Department of Food Science, Faculty of Food and Consumer Sciences, Ladoke Akintola University of Technology, Ogbomoso, Nigeria.
[d]Department of Microbiology, Faculty of Natural and Applied Sciences, Federal University of Technology and Environmental Sciences, Iyin-Ekiti, Nigeria
[*]**Corresponding author:** Ruth Adefolakemi O. Gabriel-Ajobiewe, Food and Applied Microbiology Unit, Department of Microbiology, Faculty of Life Sciences, Federal University, Oye-Ekiti, Nigeria. E-mail: adefolakemi.gabriel-ajobiewe@fuoye.edu.ng; Bartholomew Saanu Adeleke, Department of Microbiology, Faculty of Natural and Applied Sciences, Federal University of Technology and Environmental Sciences, Iyin-Ekiti, Nigeria. E-mail: bartholomew.adeleke@futes.edu.ng
DOI: 10.26599/JFB.2026.95035456
Received: July 06, 2026; **Revised received & accepted:** September 02, 2026
Citation: Odeleye, O.P., Gabriel-Ogunniyi, B.M., Adegbola, G.M., Gabriel-Ajobiewe, R.A.O., and Adeleke, B.S. (2026). Probiotics characterization of fermented tiger nut-millet-blended beverage. J. Food Bioact. 35: 57–68.

Abstract

This study investigated the functional characteristics and probiotic potential of lactic acid bacteria (LAB) isolated from a fermented tiger nut-millet beverage. The beverage was prepared using a traditional tiger nut fermentation process (sorting, cleaning, soaking, spicing, wet-grinding, fermentation, filtration, chilling, and storage), and samples were collected at 6-hour intervals throughout the 48-hour fermentation time for microbiological analysis. The isolated LAB were evaluated for probiotic properties, including tolerance to acidic pH, bile salts, and phenol. Their antibiotic susceptibility and antibacterial activities against selected pathogenic bacteria were also assessed. LAB counts increased from 2.30 to 6.40 $\log_{10}$ CFU/mL during fermentation. The isolates were identified using the API 50 CHL system and 16S rRNA gene sequencing, revealing members of the genera *Leuconostoc* and *Lactiplantibacillus*. Selected isolates exhibited strong tolerance to simulated gastrointestinal conditions, with survival rates exceeding 50% at acidic pH (2.0–3.0), bile salt concentrations (0.3% and 2%), and phenol concentrations (0.2% and 0.3%). The isolates also demonstrated susceptibility to clinically relevant antibiotics and exhibited antibacterial activity against selected foodborne pathogens, producing inhibition zones ranging from 11.0 to 20.0 mm. These findings demonstrate the probiotic potential of LAB and their suitability for developing non-dairy functional foods and nutraceutical products.

Keywords: Cereal-based beverage; Functional foods; Gastrointestinal health; Lactic acid bacteria; Probiotics.

1. Introduction

Fermented foods have been consumed for centuries because of their enhanced nutritional value, extended shelf life, improved sensory properties, and potential health benefits (Tamang et al., 2020; Marco et al., 2021). Fermentation is driven primarily by microorganisms, particularly lactic acid bacteria (LAB), yeasts, and molds, which convert carbohydrates into organic acids, alcohols, and other metabolites that improve food quality and preservation (Kitessa, 2024). These microbial activities enhance

© The author(s) 2026. Publishing Services by Tsinghua University Press
The articles published in this open access journal are distributed under the terms of the Creative Commons Attribution 4.0 International License (http://creativecommons.org/licenses/by/4.0/)

nutrient bioavailability, improve digestibility, inhibit spoilage microorganisms, and contribute to food safety (Rymuszka and Gorczynska, 2026). More recently, plant-based fermented beverages have gained considerable attention owing to the increasing consumer demand for functional foods with health-promoting properties (Adegbola et al., 2026). Functional foods are defined as foods that provide physiological benefits beyond basic nutrition and may reduce the risk of chronic diseases while promoting overall health (Debri et al., 2026). Consequently, fermented foods and beverages have become attractive dietary options because they contain beneficial microorganisms and bioactive compounds that support gastrointestinal health and improve nutritional quality.

Lactic acid bacteria are among the most important microorganisms involved in the fermentation of traditional foods and beverages worldwide. During fermentation, LAB metabolize carbohydrates to produce organic acids, enzymes, and antimicrobial compounds that inhibit spoilage and pathogenic microorganisms while enhancing food preservation and quality (Zapaśnik et al., 2022; Anumudu et al., 2024). In addition to their technological roles, many LAB species possess probiotic properties, defined as the ability to confer health benefits on the host when administered in adequate amounts (Mafe et al., 2026). These microorganisms help maintain intestinal microbial balance, strengthen the intestinal barrier, modulate immune responses, and contribute to overall gastrointestinal health. Consequently, the development of fermented foods containing viable probiotic LAB has become an important focus of food science and nutritional research (Marco et al., 2021).

The probiotic efficacy of LAB depends largely on their ability to survive the harsh conditions of the gastrointestinal tract, including exposure to gastric acidity, bile salts, and phenolic compounds (Bernatek et al., 2022; Aleman and Yadav, 2024). These metabolic compounds in the gut are known to be associated with the promotion of gut health by stimulating the growth of probiotic microorganisms and inhibiting the growth of pathogens (Tang et al., 2023). Therefore, tolerance to low pH, bile salts, and phenol is widely used as an in vitro criterion for evaluating probiotic potential (Zheng et al., 2020). Microorganisms that can withstand these adverse conditions are more likely to survive gastrointestinal transit, colonize the intestine, and exert beneficial physiological effects.

Recent studies have shown that traditional fermented foods and beverages prepared from cereals, legumes, fruits, nuts, and vegetables are valuable sources of probiotic LAB with beneficial effects on human health (Erem and Kılıç-Akyılmaz, 2024; Chen et al., 2026). Consumption of these fermented products has been associated with improved digestion, enhanced immune function, and a reduced incidence of gastrointestinal disorders. Despite the growing interest in plant-based probiotic beverages, the probiotic characteristics of LAB isolated from fermented tiger nut-millet beverages remain largely unexplored compared with those from other plant-based substrates such as soy, oat, and almond beverages.

Therefore, this study aimed to isolate, characterize, and identify LAB associated with fermented tiger nut–millet beverage and to evaluate their probiotic potential. Specifically, the isolates were assessed for tolerance to acidic pH, bile salts, and phenol, as well as their antibiotic susceptibility and antibacterial activity against selected pathogenic bacteria. The findings provide valuable insights into the probiotic potential of fermented tiger nut–millet beverage and its suitability as a promising non-dairy functional food for improving human health.

2. Materials and methods

2.1. Sample preparation

Yellow tiger nuts and finger millet were used as the primary raw materials, while date fruits and sweet potatoes served as natural sweeteners. All materials were purchased from a local market in Ado-Ekiti, Ekiti State, Nigeria, and transported to the Microbiology Laboratory, Federal University Oye-Ekiti. The samples were sorted, cleaned, washed thoroughly with sterile water under aseptic conditions, and weighed before processing. Triplicate batches (n = 3) were prepared by steeping the samples in 2,500 mL of distilled water at room temperature in sterile plastic containers. A total of 1,000 g of substrate, comprising 750 g of tiger nuts and 250 g of finger millet (4:1, w/w), was used for beverage production. Subsequently, 100 g of the selected natural sweetener was added before blending (New Silver Crest Electric Rotary Blender, SCB-9880, Zhejiang, China). Fermentation was carried out following the traditional tiger nut milk production process for 36 hours.

2.2. Isolation of lactic acid bacteria

Samples were collected from the fermenting mixture at 0, 6, 12, 18, 24, and 36 hours of fermentation. Each sample was serially diluted ten-fold in 0.1% peptone water and plated on de Mann Rogosa, and Sharpe (MRS) agar using the pour plate technique. The inoculated plates were incubated anaerobically at 37°C for 48 hours (Jenway Incubator: Jenway Ltd, Staffordshire, UK). Distinct colonies were selected and repeatedly sub-cultured on fresh MRS agar plates until pure cultures were obtained.

2.3. Cultural, morphological and biochemical characterization of LAB

The purified isolates were characterized based on colony morphology, including colony colour, size, shape, surface texture, margin, elevation, and Gram reaction, following standard procedures (Kunchala et al., 2016; Divisekera et al., 2019). Gram staining was performed using freshly cultured isolates, microscopically viewed (Microscope: Motic BA310, Xiamen, China), and observations were recorded. The isolates were further characterized using catalase, citrate utilization, oxidase, hydrogen sulphide (H_2S) production, and carbohydrate fermentation tests.

2.4. Tolerance to environmental stress

2.4.1. Growth at different temperatures

Each LAB isolate was inoculated into freshly prepared MRS broth supplemented with 1% glucose and incubated anaerobically at 15°C and 45°C for 24 hours (Sharma et al., 2016). Growth was determined by the presence of visible turbidity.

2.4.2. Growth at different sodium chloride concentrations

Pure LAB colonies were inoculated into MRS broth containing 4%, 6.5%, and 8% (w/v) NaCl. The cultures were incubated anaerobically at 37°C for 24 hours, after which growth was assessed by observing turbidity.

2.5. Identification of LAB isolates

The isolates were identified using the commercial API 50 CHL system (bioMérieux®, France) according to the manufacturer's instructions. Carbohydrate fermentation profiles generated from the API 50 CH strips were interpreted using the APIweb™ identification software. Pure cultures were maintained on MRS agar slants for subsequent analyses.

2.6. In vitro evaluation of probiotic properties

2.6.1. Acid tolerance

Acid tolerance was evaluated according to the method described by Suwannaphan (2021). Overnight cultures were harvested by centrifugation (TGL-16R Tabletop High Speed Refrigerated Centrifuge, Changsha, Hunan, China) at 5,000 rpm for 10 minutes at 4°C. The cell pellets were washed with phosphate-buffered saline (PBS; pH 7.2) and resuspended in 500 µL of MRS broth adjusted to pH 2.0, 2.5, or 3.0 using 1 N HCl. The suspensions were incubated anaerobically at 37°C for 3 hours. Samples collected at 0 and 3 hours were serially diluted, spread-plated on MRS agar, and incubated anaerobically at 37°C for 48 hours.

The percentage survival was calculated as follows:

$$\text{Survival (\%)} = \frac{\log \text{CFU } N_1}{\log \text{CFU } N_0} \times 100$$

where N_0 represents the viable cell count before incubation, and N_1 represents the viable cell count after 3 hours. Isolates with survival rates greater than 75% were considered tolerant to acidic conditions (Suwannaphan, 2021).

2.6.2. Bile salt tolerance

Bile salt tolerance was determined following the method of Suwannaphan (2021). Overnight cultures were centrifuged at 5,000 rpm for 10 minutes at 4°C, washed with PBS (pH 7.2), and resuspended in 500 µL of MRS broth supplemented with 0.3% and 2.0% (w/v) bile salts. The suspensions were incubated anaerobically at 37°C for 3 hours. Viable counts were determined at 0 and 3 hours using the procedure described above. Survival percentages were calculated using the same equation, and isolates with survival rates exceeding 75% were considered bile tolerant.

2.6.3. Phenol tolerance

Phenol tolerance was assessed according to Suwannaphan (2021). Harvested LAB cells were washed with PBS (pH 7.2) and resuspended in 500 µL of MRS broth containing 0.2% or 0.3% (w/v) phenol. The suspensions were incubated anaerobically at 37°C for 3 hours. Viable cell counts were determined before and after incubation, and survival percentages were calculated using the equation described above. Isolates exhibiting survival rates above 75% were considered phenol-tolerant.

2.7. Antibiotic susceptibility testing

The antibiotic susceptibility profiles of the LAB isolates were determined using the agar disc diffusion method following CLSI (2012) guidelines. The isolates were tested against ampicillin (AMP), cotrimoxazole (COT), gentamicin (GEN), erythromycin (ERY), tetracycline (TET), vancomycin (VAN), ciprofloxacin (CIP), meropenem (MEM), Augmentin (AUG), ceftazidime (CPZ), cefuroxime (CRX), and cephalexin (CP).

2.8. Antibacterial activity

The antibacterial activity of the LAB isolates was evaluated against *Staphylococcus aureus* ATCC 25923, *Bacillus cereus* NCIB 6349, *Pseudomonas aeruginosa* NCIB 3471, *Escherichia coli*, and *Klebsiella pneumoniae*. The test organisms were obtained from the Microbial Culture Collection of the Department of Microbiology, Obafemi Awolowo University, Ile-Ife, Nigeria. The agar well diffusion method described by Divisekera et al. (2018) was employed. Overnight cultures of the test organisms were adjusted to a 0.5 McFarland standard (1.5×10^8 CFU/mL) and spread onto nutrient agar plates. Wells of 6 mm diameter were prepared using a sterile cork borer, and 100 µL of LAB cell-free supernatant was dispensed into each well. Phosphate-buffered saline served as the negative control. Plates were incubated at 37°C for 24 hours, after which inhibition zones were measured. Antibacterial activity was interpreted according to Sanam et al. (2022) with slight modifications: inhibition zones <4 mm were considered very weak, 5 mm weak, 5–10 mm moderate, 10–20 mm strong, and 20–30 mm very strong.

2.9. Molecular identification of probiotic LAB

Only isolates exhibiting survival rates greater than 75% under acidic, bile salt, and phenol stress conditions were selected for molecular identification using 16S rRNA gene sequencing.

2.9.1. Genomic DNA extraction

Genomic DNA was extracted from six selected LAB isolates exhibiting similar biochemical and probiotic characteristics. Overnight cultures grown in MRS broth were centrifuged at 10,000 rpm for 3 minutes. The cell pellets were resuspended in Tris-EDTA buffer before DNA extraction following the manufacturer's protocol. DNA purity and integrity were assessed before PCR amplification.

2.9.2. PCR amplification and sequencing

The 16S rRNA gene was amplified using the universal bacterial primers 27F (5′-AGAGTTTGATCCTGGCTCAG-3′) and 1492R (reverse primer). PCR products were sequenced using an ABI 3100 Genetic Analyzer (ABI 3100 Genetic Analyzer, California, USA). The obtained sequences were compared with those in the NCBI database using the BLAST algorithm, and phylogenetic analysis was performed using the neighbour-joining method implemented in MEGA version 12.

2.10. Statistical analysis

All experiments were conducted in triplicate (n = 3), and results are presented as mean ± standard deviation. Statistical analyses were performed using one-way analysis of variance (ANOVA) followed by Duncan's multiple range test. Differences were considered statistically significant at $p < 0.05$.

Table 1. Lactic acid bacteria count (CFU/mL) from fermented spicy tiger nut-millet beverage

Sample Code	Log_{10} CFU/mL						
	0 hour	6 hours	12 hours	18 hours	24 hours	30 hours	36 hours
TMD F1	3.45 ± 0.23a	4.91 ± 0.27b	4.97 ± 0.69b	5.01 ± 0.60c	6.07 ± 0.60d	6.16 ± 0.80d	6.30 ± 0.75d
TMD F2	3.92 ± 0.45a	5.03 ± 0.72b	5.10 ± 0.69b	5.28 ± 0.68b	6.03 ± 0.71c	6.04 ± 0.73c	6.20 ± 0.67c
TMD F3	4.01 ± 0.47a	4.96 ± 0.80a	5.08 ± 0.76b	5.20 ± 0.77b	6.04 ± 0.73c	6.27 ± 0.75c	6.31 ± 0.70c
TMD F4	4.23 ± 0.40a	5.00 ± 0.90b	5.11 ± 0.67b	5.31 ± 0.60b	6.01 ± 0.58c	6.24 ± 0.79c	6.31 ± 0.77c
TMD F5	2.45 ± 0.32a	4.78 ± 0.84b	5.17 ± 0.82b	5.10 ± 0.67b	5.92 ± 0.99c	6.05 ± 0.88c	6.16 ± 0.81c
TMD F6	3.73 ± 0.24a	4.83 ± 0.81b	5.05 ± 0.83c	5.08 ± 0.67b	6.04 ± 0.91c	6.08 ± 0.90c	6.18 ± 0.83c
TMSP F1	3.04 ± 0.35a	4.87 ± 0.75b	5.07 ± 0.71c	5.10 ± 0.70c	6.06 ± 0.65d	6.04 ± 0.74d	6.13 ± 0.77d
TMSP F2	3.86 ± 0.50a	5.43 ± 0.70b	5.70 ± 0.79b	6.11 ± 1.04c	6.03 ± 0.76c	6.13 ± 0.74c	6.26 ± 0.69
TMSP F3	3.64 ± 0.34a	5.27 ± 0.68b	6.16 ± 0.57c	6.26 ± 0.76c	6.30 ± 0.71c	6.37 ± 0.74c	6.40 ± 0.70
TMSP F4	3.30 ± 0.50a	4.82 ± 0.35b	5.31 ± 0.73c	5.36 ± 0.73c	6.11 ± 0.86d	6.21 ± 0.83d	6.26 ± 0.80d
TMSP F5	2.30 ± 0.40a	4.91 ± 0.37b	5.25 ± 0.53b	6.28 ± 0.53c	6.30 ± 0.56c	6.34 ± 0.58c	6.38 ± 0.64c
TMSP F6	3.23 ± 0.51a	4.97 ± 0.47b	5.11 ± 0.40c	5.97 ± 0.86c	6.04 ± 0.86c	6.13 ± 0.85c	6.22 ± 0.78c
TMSP F7	2.86 ± 0.34a	4.57 ± 0.71b	5.61 ± 0.70c	5.69 ± 0.77c	5.97 ± 0.85c	6.09 ± 0.80c	6.16 ± 0.82c
TMDSP F1	2.87 ± 0.25a	4.81 ± 0.81b	5.00 ± 0.83b	5.14 ± 0.79b	6.27 ± 0.79c	6.31 ± 0.74c	6.31 ± 0.77c
TMDSP F2	3.44 ± 0.30a	4.64 ± 0.82b	4.83 ± 0.62b	4.93 ± 0.70b	5.83 ± 0.88c	5.98 ± 0.82c	6.01 ± 0.82c
TMDSP F3	2.76 ± 0.51a	4.70 ± 0.95b	4.90 ± 0.83b	4.94 ± 0.68b	5.77 ± 0.88c	5.95 ± 0.82c	6.07 ± 0.78c
TMDSP F4	3.64 ± 0.42a	4.91 ± 0.67b	4.95 ± 0.70b	5.00 ± 0.76b	5.87 ± 0.67c	6.00 ± 0.76c	6.06 ± 0.81c
TMDSP F5	2.87 ± 0.23a	4.73 ± 0.85b	4.93 ± 0.81b	4.98 ± 0.80b	5.77 ± 0.53c	5.92 ± 0.58c	6.05 ± 0.65c
TMDSP F6	3.01 ± 0.22a	4.74 ± 0.10b	4.78 ± 0.98b	4.95 ± 0.83b	5.95 ± 0.59c	6.05 ± 0.70c	6.13 ± 0.76c
TMDSP F7	2.90 ± 0.35a	4.89 ± 0.78b	4.92 ± 0.79b	4.95 ± 0.80b	5.96 ± 0.63c	5.98 ± 0.63c	6.02 ± 0.64c
Control	2.68 ± 0.42a	4.87 ± 0.57b	5.08 ± 0.48b	5.59 ± 0.34b	5.94 ± 0.71b	6.02 ± 0.54c	6.20 ± 0.60c

Values were presented as mean ± standard deviation (n = 3 for each sample). The letters across the column represent significant differences. Key: TMD F1-F6 = Tiger nut-Millet beverage sweetened with Date fruit; TMSP F1-F7 = Tiger nut-Millet beverage sweetened with Sweet potato; TMDSP F1-F7 = Tiger nut-Millet beverage sweetened with Date fruit and Sweet potato

3. Results

3.1. Lactic acid bacteria counts during fermentation

The changes in LAB counts during fermentation of the tiger nut–millet beverages are presented in Table 1. LAB populations increased progressively throughout the fermentation period in all beverage formulations. At 6 hours of fermentation, LAB counts ranged from 4.57 to 5.43 log_{10} CFU/mL, while the highest counts (6.01–6.40 log_{10} CFU/mL) were recorded after 36 hours. The sweet potato-sweetened formulations generally supported greater bacterial growth than the other formulations. Notably, TMSP F3 and TMSP F5 exhibited rapid bacterial proliferation, reaching 6.26 and 6.28 log_{10} CFU/mL, respectively, after 18 hours of fermentation.

3.2. Cultural and morphological characteristics of LAB isolates

The cultural and morphological characteristics of the LAB isolates obtained from the fermented tiger nut-millet beverages are summarized in Table S1. The isolates displayed considerable diversity in colony morphology. Colony size ranged from small to large, while colony colour varied from white and creamy to light yellow. Most isolates exhibited entire margins and smooth surfaces; however, isolates TMD4, TMD5, TMSP3, TMSP7, and TMDSP3 from the fermenting substrates displayed wrinkled colony surfaces. Colony elevation was predominantly convex, although a few isolates exhibited flat colonies. Gram staining confirmed that all isolates were Gram-positive, and microscopic examination revealed both cocci and rod-shaped morphologies.

3.3. Biochemical and physiological characteristics of the LAB isolates

The biochemical and physiological characteristics of the LAB isolates are presented in Table 2. All isolates fermented glucose, lactose, and sucrose with gas production and tested negative for catalase, citrate utilization, oxidase, and hydrogen sulphide production, consistent with the typical characteristics of LAB.

Most isolates grew at both 15°C and 45°C, indicating broad temperature tolerance. However, isolates TMD4, TMSP3, TMSP5, TMSP7, TMDSP2, and TMDSP5 failed to grow at 45°C. Furthermore, all isolates demonstrated tolerance to 4% and 6.5% NaCl, whereas only a few isolates exhibited growth at 8% NaCl, indicating variability in salt tolerance among the isolates.

Table 2. Biochemical characterization and Physiological ability of LAB isolated from naturally sweetened spicy fermented tiger nut-Millet beverage

Codes	Catalase	Citrate	Oxidase	H_2S test	Sugar Fermentation			Temperature (°C)		NaCl (%)		
					Glucose	Lactose	Sucrose	15	45	4	6.5	8
TMD1	–	–	–	–	+ (gas)	+ (gas)	+ (gas)	+	+	+	+	+
TMD2	–	–	–	–	+ (gas)	+ (gas)	+ (gas)	+	+	+	+	+
TMD3	–	–	–	–	+ (gas)	+ (gas)	+ (gas)	+	+	+	+	+
TMD4	–	–	–	–	+ (gas)	+ (gas)	+ (gas)	+	–	+	+	–
TMD5	–	–	–	–	+ (gas)	+ (gas)	+ (gas)	+	+	+	+	+
TMSP1	–	–	–	–	+ (gas)	+ (gas)	+ (gas)	+	+	+	+	+
TMSP2	–	–	–	–	+ (gas)	+ (gas)	+ (gas)	+	+	+	+	+
TMSP3	–	–	–	–	+ (gas)	+ (gas)	+ (gas)	+	–	+	+	+
TMSP4	–	–	–	–	+ (gas)	+ (gas)	+ (gas)	+	+	+	+	+
TMSP5	–	–	–	–	+ (gas)	+ (gas)	+ (gas)	+	–	+	+	–
TMSP6	–	–	–	–	+ (gas)	+ (gas)	+ (gas)	+	+	+	+	+
TMSP7	–	–	–	–	+ (gas)	+ (gas)	+ (gas)	+	–	+	+	+
TMDSP1	–	–	–	–	+ (gas)	+ (gas)	+ (gas)	+	+	+	+	+
TMDSP2	–	–	–	–	+ (gas)	+ (gas)	+ (gas)	+	–	+	+	–
TMDSP3	–	–	–	–	+ (gas)	+ (gas)	+ (gas)	+	+	+	+	+
TMDSP4	–	–	–	–	+ (gas)	+ (gas)	+ (gas)	+	+	+	+	+
TMDSP5	–	–	–	–	+ (gas)	+ (gas)	+ (gas)	+	–	+	+	–
TMDSP6	–	–	–	–	+ (gas)	+ (gas)	+ (gas)	+	+	+	+	+

Key: TMD D1-D5 = Tiger nut-Millet beverage sweetened with Date fruit; TMSP P1-P7 = Tiger nut-Millet beverage sweetened with Sweet potato; TMDSP P1-P6 = Tiger nut-Millet beverage sweetened with Date fruit and Sweet potato

3.4. Survival of LAB isolates under stimulated gastrointestinal conditions

The survival of the LAB isolates under acidic, bile salt, and phenol stress conditions is shown in Figures 1–3. At acidic pH (Figure 1), the isolates exhibited appreciable acid tolerance, with survival rates ranging from approximately 53% to 80% after 3 hours of exposure. Several isolates maintained survival rates exceeding 75%, indicating strong resistance to acidic conditions that simulate the gastric environment. Similarly, most isolates showed high tolerance to bile salts (Figure 2), maintaining survival rates above 70% at both 0.3% and 2% bile salt concentrations. These findings demonstrate the ability of the isolates to withstand conditions resembling those encountered in the small intestine. The LAB isolates also demonstrated considerable tolerance to phenol (Figure 3). Survival rates were generally highest in the medium supplemented with 0.2% phenol, indicating that the selected isolates possess adaptive mechanisms that enable survival in phenolic environments.

3.5. Identification of LAB using API 50 CHL system

The identification results obtained using the API 50 CHL system are presented in Table 3. *Lactobacillus plantarum* was the predominant species identified among the isolates, with identification confidence ranging from 74.4% to 99.9%. Isolate TMSP2 was identified as *Lactobacillus brevis* with 99.7% confidence, whereas isolate TMDSP6 was identified as *Lactobacillus pentosus* with 69.5% confidence. Overall, the API results indicated that *Lactobacillus* species predominated during fermentation of the tiger nut-millet beverages.

3.6. Antibiotic susceptibility profile of selected probiotic LAB

The antibiotic susceptibility profiles of the selected probiotic LAB isolates are presented in Table 4. Most isolates were susceptible to ampicillin, cotrimoxazole, gentamicin, erythromycin, tetracycline, vancomycin, and ciprofloxacin, exhibiting inhibition zones of ≥21 mm. An exception was isolate TMSP7, which showed resistance to ciprofloxacin. Conversely, all isolates exhibited resistance to meropenem, Augmentin, ceftazidime, cefuroxime, and cephalexin. The observed susceptibility to commonly used antibiotics, together with resistance to selected β-lactam antibiotics, indicates distinct antibiotic susceptibility patterns among the isolates.

3.7. Antibacterial activities of selected probiotic LAB

The antibacterial activities of the selected LAB isolates against clinically important bacterial pathogens are shown in Table 5. The isolates exhibited varying degrees of antibacterial activity against the test organisms. The strongest inhibitory activity was observed for isolate TMD5 against *Klebsiella pneumoniae*, producing an inhibition zone of 23 mm. Several isolates also demonstrated strong inhibition against *Escherichia coli*, *Pseudomonas aeruginosa*, *Bacillus cereus*, and *Staphylococcus aureus*, whereas a few isolates showed no detectable antibacterial activity against specific pathogens.

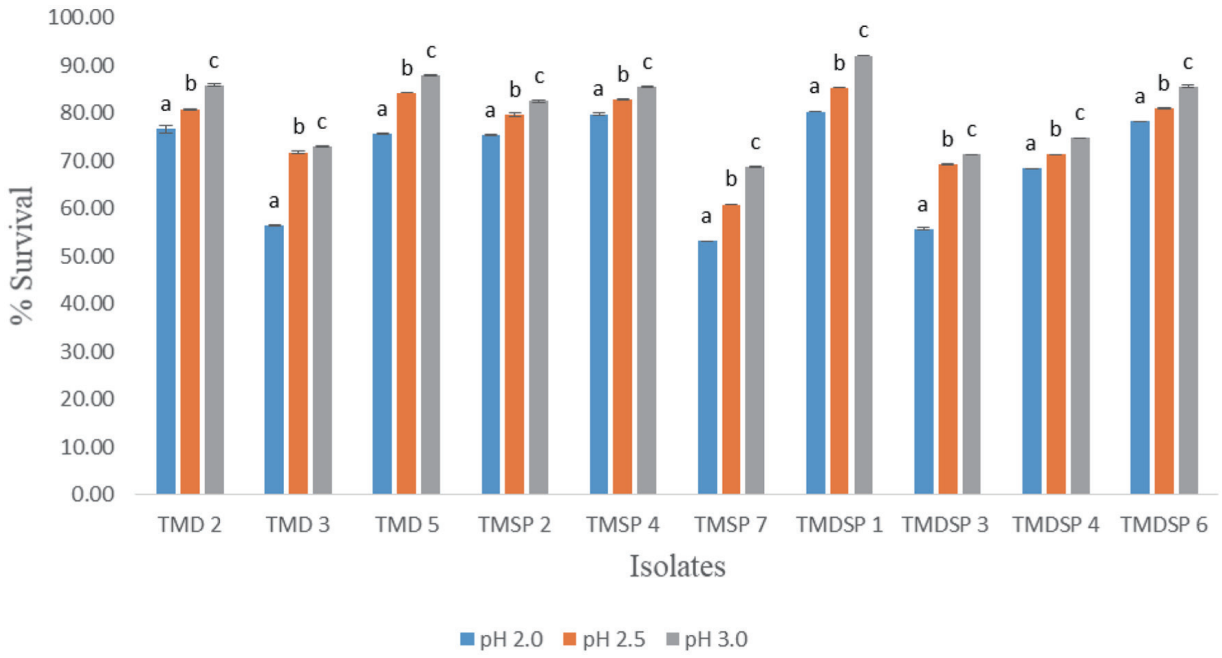


Figure 1. Percentage survival of LAB isolates at different acid levels after 3 hours of exposure. (n = 3). Data are presented as mean ± SEM (n = 3 independent replicates per isolate). Error bars denote ± SEM. For each isolate, survival was compared across the three pH levels using one-way ANOVA followed by pairwise t-tests with Bonferroni correction; survival differed significantly among all three pH levels for every isolate tested ($p < 0.05$ in all cases). Bars labeled a, b, and c within an isolate differ significantly from one another. Key: TMD (2, 3 and 5) = Bacterial Isolates from Tiger nut-Millet beverage sweetened with Date fruit; TMSP (2, 4, and 7) = Bacterial Isolates from Tiger nut-Millet beverage sweetened with Sweet potato; TMDSP (1, 3, 4 and 6) = Bacterial Isolates from Tiger nut-Millet beverage sweetened with Date fruit and Sweet potato.

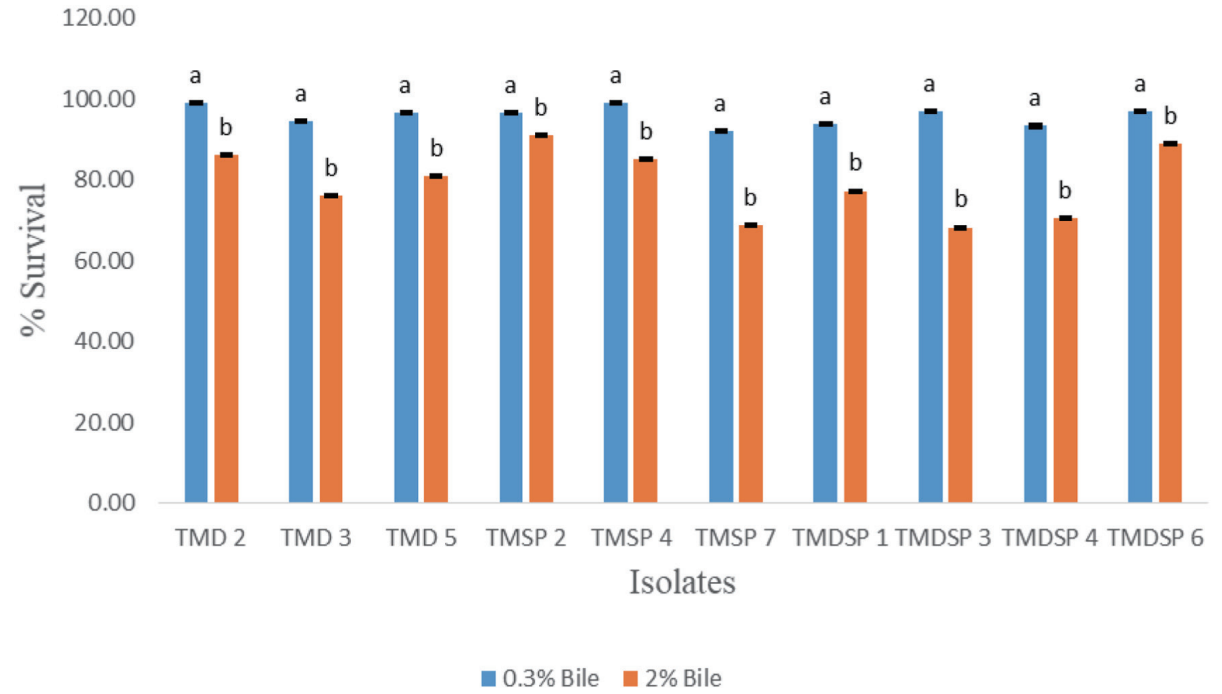


Figure 2. Percentage survival of LAB isolates at different bile salt concentrations after 3 hours of exposure (n = 3). Data are presented as mean ± SEM (n = 3). Error bars denote ± SEM. Survival at 0.3% versus 2% bile salt was compared for each isolate using Student's t-test; survival differed significantly between the two concentrations for every isolate ($p < 0.001$). Key: TMD (2, 3 and 5) = Bacterial isolates from Tiger nut-Millet beverage sweetened with Date fruit; TMSP (2, 4, and 7) = Bacterial Isolates from Tiger nut-Millet beverage sweetened with Sweet potato; TMDSP (1, 3, 4 and 6) = Bacterial Isolates from Tiger nut-Millet beverage sweetened with Date fruit and Sweet potato.

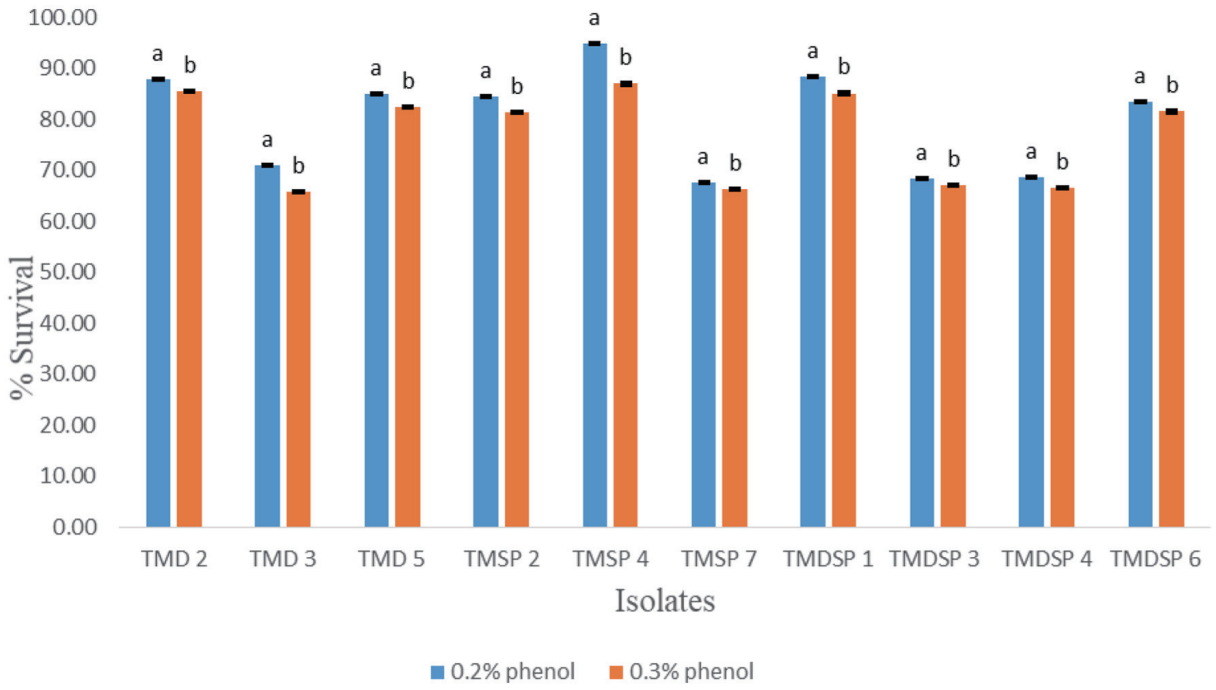


Figure 3. Percentage survival of LAB isolates at different phenol concentrations after 3 hours of exposure (n = 3). Data are presented as mean ± SEM (n = 3). Error bars denote ± SEM. Survival at 0.2% versus 0.3% phenol was compared for each isolate using Student's t-test; survival differed significantly between the two concentrations for every isolate ($p < 0.001$). Key: TMD (2, 3 and 5) = Bacterial isolates from Tiger nut-Millet beverage sweetened with Date fruit; TMSP (2, 4, and 7) = Bacterial Isolates from Tiger nut-Millet beverage sweetened with Sweet potato; TMDSP (1, 3, 4 and 6) = Bacterial Isolates from Tiger nut-Millet beverage sweetened with Date fruit and Sweet potato.

3.8. Molecular identification of selected LAB by 16S rRNA gene sequencing

The molecular identification of the selected LAB isolates based on 16S rRNA gene sequencing is presented in Table 6. Most isolates belonged to the genus *Lactiplantibacillus*, while one isolate was identified as *Leuconostoc*, both of which are commonly associated with plant-based fermentations. Isolates TMD2 and TMD5 were identified as *Lactiplantibacillus plantarum* with sequence similarities of 98.39% and 96.89%, respectively. TMDSP1 and TMDSP6 were identified as *Lactiplantibacillus pentosus*, exhibiting sequence similarities of 98.68% and 99.73%, respectively. In addition, isolate TMSP2 showed 99.61% sequence similarity with *Leuconostoc mesenteroides*.

4. Discussion

The bacterial growth patterns observed during fermentation indicated enhanced fermentative activity in the sweet potato-enriched

Table 3. Identification of isolated LAB using the standard API 50 CHL system

Isolates	LAB Significant Taxa	% accuracy	Remarks
TMD2	*Lactobacillus plantarum* 1	99.9	Excellent identification
TMD3	*Lactobacillus plantarum* 1	74.4	Good identification
TMD5	*Lactobacillus plantarum* 1	99.9	Excellent identification
TMSP2	*Lactobacillus brevis* 1	99.7	Very good identification
TMSP4	*Lactobacillus plantarum* 1	99.6	Good identification
TMSP7	*Lactobacillus plantarum* 1	99.9	Excellent identification
TMDSP1	*Lactobacillus plantarum* 1	99.9	Excellent identification
TMDSP3	*Lactobacillus plantarum* 1	90.4	Good identification
TMDSP4	*Lactobacillus plantarum* 1	98.5	Very good identification
TMDSP6	*Lactobacillus pentosus*	69.5	Doubtful profile

Key: TMD (2, 3 and 5) = Bacterial isolates from Tiger nut-Millet beverage sweetened with Date fruit; TMSP (2, 4, and 7) = Bacterial Isolates from Tiger nut-Millet beverage sweetened with Sweet potato; TMDSP (1, 3, 4 and 6) = Bacterial Isolates from Tiger nut-Millet beverage sweetened with Date fruit and Sweet potato

Table 4. Antibiotic susceptibility profile of selected probiotic LAB isolates

Antibiotics used	Disc conc. (µg)	Zone of Inhibition (mm) (Interpretation)									
		TMD 2	TMD 3	TMD 5	TMSP 2	TMSP 4	TMSP 7	TMDSP 1	TMDSP 3	TMDSP 4	TMDSP 6
Ampicillin (AMP)	10	24 (S)	25 (S)	25 (S)	24 (S)	27 (S)	25 (S)	26 (S)	21 (S)	30 (S)	25 (S)
Cotrimoxazole (COT)	25	28 (S)	28 (S)	26 (S)	28 (S)	29 (S)	27 (S)	21 (S)	25 (S)	28 (S)	22 (S)
Gentamicin (GEN)	10	26 (S)	27 (S)	26 (S)	28 (S)	31 (S)	29 (S)	28 (S)	23 (S)	27 (S)	25 (S)
Erythromycin (ERY)	5	24 (S)	29 (S)	21 (S)	24 (S)	27 (S)	28 (S)	34 (S)	31 (S)	29 (S)	24 (S)
Tetracycline (TET)	30	29 (S)	27 (S)	26 (S)	31 (S)	29 (S)	28 (S)	25 (S)	27 (S)	29 (S)	26 (S)
Vancomycin (VAN)	30	30 (S)	22 (S)	29 (S)	27 (S)	29 (S)	21 (S)	28 (S)	24 (S)	27 (S)	23 (S)
Meropenem (MEM)	10	6 (R)	15 (R)	7 (R)	9 (R)	10 (R)	8 (R)	11 (R)	9 (R)	13 (R)	10 (R)
Augmentin (AUG)	30	9 (R)	11 (R)	12 (R)	14 (R)	9 (R)	10 (R)	8 (R)	11 (R)	10 (R)	8 (R)
Ceftazidime (CPZ)	30	8 (R)	9 (R)	10 (R)	11 (R)	8 (R)	8 (R)	10 (R)	9 (R)	11 (R)	10 (R)
Cefuroxime (CRX)	10	9 (R)	12 (R)	10 (R)	13 (R)	12 (R)	9 (R)	10 (R)	9 (R)	12 (R)	11 (R)
Ciprofloxacin (CIP)	5	24 (S)	27 (S)	26 (S)	29 (S)	21 (S)	20 (R)	25 (S)	21 (S)	28 (S)	29 (S)
Cephalexin (CP)	15	10 (R)	9 (R)	12 (R)	10 (R)	8 (R)	10 (R)	9 (R)	11 (R)	10 (R)	12 (R)

Zone of inhibition (diameter in mm) for each antibiotic was measured and expressed as susceptible, S (≥21 mm), and resistant, R (≤15 mm). Key: TMD (2, 3 and 5) = Bacterial isolates from Tiger nut-Millet beverage sweetened with Date fruit; TMSP (2, 4, and 7) = Bacterial Isolates from Tiger nut-Millet beverage sweetened with Sweet potato; TMDSP (1, 3, 4 and 6) = Bacterial Isolates from Tiger nut-Millet beverage sweetened with Date fruit and Sweet potato.

Table 5. Antibacterial activities of selected probiotic LAB isolates

Test organisms	Zone of Inhibition (mm)									
	TMD 2	TMD 3	TMD 5	TMSP 2	TMSP 4	TMSP 7	TMDSP 1	TMDSP 3	TMDSP 4	TMDSP 6
Bacillus cereus NCIB 6349	12.00 ± 0.00c	11.00 ± 0.00b	0.00 ± 0.00a	15.00 ± 0.01d	0.00 ± 0.00a	15.00 ± 0.00d	0.00 ± 0.00a	11.00 ± 0.00b	15.00 ± 0.01	12.00 ± 0.00c
Staphylococcus aureus ATCC 25923	0.00 ± .00a	0.00 ± 0.00a	0.00 ± 0.00a	20.00 ± 0.01	0.00 ± 0.00a	11.00 ± 0.01b	13.00 ± 0.01c	0.00 ± 0.00a	0.00 ± 0.00a	17.00 ± 0.01d
Pseudomonas aeruginosa NCIB 3471	0.00 ± 0.00a	19.00 ± 0.02e	12.00 ± 0.01c	11.00 ± 0.00b	18.00 ± 0.01	0.00 ± 0.00a	0.00 ± 0.00a	11.00 ± 0.01b	14.00 ± 0.02d	20.00 ± 0.00f
Klebsiella pneumoniae	20.00 ± 0.00e	8.00 ± 0.00b	23.00 ± 0.02g	0.00 ± 0.00a	20.00 ± 0.01	14.00 ± 0.01c	16.00 ± 0.01d	21.00 ± 0.01f	16.00 ± 0.01d	0.00 ± 0.00a
Klebsiella edwardsii	0.00 ± 0.00a	19.00 ± 0.01e	21.00 ± 0.01f	14.00 ± 0.02d	10.00 ± 0.00b	0.00 ± 0.00a	11.00 ± 0.00c	10.00 ± 0.00b	10.00 ± 0.00b	0.00 ± 0.00a
Escherichia coli	17.00 ± 0.01f	15.00 ± 0.00d	0.00 ± 0.00a	20.00 ± 0.01h	16.00 ± 0.02e	15.00 ± 0.01d	7.00 ± 0.01b	0.00 ± 0.00a	12.00 ± 0.01c	16.00 ± 0.01e

Values were presented as mean ± standard deviation (n = 3 for each sample). The letters across the column represent significant differences. Key: TMD (2, 3 and 5) = Bacterial isolates from Tiger nut-Millet beverage sweetened with Date fruit; TMSP (2, 4, and 7) = Bacterial Isolates from Tiger nut-Millet beverage sweetened with Sweet potato; TMDSP (1, 3, 4 and 6) = Bacterial Isolates from Tiger nut-Millet beverage sweetened with Date fruit and Sweet potato.

Table 6. 16S rRNA gene sequence identification of isolated LAB strains

Isolate code	Isolate identity	Similarity (%)	GenBank Accession number
TMD2	*Lactiplantibacillus plantarum*	98.39	NR_025447.1
TMD5	*Lactiplantibacillus plantarum*	96.89	NR_117813.1
TMSP2	*Leuconostoc mesenteroides*	99.61	NR_074957.1
TMSP4	*Lysinibacillus sphaericus*	90.43	NR_042073.1
TMDSP1	*Lactiplantibacillus pentosus*	98.68	NR_113338.1
TMDSP6	*Lactiplantibacillus pentosus*	99.73	NR_029133.1

Key: TMD (2 and 5) = Bacterial isolates from Tiger nut-Millet beverage sweetened with Date fruit; TMSP (2 and 4) = Bacterial Isolates from Tiger nut-Millet beverage sweetened with Sweet potato; TMDSP (1 and 6) = Bacterial Isolates from Tiger nut-Millet beverage sweetened with Date fruit and Sweet potato.

formulations. Under favorable fermentation conditions and with sufficient carbohydrate availability, the metabolic activity and proliferation of LAB are expected to increase, consistent with the gradual rise in LAB counts observed in this study (Gallina and Barbosa, 2022). The higher LAB populations detected in sweet potato-containing samples may be associated with their increased availability of fermentable sugars, which promote acid production and bacterial growth (Albay et al., 2025). A study by Rahman et al. (2026) reported successful fermentation of sugars, fructose, sucrose, and lactose by isolated *Lactobacillus* spp. isolated from locally fermented dairy products in Dhaka city, Bangladesh, which supports their ability to break down organic substrates to produce organic acids, such as acetic and lactic acids, ethanol, and carbon dioxide. The findings of this study were consistent with those reported by Ozabor et al. (2026), who described isolated LAB colonies with smooth or rough surfaces, flat to raised elevations, white or cream pigmentation, and entire, lobate, or undulate margins from *ogi*, a traditional Nigerian cereal-based fermented food. The biochemical and morphological characteristics of the isolates were consistent with typical LAB features, suggesting the presence of a mixed LAB population comprising genera such as *Lactiplantibacillus, Pediococcus, Leuconostoc,* and *Enterococcus*, which are frequently reported in plant-based fermented beverages (Adesulu-Dahunsi et al., 2021). The selection of colonies based on distinctive morphological features, such as color, shape, size, and surface characteristics, before purification and molecular sequencing for the characterization of *Lacticaseibacillus paracasei* A35 and *Lactococcus lactis* E24 from Chinese Kefir by Li et al. (2026) aligned with the preliminary screening for LAB employed in this study.

The physiological characteristics of the isolates indicated diverse metabolic capabilities associated with both homofermentative and heterofermentative pathways (Rahman et al., 2026). The catalase-negative reaction and fermentative nature of the isolates further confirmed their classification as LAB (Kouadio et al., 2024). Similarly, Asjad et al. (2025) reported that all LAB strains isolated from fermented foods were catalase-negative. The absence of hydrogen sulfide (H_2S) production among the isolates is considered a desirable characteristic, as H_2S-producing microorganisms are generally associated with undesirable effects in fermented food systems (Lee et al., 2024). A study by Khushboo et al. (2023) also reported the absence of H_2S production among the LAB sourced from fermented and non-fermented foods, such as curd, milk, pickle, and wheat dough. Differences in temperature-dependent growth patterns indicate strain-specific adaptability, with some isolates exhibiting improved tolerance to elevated temperatures. Growth at 15°C suggests psychrotolerance, which may enhance their suitability for refrigerated storage conditions (Liu et al., 2017). In the present study, all bacterial isolates grew at 15°C, whereas only a few isolates (22.2%) failed to grow at 45°C. The ability of LAB to survive over a wide temperature range highlights their adaptability during fermentation, particularly under the fluctuating temperatures characteristic of traditional fermentation processes. The survival of all the isolates at 15°C suggests the presence of psychrotolerant LAB strains, which can function in enhancing the quality and stability of cereal-based fermentation. Evaluating LAB at both low and high temperatures is essential for optimizing fermentation processes, improving food preservation, understanding microbial ecology, and enhancing industrial and biotechnological applications (Bindu et al., 2021). The results obtained in this study were similar to the findings of Nassanga et al. (2026), who reported that 97.7% of LAB isolates grew at 15°C. Compared with previous studies (Mashau et al., 2020; Nassanga et al., 2026), the present study recorded 100% growth of LAB isolates at 15°C, indicating the presence of psychrotolerant strains, whereas 77.7% of the isolates grew at 45°C, suggesting thermotolerance. All the isolates exhibited growth at 4 and 6.5% NaCl, although 11.1% of the bacterial isolates failed to grow at 8% NaCl. Growth at 4% and 6.5% NaCl demonstrated the isolates' ability to tolerate osmotic stress and remain viable during fermentation. The variations in the salt tolerance ability of the LAB were dissimilar to the findings of Nassanga et al. (2026), who reported no growth of 6.7% and 9.1% LAB isolated from *kwete*, a maize-based fermented beverage, at 6.5% and 4% NaCl, respectively. This suggests that LAB from fermented foods may be susceptible to higher salt concentrations, which could influence their viability during prolonged fermentation or shelf-ability. Similarly, Khushboo et al. (2023) reported that all LAB strains exhibited high survival at 2% NaCl, whereas only six strains showed reduced survival at 6% NaCl. Beyond this concentration, only strain BM2 maintained a high level of salt tolerance at 10% NaCl. The results from this study agree with the findings of Isono et al. (1994), who reported the ability of four LAB isolated from fermented milk to survive at a concentration of 4% NaCl, and only one isolate exhibited survival at 6.5% NaCl supplementation in the growth medium.

Tolerance to gastrointestinal stress conditions is a fundamental criterion for evaluating potential probiotic microorganisms (Khushboo et al., 2023). Acid tolerance is a key characteristic of probiotic LAB. In the present study, all isolates survived at pH 3, indicating strong resistance to acidic conditions. LAB growth at low pH (acidic) can contribute to their survival in the fermentation medium, suppress spoilage microorganisms, and improve probiotic survival and shelf-life of cereal-based fermented foods, enhancing both the preservation and sensory attributes (Borthakur et al., 2026; Nassanga et al., 2026). The survival of LAB at low pH can help identify LAB strains with greater resistance to gastric acidity, which are viable and effective as probiotics in efficient fermentation processes for improved quality of fermented products and consistency (Nassanga et al., 2026). Optimization of process parameters to determine LAB survival at varied pH can help ascertain the functionalities to ensure improved fermented food quality and safety (Lu et al., 2022). The ability of all LAB isolates to grow at pH 3 was consistent with the findings of Zhu et al. (2022) and Nassanga et al. (2026). The predominance of *Lactiplantibacillus plantarum* in this study agrees with previous reports describing its frequent occurrence in cereal- and plant-based fermented foods due to its metabolic flexibility, probiotic potential, and ability to withstand osmotic and acidic stress (Seddik et al., 2017; Katiku et al., 2022). A study by Simatende et al. (2019) reported the dominant LAB, such as *Lactococcus lactis, Leuconostoc mesenteroides, Lb. plantarum*, *Lb. paracasei,* and *Lb. brevis* in *emasi* and *Lb. plantarum, L. mesenteroides, Lb. fermentum, Lb. brevis, Wessella confusa, Lb. acidophilus* and *Lb. lactis* in *emahewu,* which contribute to the dietary and nutritional quality of the non-alcoholic lactic acid fermented traditional foods produced for both children and adults in Eswatini. Similarly, the detection of *Levilactobacillus brevis* is consistent with previous studies highlighting its contribution to flavor development and production of antimicrobial metabolites in fermented plant-based products (Wuyts et al., 2018; Nguyen et al., 2025). Although identified with lower confidence, *Lactiplantibacillus pentosus* remains an important species because of its ecological adaptability and reported probiotic characteristics in complex fermentation systems (Abriouel et al., 2024). Comparatively, isolation and characterization of dominant LAB in the genera *Lactobacillus* and *Leuconostoc* from fermented foods with exceptional probiotic potential for functional food development have been documented (Yao et al., 2025; Zakari et al., 2025; Sliti et al., 2026).

The high survival rates recorded under acidic conditions suggest

that the LAB isolates possess effective acid tolerance mechanisms (Khushboo et al., 2023). Previous studies have demonstrated the resistance of *Leuconostoc mesenteroides* and *Lactiplantibacillus plantarum* to acid stress through mechanisms such as membrane fatty acid modification, synthesis of stress-response proteins, and activation of F_0F_1-ATPase systems, which contribute to intracellular pH regulation (Zheng et al., 2020; Lee et al., 2024).

Bile tolerance is another important characteristic for probiotic selection because bile salts in the small intestine can damage bacterial membranes, disrupt cellular proteins, and induce oxidative stress (Khushboo et al., 2023). The ability of probiotic bacteria to adapt to bile stress in the small intestine is essential for successful intestinal colonization (Sliti et al., 2026). During digestion, bile is released from the gallbladder into the duodenum, where it facilitates lipid emulsification and promotes fat digestion and nutrient absorption (Kiran et al., 2025). Under normal physiological conditions, bile concentrations in the human intestine are between 40 mM and < 1 mM (equivalent to 2 % and 0.05 %, respectively) (Sliti et al., 2026). The survival ability of the isolates under bile exposure indicates their potential to withstand intestinal conditions. This tolerance may be associated with adaptive mechanisms reported in *Lactiplantibacillus plantarum*, including membrane modification and bile salt hydrolase (BSH) activity, which reduce bile-induced cellular damage (Zheng et al., 2020; Ruiz et al., 2013). In this study, all the LAB isolates showed a high survival rate >86% at 0.3% bile concentrations. The results obtained from this study align with the findings of Sliti et al. (2026), who reported survival rates between 51.61 and 98.71% of *Leuconostoc* strains at varied bile concentrations of 0.05 % and 0.08 %, respectively. The resistance of LAB to bile salts can be facilitated by the production of bile salt hydrolase, the action of efflux pumps, and the intrinsic physiological properties of the cell (Bustos and Taranto, 2025). However, higher concentrations of bile salts can function as antimicrobials, which disrupt bacterial membrane phospholipids and damage lipid bilayers, leading to cell lysis and death.

Resistance to phenolic compounds is also relevant in probiotic evaluation because phenolic metabolites produced in the gastrointestinal tract can negatively affect bacterial membranes and intracellular components (Pacheco-Ordaz et al., 2018; Roslina et al., 2021). The ability of the LAB isolates to survive phenol exposure indicates the presence of adaptive mechanisms that enhance persistence under gastrointestinal conditions (Islam et al., 2026). These mechanisms may include enhanced membrane stability, efflux activity, and cellular stress responses. Similar phenol tolerance has been reported among *Lactiplantibacillus plantarum* and *Pediococcus acidilactici* strains, supporting their potential application as functional probiotic cultures (Zhang et al., 2018).

The antibiotic susceptibility profile of the isolates revealed consistent resistance to ceftazidime, cefuroxime, Augmentin, meropenem, and cephalexin. Such resistance patterns may reflect intrinsic resistance characteristics commonly observed among LAB, including limited antibiotic uptake due to cell wall structure, chromosomal resistance determinants, or efflux mechanisms (Gueimonde et al., 2013; Seyirt et al., 2023). Similar observations have been reported for LAB isolated from fermented foods, where susceptibility to clinically relevant antibiotics supports their potential safety for probiotic applications (Saci et al., 2025). Importantly, the absence of tetracycline resistance among the isolates represents a favorable biosafety characteristic because tetracycline resistance genes are frequently associated with horizontal transfer among gastrointestinal microorganisms (Zhou et al., 2022).

The antagonistic activity of probiotic LAB against pathogenic microorganisms is an important functional characteristic that supports their application in fermented foods and probiotic formulations (Choi et al., 2018). LAB inhibit pathogens through multiple mechanisms, including organic acid production, bacteriocin secretion, competitive exclusion, nutrient competition, and modulation of host immune responses (Malik et al., 2021). According to Gueimonde et al. (2013), probiotic strains should lack transferable antibiotic resistance determinants to minimize the risk of resistance dissemination within the gastrointestinal microbiota.

Among the evaluated isolates, TMSP2 and TMDSP6 demonstrated strong probiotic potential due to their broad-spectrum antimicrobial activity against tested pathogens. TMSP2 showed the highest inhibition activity against *Escherichia coli* and *Staphylococcus aureus* (20 mm inhibition zone), suggesting the production of antimicrobial compounds, such as organic acids, hydrogen peroxide, or bacteriocins (Aguilar-Toalá et al., 2018; Zommiti et al., 2018). Similarly, TMD3 and TMSP4 exhibited notable inhibition against *Pseudomonas aeruginosa* (19 mm and 18 mm, respectively), whereas TMD5 and TMD2 demonstrated strong activity against *Klebsiella pneumoniae* (23 mm and 20 mm, respectively). These findings support previous reports that LAB exert antimicrobial effects through acidification, nutrient depletion, and production of antimicrobial peptides, highlighting their potential use in functional foods and microbial-based therapies (Binda et al., 2020; Girma and Aemiro, 2021). Furthermore, Sliti et al. (2026) reported antimicrobial activities of *Leuconostoc* strains RP1, RP3, and SS5 against *S. typhimurium, S. enterica*, *B. cereus*, and *E. coli*, which can be due to their ability in the production of metabolic compounds, such as bacteriocins, hydrogen peroxide, organic acids, and other active antimicrobial metabolites (Khubber et al., 2022).

The molecular identification results were consistent with previous reports showing that *Leuconostoc, Lactobacillus,* and *Lactiplantibacillus* species are predominant microorganisms in cereal- and tuber-based fermented foods (Tamene et al., 2019; Kouadio et al., 2024; Abdi et al., 2025). These microorganisms contribute to acidification, flavor development, and functional properties, including stress tolerance and gastrointestinal survival (Zheng et al., 2020; Zhang et al., 2025). However, the relatively low similarity value (90.43%) observed for isolate TMSP4 suggests that it may represent a genetically distinct strain or a microorganism not typically associated with fermented food systems. Further molecular characterization using advanced identification approaches, such as whole-genome sequencing or multilocus sequence analysis, would be required to confirm its taxonomic position.

5. Conclusions

The fermented tiger nut–millet beverage contained dominant LAB belonging to the genera *Lactobacillus* and *Lactiplantibacillus*, highlighting their important roles in fermentation and potential probiotic functionality. The adaptability and performance of these LAB isolates during fermentation demonstrate their ability to tolerate simulated gastrointestinal conditions, including acid, bile, and phenolic stress. Their antibacterial activity against selected food-borne pathogens further supports their potential contribution to food safety. Therefore, the fermented tiger nut–millet beverage represents a promising non-dairy probiotic food candidate for the development of functional foods and nutraceutical products.

Acknowledgments

The authors gratefully acknowledge the support received from the affiliated institutions.

Funding

This research received no funding.

Conflict of interest

The authors have no competing interests to declare that are relevant to the content of this article.

Supplementary Material

Table S1. Cultural and morphological characteristics of LAB isolated from naturally sweetened spicy fermented tiger nut-Millet beverage.

References

Abdi, A., Gatri, E., Guilbaud, J., Bouallagui, H., Fadhlaoui, K., Garrait, G., and Ayed, L. (2025). Co-cultivation of potential probiotic strains isolated from water kefir for fermented green tea beverage. Fermentation 11(4): 169.

Abriouel, H., Caballero, G.N., Manetsberger, J., and Benomar, N. (2024). Dual effects of a bacteriocin-producing *Lactiplantibacillus pentosus* CF-6HA, isolated from fermented Aloreña table olives, as potential probiotic and antimicrobial agent. Heliyon 10(7): e28408.

Adegbola, G.M., Gabriel-Ajobiewe, R.A.O., Gabriel-Ogunniyi, B.M., Odeleye, O.P., and Adeleke, B.S. (2026). Nutritional assessment of composite postnatal diets formulated from traditionally fermented cereal blends. Edelweiss Appl. Sci. Technol. 10(3): 308–317.

Adesulu-Dahunsi, A.T., Sanni, A.I., and Jeyaram, K. (2021). Diversity and technological characterization of *Pediococcus pentosaceus* strains isolated from Nigerian traditional fermented foods. LWT 140: 110697.

Aguilar-Toalá, J.E., Garcia-Varela, R., Garcia, H.S., Mata-Haro, V., González-Córdova, A.F., Vallejo-Cordoba, B., and Hernández-Mendoza, A. (2018). Postbiotics: An evolving term within the functional foods field. Trends Food Sci. Technol. 75: 105–114.

Albay, Z., Çelebi, M., and Şimşek, B. (2025). Physicochemical, rheological, and microbiological properties of honey-fortified probiotic drinkable yogurt. Foods Raw Mater. 13(2): 320–329.

Aleman, R.S., and Yadav, A. (2024). Systematic review of probiotics and their potential for developing functional nondairy foods. Appl. Microbiol. 4(1): 47–69.

Anumudu, C.K., Miri, T., and Onyeaka, H. (2024). Multifunctional applications of lactic acid bacteria: Enhancing safety, quality, and nutritional value in foods and fermented beverages. Foods 13(23): 3714.

Asjad, T., Al-Adeeb, A., Sibomana, M., Basharat, S., Bux, E., Gu, Q., and Yu, X. (2025). Purine-degrading lactic acid bacteria isolated from fermented foods and fig fruit: evaluation of probiotic and anti-hyperuricemic properties. Probiotics Antimicrob. Proteins 18: 5853–5869.

Bernatek, M., Żukiewicz-Sobczak, W., Lachowicz-Wiśniewska, S., and Piątek, J. (2022). Factors determining effective probiotic activity: Evaluation of survival and antibacterial activity of selected probiotic products using an *in vitro* study. Nutrients 14(16): 3323.

Binda, S., Hill, C., Johansen, E., Obis, D., Pot, B., Sanders, M.E., Tremblay, A., and Ouwehand, A.C. (2020). Criteria to qualify microorganisms as "probiotic" in foods and dietary supplements. Front. Microbiol. 11: 1662.

Bindu, A., and Lakshmidevi, N. (2021). Identification and *in vitro* evaluation of probiotic attributes of lactic acid bacteria isolated from fermented food sources. Arch. Microbiol. 203: 579–95.

Borthakur, D., Sharma, B.K., and Duncan, T. (2026). Unravelling functional Bacillus strains from Ngari: A step toward sustainable probiotic applications in food systems. Annals Microbiol. 76(1): 19.

Bustos, A.Y., and Taranto, M.P. (2025). Interaction between lactic acid bacteria and bile acids: Molecular and biophysical insights. Chem. Phys. Lipids. 270: 105513.

Chen, Y., Hu, Y., Xie, Y., Cui, M., Jiang, J., Li, Y., Guo, J., Xiang, M., Tian, Z., Niu, J., and Cheng, W. (2026). A comprehensive review of lactic acid bacteria-fermented plant-based beverages: substrate types, nutritional quality, probiotic characteristics, metabolic pathways and future development trends. Crit. Rev. Food Sci. Nutr. 66(16): 2993–3021.

Choi, A.R., Patra, J.K., Kim, W.J., and Kang, S.S. (2018). Antagonistic activities and probiotic potential of lactic acid bacteria derived from a plant-based fermented food. Front. Microbiol. 9: 1963.

Debri, R.P., De Lorenzo, A., Conte, R., and Peluso, G. (2026). Functional foods as vehicles for bioactive compounds: Chemical and nutritional perspectives on health and disease prevention. Int. J. Mol. Sci. 27(5): 2293.

Divisekera, D.M.W.D., Samarasekera, J.K.R.R., Hettiarachchi, C., Gooneratne, J., Choudhary, M.I., Gopalakrishnan, S., and Wahab, A.T. (2019). Lactic acid bacteria isolated from fermented flour of finger millet, its probiotic attributes and bioactive properties. Ann. Microbiol. 69(2): 79–92.

Erem, E., and Kılıç-Akyılmaz, M. (2024). The role of fermentation with lactic acid bacteria in quality and health effects of plant-based dairy analogues. Compr. Rev. Food Sci. Food Safety 23(4): e13402.

Gallina, D.A., and Barbosa, P.M. (2022). Viability of probiotics, physicochemical and microbiological characterization of beverage (smoothie) with symbiotic yogurt and berries pulp. Res. Soc. Dev. 11(3): e19511325975.

Girma, A., and Aemiro, A. (2021). Antibacterial activity of lactic acid bacteria isolated from fermented Ethiopian traditional dairy products against food spoilage and pathogenic bacterial strains. J. Food Qual. 2021: 9978561.

Gueimonde, M., Sánchez, B., de los Reyes-Gavilán, C.G., and Margolles, A. (2013). Antibiotic resistance in probiotic bacteria. Front. Microbiol. 4: 202.

Islam, S., Hossain, T.J., Afrin, S., Paul, S., Bappi, M.S.H., Ali, F., and Ferdouse, J. (2026). Multifunctional lactic acid bacteria from sugarcane juice with probiotic properties for gut adaptation, health benefits, food preservation and quality enhancement. Sci. Rep. 16: 9994.

Isono, Y., Shingu, I., and Shimizu, S. (1994). Identification and characteristics of lactic acid bacteria isolated from Masai fermented milk in Northern Tanzania. Biosci. Biotechnol. Biochem. 58: 660–664.

Katiku, M.M., Matofari, J.W., and Nduko, J.M. (2022). Preliminary evaluation of probiotic properties and safety profile of *Lactiplantibacillus plantarum* isolated from spontaneously fermented milk, Amabere amaruranu. Heliyon 8(8): e10342.

Khubber, S., Marti-Quijal, F.J., Tomasevic, I., Remize, F., and Barba, F.J. (2022). Lactic acid fermentation as a useful strategy to recover antimicrobial and antioxidant compounds from food and by-products. Curr. Opin. Food Sci. 43: 189–198.

Khushboo, Karnwal, A., and Malik, T. (2023). Characterization and selection of probiotic lactic acid bacteria from different dietary sources for development of functional foods. Front. Microbiol. 14: 1170725.

Kiran, B.S., Bashir, O., Pawase, P.A., Dash, K.K., Amin, T., Shams, R., Shaikh, A.M., and Béla, K. (2025). A review of *in-vitro* digestibility models on diverse foods in various segments of human digestive tract. Discover Food. 5(1): 273.

Kitessa, D.A. (2024). Review on effect of fermentation on physicochemical properties, anti-nutritional factors and sensory properties of cereal-based fermented foods and beverages. Ann. Microbiol. 74: 32.

Kouadio, N.J., Zady, A.L.O., Kra, K.A.S., Diguță, F.C., Niamke, S., and Matei, F. (2024). *In vitro* probiotic characterization of Lactiplantibacillus plantarum strains isolated from traditional fermented dockounou paste. Fermentation 10(5): 264.

Kunchala, R., Banerjee, R., Datta Mazumdar, S.D., Durgalla, P., Srinivas, V., and Gopalakrishnan, S. (2016). Characterization of potential probiotic bacteria isolated from sorghum and pearl millet of the semi-arid tropics. Afr. J. Biotechnol. 15(16): 613–621.

Lee, M.G., Kang, M.J., Cha, S., Kim, T.R., and Park, Y.S. (2024). Acid tolerance responses and their mechanisms in *Lactiplantibacillus plantarum* LM1001. Food Sci. Biotechnol. 33(9): 2213–2222.

Li, J., Zhao, X., Liu, C., Gao, R., Zhang, T., Qi, W., Zhang, F., Liu, W., Kwok, L.Y., and Bao, Q. (2026). Functional characterization and application of autochthonous lactic acid bacteria from Chinese kefir for improved fermented milk quality. J. Dairy Sci.

Liu, A., Li, X., Pu, B., Ao, X., Zhou, K., He, L., Chen, S., and Liu, S. (2017). Use of psychrotolerant lactic acid bacteria (*Lactobacillus* spp. and *Leuconostoc* spp.) isolated from Chinese traditional Paocai for the quality improvement of Paocai products. J. Agric. Food Chem. 65(12): 2580–2587.

Lu, Y., Xing, S., He, L., Li, C., Wang, X., Zeng, X., and Dai, Y. (2022). Characterization, high-density fermentation, and the production of a directed vat set starter of Lactobacilli used in the food industry: A review. Foods 11(19): 3063.

Mafe, A.N., Makut, M.D., Owuna, J.E., Nkene, I.H., Edo, G.I., Salisu, S.M., and Said, M.A. (2026). Development, functional profiling, and probiotic evaluation of indigenous LAB from Nigerian fermented foods: Antimicrobial mechanisms, *in vivo* validation, and applications in food preservation and mycotoxin risk reduction. World J. Microbiol. Biotechnol. 42(6): 317.

Malik, K.M., Gehlot, T.R., Kumari, K.R., Sindhu, R.A., and Rohilla, P. (2021). Antimicrobial property of probiotics. Environ. Conserv. J. 22(SE): 33–48.

Marco, M.L., Sanders, M.E., Gänzle, M., Arrieta, M.C., Cotter, P.D., De Vuyst, L., Hill, C., Holzapfel, W., Lebeer, S., Merenstein, D., and Reid, G. (2021). The International Scientific Association for Probiotics and Prebiotics (ISAPP) consensus statement on fermented foods. Nat. Rev. Gastroenterol. Hepatol. 18(3): 196–208.

Mashau, M.E., Jideani, A.I.O., and Maliwichi, L.L. (2020). Evaluation of the shelf-life extension and sensory properties of mahewu - a non-alcoholic fermented beverage by adding *Aloe vera* (*Aloe barbadensis*) powder. Brit. Food J. 122(11): 3419–3432.

Nassanga, P., Mauriello, G., Ochaya, S.O., and and Ongeng, D. (2026). Genera of lactic acid bacteria isolated from a maize-based fermented beverage (Kwete) consumed by ethnic communities in Northern Uganda. Discov. Food 6(1): 131.

Nguyen, Q.D., Truong Thi, H.T., Ngo Thi, N.H., Nguyen, V.L., Nguyen, M.A., and Do, A.D. (2025). Whole-genome sequencing, probiotic characterization, and safety evaluation of *Levilactobacillus brevis* QD-1 and its application in soy yogurt production. Food Biotechnol. 39(4): 388–413.

Ozabor, P.T., Olumakinde, T.S., Oluokun, T.E., Oladele, J.O., and Fadahunsi, I.F. (2026). Biochemical and molecular identification of lactic acid bacteria and yeasts with technological qualities from *ogi* (a cereal-based fermented food in Nigeria). BioTechnologia (Pozn) 107(1): 45.

Pacheco-Ordaz, R., Wall-Medrano, A., Goñi, M.G., Ramos-Clamont-Montfort, G., Ayala-Zavala, J.F., and González-Aguilar, G.A. (2018). Effect of phenolic compounds on the growth of selected probiotic and pathogenic bacteria. Lett. Appl. Microbiol. 66: 25–31.

Rahman, A., Akter, M., Rahman, A., Biswas, L., Sultana, M.T., Islam, M.S., and Asaduzzaman, M. (2026). Isolation and characterization of lactic acid bacteria derived from fermented dairy products. Asian-Australas. J. Food Saf. Secur. 10(1): 43–50.

Roslina, J., Sahar, A., Shuhaimi, M., Rizal, K.M., Murni, H., and Ariff, A.B. (2021). *In vitro* evaluation of potential probiotic strain Lactococcus lactis Gh1 and its bacteriocin-like inhibitory substances for potential use in the food industry. Probiotics Antimicrob. Proteins 13(2): 422–440.

Ruiz, L., Margolles, A., and Sánchez, B. (2013). Bile resistance mechanisms in *Lactobacillus* and *Bifidobacterium*. Front. Microbiol. 4: 396.

Rymuszka, A., and Gorczynska, W. (2026). Classical food fermentations as modern biotechnological platforms: Alcoholic, acetic, butyric, lactic and propionic pathways and applications. Molecules 31(2): 333.

Saci, A., Gharbi, S., Djadouni, F., and Karkachi, N. (2025). Screening of five *Lactobacillus* bacteria with probiotic properties from indigenous Klila cheese. North Afr. J. Food Nutr. Res. 9(20): 59–73.

Sanam, M.U., Detha, A.I., and Rohi, N.K. (2022). Detection of antibacterial activity of lactic acid bacteria, isolated from Sumba mare's milk, against *Bacillus cereus*, *Staphylococcus aureus*, and *Escherichia coli*. J. Adv. Vet. Animal Res. 9(1): 53.

Seddik, H.A., Bendali, F., Cudennec, B., and Drider, D. (2017). Anti-pathogenic and probiotic attributes of *Lactobacillus salivarius* and *Lactobacillus plantarum* strains isolated from feces of Algerian infants and adults. Res. Microbiol. 168(3): 244–254.

Seyirt, S., Şanlıbaba, P., and Uymaz Tezel, B. (2023). Antibiotic resistance in probiotic microorganisms. Turk. J. Agric. Food Sci. Technol. 11(4): 746–757.

Sharma, K., Sharma, N., and Sharma, R. (2016). Identification and evaluation of in vitro probiotic attributes of novel and potential strains of lactic acid bacteria isolated from traditional dairy products of North-West Himalayas. J. Clin. Microbiol. Biochem. Technol. 2(1): 18–25.

Simatende, P., Siwela, M., and Gadaga, T.H. (2019). Identification of lactic acid bacteria and determination of selected biochemical properties in emasi and emahewu. South Afr. J. Sci. 115(11-12): 1–7.

Sliti, A., Kim, R.H., and Shin, J.H. (2026). Screening and characterization of probiotic lactic acid bacteria from Korean fermented foods for functional food development. Appl. Food Res. 6(1): 101787.

Suwannaphan, S. (2021). Isolation, identification and potential probiotic characterization of lactic acid bacteria from Thai traditional fermented food. AIMS Microbiol. 7(4): 431–446.

Tamang, J.P., Watanabe, K., and Holzapfel, W.H. (2020). Diversity of microorganisms in global fermented foods and beverages. Front. Microbiol. 11: 543.

Tamene, A., Baye, K., Kariluoto, S., Edelmann, M., Bationo, F., Leconte, N., and Humblot, C. (2019). *Lactobacillus plantarum* P2R3FA isolated from traditional cereal-based fermented food increase folate status in deficient rats. Nutrients 11(11): 2819.

Tang, H., Huang, W., and Yao, Y.F. (2023). The metabolites of lactic acid bacteria: Classification, biosynthesis and modulation of gut microbiota. Microb. Cell 10(3): 49.

Wuyts, S., Van Beeck, W., Oerlemans, E.F., Wittouck, S., Claes, I.J., De Boeck, I., Weckx, S., Lievens, B., De Vuyst, L., and Lebeer, S. (2018). Carrot juice fermentations as man-made microbial ecosystems dominated by lactic acid bacteria. Appl. Environ. Microbiol. 84(12): e00134–18.

Yao, P., Kang, M., and Effarizah, M.E. (2025). Characterization of biofilm-forming lactic acid bacteria from traditional fermented foods and their probiotic potential. Foods 14(24): 4299.

Zakari, D., Amoka, A., Idris, E., Anoze, A., Moyosore, A., Boniface, M., Bashir, A., Danjuma, S., and Omuya, A. (2025). Characterization of lactic acid bacteria from fermented cereal-based foods in Anyigba, Nigeria, for potential probiotic and bio-preservation applications. Agric. Food Bioact. Compd. 2(8): 171–182.

Zapaśnik, A., Sokołowska, B., and Bryła, M. (2022). Role of lactic acid bacteria in food preservation and safety. Foods 11(9): 1283.

Zhang, Z., Lv, J., Pan, L., and Zhang, Y. (2018). Roles and applications of probiotic *Lactobacillus* strains. Appl. Microbiol. Biotechnol. 102(19): 8135–8143.

Zhang, Z., Niu, H., Qu, Q., Guo, D., Wan, X., Yang, Q., Mo, Z., Tan, S., Xiang, Q., Tian, X., and Yang, H. (2025). Advancements in *Lactiplantibacillus plantarum*: probiotic characteristics, gene editing technologies and applications. Crit. Rev. Food Sci. Nutr. 65(29): 6623–6644.

Zheng, J., Wittouck, S., Salvetti, E., Franz, C.M., Harris, H.M., Mattarelli, P., O'toole, P.W., Pot, B., Vandamme, P., Walter, J., and Watanabe, K. (2020). A taxonomic note on the genus *Lactobacillus*: Description of 23 novel genera, emended description of the genus *Lactobacillus beijerinck* 1901, and union of Lactobacillaceae and Leuconostocaceae. Int. J. Syst. Evol. Microbiol. 70(4): 2782–2858.

Zhou, M., Cai, Q., Zhang, C., Ouyang, P., Yu, L., and Xu, Y. (2022). Antibiotic resistance bacteria and antibiotic resistance genes survived from the extremely acidity posing a risk on intestinal bacteria in an in vitro digestion model by horizontal gene transfer. Ecotoxicol. Environ. Safet. 247: 114247.

Zhu, X.M., Jiang, D.D., Yuan, B.J., and Ni, K.K. (2022). Effect of low-temperature-tolerant lactic acid bacteria on the fermentation quality and bacterial community of oat silage at 5°C vs 15°C. Fermentation 8(158): 1–9.

Zommiti, M., Cambronel, M., Maillot, O., Barreau, M., Sebei, K., Feuilloley, M., Ferchichi, M., and Connil, N. (2018). Evaluation of probiotic properties and safety of *Enterococcus faecium* isolated from artisanal Tunisian meat "Dried Ossban". Front. Microbiol. 9: 1685.

Journal of Food Bioactives
International Society for Nutraceuticals and Functional Foods
Original Research
J. Food Bioact. 2026;35:69–80

Effects of tamarind seed husk extract on abdominal visceral fat: a randomized, double-blind, placebo-controlled trial in Japanese adults with mild obesity

Hiroaki Yamada[a], Yusuke Yamashita[a], Xuan Li[a], Kenji Sato[a], Saki Shirako[a], Mariko Hirata[b], Jun Kawamura[b], Yumeo Suzuki[b], Yoshito Tsuruha[b], Tsuyoshi Takara[c] and Young-il Kim[a*]

[a]Research & Development Division, Pharma Foods International Co., Ltd., 1-49 Goryo Ohara, Nishikyo-ku, Kyoto 615-8245, Japan
[b]MP GOKYO FOOD & CHEMICAL Co., Ltd., 20F HERBIS OSAKA, 2-5-25 Umeda, Kita-ku, Osaka 530-0001, Japan
[c]Takara Clinic Medical Corporation Seishinkai, 9F Taisei Building, 2-3-2 Higashi-Gotanda, Shinagawa-ku, Tokyo 141-0022, Japan
[*]**Corresponding author:** Young-il Kim, Research & Development Division, Pharma Foods International Co., Ltd., 1-49 Goryo Ohara, Nishikyo-ku, Kyoto 615-8245, Japan. E-mail: youngil-kim@pharmafoods.co.jp
DOI: 10.26599/JFB.2026.95035457
Received: July 27, 2026; **Revised received & accepted:** September 10, 2026
Citation: Yamada, H., Yamashita, Y., Li, X., Sato, K., Shirako, S., Hirata, M., Kawamura, J., Suzuki, Y., Tsuruha, Y., Takara, T., and Kim, Y. (2026). Effects of tamarind seed husk extract on abdominal visceral fat: a randomized, double-blind, placebo-controlled trial in Japanese adults with mild obesity. J. Food Bioact. 35: 69–80.

Abstract

Tamarind seed husk, a by-product of gum production, is rich in polyphenols. We examined whether tamarind seed husk extract (TSHE) reduces abdominal visceral fat area (AVFA) in Japanese adults with mild obesity. In a randomized, double-blind, placebo-controlled trial (UMIN000057223), 112 adults (25 ≤ BMI < 30 kg/m^2) received TSHE (200 mg/day) or placebo for 12 weeks. AVFA at week 12, the primary outcome, was lower but not significantly (p = 0.077). AVFA was already significantly lower at week 4, and the percent reduction in total fat area was significant at weeks 8 and 12. Reductions were greater in participants with a baseline visceral-to-subcutaneous fat ratio ≥ 0.4. No adverse events occurred, indicating that TSHE is safe as a food ingredient. This is the first clinical trial to show that TSHE (200 mg/day) reduces visceral fat in mildly obese adults with a visceral-to-subcutaneous fat ratio ≥ 0.4.

Keywords: Tamarind seed husk; Procyanidin; Visceral fat; Randomized controlled trial; Polyphenol.

1. Introduction

Obesity is a major risk factor for lifestyle-related diseases such as dyslipidemia and diabetes, representing a significant public health concern. In Japan, obesity is defined as a body mass index (BMI) ≥ 25 kg/m^2 (Examination Committee of Criteria for Obesity Disease in Japan, 2002; Japan Society for the Study of Obesity, 2022), and a BMI of 25 to less than 30 kg/m^2 is classified as mild obesity (class 1 obesity). According to the 2023 National Health and Nutrition Survey, approximately one in four Japanese adults falls into mild obesity, representing an estimated 27 million individuals with obesity and 13 million with suspected diabetes (Ministry of Health, Labour and Welfare of Japan, 2025). These figures highlight an urgent need for strategies to prevent the onset and progression of these conditions. Although East Asians have lower obesity rates than Western populations, they are more susceptible to metabolic disorders. Consequently, even individuals with mild obesity exhibit elevated risk (Kuwabara et al., 2018). This disparity is attributed to a higher proportion of abdominal visceral fat (AVF) in East Asians at an equivalent BMI (Zenas-Trujillo et al., 2023).

In Japan, a GLP-1 receptor agonist is approved for obesity only in patients with hypertension, dyslipidemia or type 2 diabetes who have a BMI of ≥ 27 kg/m^2 with two or more obesity-related disorders, or ≥ 35 kg/m^2, and only after six months of supervised diet and exercise therapy has failed; use is restricted to certified institutions and to 68 weeks (Ministry of Health, Labour and Welfare

© The author(s) 2026. Publishing Services by Tsinghua University Press
The articles published in this open access journal are distributed under the terms of the Creative Commons Attribution 4.0 International License (http://creativecommons.org/licenses/by/4.0/)

Table 1. Composition of TSHE and of the test food

Ingredients and Nutritional components	TSHE (g/100 g)	Test food (g/two capsules)	Placebo (g/two capsules)
Tamarind seed husk extract (TSHE)	–	0.20	–
Syloid 760 (fine silicon dioxide)	–	<0.01	<0.01
Tricalcium phosphate	–	<0.01	<0.01
Calcium stearate	–	<0.01	<0.01
TK-16 (starch hydrolysate)	–	0.30	0.54
Capsule	–	0.12	0.12
Protein	0.8	0.12	0.12
Lipid	0.3	0.01	0.01
Moisture	8.6	0.04	0.04
Ash	1.2	0.01	0.01
Total carbohydrate	22.1	0.33	0.51
Total polyphenol	67.0	0.13	0.00
Energy (kcal)	–	2.13	2.59

TSHE values are expressed as g per 100 g of extract; test food and placebo values as g per two capsules, which constitute one daily dose and provide 200 mg of TSHE. Total carbohydrate was obtained by subtracting total polyphenol from crude carbohydrate, and total polyphenol was determined by the Folin-Ciocalteu method and expressed as gallic acid equivalents. – , not applicable. TSHE, tamarind seed husk extract. The capsule contents and the TSHE bulk powder were analyzed at different times.

of Japan, 2023). Gastrointestinal adverse events are common: in the Japanese and Korean phase III trial, constipation, nausea, diarrhea and vomiting occurred in 26.1%, 17.6%, 16.1% and 8.5% of participants given 2.4 mg, versus 3.0%, 4.0%, 5.9% and 2.0% on placebo (Ministry of Health, Labour and Welfare of Japan, 2023). Therefore, in Japan, there is a need for functional food ingredients that are safe for daily use and target reduction of AVF, particularly in individuals with mild obesity and elevated AVF.

Current approaches to reducing AVF through functional foods include a range of bioactive compounds, such as tea catechins (Nagao et al., 2001; Zhang et al., 2012), apple polyphenols (Akazome et al., 2010), and 3-(4-hydroxy-3-methoxyphenyl)propionic acid (HMPA) derived from fermented rice bran (Yoshino et al., 2022). Although these options are safe for daily consumption, obtaining these components through complex production methods or specialized cultivation often leads to high costs and environmental burdens.

Tamarind (*Tamarindus indica* L.) is a large tropical leguminous tree that can reach a height of up to 30 m (Nasir et al., 2026). It is characterized by remarkable longevity and is widely cultivated across Africa and Asia (Nasir et al., 2026). Furthermore, it exhibits environmental adaptability due to its nitrogen-fixing capability through symbiosis with rhizobia and a hard outer seed husk that protects the interior of the seed (Nasir et al., 2026). The seeds serve as a vital industrial resource, providing tamarind seed gum, which is utilized as a thickening and stabilizing agent (Nasir et al., 2026). During gum production, the seed husk is generated as a by-product in quantities estimated at 30,000 tons annually, most of which is currently discarded (Crispín-Isidro et al., 2019). Although treated as underutilized biomass, tamarind seed husk is rich in bioactive compounds, particularly polyphenols such as catechins and procyanidins (Wandee et al., 2022). Tamarind seed husk polyphenols have been reported to inhibit adipocyte differentiation and lipid accumulation in cultured adipocytes (Wandee et al., 2022). In addition, a tamarind seed coat extract inhibits pancreatic lipase activity *in vitro* and suppresses triglyceride absorption in rats, indicating a capacity to limit dietary lipid digestion and absorption (Souza et al., 2025). In a rat model of non-alcoholic fatty liver disease (NAFLD), tamarind seed coat extract reduced hepatic lipid accumulation and also lowered body weight (Sasidharan et al., 2014). However, its specific effects on the reduction of AVF particularly in humans have not yet been evaluated. Therefore, we conducted a randomized, double-blind, placebo-controlled trial to evaluate the effects of tamarind seed husk extract (TSHE) on the reduction of AVF in individuals with mild obesity. We hypothesized that a 12-week TSHE intake would reduce AVF compared with placebo.

2. Materials and methods

2.1. Nutritional composition and polyphenol content of TSHE

The TSHE used in the present study was a powdered extract prepared from tamarind seed husk by extraction with food-grade aqueous ethanol (the exact extraction parameters are proprietary) at a food processing facility of Pharma Foods International (Kyoto, Japan). The nutritional composition of TSHE—including moisture, crude protein, crude fat, ash, and crude carbohydrate—was analyzed by the Japan Food Research Laboratories (Tokyo, Japan). The composition of TSHE and of the test food is given in Table 1.

2.2. Polyphenol analysis of TSHE and the test food

To analyze the polymerized procyanidins that comprise the principal constituents of TSHE, thiolytic degradation of polymerized procyanidins in TSHE was performed prior to high-performance liquid chromatography (HPLC) analysis. Thiolytic degradation of authentic procyanidin B2 (Tokyo Chemical Industry, Tokyo, Japan) was also performed. Ethanol (analytical grade or higher), hydrochloric acid (35.0–37.0%, analytical grade or higher), and

2-mercaptoethanol (molecular biology grade) were purchased from FUJIFILM Wako Pure Chemical (Osaka, Japan). For sample preparation, five TSHE capsules and five placebo capsules were opened, and 400 mg of the collected powder from each group was dissolved in 20 mL of water. Separately, 200 mg of TSHE bulk powder was dissolved in 20 mL of water to serve as the raw material standard. Reference standard solutions of procyanidin B2 and epicatechin were prepared in water at approximately 1 mg/mL. The thiolysis reagent was prepared by mixing 1,250 µL of ethanol, 1.5 µL of hydrochloric acid (~12.0 mol/L), and 75 µL of 2-mercaptoethanol per sample. Then, 1,325 µL of this reagent was mixed with 675 µL of each sample solution or procyanidin B2 and incubated at 70°C for 7 h under continuous stirring. After incubation, the mixtures were filtered through No. 2 filter paper (Toyo Roshi Kaisha, Tokyo, Japan) prior to analysis.

Compounds with low molecular weight were detected by ESI-MS using an LCMS-8040 mass spectrometer (Shimadzu) operating in negative ion and full scan modes. Mass spectra were acquired for a scan range up to mass-to-charge ratio (*m/z*) of 2,000. Chromatographic separation was performed using a Shimadzu Nexera LC-40 series UHPLC system (Shimadzu) equipped with a binary pump and a YMC-Triart C18 column (2.1 mm × 100 mm, 1.9 µm; YMC, Kyoto, Japan). The mobile phases consisted of 0.1% formic acid in water (mobile phase A) and 0.1% formic acid in acetonitrile/methanol (50:50, v/v) (mobile phase B). The gradient program was as follows: 5% B at 0 min, followed by a linear gradient to 40% B over 30 min, an immediate step to 95% B (held until 35 min), and an immediate return to 5% B for 5 min of re-equilibration (total run time: 40 min). The flow rate was maintained at 0.2 mL/min, the column temperature was set to 60°C, and the injection volume was 10 µL. UV detection was also performed at a wavelength of 280 nm.

2.3. Test food

The test foods consisted of active capsules containing TSHE and placebo capsules without TSHE. The active capsules were formulated to provide a daily dose of 200 mg of TSHE (two capsules taken once daily). The detailed composition per daily dose (two capsules) is shown in Table 1. All test foods were supplied by Pharma Foods International and stored at room temperature in the dark. To ensure proper blinding, the test foods were indistinguishable in appearance, shape, color, odor, and taste.

2.4. Ethics statement

The trial protocol was approved by the Institutional Review Board of Takara Clinic, Medical Corporation Seishinkai (Tokyo, Japan; approval No. 2502-02351-0124-0D-TC, approved on 13 February 2025). The trial was conducted in strict accordance with the Declaration of Helsinki (2024) and the Ethical Guidelines for Medical and Health Research Involving Human Subjects.

This trial is reported in accordance with the CONSORT 2025 statement. All participants received detailed information about the trial both orally and in writing, and written informed consent was obtained prior to trial initiation. The trial was registered in the University Hospital Medical Information Network Clinical Trials Registry (UMIN-CTR: UMIN000057223, registered on 6 March 2025). The full trial protocol and statistical analysis plan are available from the corresponding author on reasonable request. Informed consent was obtained from all subjects involved in the study.

2.5. Participants

A total of 316 participants provided informed consent and underwent screening. Based on a previous study (Akazome et al., 2010), a sample size of approximately 50 participants per group (100 total for the final analysis) was determined to provide sufficient statistical power. To accommodate potential dropouts, 112 eligible participants were initially enrolled as the intention-to-treat (ITT) population. Participants were Japanese adult men and women with BMI ranging from 25 to less than 30 kg/m^2 at screening, whose health status was checked by a physician at enrollment. Eligible participants were enrolled in descending order of their abdominal visceral fat area (AVFA) at screening until the target sample size was reached; the minimum AVFA among the enrolled participants was 76.5 cm^2. Participants and members of the public were not involved in the design, conduct, or reporting of this trial.

Individuals meeting any of the following criteria were excluded from the trial:

- History of malignant tumors, severe cardiovascular diseases, presence of pacemakers, or ongoing treatment for chronic diseases (e.g., diabetes, dyslipidemia, hypertension, liver or kidney disease);
- Current use of medications, dietary supplements, or functional foods (e.g., FOSHU, FFC);
- Active weight-loss attempts, extreme dietary restrictions, intensive or habitual exercise (≥3 times/week), heavy alcohol consumption (≥60 g/day), or irregular lifestyle patterns;
- Pregnancy, breastfeeding, or planning to become pregnant;
- Participation in another clinical trial within 28 days prior to consent, or planned participation;
- Any other reason deemed unsuitable by the principal investigator.

2.6. Trial design

This randomized, double-blind, placebo-controlled trial was managed by Orthomedico (Tokyo, Japan), maintaining strict blinding for both investigators and participants throughout the trial period. Eligible participants were randomly assigned (1:1) to either the test food or placebo group using computer-generated block randomization. An independent allocation manager prepared the allocation table and sealed the emergency keys. These keys were kept strictly concealed until data fixation and opened only after confirming the blinding.

The trial consisted of a 12-week intervention and a 4-week post-observation period. Participants visited the site at screening, weeks 4, 8, and 12, and the end of the observation period. They took two capsules daily immediately before lunch, or before dinner if missed. At each visit, investigators assessed their health status through interviews. Throughout the trial, participants logged their daily test food intake, physical activity, alcohol consumption, step counts, and menstrual status (females only). They also recorded their dietary intake for three days before each visit. Participants maintained their usual lifestyle and ≥80% compliance, avoiding other functional foods and changes in diet or exercise. Prior to each examination, they abstained from alcohol and intense exercise for one day, and fasted for at least 10 hours before blood sampling. Discontinuation criteria included withdrawal of consent, poor compliance, significant protocol deviations, serious adverse events, or investigator discretion. Efficacy was evaluated at screening (baseline) and at weeks 4, 8, and 12 after the start of the intervention. The primary endpoint was the AVFA at

week 12 of the intervention. As this was a Phase II exploratory clinical trial, secondary endpoints were also assessed to provide supportive evidence of efficacy. These included the change from baseline and percent change in AVFA at week 12, as well as the measured values, changes from baseline, and percent changes at weeks 4 and 8. Additional secondary endpoints assessed at weeks 4, 8, and 12 included abdominal total fat area (TFA), subcutaneous fat area (SFA), body weight, BMI, body fat percentage, waist and hip circumferences, waist-to-hip ratio, fat mass, fat-free mass, and skeletal muscle mass. Blood parameters, including total cholesterol, HDL cholesterol, LDL cholesterol, triglycerides, glucose, and hemoglobin A1c, were also evaluated as measured values, changes from baseline, and percent changes.

Safety was evaluated at screening, weeks 4, 8, and 12, and the end of the post-observation period. Safety endpoints included the incidence of adverse events and deviations in standard hematological, biochemical, and urinalysis parameters. Investigators assessed anthropometric and vital parameters using standard medical equipment, and calculated BMI and waist-to-hip ratios. Computed tomography (CT) at the umbilical level quantified abdominal total, visceral (AVFA), and subcutaneous (SFA) fat areas. Changes and percent changes were calculated relative to baseline values. For laboratory analyses, venous blood was collected, and serum was separated and stored at −80°C. Standard automated analyzers processed all blood and urine samples.

2.7. Statistical analysis

All randomized participants comprised the ITT population. The full analysis set (FAS) was defined as the ITT population excluding participants who did not receive the assigned intervention, did not meet eligibility criteria, or lacked post-randomization data. The per-protocol set (PPS), primarily used for efficacy analyses, was defined by further excluding participants with less than 80% trial product compliance or major protocol deviations. The safety analysis population (SAF) included all ITT participants who received at least one dose. Baseline characteristics were summarized using the ITT population.

Primary and secondary endpoints were analyzed using linear mixed-effects models, with fixed effects for group, time point, and group × time point interaction, and covariates for baseline value and baseline × time point interaction. Random effects accounted for inter-subject variability and the model parameters were estimated via the restricted maximum likelihood (REML) method. Treatment effects were estimated as differences in estimated marginal means (EMMs) between groups, with standard errors and 95% confidence intervals. Missing values were not imputed, nor were participants with missing data entirely excluded from the analyses; instead, missingness was handled intrinsically by the linear mixed-effects models. There were no missing values in the PPS. For the SAF, the number of available data points at each time point is detailed in the respective tables.

An exploratory post hoc subgroup analysis was conducted for participants with a baseline visceral-to-subcutaneous fat ratio (VSR) ≥ 0.4. This specific cut-off was selected because a VSR of 0.4 is the established threshold for visceral-type obesity (Matsuzawa et al., 1992), above which obesity-related risk factors increase (Hiuge-Shimizu et al., 2012). To assess whether baseline imbalances between the groups in this subgroup affected the results, a post hoc sensitivity analysis of AVFA at week 12 was performed using the same linear mixed-effects modeling approach restricted to week 12, with fixed effects for group and sex and covariates for baseline AVFA, baseline body fat percentage, and baseline fat-free mass. Secondary safety endpoints, such as urinalysis and blood tests, were analyzed for all SAF participants, and the proportions of measurements outside reference ranges after the intervention were compared between groups. All statistical tests were two-sided with a significance level of 0.05. Analyses were performed using SPSS Statistics (version 23.0 or higher; IBM, Armonk, NY, USA).

3. Results

3.1. Types of polyphenols in TSHE

The thiolysates of TSHE and the contents of the TSHE capsules showed almost identical HPLC elution patterns (Figure 1). To further confirm the identity of the separated peaks, liquid chromatography-mass spectrometry (LC-MS) analysis was performed. Peak a was identified as the epicatechin monomer, exhibiting a retention time identical to that of the authentic standard, which was corroborated by the detection of *m/z* at 289 and 325. Peaks c and d coincided with the peaks observed in the thiolysate of the authentic procyanidin B2 standard. For these peaks, *m/z* values of 287 and 401 were detected. The *m/z* 401 signal is consistent with a chloride adduct (mass 35) of the epicatechin-mercaptoethanol conjugate (epicatechin mass 289 and mercaptoethanol mass 78). Furthermore, the *m/z* 287 signal corresponds to the neutral loss of a mercaptoethanol moiety (*m/z* 78) from the epicatechin-mercaptoethanol conjugate (*m/z* 365). Therefore, both signals are considered to be valid peaks representing the thiolysis products of procyanidin B2. Peaks b and e were distinct from the peaks observed in the thiolysate of authentic procyanidin B2; no *m/z* signals corresponding to known polyphenols were detected for these peaks, and they remained unidentified. These results indicate that TSHE comprises epicatechin, procyanidin B2, and highly polymerized procyanidins (epicatechin polymers), and that these components remained largely unchanged during the manufacturing process of the test food. The mass spectra are shown in Figure S1. In thiolysis of a procyanidin dimer, the terminal unit gives a free monomer and the extension unit its thioether adduct, corresponding to a theoretical HPLC peak area ratio of 1:1. The observed ratio in TSHE was 1:15. Peak b was not assigned, but counting it as an additional monomer still gives a ratio corresponding to more than 10 monomeric units. Area ratios were not converted to an exact degree of polymerization because the molar responses of epicatechin and its thioether adduct at 280 nm differ.

3.2. Participant demographics

The trial was conducted between 27 February and 14 December 2025. As shown in Figure 2, of the 316 individuals screened, 112 met the eligibility criteria and were subsequently randomized to either the TSHE group (n = 56) or the placebo group (n = 56). All 112 participants initiated the intervention and were included in the SAF, which was therefore identical to the ITT population. During follow-up, two placebo participants missed assessments (at weeks 8 and 12). Excluding 12 participants (6 per group) with insufficient compliance (< 80%), 100 participants (50 per group) were included in the PPS for efficacy analyses. Baseline characteristics of the PPS are summarized in Table 2.

3.3. Effects of TSHE on AVFA and related outcomes

Anthropometric and vital measurements showed no clinically sig-

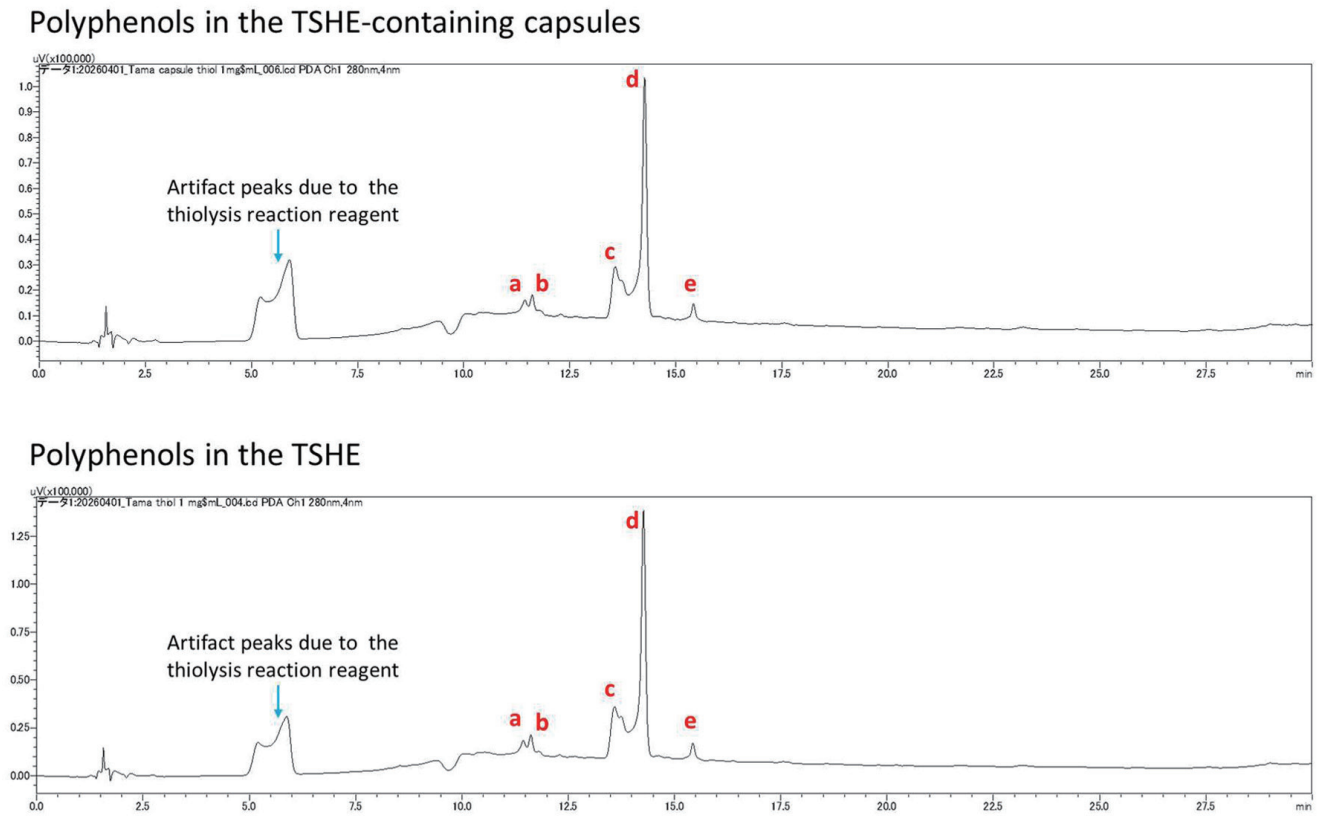


Figure 1. Comparison of HPLC elution patterns of polyphenols in the TSHE-containing capsules and in the TSHE. Upper panel: HPLC chromatogram of polyphenols extracted from the TSHE-containing capsules; lower panel: HPLC chromatogram of polyphenols from TSHE. Peak a was identified as the epicatechin monomer; peaks c and d were identified as the epicatechin-thiol adduct formed via the thiolysis of procyanidin B2; peaks b and e were unidentified. TSHE, tamarind seed husk extract.

nificant changes (Table S1). The primary and secondary efficacy outcomes are presented in Table 3. Data are expressed as EMMs with 95% confidence intervals (CIs), and p-values reflect between-group differences estimated by the linear mixed-effects model. AVFA at week 12 (primary outcome) was a trend toward lower in the TSHE group compared to the placebo group (115.9 cm^2 [95% CI: 110.0, 121.7] vs. 123.3 cm^2 [95% CI: 117.5, 129.2]), while the difference did not reach statistical significance ($p = 0.077$; Figure 3). At week 4, AVFA was significantly lower in the TSHE group than in the placebo group (114.3 cm^2 [95% CI: 108.4, 120.1] vs. 122.6 cm^2 [95% CI: 116.8, 128.5], $p = 0.048$). There was a consistent trend toward a larger percent reduction in AVFA in the TSHE group compared to the placebo group at both week 4 (−5.3% [95% CI: −10.6, 0.0] vs. 1.3% [95% CI: −4.0, 6.7], $p = 0.083$) and week 12 (−4.3% [95% CI: −9.6, 1.0] vs. 2.4% [95% CI: −2.9, 7.7], $p = 0.080$).

No significant differences were observed between groups for SFA at any time point. For TFA, the percent reduction from baseline was significantly larger in the TSHE group than in the placebo group at week 8 (−3.1% [95% CI: −6.1, −0.1] vs. 1.2% [95% CI: −1.7, 4.2], $p = 0.043$) and week 12 (−2.9% [95% CI: −6.0, 0.3] vs. 1.7% [95% CI: −1.5, 4.9], $p = 0.048$). Furthermore, the measured TFA values showed a consistent trend toward being lower in the TSHE group at week 8 (355.7 cm^2 [95% CI: 344.7, 366.8] vs. 369.7 cm^2 [95% CI: 358.7, 380.8], $p = 0.078$) and week 12 (355.9 cm^2 [95% CI: 344.3, 367.5] vs. 370.5 cm^2 [95% CI: 359.0, 382.1], $p = 0.079$).

As detailed in Table S2, among the blood parameters, fasting glucose was significantly lower in the TSHE group than in the placebo group at week 4 (88.2 mg/dL [95% CI: 85.6, 90.8] vs. 92.7 mg/dL [95% CI: 90.1, 95.3], $p = 0.017$). No significant differences were observed between groups in other outcomes.

3.4. Safety outcomes

No adverse events occurred during the trial. The incidence of laboratory values shifting outside normal reference ranges was low and generally comparable between groups (Table S3). Notably, significantly fewer participants in the TSHE group exhibited abnormal shifts for serum creatinine at the post-observation period (1.8% vs. 13.0%, $p = 0.024$) and potassium at week 4 (3.6% vs. 14.3%, $p = 0.047$) compared to the placebo group. Overall, these findings indicate that TSHE is safe for food.

3.5. Exploratory analysis in participants with a high visceral-to-subcutaneous fat ratio (VSR ≥ 0.4)

Overall, AVFA in the TSHE group showed a consistent trend toward a greater reduction compared to the placebo group, although the difference at week 12 did not reach statistical significance. To further investigate these findings, exploratory analyses were conducted in participants with a VSR ≥ 0.4, including 35 participants from the TSHE group and 30 from the placebo group. In the TSHE

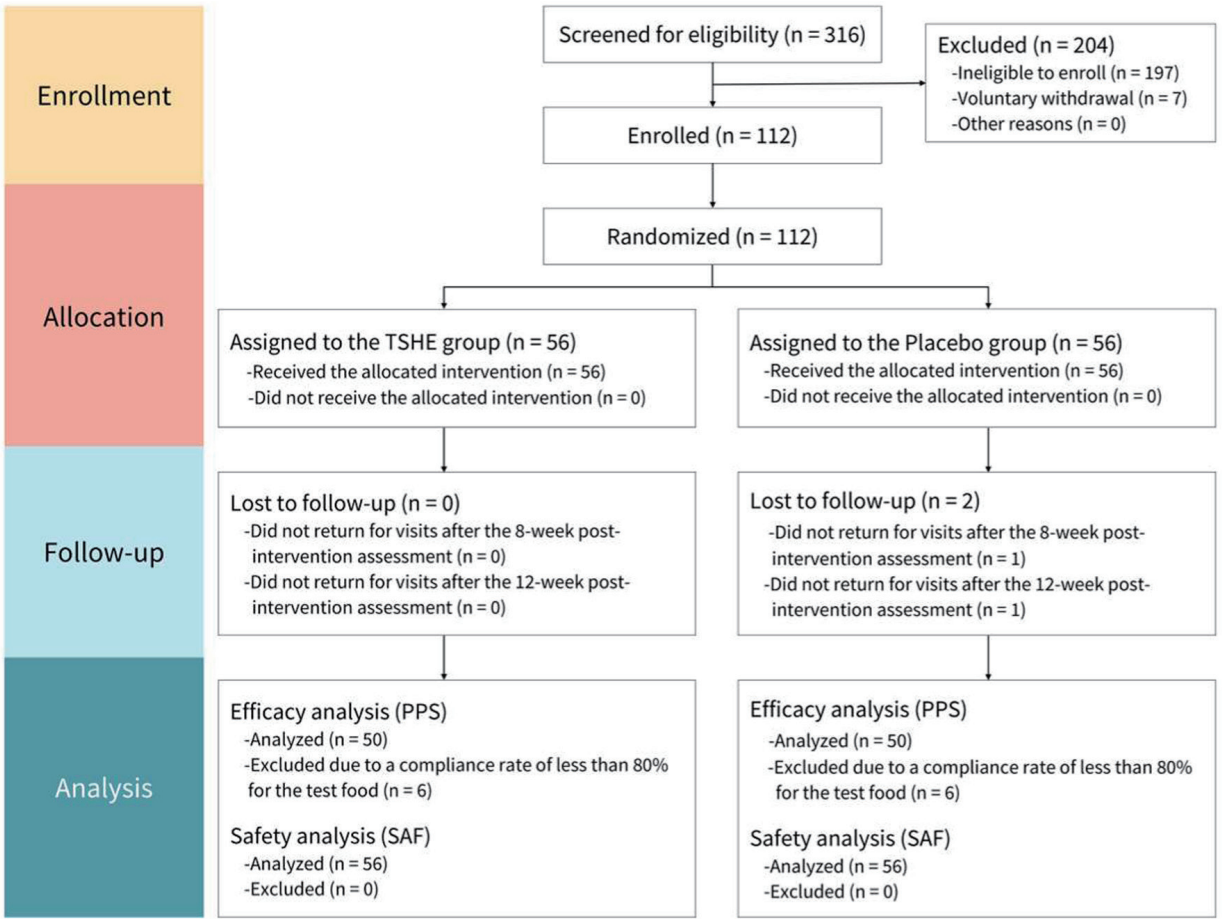


Figure 2. Flow diagram of the study design and procedures. SAF, safety analysis population; PPS, per-protocol set; TSHE, tamarind seed husk extract.

group, the mean age was 52.3 ± 8.8 years, with 23 males (65.7%) and 12 females (34.3%). In the placebo group, the mean age was 52.8 ± 9.9 years, with 28 males (93.3%) and 2 females (6.7%). At baseline, body fat percentage, fat-free mass, and muscle mass differed significantly between groups (body fat percentage: 30.6 ± 7.0% [TSHE group] vs. 27.4 ± 5.2% [placebo group], p = 0.042; fat-free mass: 51.5 ± 9.7 kg vs. 56.5 ± 6.4 kg, p = 0.018; muscle mass: 48.8 ± 9.3 kg vs. 53.5 ± 6.1 kg, p = 0.016).

Table 2. Baseline characteristics of the intention-to-treat and per-protocol sets

	ITT		PPS	
	TSHE (n = 56)	**Placebo (n = 56)**	**TSHE (n = 50)**	**Placebo (n = 50)**
Male, n (%)	30 (53.6%)	37 (66.1%)	28 (56.0%)	33 (66.0%)
Female, n (%)	26 (46.4%)	19 (33.9%)	22 (44.0%)	17 (34.0%)
Age (years)	51.0 ± 10.3 [min 21, max 70]	51.9 ± 9.7 [min 32, max 71]	50.9 ± 10.2 [min 21, max 70]	52.3 ± 9.7 [min 32, max 71]
Body weight (kg)	73.5 ± 9.7	74.9 ± 8.5	73.4 ± 9.9	74.2 ± 8.3
Height (cm)	164.1 ± 10.1	165.7 ± 8.0	164.2 ± 9.9	165.5 ± 8.1
BMI (kg/m^2)	27.2 ± 1.4	27.2 ± 1.4	27.1 ± 1.3	27.0 ± 1.3
Systolic blood pressure (mmHg)	125.8 ± 16.0	125.9 ± 15.4	125.2 ± 15.8	126.1 ± 15.2
Diastolic blood pressure (mmHg)	82.9 ± 12.1	83.2 ± 11.7	82.4 ± 12.1	82.9 ± 11.5
AVFA (cm^2)	122.4 ± 31.9	119.9 ± 37.1	123.9 ± 32.6	119.7 ± 37.5

Data are presented as mean ± SD unless otherwise indicated. AVFA, abdominal visceral fat area; BMI, body mass index; ITT, intention-to-treat population; PPS, per-protocol set; SD, standard deviation; TSHE, tamarind seed husk extract.

Table 3. Primary and secondary efficacy outcomes (n = 50, per group).

Outcome	Statistics	Week 0		Week 4		Week 8		Week 12	
		TSHE	Placebo	TSHE	Placebo	TSHE	Placebo	TSHE	Placebo
AVFA (cm^2)	Mean ± SD	123.9 ± 32.6	119.7 ± 37.5	116.1 ± 31.8* (p = 0.048)	120.8 ± 42.1	117.3 ± 36.2	119.9 ± 41.9	117.7 ± 33.9 (p = 0.077)	121.5 ± 39.5
	EMM	–	–	114.3	122.6	115.3	122.0	115.9	123.3
	95% CI	–	–	[108.4, 120.1]	[116.8, 128.5]	[109.6, 121.0]	[116.3, 127.6]	[110.0, 121.7]	[117.5, 129.2]
Δ% AVFA (%)	Mean ± SD	–	–	−5.5 ± 13.6	1.5 ± 23.1	−5.4 ± 14.8	0.5 ± 20.2	−4.5 ± 15.3	2.6 ± 22.2
	EMM	–	–	−5.3	1.3	−5.3	0.4	−4.3	2.4
	95% CI	–	–	[−10.6, 0.0]	[−4.0, 6.7]	[−10.3, −0.3]	[−4.6, 5.4]	[−9.6, 1.0]	[−2.9, 7.7]
SFA (cm^2)	Mean ± SD	247.4 ± 64.5	241.5 ± 66.5	244.6 ± 72.8	241.0 ± 65.2	243.4 ± 73.3	244.8 ± 67.4	242.9 ± 70.4	244.4 ± 66.7
	EMM	–	–	241.7	243.9	240.5	247.7	240.1	247.2
	95% CI	–	–	[234.4, 249.1]	[236.6, 251.2]	[232.6, 248.4]	[239.8, 255.5]	[232.1, 248.0]	[239.2, 255.1]
Δ% SFA (%)	Mean ± SD	–	–	−1.3 ± 12.1	0.6 ± 9.2	−1.6 ± 13.4	1.8 ± 8.4	−1.8 ± 12.6	2.0 ± 10.7
	EMM	–	–	−1.2	0.6	−1.5	1.7	−1.7	1.9
	95% CI	–	–	[−4.2, 1.8]	[−2.5, 3.6]	[−4.7, 1.6]	[−1.4, 4.9]	[−5.0, 1.5]	[−1.4, 5.2]
TFA (cm^2)	Mean ± SD	371.3 ± 66.7	361.2 ± 71.1	360.8 ± 78.9	361.8 ± 75.1	360.8 ± 81.9	364.7 ± 75.9	360.6 ± 77.2	365.9 ± 74.1
	EMM	–	–	355.8	366.8	355.7	369.7	355.9	370.5
	95% CI	–	–	[345.5, 366.1]	[356.5, 377.1]	[344.7, 366.8]	[358.7, 380.8]	[344.3, 367.5]	[359.0, 382.1]
Δ% TFA (%)	Mean ± SD	–	–	−3.1 ± 10.0	0.4 ± 9.7	−3.1 ± 11.1* (p = 0.043)	1.2 ± 9.9	−2.9 ± 11.4* (p = 0.048)	1.8 ± 11.3
	EMM	–	–	−3.1	0.4	−3.1	1.2	−2.9	1.7
	95% CI	–	–	[−5.9, −0.3]	[−2.3, 3.2]	[−6.1, −0.1]	[−1.7, 4.2]	[−6.0, 0.3]	[−1.5, 4.9]
VSR	Mean ± SD	0.5 ± 0.2	0.5 ± 0.3	0.5 ± 0.2	0.5 ± 0.3	0.5 ± 0.2	0.5 ± 0.3	0.5 ± 0.2	0.5 ± 0.3
	EMM	–	–	0.5	0.5	0.5	0.5	0.5	0.5
	95% CI	–	–	[0.5, 0.5]	[0.5, 0.6]	[0.5, 0.6]	[0.5, 0.6]	[0.5, 0.6]	[0.5, 0.6]

Data are presented as mean ± SD, or as EMM with 95% CI. Between-group differences were estimated by a linear mixed-effects model; * $p < 0.05$ versus placebo. Δ%, percent change from baseline; AVFA, abdominal visceral fat area; CI, confidence interval; EMM, estimated marginal mean; SD, standard deviation; SFA, subcutaneous fat area; TFA, total fat area; VSR, visceral-to-subcutaneous fat ratio.

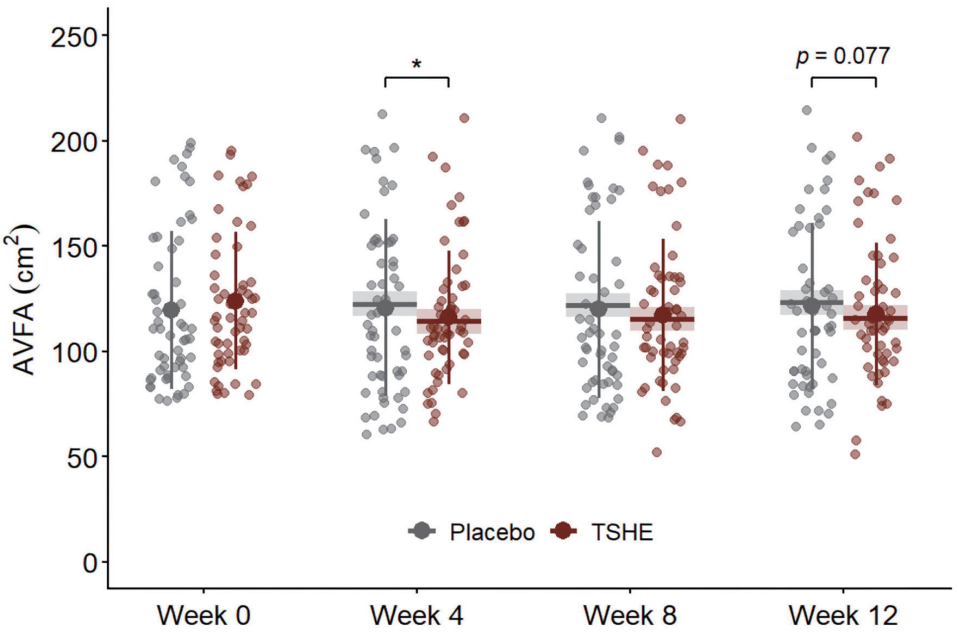


Figure 3. Abdominal visceral fat area (AVFA) at 12 weeks post-intervention (n = 50 per group). Differences between the TSHE and placebo groups were analyzed using a linear mixed-effects model with fixed effects for treatment group, time point, and the group × time point interaction, adjusting for baseline AVFA and the baseline × time point interaction. Subject-specific random effects were included to account for inter-individual variability. Individual participant values are shown as dots. Large, solid dots with vertical bars represent the mean ± SD, while EMMs and their 95% CIs are indicated by the horizontal line and shaded box, respectively. * p < 0.05 versus placebo.

As shown in Table 4, the AVFA values were significantly lower in the TSHE group than in the placebo group at week 4 (123.6 cm^2 [95% CI: 117.2, 130.0] vs. 136.2 cm^2 [95% CI: 129.2, 143.1], p = 0.010) and week 12 (127.5 cm^2 [95% CI: 121.3, 133.7] vs. 138.1 cm^2 [95% CI: 131.4, 144.8], p = 0.024). Significant between-group differences were also noted in the percent change in AVFA (−9.0% [95% CI: −14.2, −3.9] vs. 1.0% [95% CI: −4.5, 6.6], p = 0.009 at week 4; −7.2% [95% CI: −12.1, −2.3] vs. 0.5% [95% CI: −4.8, 5.8], p = 0.036 at week 8; −5.8% [95% CI: −10.6, −1.1] vs. 3.4% [95% CI: −1.8, 8.5], p = 0.011 at week 12). A similar pattern was observed for TFA. The measured values were significantly lower in the TSHE group than in the placebo group at week 4 (333.4 cm^2 [95% CI: 321.9, 344.8] vs. 351.0 cm^2 [95% CI: 338.7, 363.3], p = 0.040) and week 12 (335.7 cm^2 [95% CI: 323.5, 347.8] vs. 356.1 cm^2 [95% CI: 342.9, 369.2], p = 0.027). Significant differences were also observed for the percent change (−4.7% [95% CI: −7.9, −1.5] vs. 1.0% [95% CI: −2.5, 4.4], p = 0.018 at week 4; −3.8% [95% CI: −7.3, −0.4] vs. 2.0% [95% CI: −1.8, 5.7], p = 0.028 at week 8; −4.0% [95% CI: −7.4, −0.5] vs. 2.5% [95% CI: −1.2, 6.3], p = 0.014 at week 12). Moreover, at week 12, the TSHE group showed lower body weight (74.8 kg [95% CI: 74.1, 75.4] vs. 76.1 kg [95% CI: 75.4, 76.8], p = 0.010), BMI (26.8 kg/m^2 [95% CI: 26.6, 27.1] vs. 27.2 kg/m^2 [95% CI: 27.0, 27.5], p = 0.018), body fat percentage (28.6% [95% CI: 28.1, 29.2] vs. 29.5% [95% CI: 28.9, 30.1], p = 0.042), waist circumference (93.4 cm [95% CI: 92.3, 94.5] vs. 95.4 cm [95% CI: 94.2, 96.6], p = 0.020), hip circumference (98.4 cm [95% CI: 97.8, 99.1] vs. 99.7 cm [95% CI: 99.0, 100.4], p = 0.014), and fat mass (21.3 kg [95% CI: 20.7, 21.8] vs. 22.3 kg [95% CI: 21.7, 22.8], p = 0.013) than the placebo group. Although body fat percentage was higher in the TSHE group at baseline, the baseline-adjusted value at week 12 was significantly lower than in the placebo group. No significant differences were observed in SFA or other measured parameters, including blood variables (Table S4). A post hoc sensitivity analysis was performed with group and sex included as fixed effects and baseline AVFA, baseline body fat percentage, and baseline fat-free mass as covariates. In this analysis, AVFA at week 12 was lower in the TSHE group than in the placebo group (125.6 cm^2 [95% CI: 115.9, 135.4] vs. 136.3 cm^2 [95% CI: 124.9, 147.8]; p = 0.036; Table S5).

4. Discussion

Tamarind seed husk has attracted attention not only as an abundant by-product of tamarind seed gum production but also for its biological activity (Crispín-Isidro et al., 2019; Nasir et al., 2026; Sasidharan et al., 2014; Souza et al., 2025; Wandee et al., 2022). The present study investigated the potential of TSHE, an extract derived from tamarind seed husk, to reduce AVF accumulation. In this randomized, double-blind, placebo-controlled trial, the effects of TSHE on abdominal fat accumulation and related metabolic parameters were evaluated in Japanese adults with mild obesity (BMI of 25 to less than 30 kg/m^2).

For the primary outcome, the TSHE group showed lower AVFA at week 12 than the placebo group, although the difference was not statistically significant (Figure 3). However, at week 4, the TSHE group showed a significantly lower AVFA and a significantly greater reduction from baseline compared to the placebo group. The same direction of change was observed consistently throughout the intervention period. These results suggest that TSHE reduced AVFA in the early weeks and that this suppressive effect was sustained throughout the trial.

The Japan Society for the Study of Obesity guidelines regard abdominal visceral and subcutaneous fat as a key indicator for assessing health risks, with AVF relating to metabolic syndrome and subcutaneous fat and body weight relating to musculoskeletal disorders

Table 4. Exploratory analysis of efficacy outcomes in participants with a visceral-to-subcutaneous fat ratio (VSR) ≥ 0.4

Outcome	Statistics	Week 0		Week 4		Week 8		Week 12	
		TSHE (n = 35)	Placebo (n = 30)	TSHE (n = 35)	Placebo (n = 30)	TSHE (n = 35)	Placebo (n = 30)	TSHE (n = 35)	Placebo (n = 30)
AVFA (cm^2)	Mean ± SD	134.9 ± 32.1	136.8 ± 38.5	122.8 ± 34.6* (p = 0.010)	137.1 ± 40.3	125.9 ± 39.0	137.2 ± 40.3	126.7 ± 35.4* (p = 0.024)	139.0 ± 33.8
	EMM	–	–	123.6	136.2	126.8	136.1	127.5	138.1
	95% CI	–	–	[117.2, 130.0]	[129.2, 143.1]	[120.3, 133.3]	[129.2, 143.1]	[121.3, 133.7]	[131.4, 144.8]
Δ% AVFA (%)	Mean ± SD	–	–	−9.0 ± 12.1* (p = 0.009)	1.0 ± 18.0	−7.2 ± 15.3* (p = 0.036)	0.5 ± 13.1	−5.7 ± 15.6* (p = 0.011)	3.3 ± 13.0
	EMM	–	–	−9.0	1.0	−7.2	0.5	−5.8	3.4
	95% CI	–	–	[−14.2, −3.9]	[−4.5, 6.6]	[−12.1, −2.3]	[−4.8, 5.8]	[−10.6, −1.1]	[−1.8, 8.5]
SFA (cm^2)	Mean ± SD	220.9 ± 51.2	205.7 ± 55.6	216.3 ± 58.9	207.2 ± 51.6	216.7 ± 61.1	211.1 ± 56.7	214.6 ± 57.4	210.5 ± 54.5
	EMM	–	–	209.8	214.8	209.8	219.0	208.1	218.1
	95% CI	–	–	[200.7, 218.9]	[205.0, 224.6]	[200.0, 219.7]	[208.4, 229.7]	[199.0, 217.1]	[208.3, 227.9]
Δ% SFA (%)	Mean ± SD	–	–	−2.0 ± 13.6	1.9 ± 9.6	−1.7 ± 15.0	3.0 ± 7.8	−2.7 ± 13.4	3.2 ± 10.5
	EMM	–	–	−1.7	1.5	−1.5	2.8	−2.5	2.9
	95% CI	–	–	[−5.7, 2.3]	[−2.8, 5.9]	[−5.7, 2.7]	[−1.7, 7.3]	[−6.6, 1.6]	[−1.5, 7.3]
TFA (cm^2)	Mean ± SD	355.8 ± 66.1	342.5 ± 78.2	339.1 ± 74.6* (p = 0.040)	344.3 ± 75.2	342.6 ± 80.1	348.3 ± 80.0	341.3 ± 75.6* (p = 0.027)	349.5 ± 74.8
	EMM	–	–	333.4	351.0	336.5	355.3	335.7	356.1
	95% CI	–	–	[321.9, 344.8]	[338.7, 363.3]	[323.8, 349.3]	[341.6, 369.1]	[323.5, 347.8]	[342.9, 369.2]
Δ% TFA (%)	Mean ± SD	–	–	−4.8 ± 10.4* (p = 0.018)	1.0 ± 7.9	−3.9 ± 12.0* (p = 0.028)	2.0 ± 7.6	−4.1 ± 11.6* (p = 0.014)	2.6 ± 8.4
	EMM	–	–	−4.7	1.0	−3.8	2.0	−4.0	2.5
	95% CI	–	–	[−7.9, −1.5]	[−2.5, 4.4]	[−7.3, −0.4]	[−1.8, 5.7]	[−7.4, −0.5]	[−1.2, 6.3]
VSR	Mean ± SD	0.6 ± 0.2	0.7 ± 0.2	0.6 ± 0.2	0.7 ± 0.2	0.6 ± 0.2	0.7 ± 0.2	0.6 ± 0.2	0.7 ± 0.2
	EMM	–	–	0.6	0.7	0.6	0.7	0.6	0.7
	95% CI	–	–	[0.6, 0.7]	[0.6, 0.7]	[0.6, 0.7]	[0.6, 0.7]	[0.6, 0.7]	[0.6, 0.7]

Exploratory post hoc analysis of participants with a baseline VSR ≥ 0.4 (TSHE, n = 35; placebo, n = 30). Data are presented as mean ± SD, or as EMM with 95% CI. Between-group differences were estimated by a linear mixed-effects model; * $p < 0.05$ versus placebo. Δ%, percent change from baseline; AVFA, abdominal visceral fat area; CI, confidence interval; EMM, estimated marginal mean; SD, standard deviation; SFA, subcutaneous fat area; TFA, total fat area; VSR, visceral-to-subcutaneous fat ratio.

(Japan Society for the Study of Obesity, 2022). CT-based measurement allows visceral and subcutaneous fat areas to be quantified separately, and is therefore well suited to evaluating these distinct risks.

AVFA in the TSHE group showed a consistent trend toward a greater reduction compared to the placebo group. An exploratory subgroup analysis based on a baseline VSR ≥ 0.4 was conducted. A VSR of 0.4 is the established threshold for visceral-type obesity (Matsuzawa et al., 1992), above which obesity-related risk factors increase (Hiuge-Shimizu et al., 2012). This subgroup showed a significant reduction in AVFA at week 12. Following established guidelines (Burke et al., 2015), this subgroup analysis should be interpreted with caution. These results support the consistency of AVF reduction with TSHE. In addition, fasting glucose was significantly lower in the TSHE group in the per-protocol set at week 4. Fasting glucose is associated with AVF accumulation (Kwon and Pessin, 2013; Nawrocki, 2004), so this change may reflect the reduction in AVF. On the other hand, no significant differences were found in serum lipids, including triglycerides and cholesterol. This may be because the participants were generally healthy, with baseline lipid levels within the normal range.

In this study, TSHE reduced AVFA in participants with a VSR ≥ 0.4. However, this study did not provide direct evidence for the underlying mechanism. The TSHE used in this study contains mainly epicatechin polymers, a class of polyphenols (Figure 1). One possible mechanism is the inhibition of digestive lipase activity. Epicatechin polymers were reported to inhibit lipase and reduce fat absorption (Oliveira et al., 2015). Tamarind seed coat extracts have also been reported to inhibit lipase and reduce fat absorption *in vitro* and *in vivo* (Sasidharan et al., 2014; Souza et al., 2025). The lipase inhibitor orlistat likewise reduces AVFA in clinical settings (Shirai et al., 2019; Smith et al., 2011). These facts suggest that lipase inhibition by epicatechin and its polymers may be one of the mechanisms of the AVF reduction in this study. AVF is more metabolically active than subcutaneous fat and responds more sensitively to intervention in the short term (Freedland, 2004; Wajchenberg, 2000). Therefore, even a modest reduction in fat absorption could affect AVF at an early stage. This may explain why AVFA decreased as early as week 4.

Procyanidin B2 and its polymers have been reported to modulate the gut microbiota and show anti-obesity effects in animals (Xing et al., 2019; Yu et al., 2022). Therefore, it is possible that TSHE suppressed the accumulation of AVF by modulating the gut microbiota.

Another possible mechanism involves adipokine balance, since AVF accumulation is often associated with elevated leptin and insulin (Décordé et al., 2009; Sasidharan et al., 2014). In animal models of diet-induced obesity, both a tamarind seed coat extract and grape seed procyanidins lowered insulin and leptin, raised adiponectin, and improved insulin signaling (Décordé et al., 2009; Sasidharan et al., 2014; Yogalakshmi et al., 2014).

Several limitations of this study should be acknowledged. First, the mechanism of action, including the inhibition of fat absorption, was not directly examined in this study. Second, gut-related endpoints, such as the gut microbiota, generation of short-chain fatty acids, and metabolic hormones, were not assessed. Third, diet and physical activity were monitored but not strictly controlled; however, dietary energy intake remained stable in both groups throughout the study (data not shown), suggesting that the reduction in AVF was not attributable to changes in energy intake from foods. Fourth, the participants were limited to Japanese adults with mild obesity, so the findings may not generalize to other populations. Fifth, the subgroup analysis was an exploratory post hoc analysis. Therefore, chance findings and multiple comparison effects cannot be completely excluded, requiring cautious interpretation. In the subgroup with a VSR ≥ 0.4, baseline body fat percentage, fat-free mass, and sex distribution were imbalanced between the groups. However, in the post hoc sensitivity analysis with sex as a fixed effect and baseline body fat percentage and fat-free mass as covariates in addition to baseline AVFA, AVFA at week 12 was lower in the TSHE group than in the placebo group (Table S5), indicating that these baseline imbalances did not account for the observed effect. To confirm the specific effects of TSHE, further well-designed stratified studies considering gender and visceral fat accumulation are warranted.

At the same time, this study population is clinically important. Asian populations accumulate more AVF and develop metabolic syndrome at lower BMI than Western populations (Li et al., 2023). While obesity is defined as a BMI of 30 kg/m^2 or higher in Western countries, several organizations recommend a lower cut-off of 25 kg/m^2 for Asians (Li et al., 2023; Zhu et al., 2021). Mild obesity (BMI of 25 to less than 30 kg/m^2) with a VSR ≥ 0.4 describes exactly this group. The present finding that TSHE reduced AVFA at a practical dose in this population is therefore particularly meaningful, and suggests that TSHE may be useful as a functional food ingredient for preventing metabolic syndrome with individuals with mild obesity and a VSR ≥ 0.4.

5. Scientific innovation and practical significance

Notably, this is the first study to show that TSHE reduces abdominal visceral fat in individuals with mild obesity and a VSR ≥ 0.4. While previous studies show that reducing visceral fat requires daily doses of 600 mg for apple polyphenols or 609.3 mg for green tea catechins (Akazome et al., 2010; Zhang et al., 2012), the present study showed that TSHE was effective at 200 mg/day. Achieving efficacy at this lower dose is highly beneficial for food application, as it limits undesirable changes to the taste and physical properties of the final products. The effect of TSHE also appeared early. AVFA was significantly lower in the TSHE group than in the placebo group at week 4, the first time point evaluated after baseline, and remained lower throughout the intervention period. In the subgroup with a VSR ≥ 0.4, the percent reduction in AVFA was significant at all three time points. In the studies described above, the first CT measurement was performed at week 8 or week 12. Nagao et al. (2001) measured every four weeks but compared the groups over the whole intake period rather than at each time point. A significant reduction at week 4 has therefore not been reported for these materials. For a food taken daily, an early effect is beneficial, as it supports continued intake.

6. Conclusion

In this randomized, double-blind, placebo-controlled trial, TSHE reduced AVFA in Japanese adult participants with mild obesity and a VSR ≥ 0.4. Although the reduction in AVFA at week 12 in the per-protocol set was not statistically significant, AVFA was consistently lower in the TSHE group, and the percent reduction in TFA was significant at weeks 8 and 12. The effects were clearer in participants with a VSR ≥ 0.4. These findings support TSHE as a functional food ingredient for reducing AVFA, especially in Asian populations with mild obesity. Further studies are needed to clarify its mechanisms.

Acknowledgments

During the preparation of this manuscript, the authors used Gemini

3.1 Pro for English language editing and reference formatting. The authors have reviewed and edited the output and take full responsibility for the content of this publication. This research was funded by Pharma Foods International Co., Ltd. and MP GOKYO FOOD & CHEMICAL Co., Ltd.

Conflict of interest

H.Y., Y.Y., X.L., K.S., S.S., and Y.K. are employees of Pharma Foods International Co., Ltd.; M.H., J.K., Y.S., and Y.T. are employees of MP GOKYO FOOD & CHEMICAL Co., Ltd. These companies funded the study and supplied the test products. Because the authors are employees of the funding companies, the funders were involved in the design of the study, the interpretation of data, and the writing of the manuscript. The clinical trial was conducted independently by Orthomedico Inc., a contract research organization. T.T. is affiliated with Takara Clinic (Medical Corporation Seishinkai), which served as the trial site at the request of Orthomedico Inc.

Author contributions

Conceptualization, H.Y.; methodology, H.Y. and Y.Y.; investigation, H.Y., Y.Y. and T.T.; formal analysis, H.Y.; resources, T.T.; project administration, H.Y.; visualization, X.L. and H.Y.; writing—original draft preparation, H.Y., K.S. and X.L.; writing—review and editing, all authors; supervision, K.S. and Y.K. All authors have read and agreed to the published version of the manuscript.

Supplementary material

Figure S1. Mass spectra of peaks a, c and d in the TSHE.

Table S1. Anthropometric measurements and vital signs (safety analysis population, n = 56 per group).

Table S2. Secondary efficacy outcomes (per-protocol set, n = 50 per group).

Table S3. Primary and secondary safety outcomes (safety analysis population).

Table S4. Exploratory analysis of secondary efficacy outcomes in participants with a visceral-to-subcutaneous fat ratio (VSR) ≥ 0.4 (TSHE, n = 35; placebo, n = 30).

Table S5. Comparison of abdominal visceral fat area (cm^2) between the placebo and TSHE groups in a VSR ≥ 0.4 subgroup, with and without adjustment for covariates.

References

Akazome, Y., Kametani, N., Kanda, T., Shimasaki, H., and Kobayashi, S. (2010). Evaluation of safety of excessive intake and efficacy of long-term intake of beverages containing apple polyphenols. J. Oleo Sci. 59(6): 321–338.

Burke, J.F., Sussman, J.B., Kent, D.M., and Hayward, R.A. (2015). Three simple rules to ensure reasonably credible subgroup analyses. BMJ 351: h5651.

Crispín-Isidro, G., Hernández-Rodríguez, L., Ramírez-Santiago, C., Sandoval-Castilla, O., Lobato-Calleros, C., and Vernon-Carter, E.J. (2019). Influence of purification on physicochemical and emulsifying properties of tamarind (*Tamarindus indica* L.) seed gum. Food Hydrocoll. 93: 402–412.

Décordé, K., Teissèdre, P., Sutra, T., Ventura, E., Cristol, J., and Rouanet, J. (2009). Chardonnay grape seed procyanidin extract supplementation prevents high-fat diet-induced obesity in hamsters by improving adipokine imbalance and oxidative stress markers. Mol. Nutr. Food Res. 53: 659–666.

Examination Committee of Criteria for Obesity Disease in Japan, and Japan Society for the Study of Obesity. (2002). New criteria for obesity disease in Japan. Circ. J. 66: 987–992.

Freedland, E.S. (2004). Role of a critical visceral adipose tissue threshold (CVATT) in metabolic syndrome: implications for controlling dietary carbohydrates: a review. Nutr. Metab. (Lond.) 1: 12.

Hiuge-Shimizu, A., Kishida, K., Funahashi, T., Ishizaka, Y., Oka, R., Okada, M., Suzuki, S., Takaya, N., Nakagawa, T., Fukui, T., Fukuda, H., Watanabe, N., Yoshizumi, T., Nakamura, T., Matsuzawa, Y., Yamakado, M., and Shimomura, I. (2012). Absolute value of visceral fat area measured on computed tomography scans and obesity-related cardiovascular risk factors in large-scale Japanese general population (the VACATION-J study). Ann. Med. 44: 82–92.

Japan Society for the Study of Obesity. (2022). Guidelines for the management of obesity disease 2022. Life Science Publishing, Tokyo, Japan, (in Japanese).

Kuwabara, M., Kuwabara, R., Niwa, K., Hisatome, I., Smits, G., Roncal-Jimenez, C.A., MacLean, P.S., Yracheta, J.M., Ohno, M., Lanaspa, M.A., Johnson, R.J., and Jalal, D.I. (2018). Different risk for hypertension, diabetes, dyslipidemia, and hyperuricemia according to level of body mass index in Japanese and American subjects. Nutrients 10: 1011.

Kwon, H., and Pessin, J.E. (2013). Adipokines mediate inflammation and insulin resistance. Front. Endocrinol. 4: 71.

Li, Z., Daniel, S., Fujioka, K., and Umashanker, D. (2023). Obesity among Asian American people in the United States: a review. Obesity 31: 316–328.

Matsuzawa, Y., Fujioka, S., Tokunaga, K., and Tarui, S. (1992). Classification of obesity with respect to morbidity. Exp. Biol. Med. 200: 197–201.

Ministry of Health, Labour and Welfare of Japan. (2023). Optimal use promotion guideline: semaglutide (genetical recombination) (Wegovy subcutaneous injection). November 2023 (revised May 2025). https://www.pmda.go.jp/files/000275486.pdf. Accessed 18 June 2026. (in Japanese).

Ministry of Health, Labour and Welfare of Japan. (2025). The national health and nutrition survey 2023. https://www.mhlw.go.jp/stf/newpage_45540.html. Accessed 18 June 2026. (in Japanese).

Nagao, T., Meguro, S., Soga, S., Otsuka, A., Tomonobu, K., Fumoto, S., Chikama, A., Mori, K., Yuzawa, M., Watanabe, H., Hase, T., Tanaka, Y., Tokimitsu, I., Shimasaki, H., and Itakura, H. (2001). Tea catechins suppress accumulation of body fat in humans. J. Oleo Sci. 50(9): 717–728.

Nasir, F., Javaid, M.A., Hanif, U., Sanghvi, G., Rekha, M.M., Jayabalan, K., Panigrahi, R., Rasheed, M., and Ndagire, C.T. (2026). Extraction and functional applications of tamarind seed polysaccharides as natural thickening agents in food systems. Eur. Food Res. Technol. 252: 173.

Nawrocki, A. (2004). The delicate balance between fat and muscle: adipokines in metabolic disease and musculoskeletal inflammation. Curr. Opin. Pharmacol. 4: 281–289.

Oliveira, R., Gonçalves, G., Inácio, F., Koehnlein, E., De Souza, C., Bracht, A., and Peralta, R. (2015). Inhibition of pancreatic lipase and triacylglycerol intestinal absorption by a pinhão coat (*Araucaria angustifolia*) extract rich in condensed tannin. Nutrients 7: 5601–5614.

Sasidharan, S.R., Joseph, J.A., Anandakumar, S., Venkatesan, V., Ariyattu Madhavan, C.N., and Agarwal, A. (2014). Ameliorative potential of *Tamarindus indica* on high fat diet induced nonalcoholic fatty liver disease in rats. Sci. World J. 2014: 507197.

Shirai, K., Tanaka, M., Fujita, T., Fujii, Y., Shimomasuda, M., Sakai, S., and Samukawa, Y. (2019). Reduction of excessive visceral fat and safety with 52-week administration of lipase inhibitor orlistat in Japanese: long-term clinical study. Adv. Ther. 36: 217–231.

Smith, S.R., Stenlof, K.S., Greenway, F.L., McHutchison, J., Schwartz, S.M., Dev, V.B., Berk, E.S., and Kapikian, R. (2011). Orlistat 60 mg reduces

visceral adipose tissue: a 24-week randomized, placebo-controlled, multicenter trial. Obesity 19: 1796–1803.

Souza, G.H., Paes Silva, B., Viana Neto, G.A., Finimundy, T.C., Santos, T.F.D., Bueno, P.S.A., Souza, F.O., Pilau, E.J., Barros, L., Comar, J.F., Bracht, L., Peralta, R.M., Bracht, A., and Sá-Nakanishi, A.B. (2025). *Tamarindus indica* sub-products as potential tools for simultaneous management of diabetes and obesity. Food Funct. 16: 1969–1991.

Wajchenberg, B.L. (2000). Subcutaneous and visceral adipose tissue: their relation to the metabolic syndrome. Endocr. Rev. 21(6): 697–738.

Wandee, R., Sutthanut, K., Songsri, J., Sonsena, S., Krongyut, O., Tippayawat, P., Tukummee, W., and Rittirod, T. (2022). Tamarind seed coat: a catechin-rich source with anti-oxidation, anti-melanogenesis, anti-adipogenesis and anti-microbial activities. Molecules 27: 5319.

Xing, Y., Lei, G., Wu, Q., Jiang, Y., and Huang, M. (2019). Procyanidin B2 protects against diet-induced obesity and non-alcoholic fatty liver disease via the modulation of the gut microbiota in rabbits. World J. Gastroenterol. 25(8): 955–966.

Yogalakshmi, B., Bhuvaneswari, S., Sreeja, S., and Anuradha, C.V. (2014). Grape seed proanthocyanidins and metformin act by different mechanisms to promote insulin signaling in rats fed high calorie diet. J. Cell Commun. Signal. 8: 13–22.

Yoshino, S., Kawakami, H., Yuki, T., Sato, T., and Fukuhara, I. (2022). Effects of a food containing fermented rice bran on the reduction of abdominal visceral fat area: a randomized, double-blind, placebo-controlled, parallel-group trial. Jpn. Pharmacol. Ther. 50: 1031–1040(in Japanese).

Yu, Y., Chen, P., Li, X., Shen, S., and Li, K. (2022). Persimmon proanthocyanidins with different degrees of polymerization possess distinct activities in models of high fat diet induced obesity. Nutrients 14: 3718.

Zenas-Trujillo, G.Z., Trujillo-Ramirez, I., Carhuavilca-Torres, J.M., Ayala-Mendivil, R.E., and Vera-Ponce, V.J. (2023). Prevalence of metabolically-obese normal-weight worldwide: systematic review and meta-analysis. J. Endocrinol. Metab. 13(3): 104–113.

Zhang, Y., Yu, Y., Li, X., Meguro, S., Hayashi, S., Katashima, M., Yasumasu, T., Wang, J., and Li, K. (2012). Effects of catechin-enriched green tea beverage on visceral fat loss in adults with a high proportion of visceral fat: a double-blind, placebo-controlled, randomized trial. J. Funct. Foods 4: 315–322.

Zhu, L., Yang, W.J., Spence, C.B., Bhimla, A., and Ma, G.X. (2021). Lean yet unhealthy: Asian American adults had higher risks for metabolic syndrome than non-Hispanic White adults with the same body mass index: evidence from NHANES 2011-2016. Healthcare 9: 1518.

Journal of Food Bioactives
International Society for Nutraceuticals and Functional Foods
Original Research
J. Food Bioact. 2026;35:81–89

Effects of egg white hydrolysate on facial swelling: a randomized, double-blind, placebo-controlled, crossover trial

Aoi Tamura[a], Utano Nakamura[a], Saki Shirako[a], Tsuyoshi Takara[b], Yusuke Yamashita[a], Kenji Sato[a] and Young-il Kim[a*]

[a]R&D Division, Pharma Foods International Co., Ltd., 1-49 Goryo-Ohara, Nishikyo-ku Kyoto, 615 8245, Japan
[b]Medical Corporation Seishinkai, Takara Clinic, Taisei Bldg. 9F, 2-3-2 Higashigotanda, Shinagawa-ku, Tokyo 141 0022, Japan
[*]**Corresponding author:** Young-il Kim, R&D Division, Pharma Foods International Co., Ltd., 1-49 Goryo-Ohara, Nishikyo-ku, Kyoto, 615 8245, Japan. E-mail: youngil-kim@pharmafoods.co.jp
DOI: 10.26599/JFB.2026.95035458
Received: July 30, 2026; **Revised received & accepted:** September 07, 2026
Citation: Tamura, A., Nakamura, U., Shirako, S., Takara, T., Yamashita, Y., Sato, K., and Kim, Y. (2026). Effects of egg white hydrolysate on facial swelling: a randomized, double-blind, placebo-controlled, crossover trial. J. Food Bioact. 35: 81–89.

Abstract

This study evaluated whether egg white hydrolysate (EWH) reduces morning facial swelling in healthy adults who routinely experience this condition (UMIN000057170). Seventy-six participants were randomly assigned to an EWH-first or placebo-first sequence in a double-blind, placebo-controlled, crossover trial. Participants ingested 250 mg of EWH or placebo once daily before bedtime for one week, separated by a 2-week washout. The primary outcome was the morning Visual Analogue Scale (VAS) score for facial swelling after 1-week intervention. Secondary outcomes included other subjective swelling and coldness sensations, and calf and ankle circumferences. A total of 61 participants were included in the final analysis. EWH intake significantly reduced the VAS score for morning facial swelling compared with placebo after one week (VAS: 54.8 ± 2.6 vs. 58.8 ± 2.6; $P = 0.037$). Therefore, EWH has the potential to serve as a functional food ingredient that reduces transient facial swelling and improves quality of life in healthy adults.

Keywords: Peptide; Egg white; Swelling; Edema; Clinical trial.

1. Introduction

Edema, defined as swelling caused by an accumulation of extracellular fluid, can be broadly categorized into generalized edema and localized edema. Generalized edema affects the entire body or large regions and is typically associated with systemic abnormalities such as cardiovascular, renal, hepatic, or hormonal dysfunction. In contrast, localized edema is confined to specific areas and commonly arises from a disruption of microcirculation and fluid homeostasis, such as increased vascular permeability, inflammation, impaired lymphatic drainage or temperature-related vascular responses. Examples of localized edema include chilblains, insect bites, sprains, allergic reactions, and lymphedema. Morning swelling of the face and neck in otherwise healthy individuals also represents a form of localized and transient edema, characterized by temporary fluid accumulation that resolves spontaneously after waking.

The primary mechanism of morning facial swelling is a postural fluid shift driven by gravity during sleep; venous pressure becomes more uniform in the supine position, interstitial fluid redistributes toward the face and neck, and lymphatic drainage decreases (Tsukahara et al., 2004). Conversely, upright activity during the daytime increases venous pressure in the lower limbs due to gravity, making calf and ankle swelling more prominent in the evening (Mortimer, 1995). Previous studies have also demonstrated clear diurnal variations in swelling and skin thickness; skin thickness significantly decreases from morning to afternoon in the face, forearm, and upper arm, whereas they significantly increase in the thigh and calf (Jogamoto and Hato, 2019; Tsukahara et al., 2001).

However, not all individuals experience this symptom, indicat-

© The author(s) 2026. Publishing Services by Tsinghua University Press
The articles published in this open access journal are distributed under the terms of the Creative Commons Attribution 4.0 International License (http://creativecommons.org/licenses/by/4.0/)

ing substantial individual difference in susceptibility. Women are particularly prone to swelling due to estrogen-mediated water retention, while other factors such as microinflammation, reduced lymphatic flow, cold sensitivity, and dietary factors—such as high salt or alcohol intake—can further exacerbate the condition (Ely et al., 2006; Jogamoto and Hato, 2019). In addition to the physical sensation of swelling itself, the accompanying heaviness and discomfort can trigger negative emotions and potentially reduce overall quality of life (QOL) (Cooper, 2018). These facts highlight the need for interventions that improve microcirculation and fluid homeostasis, thereby enhancing daily comfort and well-being in susceptible individuals.

Previous studies examining the alleviation of facial or lower-leg swelling have used polyphenol-rich ingredients such as lemon-derived hesperidin (Nakamura et al., 2019) and French maritime pine bark extract (Cesarone et al., 2005), which contain various polyphenols like flavonoids and phenolic acids. However, the bioavailability of polyphenols is highly dependent on the intestinal environment, as their health benefits rely on metabolic transformation by the gut microbiota. (Li et al., 2025; Marín et al., 2015). Food-derived peptides produced by enzymatic hydrolysis of proteins can also exert diverse beneficial functions in humans. Although most ingested peptides are degraded into amino acids during digestion in the small intestine, recent research has highlighted that certain food-derived peptides are absorbed as bioactive peptides (Matsui, 2018; Sato, 2022).

Egg white hydrolysate (EWH; Runpep®, Pharma Foods International, Kyoto, Japan) is a peptide mixture, which is produced from a by-product of food manufacturing such as mayonnaise industry. EWH has been reported to have antihypertensive activity and to improve peripheral blood flow in animal models (Sakashita, 2014). A clinical study further demonstrated that it promotes thoracic blood flow during endurance exercise in healthy adults (Shirato et al., 2008).

Based on anecdotal observations suggesting improvement of facial swelling following EWH intake, this study aimed to evaluate the effects of EWH intake on facial swelling in healthy Japanese adults who routinely experience morning facial swelling.

2. Materials and methods

2.1. Size-exclusion chromatography

The molecular weight distribution of peptides in EWH was analyzed by size-exclusion chromatography (SEC), which was outsourced to Japan Food Research Laboratories (Tokyo, Japan). The SEC was performed using a high-performance liquid chromatography system (LC-20 AD, Shimadzu, Kyoto, Japan) equipped with a TSKgel G2500PW$_{XL}$ column (7.8 mm i.d. × 300 mm, Tosoh, Tokyo, Japan). The mobile phase was 45% acetonitrile solution containing 0.1 % trifluoroacetic acid at a flow rate of 0.5 mL/min. Elution was monitored by UV absorbance at 220 nm. A molecular weight calibration curve was generated using standard peptides and proteins, including cytochrome C (12,327), aprotinin (6,512 Da), bacitracin (1,450 Da), angiotensin II (1,046 Da), Gly-Gly-Tyr-Arg (451 Da), and Gly-Gly-Gly (189 Da).

2.2. Test products

EWH was produced by digesting dried egg white with three types of proteases—Papain 300 (BIOCON Japan, Nagoya, Japan), Protease S Amano G and Protease N Amano (Amano Enzyme, Nagoya, Japan) —and one peptidase Peptidase R (Amano Enzyme).

Test product, tablet containing 125 mg of EWH, was prepared by Aliment Industry (Nambu, Japan). Peptide content in EWH was 76.5% (95.6 mg) based on nitrogen content obtained by the Kjeldahl method. The placebo contained the same ingredients as the test products, except that EWH was replaced with an equivalent amount of microcrystalline cellulose (Table 1). The test products and placebo were indistinguishable in appearance, shape, color, odor, and taste.

Table 1. Composition of test product and placebo per daily intake (mg / 2 tablets / day)

Ingredients	Test product	Placebo
EWH (Peptide content)	250 (191.2)	0
Microcrystalline cellulose	233	483
Reduced maltose syrup	90	90
Anti-caking agent	9.0	9.0
Magnesium stearate	12	12
Disintegrant	6.0	6.0

2.3. Participants

Participants were recruited through "Go-Tohroku" (https://www.go106.jp/), a monitor recruitment website operated by OrthoMedico (Tokyo, Japan). Recruitment was conducted between February and March 2025. None of the participants were affiliated with the study sponsors or the funding organization. A total of 154 candidates were requested to report scores in facial swelling using a visual analogue scale (VAS) "I feel facial swelling" on the morning of the screening examination. Subjective facial swelling was evaluated using the VAS, ranging from 0 mm ("best imaginable state") to 100 mm ("worst imaginable state"). The target sample size was determined based on an unpublished pilot study performed in Pharmafoods International (Approval No. PF0154) using R (version 4.4.2), which estimated an intervention effect of 10.3 mm on the primary outcome (morning VAS score for facial swelling). Using a pooled standard deviation (SD) of 22.7 and an inter-individual variability index of 1.7, the required sample size was calculated to be 35 participants per sequence to achieve a significant level (α) of 5% and a power (1-β) of 99.9% (total n = 70). To account for potential dropouts, we finally enrolled 38 participants per sequence, resulting in a total of 76 participants (62 females and 14 males) with VAS scores higher than 50 mm.

Eligibility criteria:

1. Healthy Japanese adults.
2. Routinely experiencing facial swelling.
3. Screening VAS score for "I feel swelling face" at morning assessment ≥ 50 mm.

Exclusion criteria included:

1. Current medical treatment or a history of malignant tumor, heart failure, or myocardial infarction.
2. Presence of a pacemaker or implantable cardioverter-defibrillator.
3. Ongoing treatment for chronic diseases such as cardiac arrhythmia, liver disorder, chronic kidney disease, cerebrovascular disorder, rheumatic disease, diabetes mellitus, dyslipidemia, hypertension.

4. Current use of "Foods for Specified Health Uses" or "Foods with Functional Claims".
5. Current use of medications (including herbal medicines) or supplements.
6. Allergies to medicines or foods related to test products, particularly egg allergies.
7. Body Mass Index (BMI) < 18.5 kg/m^2 or ≥ 30 kg/m^2.
8. Irregular lifestyle due to working late-night shift work or similar factors.
9. Current participation in exercise or dietary therapy under medical supervision.
10. Current condition or history of drug or alcohol dependence.
11. Alcohol intake >60 g/day on ≥4 days per week.
12. Caffeine intake ≥400 mg/day (approximately three mugs of coffee).
13. Current treatment for psychiatric disorder (including depressive symptoms) or sleep disorders.
14. Habitual high sodium intake.
15. Current pregnancy, lactation, or plans to become pregnant during study.
16. Participation in another clinical study within 28 days prior to enrollment or planned participation during the study period.
17. Any other condition judged by the investigator to make the participant unsuitable for the study.

2.4. Study design

This study was conducted as a randomized, double-blind, placebo-controlled, crossover trial. The study schedule is shown in Table 2. The trial was conducted between May and July 2025. Eligible participants (n=76) were randomly assigned to either EWH-first or placebo-first sequence. The allocation sequence was generated by an independent manager using R (version 4.3.2) with a sex-stratified, and random-block algorithm. To ensure blinding, identification numbers were assigned to the test products by the sponsor, and the allocation codes were kept strictly confidential until study completion. Emergency keys were stored in individually sealed envelopes. All parties, including investigators, medical staffs, and analysts, remained blinded until data fixation and finalization of the statistical analysis plan. The blind was broken only after confirming that all sealed envelopes remained intact.

The study consisted of two 1-week intervention periods (Period I and Period II) separated by a 2-week washout period. The intervention period was set to 1 week as significant improvements were already observed after 1-week intervention in the pilot study. In Period I, participants in the EWH-first sequence consumed test products containing 250 mg of EWH, while those in the placebo-first sequence consumed the placebo for one week. The dosage of EWH was determined based on the effective dose in the pilot study. After a 2-week washout period, participants crossed over to the alternative product for one week in Period II. In both periods, participants were instructed to take two tablets with water or lukewarm water within one hour before bedtime. Participants were instructed to visit either Takara Clinic, Medical Corporation Seishinkai (Tokyo, Japan) or Nerima Medical Association Minami-machi Clinic (Tokyo, Japan) at baseline and at day 8 of Period I and II, where assessments were performed.

This study was approved by the Ethical Committee of the Takara Clinic, Medical Corporation Seishinkai on February 12, 2025 (Approval Number: 2502-02351-0123-2A-TC). Subsequently, the study was registered with the University Hospital Medical Information Network Clinical Trials Registry (UMIN-CTR) on February 28, 2025, under the title "Effects of consumption of the test food on the swelling in healthy Japanese: a randomized, placebo-controlled, double-blind, crossover comparison trial" (Registration Number: UMIN000057170, URL: https://center6.umin.ac.jp/cgi-open-bin/ctr/ctr_view.cgi?recptno=R000065348). The trial was conducted in accordance with the Declaration of Helsinki (revised in 2024) and the Ethical Guidelines for Medical and Health Research Involving Human Subjects, with full consideration given to medical ethics.

2.5. Study outcomes

Outcomes were assessed at baseline and on the final days of intervention Period I and II. Participants were instructed to perform the morning assessment within 60 min of waking up and the evening assessment between 17:00 and 18:00.

For all parameters (unless otherwise specified), statistical comparisons were performed using three metrics after 1-week intervention: (1) raw scores, (2) changes from baseline, and (3) diurnal changes (morning-to-evening differences).

The primary endpoint was defined as the morning raw score after 1-week intervention. Secondary outcomes included as follows:

1. Facial swelling dynamics — Morning change from baseline, evening raw score, the evening change from baseline, and the morning-to-evening diurnal change after 1-week intervention.
2. Other subjective parameters — Assessed using VAS items targeting specific body parts and emotional response, including swelling around the eyes ("I feel swelling around eyes"), facial contour sharpness ("I feel like contour is not sharp"), lower-leg swelling ("I feel swelling lower legs"), ankle swelling ("I feel swelling the ankle [such as my shoes or socks feeling tight]"), coldness ("my hands and feet are cold"), temporary negative mood due to dark circles ("I feel temporarily down due to severe dark circles under my eyes"), and tired appearance ("I feel temporarily down due to a tired appearance").
3. Lower Limb Circumferences — Calf circumference measured horizontally at the thickest part of the lower leg in a standing position using a flexible tape; ankle circumference measured just above the lateral malleolus. These parameters were measured at either Takara Clinic or Minami-machi Clinic.
4. Anthropometric Parameters — Body weight measured using a standard scale; BMI calculated as weight divided by the square of height (kg/m^2). These parameters were measured at either Takara Clinic or Minami-machi Clinic.

Participant health was monitored through medical interviews conducted on examination days and a three-day dietary survey using the Calorie and Nutrition Diary prior to each visit. Daily logbooks were used to record test product intake, physical condition, medication use, and lifestyle factors. Adverse events (AEs) were identified and summarized based on interviews and logbooks. In the case of AEs, the principal investigator provided appropriate medical management and determined whether study participation should continue and decided whether emergency unblinding was necessary. The investigator also evaluated and reported the causal relationship between AEs and the test product based on predefined criteria.

2.6. Statistical analysis

Efficacy parameters were measured at baseline and the final days

Table 2. Schedule of enrollment, interventions, and assessments throughout the clinical trial

	Screening (Scr)									Period I							
	Briefing Session	Scr-3days	Scr-2days	Scr-1day	Scr	Enroll-ment	BL-3days	BL-2days	BL-1day	Baseline (BL) Day1		Day5	Day6	Day7	Day8 (Assessment)	
										AM	PM				AM	PM
Registration						•										
Eligibility screening	•															
Informed consent	•															
Other procedures	•															
Intervention																
EWH/Placebo											←	—	→			
Assessment																
VAS					•					•	•				•	•
Measurement of calf										•	•				•	•
Measurement of ankle										•	•				•	•
Physical measurements					•					•	•				•	•
Urinalysis					•											
Blood chemistry					•											
Daily log										←	—	—	—	→		
Dietary assessment		•	•	•			•	•	•			•	•	•		

	Wash out (2 weeks)			Period II							
	BL-3days	BL-2days	BL-1day	Baseline (BL) Day1		Day5	Day6	Day7	Day8 (Assessment)	
				AM	PM				AM	PM
Registration										
Eligibility screening										
Informed consent										
Other procedures										
Intervention										
EWH/Placebo					←	—	—	→		
Assessment										
VAS				•	•				•	•
Measurement of calf				•	•				•	•
Measurement of ankle				•	•				•	•
Physical measurements				•	•				•	•
Urinalysis										
Blood chemistry										
Daily log				←	—	—	—	→		
Dietary assessment	•	•	•			•	•	•		

Scr = Screening, BL = Baseline. “Scr-3days” indicates 3days before screening. “BL-3days” indicates 3days before baseline. “•” indicates an item performed during the specified period.”↔” indicates an item performed daily by the participants throughout the specified period. AM refers to the period within 60 min after waking up, and PM refers to the period between 17:00 and 18:00.

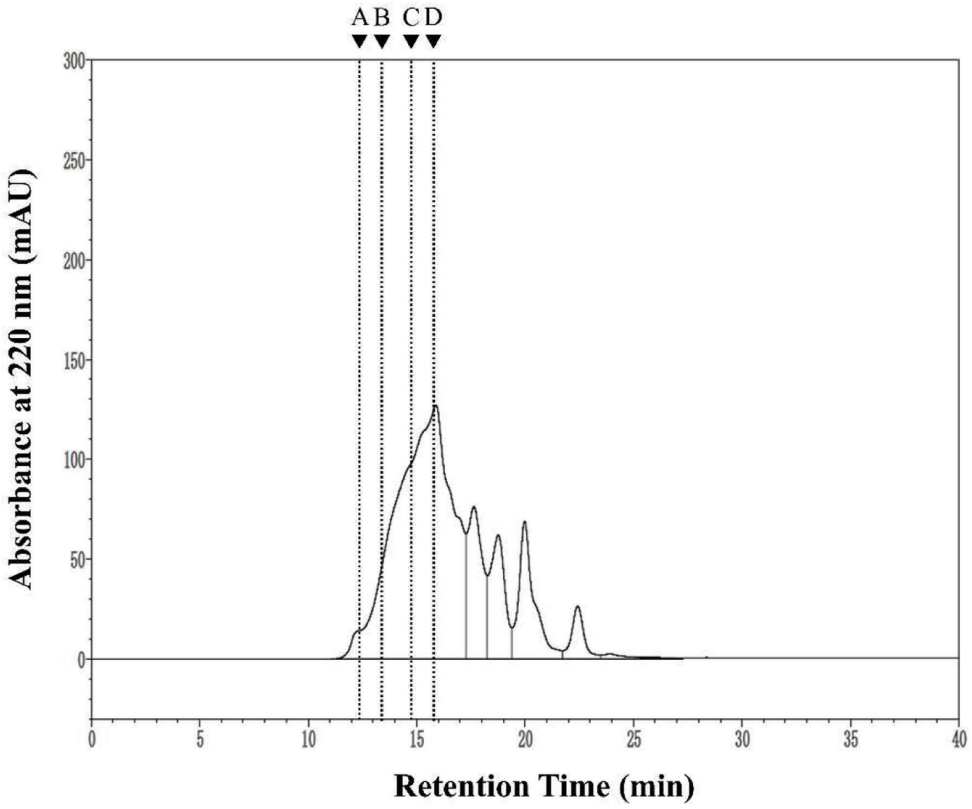


Figure 1. Size-exclusion chromatogram of peptides in EWH. Molecular weights were estimated based on the retention times of standard proteins and peptides. Arrows A, B, C, and D indicate estimated elution position of molecular weights of 6,000, 3,000, 1,000, and 500 Da, respectively. Peak area > 6,000, 3,000–6,000, 1,000–3,000, 500–1,000, < 500 were calculated.

of each period. The change from baseline was calculated for each intervention. Participant demographics for the enrolled and analyzed populations were summarized as means ± SD and compared using Welch's *t*-test. Primary and secondary outcomes were analyzed using a general linear mixed model including group (sequence), participants nested within groups, period, and food as fixed factors to evaluate treatment, sequence, and period effects. The definitions of treatment, sequence, and period effects are as reported by Lim and In (2021). Results are presented as means ± SD and estimated marginal means (EMMs) with 95% confidence intervals (95% CIs). All statistical tests were two-sided with a 5% significance level, using SPSS Statistics (version 23). Secondary outcomes were exploratory; thus, no multiplicity adjustments were made.

3. Results

3.1. Molecular weight distribution of peptides in EWH

SEC chromatogram is shown in Figure 1. Most peptides were eluted in the fraction corresponding to a molecular wight less than 6,000 Da. The molecular weight distribution of peptides in EWH is shown in Table 3. Based on peak areas, peptides with molecular weights less than 500 Da and those between 500 and 1,000 Da accounted for 57 % and 18 % of the total peak area, respectively. SEC analysis revealed that EWH predominantly consisted of low molecular weight peptides less than 500 Da.

3.2. Participants

As shown in Figure 2, a total of 154 candidates were screened, 76 were enrolled and equally assigned to two sequences. The EWH-first sequence consisted of 38 participants (mean age: 43.4 ± 10.2), and the placebo-first sequence consisted of 38 participants (mean age: 42.5 ± 11.1). During the trial, 15 participants were excluded from the analysis for the following reasons: 5 failed to receive the assigned intervention in Period I, 5 had a compliance rate of less than 80% and 5 violated dietary restrictions by consuming prohibited supplements or blood-flow-enhancing foods. Consequently, the per-protocol-set (PPS) for the final analysis consisted of 61 participants (EWH-first; n = 31 [25 females, 6 males]; placebo-first, n = 30 [23 females, 7 males]). The baseline characteristics of both the enrolled and analyzed participants are summarized in

Table 3. Molecular weight distribution of peptides in EWH

Molecular weight range (Da)	Peak area (%)
>6,000	1
3,000–6,000	4
1,000–3,000	20
500–1,000	18
<500	57
Total	100

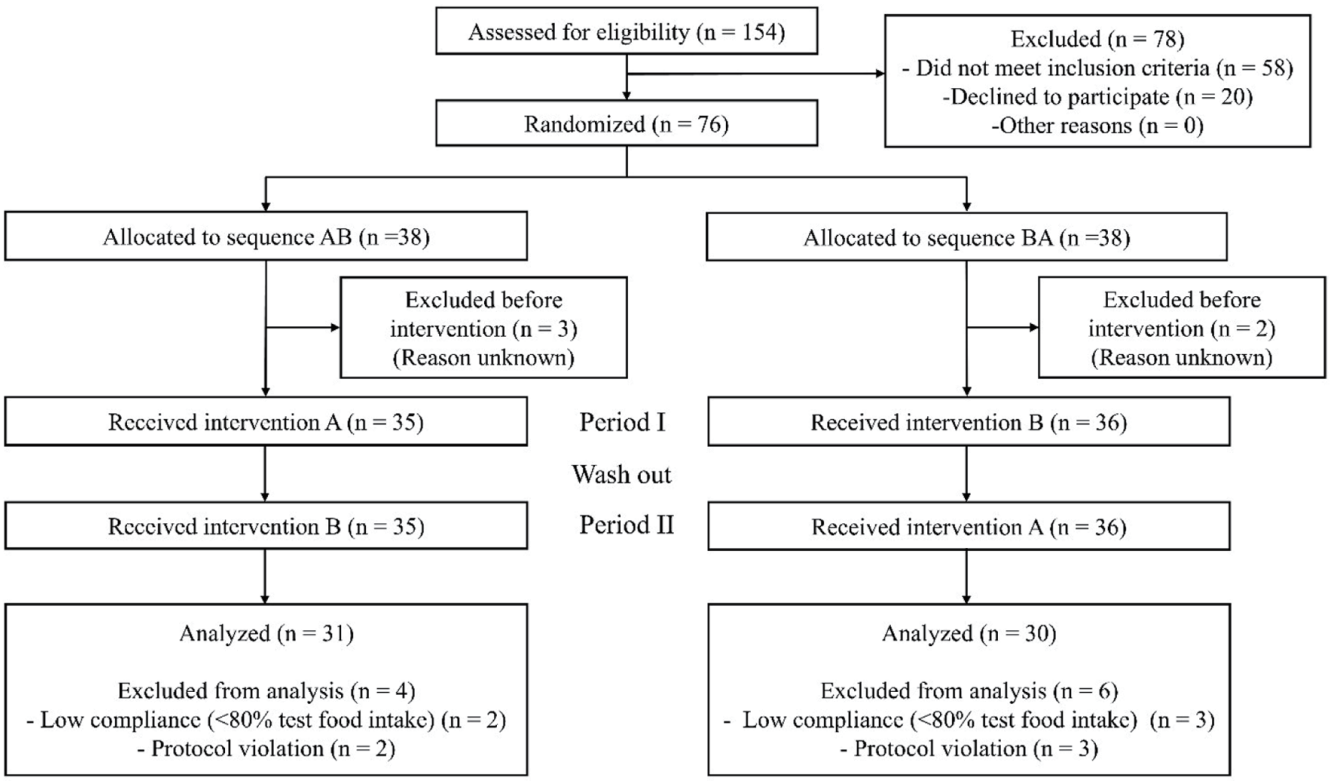


Figure 2. CONSORT flow diagram of participants throughout the study. A = the test product, B = placebo

Table 4. No significant differences were observed between the sequences in both the enrolled and analyzed participants regarding age, height, body weight, BMI, systolic blood pressure, diastolic blood pressure, and baseline VAS scores for facial swelling.

3.3. Outcomes

Table 5 summarizes the results presented as the mean, SDs, EMMs with standard error (SEs) and 95% CIs, and the inter-group differences (⊿). Regarding the primary outcome, the morning VAS score for facial swelling after 1-week was significantly improved in the EWH period (EMM ± SE: 54.8 ± 2.6) compared with the placebo period (58.8 ± 2.6), with a mean difference of −4.1 (P = 0.037). No significant differences were observed regarding the sequence effect and period effect. While no significant inter-group differences were found for any secondary outcomes (Tables S1–S3), VAS score for swelling around eyes showed a trend toward improvement (P = 0.073) (Table 5).

3.4. Safety

The present sample was well tolerated, and no adverse events were

Table 4. Baseline characteristics of participants

Item	Enrolled participants			Analyzed participants		
	Sequence AB Group (n = 38)	Sequence BA Group (n = 38)	*P* value	Sequence AB Group (n = 31)	Sequence BA Group (n = 30)	*P* value
Age (years)	43.4 ± 10.2	42.5 ± 11.1	0.707	44.4 ± 10.5	44.0 ± 11.0	0.870
Height (cm)	161.7 ± 6.7	163.4 ± 7.0	0.272	161.3 ± 6.4	164.3 ± 7.5	0.093
Body weight (kg)	62.2 ± 7.4	61.1 ± 9.7	0.570	62.4 ± 7.4	62.4 ± 9.5	0.976
BMI (kg/m^2)	23.8 ± 2.5	22.7 ± 2.3	0.068	24.0 ± 2.6	23.0 ± 2.1	0.102
Systolic blood pressure (mmHg)	113.5 ± 18.8	113.5 ± 18.1	1.000	111.9 ± 14.4	115.8 ± 18.5	0.363
Diastolic blood pressure (mmHg)	74.5 ± 13.4	74.8 ± 12.4	0.901	73.9 ± 10.8	76.3 ± 12.8	0.432
VAS score for facial swelling (mm)	69.6 ± 12.9	69.5 ± 9.9	0.953	69.6 ± 12.2	68.7 ± 9.4	0.744

Data are presented as means ± standard deviation, and *P*-value was calculated using the student's *t*-test. VAS was assessed on a 100 mm scale, where 0 mm represents "not at all" and 100 mm represents "very much." A = the test product, B = placebo

Table 5. Subjective outcomes measured during the AM assessments

Item	Time point	EWH						Placebo						Group comparison				*P* value		
		Mean	SD	EMM	SE	95% CI-	95% CI+	Mean	SD	EMM	SE	95% CI-	95% CI+	⊿	SE	95% CI-	95% CI+	Treatment effect	Sequence effect	Period effect
Facial swelling (mm)	BL	66.3	10.4	66.3	1.4	63.7	69.0	65.5	10.6	65.5	1.4	62.8	68.2	0.8	1.4	−1.9	3.5	–	0.995	0.830
	Day7	54.8	22.1	54.8	2.6	49.6	59.9	58.9	18.6	58.8	2.6	53.7	64.0	−4.1	1.9	−7.9	−0.2	0.037*	0.085	0.870
	(Day7-BL)	−11.5	19.8	−11.6	2.2	−15.9	−7.2	−6.6	14.9	−6.7	2.2	−11.0	−2.3	−4.9	2.2	−9.3	−0.5	0.029*	0.030*	0.783
Swelling around the eyes (mm)	BL	62.7	17.5	62.6	2.3	58.0	67.2	62.7	18.4	62.7	2.3	58.2	67.3	−0.1	2.4	−5.0	4.8	–	0.601	0.162
	Day7	56.1	22.4	56.1	2.6	50.8	61.3	59.9	19.7	59.8	2.6	54.6	65.1	−3.8	2.1	−7.9	0.4	0.073	0.051	0.845
	(Day7-BL)	−6.5	16.7	−6.6	2.1	−10.7	−2.4	−2.8	16.5	−2.9	2.1	−7.0	1.2	−3.7	2.7	−9.0	1.7	0.176	0.019*	0.257
Lack of definition in facial contour (mm)	BL	59.5	18.3	59.4	2.2	55.1	63.8	63.1	16.0	63.1	2.2	58.8	67.5	−3.7	2.4	−8.5	1.1	–	0.310	0.243
	Day7	55.9	21.0	55.8	2.5	50.7	60.8	57.6	19.7	57.5	2.5	52.5	62.5	−1.8	2.0	−5.9	2.3	0.390	0.019*	0.310
	(Day7-BL)	−3.6	13.8	−3.7	2.0	−7.6	0.2	−5.5	17.4	−5.6	2.0	−9.5	−1.7	1.9	2.6	−3.2	7.1	0.456	0.017*	0.776
Calf swelling (mm)	BL	62.0	22.5	61.9	2.6	56.7	67.1	65.0	18.3	64.9	2.6	59.7	70.1	−3.0	2.2	−7.4	1.4	–	0.145	0.479
	Day7	56.8	22.8	56.6	2.7	51.2	62.0	58.1	21.5	58.0	2.7	52.6	63.3	−1.3	2.4	−6.0	3.4	0.576		0.743
	(Day7-BL)	−5.2	16.8	−5.3	2.1	−9.4	−1.1	−6.9	16.4	−7.0	2.1	−11.1	−2.8	1.7	2.9	−4.2	7.5	0.567	0.022*	0.791
Ankle swelling (e.g., shoes or socks feel tight) (mm)	BL	58.7	24.1	58.6	2.7	53.3	64.0	62.8	17.5	62.7	2.7	57.4	68.1	−4.1	2.3	−8.8	0.5	–	0.154	0.504
	Day7	54.2	22.1	54.1	2.7	48.8	59.5	57.9	21.3	57.8	2.7	52.5	63.2	−3.7	2.4	−8.4	1.0	0.124	0.013*	0.670
	(Day7-BL)	−4.5	15.3	−4.5	2.0	−8.4	−0.6	−4.9	15.8	−4.9	2.0	−8.8	−1.0	0.4	2.4	−4.4	5.3	0.864	0.092	0.822
Coldness in hands and feet (mm)	BL	39.3	23.7	39.3	3.1	33.2	45.3	38.9	24.7	39.0	3.1	33.0	45.1	0.2	3.4	−6.5	7.0	–	0.341	0.011*
	Day7	33.7	23.3	33.6	3.1	27.5	39.7	34.8	24.8	34.9	3.1	28.8	40.9	−1.2	2.9	−7.1	4.6	0.670	0.686	0.008**
	(Day7-BL)	−5.6	25.6	−5.7	2.9	−11.5	0.1	−4.1	20.1	−4.2	2.9	−10.0	1.6	−1.5	4.1	−9.7	6.7	0.717	0.097	0.816
Temporary depressed mood due to prominent blue dark circles (mm)	BL	45.5	24.5	45.5	3.1	39.2	51.7	45.3	24.3	45.3	3.1	39.0	51.5	0.2	2.3	−4.5	4.9	–	0.801	0.765
	Day7	41.3	23.6	41.3	3.1	35.1	47.4	41.2	24.1	41.2	3.1	35.1	47.4	0.0	2.1	−4.2	4.3	0.987	0.880	0.939
	(Day7-BL)	−4.2	17.2	−4.2	2.1	−8.3	−0.1	−4.0	15.1	−4.0	2.1	−8.2	0.1	−0.2	2.8	−5.8	5.5	0.953	0.846	0.760
Temporary depressed mood due to a tired-looking face (mm)	BL	55.7	20.7	55.6	2.7	50.3	61.0	55.4	21.3	55.4	2.7	50.0	60.8	0.2	2.5	−4.9	5.3	–	0.902	0.577
	Day7	48.5	21.9	48.5	2.9	42.7	54.3	49.7	23.3	49.7	2.9	43.9	55.5	−1.2	2.0	−5.3	2.8	0.547	0.703	0.223
	(Day7-BL)	−7.2	16.7	−7.2	2.3	−11.7	−2.6	−5.7	18.7	−5.7	2.3	−10.3	−1.2	−1.4	2.7	−6.9	4.0	0.601	0.683	0.702

BL = Baseline, SD = standard deviation, EMM = estimated marginal means, SE = standard error, 95% CI- = 95% confidence interval (lower bound), 95% CI+ = 95% confidence interval (upper bound), ⊿ = difference in estimated marginal means. *$P < 0.05$, ** $P < 0.01$ compared with the placebo group at the same time point (between-group comparison based on a general linear mixed model). VAS was assessed on a 100 mm scale, where 0 mm represents "not at all" and 100 mm represents "very much".

observed throughout the study period with the intake of either the placebo or EWH (Table S4).

4. Discussion

This study evaluated whether 1-week daily intake of EWH improves morning facial swelling in healthy Japanese adults who routinely experience this condition. The primary outcome—morning VAS scores for facial swelling on the final days of each period—showed a statistically significant improvement during by intake of the EWH compared to the placebo across both sequences.

Previously, several functional peptides have been reported to exert diverse bioactive activities, including antihypertensive effects and improvement in skin moisture (Jia et al., 2021; Premchanth Jyothi et al., 2023; Ucak et al., 2021). To the best of our knowledge, this is the first study to demonstrate that bioactive peptides can reduce facial swelling in healthy individuals. Notably, EWH shows a clear advantage in terms of its effective dose. Whereas collagen peptide—one of the most studied functional peptides—requires daily intake of approximately 1–10 g to achieve measurable effects (Danessa et al., 2025), EWH exerts efficacy at least 250 mg. This highly practical and sustainable dosage suggests that EWH may serve as a promising ingredient for functional foods aiming at supporting vascular health and improving subject-reported QOL.

Morning facial swelling is primarily caused by hemodynamic changes related to sleep posture, specifically increased venous pressure and decreased lymphatic drainage in the facial region. Therefore, improved microcirculation is considered a plausible mechanism underlying the observed effect. *In vitro* studies have shown that EWH stimulates nitric oxide (NO) production in endothelial nitric oxide synthase (eNOS) - stably expressing human embryonic kidney 293 cell line (Sakashita, 2014) and *in vivo* studies have demonstrated increased plantar blood flow in normal rats and thoracic blood flow during endurance exercise in humans after EWH intake (Sakashita, 2014; Shirato et al., 2008). Such NO-dependent circulatory improvement may reduce posture-induced fluid retention observed in the morning.

In addition, vascular permeability is known to increase with inflammation, suggesting that mild, subclinical inflammation may exacerbate morning swelling in some individuals. Low physiological levels of eNOS-derived NO exert anti-inflammatory effects by inhibiting neutrophil adhesion and platelet aggregation, whereas excessive NO produced via inducible nitric oxide synthase (iNOS) during inflammatory states can increase vascular permeability and worsen swelling (Bian et al., 2008; Cyr et al., 2020). Although inflammatory markers were not evaluated in this study, it remains possible that peptides contained in EWH contributed to the improvement in swelling by suppressing mild inflammation that amplifies morning facial swelling.

This study has several limitations. First, the evaluation of facial swelling relied solely on subjective assessments. Because this was the first study to investigate the effects of EWH on morning facial swelling and its efficacy was difficult to predict, objective measurements that could impose additional burden on participants were not implemented. Although significant subjective improvements were observed in this placebo-controlled, double-blind, crossover trial, future studies incorporating quantitative assessments such as 3D facial scanning, ultrasound for skin thickness, tissue hydration meters are needed to elucidate the underlying mechanisms.

Second, this study did not directly measure physiological changes related to the hypothesized mechanism, including NO production and blood flow in the present participants. Therefore, the mechanistic pathways discussed herein remain hypothetical and rely on previous *in vitro* and *in vivo* findings without a direct link to the present clinical data. Future studies incorporating relevant biomarkers and hemodynamic measurements are required to establish the causal relationship between EWH intake and swelling reduction.

Third, the study population consisted exclusively of individuals who routinely perceived high levels of morning swelling. Therefore, the effects of EWH in individuals who do not typically experience swelling, as well as the physical or biochemical differences between those who do and do not experience morning swelling, remain unclear and warrant further investigation.

Finally, the specific bioactive peptide sequences for the physiological effects of EWH have not yet been identified. We are currently conducting qualitative and quantitative analyses of peptides absorbed into human bloodstream after EWH ingestion to determine which components contribute to the reduction of facial swelling *in vivo*.

5. Conclusion

In conclusion, daily intake of EWH for one week was confirmed to alleviate transient facial swelling in the morning among healthy Japanese adults who routinely experience this condition. Furthermore, the test product was found to be safe under the conditions of this study.

Data availability

The datasets generated and analyzed in this study are available from the corresponding author upon reasonable request.

Institutional review board statement

The study was conducted in accordance with the Declaration of Helsinki (revised in 2024) and approved by the Ethical Committee of the Takara Clinic, Medical Corporation Seishinkai on February 12, 2025 (Approval Number: 2502-02351-0123-2A-TC). Prior to the start of the study, the contents were registered with UMIN-CTR, which is managed by UMIN on February 28, 2025, under the title “Effects of consumption of the test food on the swelling in healthy Japanese: a randomized, placebo-controlled, double-blind, crossover comparison trial” (Registration Number: UMIN000057170,URL:https://center6.umin.ac.jp/cgi-open-bin/ctr/ctr_view.cgi?recptno=R000065348

Informed consent statement

Informed consent was obtained from all participants involved in the study.

Funding

This study was only carried out by the budget of Pharma Foods International (Kyoto, Japan).

Conflict of interest

The six authors (AT, UN, SS, YY, KS and YK) declare potential

financial conflicts of interest related to this study. This study was funded by Pharma Foods International, which provided the necessary consumables and may derive financial benefit from the publication of this manuscript. In addition, the author (YK) is the director of Pharma Foods International and holds shares in a company that may have potential financial benefits or losses from the publication of this paper.

Supplementary Material

Suppl 1. Objective outcomes measured during the AM assessments.

Suppl 2. Measured values of all outcomes during the PM assessments.

Suppl 3. Diurnal changes in all outcomes between the AM and PM assessments.

Suppl 4. Incidence of adverse events during the study period.

References

Bian, K., Doursout, M.F., and Murad, F. (2008). Vascular System: Role of Nitric Oxide in Cardiovascular Diseases. J. Clin. Hypertens. (Greenwich) 10(4): 304–310.

Cesarone, M.R., Belcaro, G., Rohdewald, P., Pellegrini, L., Ippolito, E., Scoccianti, M., Ricci, A., Dugall, M., Cacchio, M., Ruffini, I., Fano, F., Acerbi, G., Vinciguerra, M.G., Bavera, P., Di Renzo, A., Errichi, B.M., and Mucci, F. (2005). Prevention of Edema in Long Flights with Pycnogenol®. Clin. Appl. Thromb. Hemost. 11(3): 289–94.

Cooper, G. (2018). The impact of chronic oedema on quality of life in the elderly. Br. J. Community Nurs. 23(Sup4): S10–S12.

Cyr, A.R., Huckaby, L.V., Shiva, S.S., and Zuckerbraun, B.S. (2020). Nitric Oxide and Endothelial Dysfunction. Crit. Care Clin. 36(2): 307–321.

Danessa, G., Notario, D., and Regina, R. (2025). Effects of collagen-based supplements on skin's hydration and elasticity: A systematic review and meta-analysis. Indian J. Dermatol. Venereol. 91(6): 730–740.

Ely, J.W., Osheroff, J.A., Chambliss, M.L., and Ebell, M.H. (2006). Approach to Leg Edema of Unclear Etiology. J. Am. Board Fam. Med. 19(2): 148–160.

Jia, L., Wang, L., Liu, C., Liang, Y., and Lin, Q. (2021). Bioactive peptides from foods: production, function, and application. Food Funct. 12(16): 7108–7125.

Jogamoto, A., and Hato, N. (2019). Lower leg swelling in female hospital nurses. Jpn. J. Health Promot. 21(1): 1–9.

Li, H., Gao, J., Peng, W., Sun, X., Qi, W., and Wang, Y. (2025). Dietary Polyphenols-Gut Microbiota Interactions: Intervention: Strategies and Metabolic Regulation for Intestinal Diseases. Biology. 14(12): 1705.

Lim, C-Y., and In, J. (2021). Considerations for crossover design in clinical study. Korean J. Anesthesiol. 74(4): 293–299.

Marín, L., Miguélez, E.M., Villar, C.J., and Lombó, F. (2015). Bioavailability of Dietary Polyphenols and Gut Microbiota Metabolism: Antimicrobial Properties. BioMed. Res. Int. 2015: 905215.

Matsui, T. (2018). Are Peptides Absorbable Compounds? J. Agric. Food Chem. 66(2): 393–394.

Mortimer, P.S. (1995). Managing lymphedema. Clin. Exp. Dermatol. 20(2): 98–106.

Nakamura, Y., Yoshikawa, K., Nakamura, T., Hoshino, T., Yamashita, S., and Takara, T. (2019). Verification Study of Reduction in Facial Swelling with Intake of Enzyme-treated Lemon-derived Hesperidin -A Randomized, Double-blind, Placebo-controlled, Crossover Trial-. Jpn. Pharmacol Ther. 47(2): 211–228.

Premchanth Jyothi, S., Vinod, D., Lakshmi Satheesh, A., Sankar Rajeevan, J., Kannamathu, R., Pranav Biju, N., and Sandhya, S. (2023). Recent Advances in Bioactive Peptides as Functional Food for Health Promotions and Medicinal Applications. Protein Pept. Lett. 30(8): 626–639.

Sakashita, M. (2014). New Horizons for Egg White Peptide (Runpep®): Improving Blood Flow and Addressing Sarcopenia. Food Style 21 18(1): 85–87.

Sato, K. (2022). Metabolic Fate and Bioavailability of Food-Derived Peptides: Are Normal Peptides Passed through the Intestinal Layer To Exert Biological Effects via Proposed Mechanisms? J. Agric. Food Chem. 70(5): 1461–1466.

Shirato, M., Suga, M., Yoshida, Y., Kim, M., Demachi, K., and Yoshida, T. (2008). Effects of egg white-derived peptide intake on thermoregulatory response and energy metabolism during endurance exercise. JPFNI (Tairyoku Eiyou Menekigakuzasshi) 18(1): 28–38.

Tsukahara, K., Takema, Y., Moriwaki, S., Fujimura, T., and Imokawa, G. (2001). Dermal fluid translocation is an important determinant of the diurnal variation in human skin thickness. Br. J. Dermatol. 145(4): 590–596.

Tsukahara, K., Moriwaki, S., Hotta, M., Fujimura, T., and Kitahara, T. (2004). A study of diurnal variation in wrinkles on the human face. Arch. Dermatol. Res. 296(4): 169–174.

Ucak, I., Afreen, M., Montesano, D., Carrillo, C., Tomasevic, I., Simal-Gandara, J., and Barba, F.J. (2021). Functional and Bioactive Properties of Peptides Derived from Marine Side Streams. Mar. Drugs. 19(2): 71.

Journal of Food Bioactives

The Journal of Food Bioactives (JFB), a publication of the International Society for Nutraceuticals and Functional Foods (ISNFF), aims to bring together the results of fundamental and applied research on food bioactives, functional food ingredients, nutraceuticals and natural health products that are known to possess or perceived to have health-promoting properties.

Reviews

1

Matcha (Japanese ground green tea) and cognitive function

Klaus W. Lange, Yukiko Nakamura

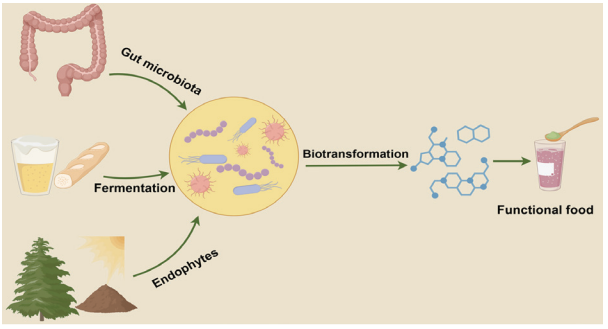
Matcha is a finely ground powder made from shade-grown green tea leaves.

12

Microbial biotransformation of plant-derived bioactive compounds: structural modifications, enhanced bioavailability, and functional food applications

Ying Ni, Wensheng Zhang, Yao Sun, Zhengyong Yu, Youhua Xu

Plant-derived bioactive compounds, including polyphenols, polysaccharides, alkaloids, terpenoids/saponins, lignans and glucosinolates, are widely valued for their health-promoting potential, yet poor bioavailability and, in several cases, biological inactivity in native form limit their translation into functional food ingredients.



24

Coreopsis tinctoria and its bioactives in the prevention and management of diabetes and diabetic complications

Wenyu Zhang, Yixing Zhu, Junfeng Shen, Alexander Gosslau

Diabetes, one of the major metabolic diseases, has become a major public health concern worldwide leading to chronic lesions in various organs such as kidney and cardiovascular disease, severely impacting quality of life and life expectancy.

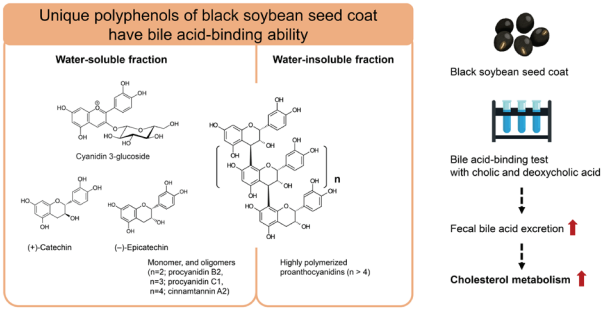
Original Research

38

In vitro bile acid-binding ability of black soybean seed coat

Naho Mizuno-Nagata, Hitoshi Ashida, Toshiya Toda

Bile acid-binding ability with dietary components is known to modulate cholesterol metabolism.

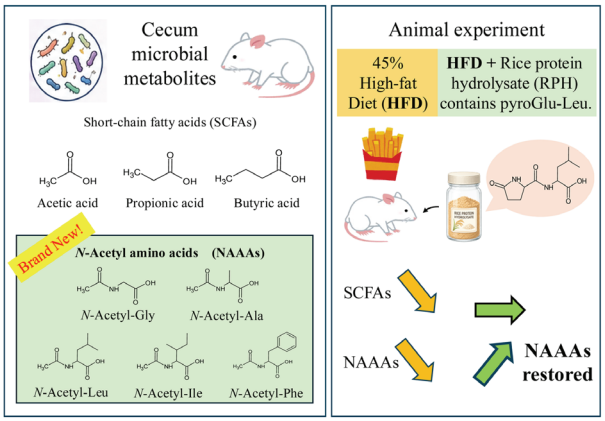


46

Pyroglutamyl peptide–rich rice protein hydrolysate restores cecal *N*-acetyl amino acids in high-fat-diet–fed rats, outperforming short-chain fatty acids as early microbial markers

Satoshi Miyauchi, Shiro Kajiwara, Tomoko Asai, Yasutaka Shigemura, Kenji Sato

Pyroglutamyl-leucine (pyroGlu-Leu) is a food-derived modified peptide known to modulate the gut microbiota.

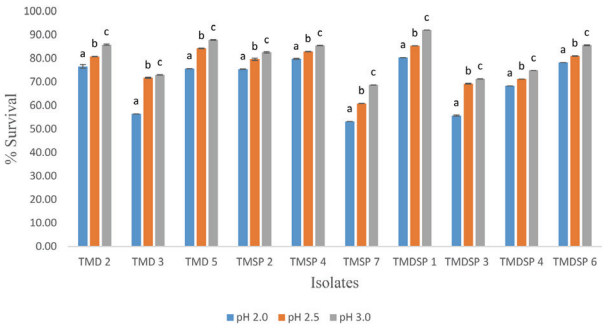


57

Probiotics characterization of fermented tiger nut-millet-blended beverage

Olawale Peter Odeleye, Blessing Mosopeoluwa Gabriel-Ogunniyi, Grace Mosunmola Adegbola, Ruth Adefolakemi O. Gabriel-Ajobiewe, Bartholomew Saanu Adeleke

This study investigated the functional characteristics and probiotic potential of lactic acid bacteria (LAB) isolated from a fermented tiger nut-millet beverage.

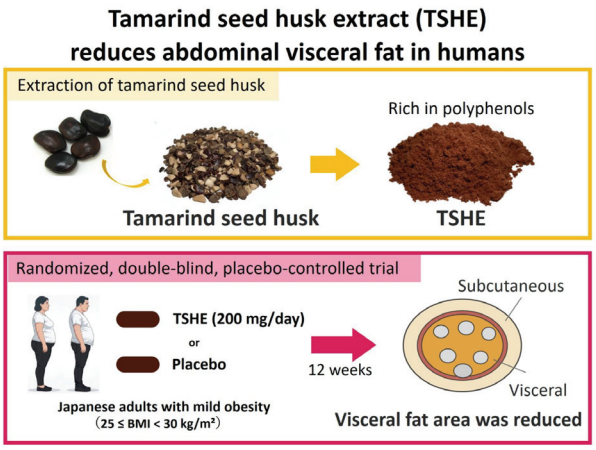


69

Effects of tamarind seed husk extract on abdominal visceral fat: a randomized, double-blind, placebo-controlled trial in Japanese adults with mild obesity

Hiroaki Yamada, Yusuke Yamashita, Xuan Li, Kenji Sato, Saki Shirako, Mariko Hirata, Jun Kawamura, Yumeo Suzuki, Yoshito Tsuruha, Tsuyoshi Takara, Young-il Kim

Tamarind seed husk, a by-product of gum production, is rich in polyphenols.

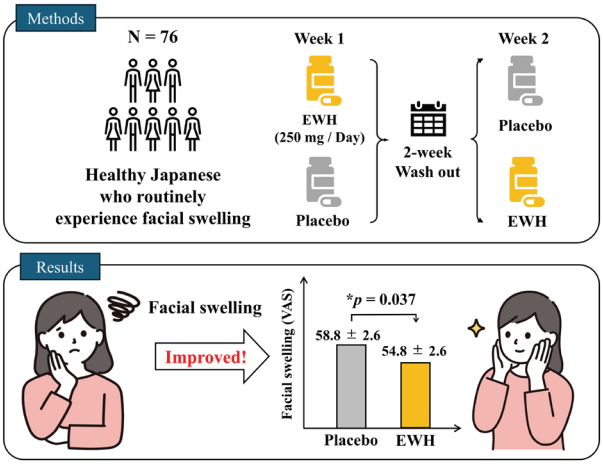


81

Effects of egg white hydrolysate on facial swelling: a randomized, double-blind, placebo-controlled, crossover trial

Aoi Tamura, Utano Nakamura, Saki Shirako, Tsuyoshi Takara, Yusuke Yamashita, Kenji Sato, Young-il Kim

This study evaluated whether egg white hydrolysate (EWH) reduces morning facial swelling in healthy adults who routinely experience this condition (UMIN000057170).



Journal of Food Bioactives

TABLE OF CONTENTS

Reviews

Matcha (Japanese ground green tea) and cognitive function
Klaus W. Lange, Yukiko Nakamura 1

Microbial biotransformation of plant-derived bioactive compounds: structural modifications, enhanced bioavailability, and functional food applications
Ying Ni, Wensheng Zhang, Yao Sun, Zhengyong Yu, Youhua Xu 12

***Coreopsis tinctoria* and its bioactives in the prevention and management of diabetes and diabetic complications**
Wenyu Zhang, Yixing Zhu, Junfeng Shen, Alexander Gosslau 24

Original Research

***In vitro* bile acid-binding ability of black soybean seed coat**
Naho Mizuno-Nagata, Hitoshi Ashida, Toshiya Toda 38

Pyroglutamyl peptide–rich rice protein hydrolysate restores cecal *N*-acetyl amino acids in high-fat-diet–fed rats, outperforming short-chain fatty acids as early microbial markers
Satoshi Miyauchi, Shiro Kajiwara, Tomoko Asai, Yasutaka Shigemura, Kenji Sato 46

Probiotics characterization of fermented tiger nut-millet-blended beverage
Olawale Peter Odeleye, Blessing Mosopeoluwa Gabriel-Ogunniyi, Grace Mosunmola Adegbola, Ruth Adefolakemi O. Gabriel-Ajobiewe, Bartholomew Saanu Adeleke 57

Effects of tamarind seed husk extract on abdominal visceral fat: a randomized, double-blind, placebo-controlled trial in Japanese adults with mild obesity
Hiroaki Yamada, Yusuke Yamashita, Xuan Li, Kenji Sato, Saki Shirako, Mariko Hirata, Jun Kawamura, Yumeo Suzuki, Yoshito Tsuruha, Tsuyoshi Takara, Young-il Kim 69

Effects of egg white hydrolysate on facial swelling: a randomized, double-blind, placebo-controlled, crossover trial
Aoi Tamura, Utano Nakamura, Saki Shirako, Tsuyoshi Takara, Yusuke Yamashita, Kenji Sato, Young-il Kim 81